

**“Role of aberrant vimentin expression in human oral pre-cancer and cancer”**

**By**

**Crismita Clement Dmello  
(LIFE09201004021)**

**Tata Memorial Centre  
Mumbai**

*A thesis submitted to the  
Board of Studies in Life Sciences  
In partial fulfillment of requirements  
for the Degree of*

**DOCTOR OF PHILOSOPHY  
of  
HOMI BHABHA NATIONAL INSTITUTE**



**April, 2017**

# Homi Bhabha National Institute

## Recommendations of the Viva Voce Committee

As members of the Viva Voce Committee, we certify that we have read the dissertation prepared by Ms. Crismita Clement Dmello entitled "Role of aberrant vimentin expression in human oral pre-cancer and cancer" and recommend that it may be accepted as fulfilling the thesis requirement for the award of Degree of Doctor of Philosophy.

	11/4/17
Chairman – Dr. Sorab N. Dalal	Date:
	11/4/17
Guide/Convener – Dr. Milind Vaidya	Date:
	11/4/17
Member 1 – Dr. Amit Dutt	Date:
	11/4/17
Member 2 – Dr. Sanjeev Waghmare	Date:
	11/04/2017
External Examiner – Dr. Maithreyi Narasimha	Date:

Final approval and acceptance of this thesis is contingent upon the candidate's submission of the final copies of the thesis to HBNI.

I hereby certify that I have read this thesis prepared under my direction and recommend that it may be accepted as fulfilling the thesis requirement.

Date: 11/4/17  
Place: Navi Mumbai

  
Dr. Milind Vaidya  
Guide

## STATEMENT BY AUTHOR

This dissertation has been submitted in partial fulfillment of requirements for an advanced degree at Homi Bhabha National Institute (HBNI) and is deposited in the library to be made available to borrowers under rules of the HBNI.

Brief quotations, from this dissertation, are allowable without special permission provided that accurate acknowledgement of source is made. Requests for permission for extended quotation from or reproduction of this manuscript in whole or in part may be granted by the Competent Authority of HBNI when in his or her judgment, the proposed use of the material is in the interests of scholarship. In all the other instances, however, permission must be obtained from the author.

Navi Mumbai

Date: 31<sup>st</sup> August, 2016



Crismita Clement Dmello

## DECLARATION

I, hereby declare that the investigation presented in the thesis has been carried out by me. The work is original and has not been submitted earlier as a whole or in part for a degree/diploma at this or any other Institution or University.

Navi Mumbai

Date: 31<sup>st</sup> August, 2016



Crismita Clement Dmello

## List of Publications arising from the thesis

### Journal

1. Crismita Dmello, Sharada Sawant, Hunain Alam, Prakash Gangadaran, Saie Mogre, Richa Tiwari, Zinia D'Souza, Manish Narkar, Rahul Thorat, Komal Patil, Devendra Chaukar, Shubhada Kane, Milind Vaidya, Vimentin regulates differentiation switch via modulation of keratin 14 levels and their expression together correlates with poor prognosis in oral cancer patients. *PloS one*. 2017;12(2):e0172559.
2. Crismita Dmello, Sharada Sawant, Hunain Alam, Prakash Gangadaran, Richa Tiwari, Harsh Dongre, Neha Rana, Sai Barve, Daniela Elena Costea, Davendra Chaukar, Shubhada Kane, Harish Pant, Milind Vaidya, Vimentin mediated regulation of cell motility through modulation of beta4 integrin protein levels in oral tumor derived cells, *The international journal of biochemistry & cell biology*, 70 (2015) 161-172.

### Conferences (Abstracts published)

1. **Crismita Dmello**, Sharada Sawant, Milind Vaidya “Role of aberrant vimentin expression in early and late events of human oral cancer”, *Journal of Carcinogenesis*, 2015; 14 (Suppl 1): S21–S38. Published online 2015 Feb 10
2. **Crismita Dmello**, Sharada Sawant, Milind Vaidya “Development of an in vitro carcinogenesis model to test the transformation potential of vimentin”, *European Journal of Cancer*, Feb 2016; [http://dx.doi.org/10.1016/S0959-8049\(16\)31953-0](http://dx.doi.org/10.1016/S0959-8049(16)31953-0)

### Conferences and workshops attended

#### 1. Oral presentation

1. Received award for oral presentation at the fifth international conference of the Carcinogenesis Foundation (USA) on “Molecular pathways to therapeutics: new

paradigms and challenges in oncology”, organized in India in collaboration with ACTREC-TMC from 11th to 13th February, 2015 at Advanced Centre for Treatment Research and Education in Cancer (ACTREC), Navi Mumbai, India.

2. Received award for oral presentation at the 11<sup>th</sup> National Research Scholars Meet in Life Sciences (NRSML), 2015 held from 17th to 18th December 2015 at Advanced Centre for Treatment, Research and Education in Cancer, Kharghar, Navi Mumbai.

## **2. Poster presentations**

1. Presented a poster entitled “Development of an in vitro carcinogenesis model to test the transformation potential of vimentin” at the TMC Platinum Jubilee ‘A conference of new ideas in cancer: challenging dogmas’ held from 26<sup>th</sup> to 28<sup>th</sup> February, 2016 at National Centre for the Performing Arts, Nariman Point, Mumbai
2. Presented a poster entitled “Vimentin mediated regulation of differentiation switch via keratin 14 modulation in oral squamous cell carcinoma derived cell line” at the Intermediate Filaments Gordon Research Seminar (GRS) and at Intermediate Filaments Gordon Research conference (GRC), on Intermediate Filaments at the Crossroads Between Health and Disease held from June 14-20, 2014 at Mount Snow, West Dover, VT, USA.
3. Presented a poster entitled “Vimentin mediates epithelial cell motility by destabilizing  $\alpha 6\beta 4$  integrin associated adhesion complex” at the 37<sup>th</sup> All India Cell Biology Conference on Cell Dynamics and Cell Fate held from December 22<sup>nd</sup> 2013 to December 24<sup>th</sup> 2013 at J N Tata Auditorium, Indian Institute of Science, Bangalore.

4. Presented a poster entitled “Down-regulation of vimentin using RNA interference leads to decreased *in vitro* tumorigenic potential and motility” at monsoon retreat 2012 held at ACTREC, Navi Mumbai

### **3. Other Participations**

1. Participated in the “Science Communication Workshop” organized by “The Wellcome Trust/DBT India Alliance” held on 21-22 march, 2016 at Lemon Tree Premier, Hyderabad.
2. Participated in the “10<sup>th</sup> Annual Surgical Oncology Conference 'Oncosurg 2014" from 21st - 23rd November 2014, held at Tata Memorial Hospital, Mumbai.
3. Part of organising committee of “9<sup>th</sup> national research scholars meet in life sciences” held at ACTREC, Kharghar, Navi Mumbai from 19th-20th December 2013
4. Participated in the workshop and mini-symposium on ‘Cancer Informatics – Analysis and Informatics of Microarray Data’ organized jointly by the National Centre for Cell Science & the Bioinformatics Centre, University of Pune, on 13 and 14 September, 2012.
5. Participated in the conference held by Indian association for cancer research (IACR) at ACTREC, Navi Mumbai in 2012
6. Participated in the 1ST Annual Global Cancer Genomics Consortium–Tata Memorial Centre (GCGC-TMC) Symposium on 10th-12th Nov 2011
7. Attended meeting on Gynaecology Cancers AOGIN (Asia Oceania research organization on Genital Infections and Neoplasia, India) on 5-6th November 2011

Navi Mumbai

Date: 31<sup>st</sup> August, 2016



Crismita Clement Dmello

## **Dedicated To**

I dedicate my 6 years of PhD work to my parents, Mommu and Papuu for being there.....  
with me, for me and by me.....in sickness and in wellness, in joys and sorrows, in pain and in  
comfort, in failures and in success.....and in all decision making and solutions.

## **Acknowledgements**

*PhD is not a degree but a process, which programs you to perform beyond your capabilities, to comprehend beyond your understanding, to imagine beyond your imagination and most importantly to sustain beyond all odds. During this process one comes across several people who either take you through the path or direct you to the correct path. I take this opportunity to remember all those navigators to whom I will always be indebted. They have not only helped me rise after every fall but have also taught me patience and optimism which are key factors required in research.*

*To top the list is my supervisor, mentor and guardian Dr. Milind Vaidya. I am fortunate to find all the traits in one person. He not only took me through this journey of PhD but while attaining the goal he taught me patience, trust and persistence. I would always wonder about his boundless optimism, which appeared unrealistic most of the times, but I now realize that hope and optimism are the only catalyst to accelerate your reaction (PhD). I will always cherish his ideologies and his approach towards life and science. My second mentor is the pioneer of the vimentin project in my laboratory, Mrs. Sharda Sawant. Thank you Sharada Ma'am for your abundant support and guidance especially in human tumor tissue related work. I will always remember the daily snacks that you offered me during my paper/thesis writing sessions.*

*I am very thankful to our Director Prof. Shubhada V. Chiplunkar for giving me an opportunity to be a part of this prestigious institution and creating an excellent research environment at ACTREC. I would like to thank Deputy Director Dr. Sudeep Gupta for the infrastructure and facilities. I would also like to acknowledge the financial, academic and technical support provided by them. I am deeply grateful to our former director Dr. R. Sarin and former deputy director Dr. S. Zingde for their support and encouragement.*

*I am extremely thankful to my Doctoral Committee members- Dr. Sorab Dalal, Dr. Amit Dutt and Dr. Sanjeev Waghmare for their invaluable suggestions and critical assessment of the progress of my research work. I was benefited greatly from the ideas given by Dr. Sorab Dalal during my DC meetings, this helped me a lot, to develop my project and reanalyze the data carefully. I am very grateful to my former chairperson Dr. Girish Maru and former DC member late Dr. Rajiv Kalraiya for their valuable suggestions and also help in terms of reagents sharing.*

*I owe my deepest gratitude to my former and current labmates. My super senior Dr. Deepak Kanojia, whom I only know by the reagents and methods he developed, since he completed his PhD before I joined. My senior Dr. Hunain Alam, was the first one to introduce me to the world of research. He not only taught me the techniques but also trained me to do research with discipline and dedication. I am thankful to my senior Dr. Sapna Iyer for teaching me patience and understanding in science. She also taught me some of the techniques involved in tissue culture. My senior Dr. Biharilal Soni alias Soniji taught me 2D and Mass spectrometry. I will always miss his kindness, loud laughter and importantly yummy food cooked by him. I am grateful to my batchmate, labmate and roommate Ms. Richa Tiwari for always being there to help me out in my problems both scientific and personal. I learned a lot from the scientific discussions we had in the laboratory and in our hostel room. I am thankful to Mr. Pratik Chaudhari, for always offering infinite support and strength to move forward. His scientific suggestions and personal advice has helped me throughout during PhD. I am privileged for having Saumaya as a postdoctoral fellow in our laboratory, who has provided support both scientifically and personally. I would like to thank Rajesh for helping me in animal work, washing and packing of glassware and ordering reagents. I would like to thank Sridhar for his immense help with animal work and in the washing and packing of glassware. I am also thankful to Prema Ma'am and Yashwant sir for helping me*

out with all the laboratory and official formalities. I am grateful to Kishore and Ram More for their help with laboratory work. My research would not have been possible without their constant support. I would like to thank Mr. Harsh Dongre for his constant unconditional help in data analysis and in any computer related issues. I have learned a lot from him. I would like to wholeheartedly thank all my trainees Sai, Saie, Cyrus, Nandini, Swapnita, Nikhil, Jashkaran, Latika, Neha, Pallavi, Manish, Ravi, Arti, Komal, Anagha, Zinia, without whom my work would not have been completed on time. Special thanks to my last trainee Zinia for helping me in thesis writing. I am also thankful to former lab members Prakash, Vidhi, Archana and Swapnil and current lab members Sylvania, Sunita, Ankur, Fatima, Krishna, Yashvi, Chetan, Shruti and Abhishek for their company. I am thankful to our staff physician who has promptly addressed all my health issues. I am immensely grateful to the oral cancer patients, who consented to be a part of this study, for their generosity.

I would like to thank the entire ACTREC students' community for all their support and cooperation throughout the tenure. My special thanks to all my batchmates (Abira, Aditi, Asif, Gauri, Indrajit, Madhura, Nikhat, Piyush, Poonam, Prasad, Raja, Rajan, Ram, Richa, Rushikesh, Saikat, Satish, Shyam, and Yasser) for all their help in terms of scientific ideas and reagents as well. I would also like to thank other seniors and juniors of ACTREC especially, Amit Singh, Amit Fulzale, Akhil, Manohar, Dilip, Rupa, Kedar, Shrikanto, Gopal, Bhavik and Shalaka for their constant help in terms of reagents or understanding the techniques. I will always cherish the memories shared with my former and current hostel roommates Richa, Aditi, Poonam, Khrivono Kheki, Shilpi, Priya, Raikamal and Sudheshna

I am extremely thankful to Dr. Ingle, Dr. Thorat and other staff of the animal house for supplying and helping me with animal work. I would like to thank Vaishali, Tanuja and Jaiaraj for their immense help in confocal, inverted and upright microscopy. I thank Rekha and Shamal for their help in flow cytometry experiments. I thank Sashi and Prashant for their help in proteomics. I am also thankful to Naresh and Sharada for their help in sequencing. My special thanks to the common facility staff especially Mr. Uday Dandekar for being a solution to all technical issues related to equipments and machines. I am also thankful to the Hostel, Photography, Stores, Purchase, Library, Engineering, Security, Workshop, Administration, Accounts and Pharmacy department for their help and co-operation. I am grateful to Dr. Daniela, Prof. Goldman, Dr. Livio, Prof. Magin, Dr. Sorab and all the PIs of ACTREC for sharing cell line, reagents and plasmid constructs. I am thankful to Mrs. Tejaswini Modak (Online trainer and instructor for English Writing Skills, Centre for e-learning and Training) for corrections related to English spelling and grammar of my manuscripts. I gratefully acknowledge the funding sources that made my Ph.D. work possible. I was funded by the fellowship from ACTREC and my work was supported by the Department of Biotechnology (DBT). I would also like to thank the Sam Mistry Fund (Tata Memorial Centre) and Homi Bhabha National Institute (HBNI) for travel fellowship to attend the Gordon conference.

I would like to thank my husband, my life; Mr. Nigel Gomes for trusting, supporting and believing in me. I thank him for being the reason of all my happiness, hope and peace. I thank my parents-in-law Francis Gomes and Elizabeth Gomes for equally supporting and understanding me under all circumstances. My parents Clement and Rosy Dmello for making me what I am today and my brother Carol Dmello for encouraging and supporting me against all odds. I thank my bhabhi Arina and my little nephew Arnold for making my life so beautiful and cheerful. I wish to thank all who have contributed in some or the other way towards completion of my PhD degree.

Above all, I thank "God" for his uncountable blessings and mercy on me.

**Crismita Clement Dmello**

## Contents

<b>List of Illustrations</b>	
<b>List of Figures</b>	
<b>List of Tables</b>	
<b>Abbreviations</b>	1
<b>Synopsis</b>	3
<b>Chapter 1: Introduction</b>	19
1.1 Key Question	22
1.2 Objectives	22
1.2.1 To study the phenotypic and molecular changes associated with vimentin in OSCC derived cell line.	22
1.2.2 To delineate the molecular pathways by which vimentin confers a particular phenotype to the cancer cell.	22
1.2.3 To study role of vimentin in early events of human oral cancer development.	22
<b>Chapter 2: Review of Literature</b>	23
2.1 Human oral cancer	24
2.1.1 Epidemiology	24
2.1.2 Risk factors	24
2.1.3 Tumorigenesis	25
2.2 Human oral pre-cancer	26
2.2.1 Types of Oral premalignant lesions (OPLs)	26
2.2.1.1 Leukoplakia	26
2.2.1.2 Erythroplakia	26
2.2.1.3 Oral Submucous Fibrosis (OSMF)	27
2.2.1.4 Lichen planus	27
2.2.2 Diagnosis	27
2.2.3 Treatment	28
2.2.4 Challenges	28
2.3 Intermediate Filaments	29
2.3.1 Structure and assembly of IFs	30
2.3.2 Functions of intermediate filaments	31
2.3.2.1 Structural functions of IFs	32
2.3.2.2 Role of IFs in cellular processes	32
2.3.2.3 Role of nuclear IFs in controlling nuclear organisation	32
2.3.2.4 Role of IFs in vesicular trafficking	33
2.3.3 Diseases associated with intermediate filaments	33
2.3.4 Intermediate filament (IF) proteins and cancer	35
2.3.5 Vimentin	36
2.3.5.1 Structure	37
2.3.5.2 Post translational modifications of vimentin	37
2.3.5.3 Functions of vimentin	38
2.3.5.3.1 Role of vimentin in normal development and differentiation	38
2.3.5.3.2 Role of vimentin in precancerous lesions	38
2.3.5.3.3 Role of vimentin in cancer	39
2.3.5.3.4 Role of vimentin in Epithelial mesenchymal transition (EMT)	40
2.3.5.3.5 Role of vimentin in cell signaling	41

2.3.6 Vimentin and $\alpha 6\beta 4$ integrin	42
2.3.6.1 Vimentin and $\alpha 6\beta 4$ integrin in cancer	43
2.3.7 Vimentin and differentiation state of cancer cell	44
2.3.8 Vimentin and keratin in cancer cell differentiation	44
<b>Chapter 3: Materials and Methods</b>	<b>46</b>
3.1 List of Cell lines, antibodies and reagents	47
3.2 Routine maintenance of cells	50
3.3 Other reagents	50
3.4 Revival of cells	51
3.5 Subculture/Trypsinization and transfer of cells	52
3.6 Freezing and cryopreservation of cells	52
3.7 Plasmid and cloning	52
3.8 Validation of shRNA constructs	54
3.9 Virus production	55
3.10 Preparation of whole cell lysates	55
3.11 Protein estimation by modified Lowry's method	56
3.12 SDS PAGE	56
3.13 Western blotting	56
3.14 Zymography	57
3.15 Co-immunoprecipitation	58
3.16 Protein estimation by RC DC Kit	58
3.17 Two-dimensional polyacrylamide gel electrophoresis (2DE)	59
3.18 Coomassie staining	60
3.19 In gel tryptic digestion and Mass spectrometry	60
3.20 RNA extraction	61
3.21 Reverse transcriptase - Polymerase chain reaction (RT-PCR)	61
3.22 Real-Time Quantitative PCR	62
3.23 Immunofluorescence	64
3.24 Immuno-electron microscopy	65
3.25 Induction of EMT and stimulation of $\beta 4$ integrin signaling	65
3.26 Cell proliferation / MTT (3-(4,5-Dimethylthiazol-2-yl)-2,5-Diphenyltetrazolium Bromide) viability assay	66
3.27 Adhesion assay	66
3.28 Live cell spreading assay	67
3.29 Colony-forming assay	67
3.30 Soft agar colony forming assay	67
3.31 Single cell migration assay	68
3.32 <i>In vitro</i> wound healing assay for migration	68
3.33 Boyden chamber cell invasion assay	68
3.34 Development of <i>in vitro</i> carcinogenesis model	69
3.35 Tumorigenicity assays	69
3.36 Histology and immunohistochemistry	70
3.37. Statistical analysis	71
<b>Chapter 4: Results</b>	<b>72</b>
4.1 Vimentin mediates regulation of cell motility through modulation of $\beta 4$ integrin protein levels in oral tumor derived cells	73
4.1.1 Downregulation of vimentin decreases <i>in vitro</i> transformation potential and invasiveness of OSCC derived cell line AW13516	73
4.1.2 Vimentin downregulation results in a more spread morphology	75

4.1.3 Vimentin regulates $\beta$ 4 integrin levels	76
4.1.4 Changes in vimentin expression directly correlate with the alterations in the levels of $\beta$ 4 integrin in squamous cell carcinoma (SCC) derived cell lines	78
4.1.5 Plectin could be a possible linker connecting $\beta$ 4 integrin with vimentin intermediate filament protein	80
4.1.6 Vimentin knockdown results in increased localization of hemidesmosomal proteins ( $\beta$ 4 integrin and plectin) at membrane-substrate front	81
4.1.7 Vimentin knockdown results in increased colocalization between $\beta$ 4 integrin and plectin	82
4.1.8 Vimentin knockdown results in enhanced interaction between $\beta$ 4 integrin and plectin	84
4.1.9 Functional consequence of $\beta$ 4 integrin upregulation in vimentin knockdown cells	85
4.1.10 Vimentin knockdown cells show decreased spreading and migration on fibronectin	87
4.1.11 Downstream molecules associated with $\beta$ 4 integrin mediated adhesive phenotype	88
4.1.12 Vimentin knockdown results in decreased protein turnover of $\beta$ 4 integrin and plectin	89
4.1.13 Downregulation of $\beta$ 4 integrin in vimentin knockdown background rescues vimentin knockdown phenotype	91
4.1.14 $\beta$ 4 integrin downregulation rescued the vimentin knockdown phenotype	93
4.1.15 High vimentin and low $\beta$ 4 integrin protein levels are associated with poor survival	94
4.1.16 Summary of part 1	97
4.2 Vimentin regulates differentiation switch via modulation of Keratin 14 levels and their expression together correlates with poor prognosis in oral cancer patients	98
4.2.1 Downregulation of vimentin results in alteration in the keratin profile of the OSCC derived cell line AW13516	98
4.2.2 Validation of K14 depletion upon vimentin downregulation	102
4.2.3 Vimentin modulates the differentiation status of the epithelial cells	104
4.2.4 Vimentin modulates the tumorigenic potential of the epithelial cells	106
4.2.5 Vimentin positively regulates the expression of K5/K14 pair across different stratified epithelia derived cell lines	107
4.2.6 Vimentin knockdown phenotype was rescued upon re-expression of K5/K14 pair	109
4.2.7 $\Delta$ Np63 could be a possible target of vimentin, to bring about the modulation of K5/14 expression	111
4.2.8 Activation of Notch1 may be a cause or a consequence of $\Delta$ Np63 downregulation in vimentin knockdown background	114
4.2.9 High expression of vimentin-K14 together correlates with recurrence and poor survival of oral cancer patients	116
4.2.10 Summary of part 2	119
4.3 Evaluation of transformation potential of vimentin in the development of human oral cancer	120
4.3.1 Characterization of DOK for vimentin expression	120

4.3.2 Overexpression of vimentin in DOK cell line	121
4.3.3 Development of <i>in vitro</i> carcinogenesis model using benzo[a]pyrene	124
4.3.4 Molecular changes associated with the vimentin overexpressing and its vector control cells in response to benzo[a]pyrene treatment	126
4.3.5 Summary of objective 3	128
<b>Chapter 5: Discussion</b>	<b>129</b>
5.1 Overall summary of the role of vimentin deduced in this study	144
<b>Chapter 6: Summary and Conclusion</b>	<b>145</b>
<b>Bibliography</b>	<b>149</b>

## List of Illustrations

Figure 2.1 Schematic depictions of the structure and assembly groups of IFs.	31
Figure 4.1.16 Schematic depiction of the role of vimentin in modulating $\beta$ 4 integrin surface levels to regulate migration, in carcinoma derived cells.	97
Figure 4.2.10 Schematic representation depicting role of vimentin in modulating K5/K14 expression to regulate differentiation, in carcinoma derived cells.	119
Figure 4.3.5 Schematic depiction of the possible role of vimentin in early events of transformation.	128
Figure 5.1 Schematic representation of the role of vimentin in oral precancer and cancer.	144

## List of Figures

Figure 4.1.1 Generation of vimentin knockdown clones in oral SCC derived cell line.	74
Figure 4.1.2 Vimentin knockdown cells show elongated morphology	75
Figure 4.1.3 Vimentin knockdown cells show upregulation of $\beta$ 4 integrin protein levels	77
Figure 4.1.4 Vimentin negatively regulates $\beta$ 4 integrin protein levels in SCC derived cells	79
Figure 4.1.5 Vimentin knockdown cells show upregulation of plectin protein levels	80
Figure 4.1.6 Vimentin knockdown cells showed increased localization of $\beta$ 4 integrin at the cell membrane to substratum front.	81
Figure 4.1.7 $\beta$ 4 integrin/plectin colocalize strongly at the membrane upon vimentin knockdown.	83
Figure 4.1.8 Vimentin downregulation results in increased $\beta$ 4 integrin-plectin interaction.	84
Figure 4.1.9 Functional consequences of upregulation of $\beta$ 4 integrin in vimentin depleted cells	86
Figure 4.1.10 Phenotypic effects of vimentin downregulation on fibronectin coated surface	87
Figure 4.1.11 Vimentin knockdown cells show increased adhesion associated signaling.	89
Figure 4.1.12 Vimentin regulates the turnover of $\beta$ 4 integrin and plectin	90
Figure 4.1.13 Downregulation of $\beta$ 4 integrin in vimentin knockdown background	92
Figure 4.1.14 Effect of $\beta$ 4 integrin knockdown on its mechanical and signaling function	93
Figure 4.1.15 High vimentin and low $\beta$ 4 integrin staining intensity together correlates with poor survival in oral SCC patients.	95
4.2.1 Downregulation of vimentin resulted in change in the global keratin profile of the oral SCC derived cell line AW13516.	99
Figure 4.2.2 Vimentin knockdown cells show downregulation of both K5 and K14 at mRNA as well as protein level	103
Figure 4.2.3 Phenotypic alterations associated with K5/K14 downregulation as a consequence of vimentin depletion.	105
Figure 4.2.4 Tumorigenic potential of the vimentin knockdown clones	106
Figure 4.2.5 Vimentin mediated positive regulation of K5/K14 levels is not a cell line specific phenomenon	108
Figure 4.2.6 Vimentin knockdown phenotype was rescued upon re-expression of K5/K14 together, in vimentin knockdown background.	110
Figure 4.2.7 $\Delta$ Np63 $\alpha$ may not be the sole regulator of K5/K14 expression in vimentin mediated regulation of differentiation.	113

Figure 4.2.8 Notch1 (independently or through NF-kb) may regulate the expression of $\Delta$ Np63	115
4.2.9 High expression of vimentin-K14 together correlates with recurrence and poor survival of oral cancer patients	117
Figure 4.3.1 Characterization of DOK for vimentinexpression and <i>invitro</i> transformation potential.	121
Figure 4.3.2 Vimentin overexpression did not lead to any transformation related phenotypic alterations	123
Figure 4.3.3 Vimentin overexpressing cells showed increased <i>invitro</i> transformation potential in response to benzo[a]pyrene treatment	125
Figure 4.3.4 Vimentin overexpressing cells treated with benzo[a]pyrene showed transformation related molecular signatures.	127

## List of Tables

Table 2.1 Classification of IFs based on their cell, tissue, differentiation and developmental specific expression patterns	30
Table 2.2 Diseases associated with IFs	35
Table 3.1 List of cell lines with their particulars	47
Table 3.2 List of reagents with their particulars	47
Table 3.3 List of antibodies with their particulars	49
Table 3.4 List of vimentin shRNA sequences along with their site	53
Table 3.5 Calcium phosphate transfection mix	55
Table 3.6 Conditions for IEF	59
Table 3.7 RT-PCR primer sequences	62
Table 3.8 QRT-PCR primer sequences	63
Table 4.1 Correlation of co-expression of vimentin with clinic-pathological parameters of the OSCC patients (n=74)	96
Table 4.2 List of proteins identified using MALDI analysis	101
Table 4.3 Correlations of co-expression of vimentin and $\beta$ 4 integrin with clinicopathological parameters of the OSCC patients	118

## Abbreviations

2D gel	Two-dimensional gel
BP	Benzo[a]pyrene
BSA	Bovine Serum Albumin
CHX	Cycloheximide
CQ	Chloroquine
DAPI	Diamidino-2-phenylindole dihydrochloride
DEPC	Diethylpyrocarbonate
ECL	Enhanced Chemiluminescence
ECM	Extracellular matrix
EDTA	Ethylene Diamine Tetra Acetic acid
EMT	Epithelial mesenchymal transition
Ex/Em	Extension/emission
FBS	Fetal Bovine Serum
fn	Fibronectin
H	Hour
HRPO	Horse Radish Peroxidase
IFs	Intermediate filaments
IHC	Immunohistochemistry
IP	Immunoprecipitation
K	Keratin
K5/14	Keratin 5 and Keratin 14
kDa	Kilo Dalton
LB	Luria Bertani
ln5	laminin-5
MALDI	Matrix-assisted laser desorption ionization
MET	Mesenchymal epithelial transition
MMP	Matrix metalloproteinase
NF- $\kappa$ B	Nuclear factor-kappaB
NICD	Notch intracellular domain
NP-40	Nonidet P-40
ns	Non-significant
OSCC	Oral squamous cell carcinoma
PBS	Phosphate Buffered Saline
PCNA	Proliferating cell nuclear antigen
PCR	Polymerase Chain Reaction
PVDF	Poly VinyleneDiFlouride
QRT-PCR	Quantitative real time polymerase chain reaction
RT-PCR	Reverse transcriptase polymerase chain reaction
RT	Room temperature

SCC	Squamous cell carcinoma
SDS	Sodium Dodecyl Sulphate
SEM	Standard error mean
TEMED	N, N, N', N',-Tetramethylethylenediamine
TGF- $\beta$ 1	Transforming growth factor beta1
uc	Uncoated



## Homi Bhabha National Institute

### Ph. D. PROGRAMME

**1. Name of the Student:** Ms. Crismita Clement Dmello

**2. Name of the Constituent Institution:** Tata Memorial Centre, Advanced Centre for  
Treatment Research and Education in Cancer

**3. Enrolment No.:** LIFE09201004021

**4. Title of the Thesis:** “Role of aberrant vimentin expression in human oral pre-cancer and cancer”

**5. Board of Studies:** Life Sciences

### SYNOPSIS

#### Introduction

Oral cancers are one of the leading cancers in India. In Indian males, it accounts for approximately 30% of the overall cancer burden. The major hurdle over the years in the oral cancer scenario, is diagnosing oral cancer at an early stage [1]. Some of the oral cancers arise from precursor lesions like leukoplakia (a predominantly white lesion), erythroplakia (a predominantly reddish lesion), lichen planus, and submucous fibrosis (SMF). The malignant transformation rates of leukoplakia range from less than 1% to 18%. In Indian studies, the rate of malignant transformation ranges from 0.13% to 2.2% per year [2]. The ability of current clinical/histological methods to predict which lesions further progress into malignancy is limited. Also, regional lymph node metastasis, local recurrence and second primary tumors result

in high morbidity and mortality especially when the disease is in an advanced stage at initial diagnosis [3].

Vimentin (a type III intermediate filament protein) expression has recently gained importance from the point of view of identifying the mesenchymal origin of a cell, as a prognostic marker to predict the biology of the tumor and to detect micro-metastasis [4]. Overexpression of vimentin is seen in various carcinomas like, prostate, gastrointestinal, breast, etc. [5]. Our laboratory along with others has shown correlation between aberrant vimentin expression and late events of tumorigenesis like, lymph node metastasis, recurrence and poor survival [6-8]. Vimentin is now being perceived not only as a canonical marker but also as a driver of epithelial–mesenchymal transition (EMT) [4]. During the process of EMT, the cell acquires a characteristic flattened morphology (mesenchymal like) due to loss of cell-cell and cell-substrate contacts. Parallely, there is a dramatic reprogramming of epithelial-specific keratins, to now initiate the expression of mesenchyme specific protein vimentin [9]. Whether vimentin is a cause or a consequence of the dedifferentiation state of the tumor cell is not well understood. It has been shown that vimentin might play a functional role in epithelial cell migration associated with stress or pathological situations [10, 11]. Conversely, in mesenchymal epithelial transition (MET) vimentin levels decrease leading to the inhibition of *in vitro* cell invasion [12]. Though, the contribution of vimentin in cancer cell migration and invasion is well established, the role of regulatory molecules/signaling pathways involved are not yet well defined.

Our group for the first time has reported an aberrant expression of vimentin in human oral precancerous lesions [13]. Also, our recent data showed a sequential increase in the expression of vimentin from early stages, in a 4-Nitroquinoline 1-oxide (4NQO) induced-model of rat lingual carcinogenesis [14]. The presence of vimentin in early events of oral

tumorigenesis is suggestive of its active or a passive contribution in bringing about this process.

**Rationale:**

We have shown the expression of vimentin in leukoplakia and SMF, which are known premalignant lesions of human oral cancer. Its presence in premalignant lesions suggests the possibility of its role in early oncogenesis. Also, role of vimentin in tumor progression and invasion has been reported but the molecular mechanisms underlying the same is not clear. Hence we overexpressed vimentin in a premalignant lesion derived cell line and downregulated it in OSCC derived cell line, to study the role of aberrant vimentin expression in human oral pre-cancer and cancer.

**Key question:**

Does vimentin contribute in the early and late events of human oral oncogenesis?

**Objectives:**

1. To study the phenotypic and molecular changes associated with vimentin in OSCC derived cell line.
2. To delineate the molecular pathways by which vimentin confers a particular phenotype to the cancer cell.
3. To study role of vimentin in early events of human oral cancer development.

## **Materials and methods:**

### **Ethics statement**

This study was approved by the “Human Ethics Committee”, Tata memorial centre, India (Reg Number: DCGI: ECR/149/Inst/MH/2013). All protocols for animal studies were approved by the “Institutional Animal Ethics Committee (IAEC)” (Approval ID: 19/2014).

### **Cell lines and their maintenance**

The cell lines AW13516 and AW8507 derived from SCC of tongue [15] and SCC29B from SCC of buccal mucosa [16] were cultured in IMDM with 10% fetal bovine serum (fbs) and antibiotics. A431 (derived from epidermoidcarcinoma) and HEK-293 cells were cultured in DMEM with 10% fbs and antibiotics. DOK cells, derived from human dysplastic oral mucosa (a kind gift from Dr. Daniela Elena Costea, Norway) were cultured as described previously [17].

### **Plasmids and retroviral constructs**

Effective shRNA sequences vim3A and vim3B were transfected using lipofectamine 2000 to generate vimentin knockdown clones in AW13516 cells. For vimentin overexpression, emerald GFP vimentin retroviral construct (a kind gift from Dr. Robert Goldman, Feinberg School of Medicine, Northwestern University, USA) was used. Vimentin- $\beta$ 4 integrin double knockdown and vector control clones were generated by transducing  $\beta$ 4 integrin shRNA and scrambled shRNA cloned in pCLXSN retroviral vector (a kind gift from Dr. Livio Trusolino, Italy) in vimentin knockdown clone shvim2. Emerald GFP-K14 construct was generated by amplifying K14 gene sequence from K14-pEGFP-N3 construct and subcloned in emerald GFP-pQCXIP vector. K5 pLNCX2 retroviral construct was a kind gift from Professor Thomas Magin, Germany. For the cloning of  $\Delta$ Np63 $\alpha$ , its cDNA was prepared from HaCat cell line and was cloned in pLNCX2 vector containing N-terminal flag tag sequence.

**Quantitative real-time PCR (qRT-PCR)/reverse transcriptase PCR (RT-PCR), western blotting, sub-cellular fractionation, immunoprecipitation (IP), scratch wound migration assay, soft agar assay and zymography**

QRT-PCR/RT-PCR was performed as described previously [18]. Cell lysates for western blotting were prepared in SDS lysis buffer. Isolation of cytoplasmic and nuclear fractions was done as per manufacturer's protocol (CelLyticNuCLEAR Extraction Kit (Sigma, product code NXTRACT)). For immunoprecipitation, cell lysates were made by pooling both NP-40 (1%) and Empigen (2%) fractions as described previously [19]. Scratch wound migration assay, soft agar assay [20] and gelatin zymography [21] were performed as described previously.

**Immunofluorescence and immuno-electron microscopy**

Immunofluorescence staining [22] and immuno-electron microscopy [23] were performed as described previously.

**Cell-ECM adhesion assay, transwell migration assay, invasion assay, induction of EMT and stimulation of  $\beta$ 4 integrin signaling**

Cell-laminin-5/cell-fibronectin adhesion and invasion assays were performed as described previously [24]. Transwell migration assays were performed in a manner similar to invasion assays, without coating the inserts [24]. The methodology followed for the induction of EMT and stimulation of  $\beta$ 4 integrin signaling is as described previously [24].

**Cell proliferation, clonogenic and tumorigenicity assays**

Cell proliferation, clonogenic and tumorigenicity assays were performed as described previously [18]

## **High salt Keratin extraction, two-dimensional (2D) gel electrophoresis and mass spectroscopy**

High salt Keratin extraction, 2D gel electrophoresis and mass spectroscopy were performed as previously described [25].

## **Development of *in vitro* carcinogenesis model using benzo[a]pyrene**

Cells (vimentin overexpressing and its vector control) were treated with benzo[a]pyrene once in a week for 1 h till atleast one of the groups showed formation of colonies in the soft agar assay, marking the attainment of a transformed state [26].

## **Immunohistochemistry (IHC) and statistical analysis**

Tissue samples were collected from the operation theatre of Tata Memorial Hospital, India. IHC was carried out as described previously [14]. Statistical analysis was carried out as described previously [20]. A *p* value of less than 0.05 was considered statistically significant.

## **Results**

### **Objective 1 and 2:**

#### **Part 1**

### **Vimentin mediates regulation of cell motility through modulation of $\beta 4$ integrin protein levels in oral tumor derived cells**

#### *a) Vimentin regulates $\beta 4$ integrin levels*

As a first step, we generated a vimentin knockdown system and found a reduction in *in vitro* migration and invasion in vimentin deficient state. Interestingly, we found substantial difference in the cell spreading between vimentin knockdown and vector control clones. Next, to determine the cause of difference in cell morphology;  $\alpha 6\beta 4$  integrin levels (which govern cell spreading) were examined.  $\beta 4$  integrin levels were found to be upregulated at protein level while its transcript levels stayed unaffected with vimentin downregulation. Both protein and RNA levels of  $\alpha 6$  integrin remained unaltered. Also, other SCC derived cell lines

AW13516, AW8507, SCC29B and A431 displayed inverse relation between the status of vimentin and  $\beta 4$  integrin protein levels. As a proof of principle, exogenous expression of vimentin in A431 demonstrated decrease in  $\beta 4$  integrin levels compared to the vector control clone A431vc.

*b) Vimentin knockdown results in increased localization of hemidesmosomal proteins ( $\beta 4$  integrin and plectin) at membrane-substrate front*

Plectin is known to link  $\beta 4$  integrin to the intermediate filament cytoskeleton [27]. Co-immunoprecipitation with vimentin was able to pull down both plectin and  $\beta 4$  integrin. Further, in vimentin knockdown clones, plectin protein levels were seen to be increased without any change at its transcript levels. Our immuno-electron microscopy data showed extensive localization of  $\beta 4$  integrin at the membrane-substrate front in vimentin knockdown as compared to vector control cells. Also, at the wound front,  $\beta 4$  integrin and plectin showed higher co-localization in vimentin knockdown as compared to vector control cells.

*c) Functional consequence of  $\beta 4$  integrin upregulation in vimentin knockdown cells*

As assessed using cell-ECM adhesion assay, the attachment of vimentin knockdown clone to laminin-5 increased significantly with time as compared to vector control clone. Consistent with our results of adhesion assay, vimentin knockdown cells showed more spread morphology on laminin-5 while migration on laminin-5 was significantly reduced as compared to vector control cells. Treatment with adhesion blocking antibody of  $\beta 4$  integrin (ASC-8), which abrogates laminin-5- $\beta 4$  integrin interaction [28], demonstrated higher *in vitro* invasive potential in vimentin knockdown as compared to vector control clones. Further,  $\beta 4$  integrin downregulation rescued the vimentin knockdown phenotype.

*d) Vimentin knockdown results in decreased protein turnover of  $\beta 4$  integrin and plectin*

Upon cycloheximide (inhibitor of protein biosynthesis) treatment,  $\beta 4$  integrin levels remained almost unaffected in vimentin knockdown while 40% reduction was observed in the vector

control cells. Treatment with lysosomal inhibitor chloroquine (CQ) resulted in decrease in  $\beta$ 4 integrin protein levels in vimentin knockdown while the vector control clone showed an increase of 2.7 fold. Further, plectin followed similar stability trend in vimentin knockdown and vector control clones as observed for  $\beta$ 4 integrin.

*e) High vimentin-low  $\beta$ 4 integrin expression is together associated with poor survival*

Immunohistochemistry analysis showed an inverse relationship between  $\beta$ 4 integrin and vimentin expression (Spearman's nonparametric correlation = -0.200,  $p=0.044$ ,  $n=74$ ) in oral tumor tissues, which corroborated with our *in vitro* findings. Significant correlation was observed between high vimentin-low $\beta$ 4 integrin staining intensity and stage ( $p=0.05$ ), tumor size ( $p=0.037$ ), node status ( $p=0.021$ ) and poor survival ( $p=0.008$ ).

## **Part 2**

### **Vimentin regulates differentiation switch via modulation of Keratin 14 levels and their expression together correlates with poor prognosis in oral cancer patients**

*a) Downregulation of vimentin results in alteration in the keratin profile of the OSCC derived cell line AW13516*

The global keratin profile revealed the identity of the differentially expressed proteins across the clones, one among which was found to be K14. Further, binding partner of K14, which is K5, was also seen to be downregulated at both protein and mRNA level in vimentin knockdown clones. Previous report from our laboratory has shown direct evidence wherein K5/K14 pair is able to regulate cell proliferation, differentiation and neoplastic progression in the same system AW13516 [18]. Surprisingly, we did not see any obvious differences in the proliferation potential of the vimentin knockdown as compared to the vector control cells using MTT assay. However, vimentin downregulation led to increased expression of differentiation specific markers, K1, involucrin, filaggrin and loricrin respectively while expression of multipotent stem cell marker Oct-4 decreased significantly. Re-expression of

K5/K14 pair in vimentin knockdown background showed reversal of vimentin knockdown phenotype. Next, we wanted to investigate the molecular regulator, through which vimentin modulates the expression of K5/K14.  $\Delta$ Np63 is known to directly regulate the expression of K5/K14 pair during the program of keratinocyte stratification [29, 30]. Therefore, flag tagged  $\Delta$ Np63 $\alpha$  (since  $\Delta$ Np63 $\alpha$  is a major isoform expressed in keratinocytes [31]) was stably re-expressed in vimentin knockdown clone. The differentiation status (defined by the expression of differentiation specific markers) remained unchanged while the expression of Oct-4 showed only a marginal increase (not significant) upon  $\Delta$ Np63 $\alpha$  upregulation in vimentin knockdown background.

*b) Activation of Notch1 may be a cause or a consequence of  $\Delta$ Np63 downregulation in vimentin knockdown background*

$\Delta$ Np63 and notch regulate each other by a negative feedback loop [31]. Vimentin knockdown clone showed an increase in activated Notch1 (NICD) levels as compared to vector control clone. Correspondingly, its levels showed a significant decrease upon  $\Delta$ Np63 $\alpha$  overexpression. The other candidate molecule which may modulate the level of  $\Delta$ Np63 is nuclear factor-kappaB (NF- $\kappa$ B), since it negatively regulates  $\Delta$ Np63 either through notch or independently as a part of the differentiation program [32]. Increased nuclear localization of NF- $\kappa$ B (p65) was observed upon vimentin downregulation, while the inverse was seen in  $\Delta$ Np63 $\alpha$  overexpressing clone

*c) High expression of vimentin-K14 together correlates with recurrence and poor survival of oral cancer patients*

IHC analysis of OSCC tissues showed positive correlation of high vimentin-K14 staining intensity with recurrence ( $p=0.001$ ) and poor disease free survival ( $p=0.005$ ).

### **Objective 3**

#### **Evaluation of transformation potential of vimentin in the development of human oral cancer**

##### *a) Overexpression of vimentin in DOK cell line*

The emerald vimentin retroviral construct was used to transduce DOK cell line. Phenotypically the vimentin overexpressing clones were more migratory and proliferating as compared to the vector control clones. Vimentin overexpression did not change the *in vitro* transformation potential of the cells as assessed using soft agar colony formation assay. Vimentin overexpressing clones showed an increase in the expression of the EMT regulator twist while, a significant decrease was seen in the expression of epithelial specific marker, E-cadherin. Also the expression of stemness related marker nanog was found to be upregulated in vimentin overexpressing clones.

##### *b) Development of in vitro carcinogenesis model using benzo[a]pyrene*

Benzo[a]pyrene was used as a procarcinogen to develop an *in vitro* carcinogenesis model in vimentin overexpressing and its vector control cells, after checking for its metabolic competence. Benzo[a]pyrene treatment was carried on till transformation was reached, as assessed using soft agar colony formation assay. 35<sup>th</sup> week marked the appearance of visible colonies on soft agar plate. The number of colonies was significantly higher in vimentin overexpressing clone as compared to the vector control clone at the 35<sup>th</sup> week of benzo[a]pyrene treatment. Molecular changes associated with transformation like downregulation of p21, E-cadherin, involucrin, etc and upregulation of stemness related markers (Nanog, Sox2, Oct-4), were more prominent in benzo[a]pyrene treated vimentin overexpressing clones as compared to its vector control clones.

## **Summary and Conclusion:**

Vimentin knockdown resulted in increased  $\beta 4$  integrin surface levels leading to strong adhesive contacts. This manifested into decreased motility. Interestingly, along with  $\beta 4$  integrin, its linker protein plectin was also upregulated with vimentin downregulation probably due to decreased targeting of these molecules to proteasomal and lysosomal machinery. A similar inverse correlation was observed between vimentin and  $\beta 4$  integrin in human oral cancer tissue samples. This study provides insights into the role of vimentin in mediating tumor cell migration by modulation of  $\beta 4$  integrin levels. Furthermore, vimentin and  $\beta 4$  integrin together may be used to predict the biology of oral cancer progression.

In addition, studies to understand whether vimentin is contributing and not merely associated with the transition from a more differentiated epithelial phenotype to a dedifferentiated state, showed reduction in the expression of K5/K14 pair upon vimentin downregulation. Our study deciphers the role of vimentin in modulating the expression of K5/K14 pair partly through  $\Delta Np63$ , to regulate differentiation state of a transformed cell. Furthermore, vimentin-K14 expression may be clinically relevant in order to prognosticate the fate of the OSCC

Finally, experiments to understand whether expression of vimentin is one of the causes or a consequence of the development of human oral cancer showed that, vimentin overexpression by itself is not enough to bring about transformation. Nevertheless, its forced expression in the initial stage proves to be advantageous to the cell in order to push itself towards transformation in presence of a carcinogenic stimulus.

Collectively, vimentin has emerged as one of the drivers of key events, beneficial for tumor progression. Further studies are required to understand the role of vimentin in initial stages of human oral oncogenesis.

## **References**

1. Coelho KR. Challenges of the oral cancer burden in India. *Journal of cancer epidemiology*. 2012;2012:701932. doi: 10.1155/2012/701932. PubMed PMID: 23093961; PubMed Central PMCID: PMC3471448.
2. Nair DR, Pruthy R, Pawar U, Chaturvedi P. Oral cancer: Premalignant conditions and screening--an update. *Journal of cancer research and therapeutics*. 2012;8 Suppl 1:S57-66. doi: 10.4103/0973-1482.92217. PubMed PMID: 22322734.
3. da Silva SD, Ferlito A, Takes RP, Brakenhoff RH, Valentin MD, Woolgar JA, et al. Advances and applications of oral cancer basic research. *Oral oncology*. 2011;47(9):783-91. doi: 10.1016/j.oraloncology.2011.07.004. PubMed PMID: 21802978.
4. Kidd ME, Shumaker DK, Ridge KM. The role of vimentin intermediate filaments in the progression of lung cancer. *American journal of respiratory cell and molecular biology*. 2014;50(1):1-6. doi: 10.1165/rcmb.2013-0314TR. PubMed PMID: 23980547; PubMed Central PMCID: PMC3930939.
5. Satelli A, Li S. Vimentin in cancer and its potential as a molecular target for cancer therapy. *Cellular and molecular life sciences : CMLS*. 2011;68(18):3033-46. doi: 10.1007/s00018-011-0735-1. PubMed PMID: 21637948; PubMed Central PMCID: PMC3162105.
6. Sawant S, Vaidya M, Chaukar D, Alam H, Dmello C, Gangadaran P, et al. Clinical significance of aberrant vimentin expression in oral premalignant lesions and carcinomas. *Oral diseases*. 2014;20(5):453-65. doi: 10.1111/odi.12151. PubMed PMID: 23865921.
7. Liu LK, Jiang XY, Zhou XX, Wang DM, Song XL, Jiang HB. Upregulation of vimentin and aberrant expression of E-cadherin/beta-catenin complex in oral squamous cell carcinomas: correlation with the clinicopathological features and patient outcome. *Modern pathology : an official journal of the United States and Canadian Academy of Pathology, Inc*. 2010;23(2):213-24. doi: 10.1038/modpathol.2009.160. PubMed PMID: 19915524.
8. Otsuki S, Inokuchi M, Enjoji M, Ishikawa T, Takagi Y, Kato K, et al. Vimentin expression is associated with decreased survival in gastric cancer. *Oncology reports*. 2011;25(5):1235-42. doi: 10.3892/or.2011.1185. PubMed PMID: 21327330.
9. Mendez MG, Kojima S, Goldman RD. Vimentin induces changes in cell shape, motility, and adhesion during the epithelial to mesenchymal transition. *FASEB journal : official publication of the Federation of American Societies for Experimental Biology*. 2010;24(6):1838-51. doi: 10.1096/fj.09-151639. PubMed PMID: 20097873; PubMed Central PMCID: PMC2874471.
10. Gilles C, Polette M, Zahm JM, Tournier JM, Volders L, Foidart JM, et al. Vimentin contributes to human mammary epithelial cell migration. *Journal of cell science*. 1999;112 ( Pt 24):4615-25. PubMed PMID: 10574710.
11. Vuoriluoto K, Haugen H, Kiviluoto S, Mpindi JP, Nevo J, Gjerdrum C, et al. Vimentin regulates EMT induction by Slug and oncogenic H-Ras and migration by governing Axl expression in breast cancer. *Oncogene*. 2011;30(12):1436-48. doi: 10.1038/onc.2010.509. PubMed PMID: 21057535.
12. Dong P, Kaneuchi M, Watari H, Hamada J, Sudo S, Ju J, et al. MicroRNA-194 inhibits epithelial to mesenchymal transition of endometrial cancer cells by targeting oncogene BMI-1. *Molecular cancer*. 2011;10:99. doi: 10.1186/1476-4598-10-99. PubMed PMID: 21851624; PubMed Central PMCID: PMC3173388.
13. Sawant SS, Vaidya M, Chaukar DA, Alam H, Dmello C, Gangadaran P, et al. Clinical significance of aberrant vimentin expression in oral premalignant lesions and carcinomas. *Oral diseases*. 2014;20(5):453-65. doi: 10.1111/odi.12151. PubMed PMID: 23865921.

14. Bihari Lal Soni AM, Harsh Pawar, Sharada S. Sawant, Anita Borges,, Ranganathan Kannan AP, Arvind D. Ingle, Hindahally Chandregowda Harsha,, Vaidya MM. Quantitative proteomic analysis of different stages of rat lingual carcinogenesis. *Clinical Communications-Oncology*. 2014;1(1). doi: 10.4103/WKMP-0062.132172.
15. Tatake RJ, Rajaram N, Damle RN, Balsara B, Bhisey AN, Gangal SG. Establishment and characterization of four new squamous cell carcinoma cell lines derived from oral tumors. *Journal of cancer research and clinical oncology*. 1990;116(2):179-86. PubMed PMID: 1691185.
16. Telmer CA, An J, Malehorn DE, Zeng X, Gollin SM, Ishwad CS, et al. Detection and assignment of TP53 mutations in tumor DNA using peptide mass signature genotyping. *Human mutation*. 2003;22(2):158-65. doi: 10.1002/humu.10248. PubMed PMID: 12872257.
17. Chang SE, Foster S, Betts D, Marnock WE. DOK, a cell line established from human dysplastic oral mucosa, shows a partially transformed non-malignant phenotype. *International journal of cancer Journal international du cancer*. 1992;52(6):896-902. PubMed PMID: 1459732.
18. Alam H, Sehgal L, Kundu ST, Dalal SN, Vaidya MM. Novel function of keratins 5 and 14 in proliferation and differentiation of stratified epithelial cells. *Molecular biology of the cell*. 2011;22(21):4068-78. doi: 10.1091/mbc.E10-08-0703. PubMed PMID: 21900500; PubMed Central PMCID: PMC3204069.
19. Srikanth B, Vaidya MM, Kalraiya RD. O-GlcNAcylation determines the solubility, filament organization, and stability of keratins 8 and 18. *The Journal of biological chemistry*. 2010;285(44):34062-71. doi: 10.1074/jbc.M109.098996. PubMed PMID: 20729549; PubMed Central PMCID: PMC2962505.
20. Iyer SV, Dange PP, Alam H, Sawant SS, Ingle AD, Borges AM, et al. Understanding the role of keratins 8 and 18 in neoplastic potential of breast cancer derived cell lines. *PloS one*. 2013;8(1):e53532. doi: 10.1371/journal.pone.0053532. PubMed PMID: 23341946; PubMed Central PMCID: PMC3546083.
21. Dange MC, Agarwal AK, Kalraiya RD. Extracellular galectin-3 induces MMP9 expression by activating p38 MAPK pathway via lysosome-associated membrane protein-1 (LAMP1). *Molecular and cellular biochemistry*. 2015;404(1-2):79-86. doi: 10.1007/s11010-015-2367-5. PubMed PMID: 25739356.
22. Raul U, Sawant S, Dange P, Kalraiya R, Ingle A, Vaidya M. Implications of cytokeratin 8/18 filament formation in stratified epithelial cells: induction of transformed phenotype. *International journal of cancer Journal international du cancer*. 2004;111(5):662-8. doi: 10.1002/ijc.20349. PubMed PMID: 15252834.
23. Yamashita S, Okada Y. Heat-induced Antigen Retrieval in Conventionally Processed Epon-embedded Specimens: Procedures and Mechanisms. *The journal of histochemistry and cytochemistry : official journal of the Histochemistry Society*. 2014;62(8):584-97. doi: 10.1369/0022155414537899. PubMed PMID: 24850662.
24. Dmello C, Sawant S, Alam H, Gangadaran P, Tiwari R, Dongre H, et al. Vimentin mediated regulation of cell motility through modulation of beta4 integrin protein levels in oral tumor derived cells. *The international journal of biochemistry & cell biology*. 2015. doi: 10.1016/j.biocel.2015.11.015. PubMed PMID: 26646105.
25. Alam H, Kundu ST, Dalal SN, Vaidya MM. Loss of keratins 8 and 18 leads to alterations in alpha6beta4-integrin-mediated signalling and decreased neoplastic progression in an oral-tumour-derived cell line. *Journal of cell science*. 2011;124(Pt 12):2096-106. doi: 10.1242/jcs.073585. PubMed PMID: 21610092.
26. Damiani LA, Yingling CM, Leng S, Romo PE, Nakamura J, Belinsky SA. Carcinogen-induced gene promoter hypermethylation is mediated by DNMT1 and causal for

- transformation of immortalized bronchial epithelial cells. *Cancer research*. 2008;68(21):9005-14. doi: 10.1158/0008-5472.CAN-08-1276. PubMed PMID: 18974146.
27. Rezniczek GA, de Pereda JM, Reipert S, Wiche G. Linking integrin alpha6beta4-based cell adhesion to the intermediate filament cytoskeleton: direct interaction between the beta4 subunit and plectin at multiple molecular sites. *The Journal of cell biology*. 1998;141(1):209-25. PubMed PMID: 9531560; PubMed Central PMCID: PMC2132717.
28. Egles C, Huet HA, Dogan F, Cho S, Dong S, Smith A, et al. Integrin-blocking antibodies delay keratinocyte re-epithelialization in a human three-dimensional wound healing model. *PloS one*. 2010;5(5):e10528. doi: 10.1371/journal.pone.0010528. PubMed PMID: 20502640; PubMed Central PMCID: PMC2873945.
29. Romano RA, Birkaya B, Sinha S. A functional enhancer of keratin14 is a direct transcriptional target of deltaNp63. *The Journal of investigative dermatology*. 2007;127(5):1175-86. doi: 10.1038/sj.jid.5700652. PubMed PMID: 17159913.
30. Romano RA, Ortt K, Birkaya B, Smalley K, Sinha S. An active role of the DeltaN isoform of p63 in regulating basal keratin genes K5 and K14 and directing epidermal cell fate. *PloS one*. 2009;4(5):e5623. doi: 10.1371/journal.pone.0005623. PubMed PMID: 19461998; PubMed Central PMCID: PMC2680039.
31. Nguyen BC, Lefort K, Mandinova A, Antonini D, Devgan V, Della Gatta G, et al. Cross-regulation between Notch and p63 in keratinocyte commitment to differentiation. *Genes & development*. 2006;20(8):1028-42. doi: 10.1101/gad.1406006. PubMed PMID: 16618808; PubMed Central PMCID: PMC1472299.
32. Dotto GP. Crosstalk of Notch with p53 and p63 in cancer growth control. *Nature reviews Cancer*. 2009;9(8):587-95. doi: 10.1038/nrc2675. PubMed PMID: 19609265.

## Publications

1. **Crismita Dmello**, SharadaSawant, HunainAlam, PrakashGangadaran, RichaTiwari, Harsh Dongre, NehaRana, SaiBarve, Daniela Elena Costea, DavendraChaukar, Shubhada Kane, Harish Pant, Milind Vaidya, Vimentin mediated regulation of cell motility through modulation of beta4 integrin protein levels in oral tumor derived cells, *The international journal of biochemistry & cell biology*, 70 (2015) 161-172.
2. SharadaSawant, Milind Vaidya, DevendraChaukar, HunainAlam, **Crismita Dmello**, PrakashGangadaran, SadhanaKannan, Shubhada Kane, PreranaDange, NigamanandaDey, K Ranganathan, Anil D'Cruz, Clinical significance of aberrant vimentin expression in oral premalignant lesions and carcinomas, *Oral diseases*, 20 (2014) 453-65.
3. Surya Singh, HunainAlam, **Crismita Dmello**, Milind Vaidya, Murali Krishna Chilakapati, Raman spectroscopic study of keratin 8 knockdown oral squamous cell carcinoma derived cells, *Proc. of SPIE*, 8225 (2012) 82251C-1

## Communicated Manuscript

**Crismita Dmello**, SharadaSawant, HunainAlam, PrakashGangadaran, SaieMogre, RichaTiwari, Manish Narkar, Rahul Thorat, KomalPatil, DavendraChaukar, Shubhada Kane, Milind Vaidya, Vimentin regulates differentiation switch via modulation of Keratin 14 levels and their expression together correlates with poor prognosis in oral cancer patients (*European journal of cell biology*, under Review).

## Manuscript in preparation

**Crismita Dmello**, SharadaSawant, Milind Vaidya, Evaluation of transformation potential of vimentin in the development of human oral cancer

## Conferences and workshops attended

1. Oral presentation
  1. Received award for oral presentation at the fifth international conference of the Carcinogenesis Foundation (USA) on “Molecular pathways to therapeutics: new paradigms and challenges in oncology”, organized in India in collaboration with ACTREC-TMC from 11th to 13th February, 2015 at Advanced Centre for Treatment Research and Education in Cancer (ACTREC), Navi Mumbai, India.
  2. Received award for oral presentation at the 11<sup>th</sup> National Research Scholars Meet in Life Sciences (NRSML), 2015 held from 17th to 18th December 2015 at Advanced Centre for Treatment, Research and Education in Cancer, Kharghar, Navi Mumbai.
2. Poster presentations
  1. Presented a poster entitled “Development of an *in vitro* carcinogenesis model to test the transformation potential of vimentin” at the TMC Platinum Jubilee ‘A conference of new ideas in cancer: challenging dogmas’ held from 26<sup>th</sup> to 28<sup>th</sup> February, 2016 at National Centre for the Performing Arts, Nariman Point, Mumbai
  2. Presented a poster entitled “Vimentin mediated regulation of differentiation switch via keratin 14 modulation in oral squamous cell carcinoma derived cell line” at the Intermediate Filaments Gordon Research Seminar (GRS) and at Intermediate Filaments Gordon Research conference (GRC), on Intermediate Filaments at the Crossroads Between Health and Disease held from June 14-20, 2014 at Mount Snow, West Dover, VT, USA.
  3. Presented a poster entitled “Vimentin mediates epithelial cell motility by destabilizing  $\alpha 6\beta 4$  integrin associated adhesion complex” at the 37<sup>th</sup> All India Cell Biology Conference on Cell Dynamics and Cell Fate held from December 22<sup>nd</sup> 2013 to December 24<sup>th</sup> 2013 at J N Tata Auditorium, Indian Institute of Science, Bangalore.
  4. Participated and presented a poster entitled “Down-regulation of vimentin using RNA interference leads to decreased *in vitro* tumorigenic potential and motility” at monsoon retreat 2012 held at ACTREC, Navi Mumbai
3. Other Participations
  1. Participated in the “Science Communication Workshop” organized by “The Wellcome Trust/DBT India Alliance” held on 21-22 march, 2016 at Lemon Tree Premier, Hyderabad.
  2. Participated in the “10<sup>th</sup> Annual Surgical Oncology Conference 'Oncosurg 2014'” from 21<sup>st</sup> - 23<sup>rd</sup> November 2014, held at Tata Memorial Hospital, Mumbai.
  3. Part of organising committee of “9<sup>th</sup> national research scholars meet in life sciences” held at ACTREC, Kharghar, Navi Mumbai from 19<sup>th</sup>-20<sup>th</sup> December 2013

4. Participated in the workshop and mini-symposium on 'Cancer Informatics – Analysis and Informatics of Microarray Data' organized jointly by the National Centre for Cell Science & the Bioinformatics Centre, University of Pune, on 13 and 14 September, 2012.
5. Participated in the conference held by Indian association for cancer research (IACR) at ACTREC, Navi Mumbai in 2012
6. Participated in the 1ST Annual Global Cancer Genomics Consortium–Tata Memorial Centre (GCGC-TMC) Symposium on 10th-12th Nov 2011
7. Attended meeting on Gynaecology Cancers AOGIN (Asia Oceania research organization on Genital Infections and Neoplasia, India) on 5-6th November 2011

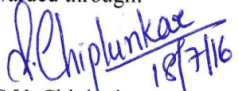
Signature of Student: 

Date: 7/7/16

**Doctoral Committee:**

S.No.	Name	Designation	Signature	Date
1.	Dr. S. N. Dalal	Chairperson		7/7/16
2.	Dr. M. M. Vaidya	Guide/Convener		7/7/16
3.	Dr. Amit Dutt	Member		7/7/16
4.	Dr. S. Waghmare	Member		7/7/16

Forwarded through:

  
 Dr. S.V. Chiplunkar  
 Director, ACTREC  
 Chairperson,  
 Academics and Training Program,  
 ACTREC

**Dr. S. V. Chiplunkar**  
 Director  
 Advanced Centre for Treatment, Research &  
 Education in Cancer (ACTREC)  
 Tata Memorial Centre  
 Kharghar, Navi Mumbai - 410 210.

  
 Prof. K. Sharma  
 Director, Academics,  
 Tata Memorial Centre

**PROF. K. S. SHARMA**  
 DIRECTOR (ACADEMICS)  
 TATA MEMORIAL CENTRE,  
 PAREL, MUMBAI

# Chapter 1: Introduction

## 1. Introduction

Oral cancers are one of the leading cancers in India. In Indian males, these account for approximately 30% of the overall cancer burden [1]. Majority of oral cancers in Indian scenario are preceded by precursor lesions like leukoplakia (a predominantly white lesion), erythroplakia (a predominantly reddish lesion), lichen planus and submucous fibrosis. The malignant transformation rates of leukoplakia range from less than 1% to 18%. In Indian studies, the rate of malignant transformation ranges from 0.13% to 2.2% per year [2]. Further, regional lymph node metastasis, local recurrence and second primary tumors result in high morbidity and mortality especially when the disease is in advanced stage at initial diagnosis [3]. Ability of current clinical/histological methods to predict which lesions would further progress into malignancy is limited. Hence development of biological markers which will prove as an adjunct to histodiagnosis has become essential.

Vimentin (a type III intermediate filament protein) expression has recently gained importance to identify mesenchymal origin of a cell, as a prognostic marker to predict the biology of the tumor and to detect micrometastasis [4, 5]. Previous report from our laboratory has shown the expression of vimentin in oral leukoplakia and submucous fibrosis, which are known premalignant lesions for human oral cancer [6]. Further, our group has documented sequential increase in the aberrant expression of vimentin from early stages, in 4NQO-model of rat lingual carcinogenesis [7]. The presence of vimentin in early events of oral tumorigenesis is suggestive of its active or a passive contribution in bringing about this process.

Overexpression of vimentin is seen in various carcinomas like, prostate, gastrointestinal, breast, lung and also melanomas [5]. Our laboratory along with others has shown correlation of aberrant vimentin expression with late events of tumorigenesis like, lymph node metastasis,

recurrence and poor survival [6]. Though, several reports have suggested the role of vimentin in tumor cell migration and invasion [8, 9], the molecular mechanism/s underlying these phenotypes is/are still under investigation. On these lines, Vuoriluoto et al. have shown vimentin mediated regulation of receptor tyrosine kinase Axl, to bring about cancer cell migration during epithelial mesenchymal transition (EMT) [10]. Conversely, in mesenchymal epithelial transition (MET) vimentin levels decrease leading to the inhibition of *in vitro* cell invasion [11].

Integrin pairs of  $\alpha6\beta4$  and  $\alpha6\beta1$  are also one of the major contributors of cell spreading and motility, in case of carcinomas [12]. Although, the primary function of  $\alpha6\beta4$  integrin in stratified epithelia is to form stable contacts with underlying basement membrane; in carcinomas, it is known to stimulate signaling molecules to enhance migration and invasion [13].  $\alpha6\beta4$  integrin is known to exclusively interact with intermediate filaments in stratified epithelia. Coherently, vimentin- $\alpha6\beta4$  integrin interaction is known to exist in endothelial cells [14]. Hence, it is worthwhile to investigate the role of  $\alpha6\beta4$  integrin in regulation of vimentin mediated tumor cell motility.

Vimentin is being perceived not only as a canonical marker but also as a driver of epithelial–mesenchymal transition (EMT) [4]. During the process of EMT, the cell acquires a characteristic flattened morphology (mesenchymal like) due to loss of cell-cell and cell-substrate contacts. Parallely, there is a dramatic reprogramming of epithelial-specific keratins, to initiate the expression of mesenchyme specific protein vimentin [15]. In this regard, expression of vimentin has been shown to significantly correlate with the poorly-differentiated and fibroblastic phenotype of the breast cancer derived cell lines [16]. However, the molecular mechanisms involved in vimentin mediated maintenance of undifferentiated state of tumor cell are not yet

clear. Therefore it will be interesting to understand, whether vimentin is a cause or a consequence of the dedifferentiated state of the tumor cell.

Thus, our preliminary results suggested role of vimentin in tumor progression and invasion. However, the molecular mechanisms underlying the same are not clear. Also, our interesting observations in oral premalignant lesions showed expression of vimentin in leukoplakia and submucous fibrosis (SMF), suggesting the possibility of its role in early oncogenesis. Based on these observations and literature the key question raised was:

### **1.1 Key question:**

Does vimentin contribute in the early and late events of human oral oncogenesis?

### **1.2 Objectives**

1.2.1 To study the phenotypic and molecular changes associated with vimentin in OSCC derived cell line.

1.2.2 To delineate the molecular pathways by which vimentin confers a particular phenotype to the cancer cell.

1.2.3 To study role of vimentin in early events of human oral cancer development.

# Chapter 2: Review of Literature

## **2. Review of literature**

### **2.1 Human oral cancer:**

#### **2.1.1 Epidemiology**

Squamous cell carcinoma is the most common cancer in the head and neck region of the body, among which oral squamous cell carcinoma predominates over the others [17]. Oral squamous cell carcinoma is a heterogeneous group of cancers arising from different parts of the oral cavity and is the sixth most common cancer reported globally [1]. The 5-year survival rate (40-50%) of oral cancer has not changed over several decades, in spite of continuous improvement in surgical techniques and adjuvant therapies [18]. 48% of these group of cancers are located in the oral cavity and 90% of these are oral squamous cell carcinomas (OSCC) [19]. It has an annual incidence of over 300,000 cases, of which 62% arise in developing countries. In comparison with the USA population, where oral cavity cancer represents only about 3% of malignancies, it accounts for over 30% of all cancers in India [1].

#### **2.1.2 Risk factors**

The common risk factors for oral cancer in Indian scenario are excessive alcohol consumption, use of tobacco like cigarettes, smokeless tobacco, betel nut chewing and human papilloma virus (HPV) [20]. Excessive tobacco usage increases the risk of cancer by 5-fold to 25-fold. Nicotine and polycyclic aromatic hydrocarbons present in tobacco are the main compounds responsible for the tobacco associated cancers. Smoking along with alcohol consumption increases the risk of cancer by 40 folds [21]. Mutations in TP53 gene are largely associated with alcohol and tobacco associated cancer. Viruses like HPV and Epstein-Barr virus (EBV) have been linked with the pathogenesis of head and neck squamous cell carcinoma (HNSCC) [22, 23]. HPV associated HNSCCs contribute to around 25% of all HNSCCs. HPV

uses its E6 and E7 oncoproteins to cause cancer [24]. According to molecular studies, E6 and E7 viral oncoproteins inactivate the TP53 and retinoblastoma tumor suppressor gene products in order to transform the cell [24].

The less common risk factors for oral cancer are poor dental care and poor diet. Among this, dietary factors like vitamin A deficiency and the iron deficiency associated with Plummer-Vinson syndrome are reported to be important risk factors for oral and pharyngeal cancers [25, 26]. Occupational hazards like exposure to chromium, nickel, radium, mustard gas, and byproducts of leather tanning and wood working are also linked to sinonasal cancers [27, 28].

### **2.1.3 Tumorigenesis**

Constant exposure to cancer causing agents results in alterations in key genes leading to tumorigenesis [26]. Described below are the details of oncogenes and tumor suppressor genes that are commonly altered in oral cancer.

Cyclin D1 is known to play a role in activation of cell cycle progression. Amplification (30% to 50%) and overexpression of Cyclin D1 is seen in HNSCC patients [29]. EGFR normally plays an important role in the induction of cell differentiation and proliferation upon activation. Overexpression of EGFR is seen in more than 95% of HNSCCs and is associated with decreased progression-free survival (PFS), decreased overall survival (OS) and increased resistance to radiation [26, 30]. TP53 is known to display several tumor suppressor functions. Mutations in TP53 gene (40% to 60%) are seen in head and neck cancer, and this mutation is associated with the progression from premalignancy to advanced stage and also with early recurrence [31, 32]. CDKN2A (formerly P16) is another tumor suppressor gene which regulates the cell cycle by causing the inhibition of cyclin-dependent kinase. Loss of chromosomal region 9p21 leading to

inactivation of the CDKN2A gene; occurs early in the progression of a majority of the HNSCC patients [33].

## **2.2 Human oral pre-cancer**

### **2.2.1 Types of Oral premalignant lesions (OPLs)**

In the Indian scenario, a majority of the oral cancers arise from precancerous lesions. Early detection of oral premalignant lesions (OPLs) is central to the improvement of prognosis of oral cancer. Some of the oral cancers arise from precursor lesions like leukoplakia (a predominantly white lesion), erythroplakia (a predominantly reddish lesion), submucous fibrosis (SMF) and lichen planus [34]. In Indian studies, the rate of malignant transformation ranges from 0.13% to 2.2% per year [2].

Following are the commonly seen precancerous lesions of oral mucosa,

#### **2.2.1.1 Leukoplakia**

Leukoplakia is usually defined as “a white patch or plaque that cannot be characterized, clinically or pathologically, as any other disease” [34]. The percentage of malignant transformation in case of leukoplakia is between 1-18% [18]. Clinically, leukoplakia can be divided into two subtypes, homogenous lesions, which are characterized by uniformly flat, thin, white, showing shallow cracks of the surface keratin and non-homogenous lesions which are red lesions that may be either irregularly flat or nodular. Verrucous leukoplakia, which falls in a non-homogenous leukoplakia type, is known to show increased transformation and therapy resistance [35].

#### **2.2.1.2 Erythroplakia**

Erythroplakia and/or erythroleukoplakia are a red patch of the oral mucosa which is correlated with significantly higher rates of dysplasia, carcinoma *in situ* and invasive carcinoma

as compared to leukoplakia [34, 35]. The soft palate, floor of the mouth and the buccal cavity are the most commonly affected regions in the case of erythroplakia. Histopathologically, oral lesions showing erythroplakia are mainly moderate or severe dysplasia grade. Congruently, its malignant transformation rates are also very high (vary from 14% to 50%) [35].

### **2.2.1.3 Oral Submucous Fibrosis (OSMF)**

Schwartz in 1952 defined OSMF as a “chronic and potentially malignant disorder characterized by juxta-epithelial fibrosis of the oral cavity” [35]. It is reported to show a malignant transformation rate of 7%-30%. OSMF is predominantly seen in Indians mainly due to the chewing of betel quid containing areca nut. OSMF occurs in the second and third decade of life, in both the sexes while in the pediatric age group it is comparatively rare [34, 35].

### **2.2.1.4 Lichen planus**

Lichen planus is a chronic inflammatory mucocutaneous disease [36] and it is reported to be a less frequently occurring premalignant disorder (0.62%) [35]. Lichen planus commonly occurs in the fifth decade of life and is more common in females as compared to males [36].

## **2.2.2 Diagnosis**

Oral squamous cell carcinomas (OSCCs) are usually preceded by the visible changes of the oral mucosa, e.g. oral premalignant lesions [37]. A thorough mucosal examination as a part of a routine dental examination helps to screen for oral cancer in a regular manner. This method is shown to be useful and is currently accepted practice for the detection of oral cancer and premalignancy [38]. The diagnosis of lesions appearing on oral mucosa may be enhanced by the use of adjunctive aids such as toluidine blue, diffused white light, chemiluminescence or loss of tissue autofluorescence [39]. Early diagnosis is crucial in the treatment of oral cancer since it significantly increases the survival rates of OSCC [40].

### **2.2.3 Treatment**

Till 1960 to 1980 the primary curative management of patients with head and neck was done by only surgery and radiation therapy (RT). In 1991, the concept of organ preservation emerged by combining chemotherapy and RT. The treatment modality is decided depending upon the stage of cancer, for example, Stage T1 or T2 without nodal involvement (N0) are treated either with surgery or with radiation depending on the subsite and the expertise of the clinical team. T2 tumors, or exophytic T3, N0-N1 tumors are shown to benefit from a combination of both surgery and radiation. Concurrent chemoradiation therapy is generally preferred for T3 or T4 primary tumors with N2 or N3 lymphadenopathy in the situations where the tumor is unresectable, or even if the tumor is resectable but organ preservation is desired [26]. Recent advancement in the treatment of HNSCC is the introduction of targeted therapy and concurrent radiotherapy. This treatment is useful for patients who are not candidates for therapy with platinum and radiation [41].

### **2.2.4 Challenges**

The major hurdles over the years in the oral cancer scenario have been in terms of their high risk of developing a second primary cancer, lymph node metastasis and failure in diagnosis and treatment of oral cancer at an early stage. Therefore, the early detection and prevention of oral cancer and premalignancy are quite important [1, 42]. The ability of current clinical/histological methods to predict which lesions will further progress into malignancy is limited. Hence the development of biological markers which will prove as an adjunct to histo-diagnosis has become essential.

### **2.3 Intermediate filaments (IFs)**

Aberrant expression of intermediate filament proteins like keratins and vimentin is widely reported since last two decades. Further, investigation of the diagnostic, prognostic and therapeutic potential of these molecules would be useful to screen and treat oral cancer patients. Intermediate filaments, along with microtubules and microfilaments, form the cytoskeletal organization of the cell. They have an average diameter of 7-11 nm and is mainly responsible for the structural appearance of the cytoplasm [43]. Along with this, they play an important role in cell division, motility and various other cellular processes [44, 45]. Around 70 IF genes code for the diverse group of IF proteins in the human genome (Human Intermediate Filament Mutation Database; <http://www.interfil.org>). On the basis of their cell, tissue, differentiation and developmental specific expression patterns, IFs are classified into six major groups (Table 2.1). Group I–IV constitute the IFs localized to the cell cytoplasm while group V forms the Ifs lamins localized to the nucleus. The last group is the “orphan” group, which involves cytoplasmic IFs expressed in the eye lens [46].

**Table 2.1: Classification of IFs based on their cell, tissue, differentiation and developmental specific expression patterns.** Adapted from [46]

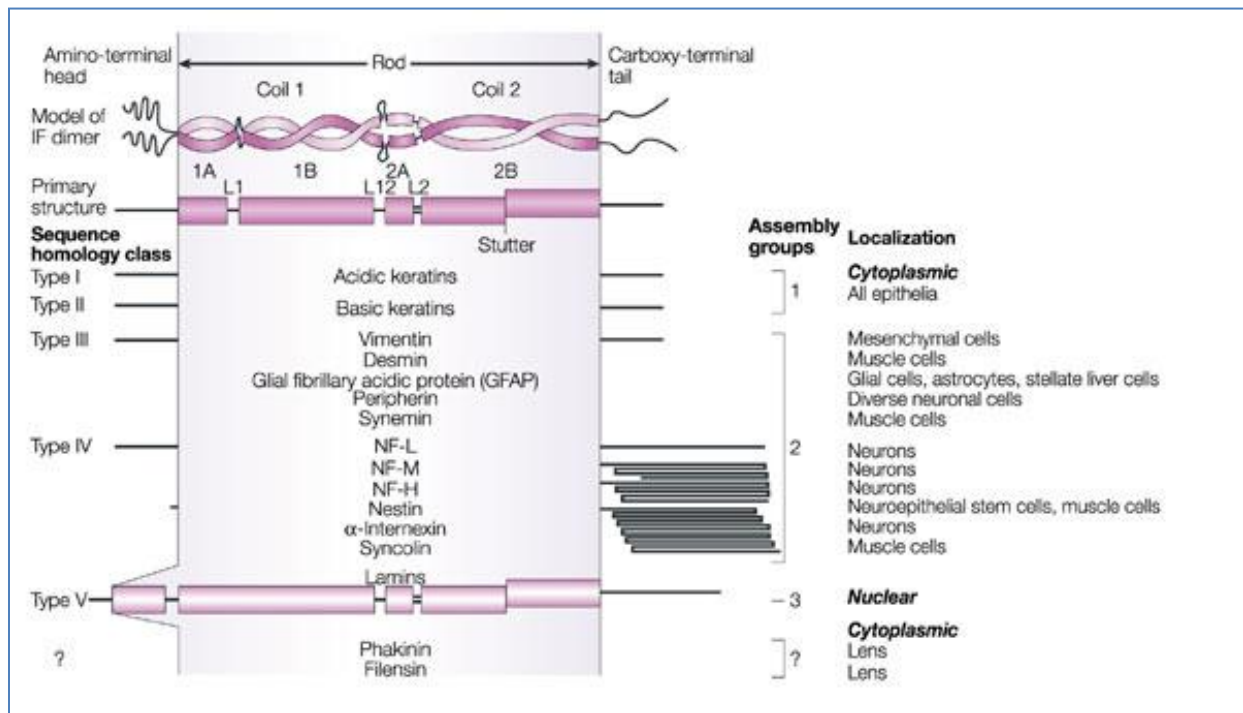
Type	Cell types	Localization	Proteins
<b>I</b>	Epithelia	Cytoplasm	Acid keratins (pI < 5.7) 17 human epithelial keratins; K9-K28
	Hair	Hair	11 human hair keratins; K31-40 (Ha 1-8)
<b>II</b>	Epithelia	Cytoplasm	Basic keratins (pI < 6.0) 20 human epithelial keratins; K1-8, K71- 80
	Hair	Hair	6 human hair keratins; K81 – 86 (Hb 1-6)
<b>III</b>	Muscle	Cytoplasm	Desmin
	Mesenchymal		Vimentin
	Neurons		Peripherin
	Astrocytes and glia		GFAP
<b>IV</b>	Neurons	Cytoplasm	NF-L
	Neurons		NF-M
	Neurons		NF-H
	Neurons		$\alpha$ -internexin
	Muscle		Synemin $\alpha$
	Muscle		Synemin $\beta$ (desmuslin)
	Muscle		Syncoilin
	Neuroepithelia		Nestin
<b>V</b>	Ubiquitous	Nuclear lamina	Lamin A/C
			B1
			B2
<b>Orphan</b>	Eye lens	Cytoplasm	Phakinin (CP49) Filensin (CP115)

### 2.3.1 Structure and assembly of IFs

IFs are made up of a non-helical N-terminal head (amino-end), a central  $\alpha$ -helical coiled-coil domain and a non-helical C-terminal tail (carboxy-end) [46]. As per the X-ray diffraction data analysis, the rods of two polypeptide chains intertwine to give rise to a coiled-coil structure. This data was further substantiated by sequence data and model building. The surface of the  $\alpha$ -helical domain is hydrophobic due to the presence of repeats of hydrophobic amino acids at the

first and fourth of every seven residues. This hydrophobicity facilitates the coiling between two IF polypeptides. [47]. The assembly of IF is initiated with the formation of parallel  $\alpha$ -helical coiled-coil dimers through four heptad repeat-containing regions designated 1A, 1B, 2A and 2B, separated by non-coiled linkers, L1, L12 and L2. Once the dimers are formed they arrange laterally into antiparallel manner to form unit length filaments (~60 nm long), which later anneal longitudinally to form immature filaments. Immature filaments undergo extensive compaction to finally form mature filaments [46].

**Figure 2.1: Schematic depiction of the structure and assembly groups of IFs.** Adapted from [48].



### 2.3.2 Functions of intermediate filaments

IFs form important cytoskeletal machinery which contributes to the regulation of cell architecture and functions. The wide array of functions performed by IFs can be attributed to the differences in their N-terminal head and C-terminal tail domains, to their stage and tissue specific expression and to their post-translational modifications [49].

### **2.3.2.1 Structural functions of IFs**

Traditionally IFs were thought to play a dedicated role of supporting cell strength and maintaining tissue structure in a static manner. Additionally, IFs were also shown to confer resistance against mechanical and non-mechanical stress and deformation. For example simple epithelial-specific keratins are known to modulate cell stiffness in hepatic cells while mesenchymal specific vimentin is also known to provide elastic properties and protection against compressive stress [50, 51].

### **2.3.2.2 Role of IFs in cellular processes**

IFs are reported to regulate multiple cellular functions. IFs, microtubules and microfilaments are in constant communication with each other through proteins known as cytolinkers, since modulation of one affects the other two networks. This consequently, affects one or the other cellular processes [52, 53]. For instance, direct communication between vimentin and actin is shown to regulate cell stiffness [54, 55]. Additionally, IFs are shown to play important role in cell signaling (eg modulation of ERKs (extracellular-signal-regulated kinases) by vimentin [56]), cell cycle (eg keratins are involved in the regulation of cell cycle [57]), apoptosis (eg both keratins [58] and lamins [59] have a role in apoptosis), cell migration and cancer (eg vimentin, keratins and nestin regulate migration and cancer progression [60-63]).

### **2.3.2.3 Role of nuclear IFs in controlling the nuclear organization**

Nuclear lamins are known to form nuclear lamina by interacting with the inner nuclear membrane as well as chromatin [64]. Studies have shown that nuclear lamina plays an important role during mitosis wherein breakdown and reformation of the nuclear envelope are the key events [65]. Experiments using an intracellular injection of anti-lamin antibodies showed defect in the decondensation of the chromosomes following mitosis [66]. This suggested that the

nuclear lamina may interact either directly or indirectly with the chromosome and the nuclear envelope. Interestingly, studies have also indicated the role of nuclear lamina in distribution of the nuclear pore complexes in the nuclear membrane [67].

#### **2.3.2.4 Role of IFs in vesicular trafficking**

Emerging reports have substantial evidence to show that IFs and vesicular transport are linked [49]. Studies have demonstrated the role of IFs in early stages of endocytosis, for example, in Sertoli cells, seminiferous tubule and testis, Rab4 is shown to interact with vimentin to play a role in sorting of early endosomes and endocytic recycling vesicles [49]. Along with vesicular trafficking, IFs have been shown to play a role in distribution and motility of late endocytic vesicles and compartments, for instance, in astrocytes, vimentin along with GFAP is shown to regulate endocytosis and motility of endosome and lysosome [49].

#### **2.3.3 Diseases associated with intermediate filaments**

The pioneering research that mutations in K5 and 14 led to epidermal fragility in mice and epidermolysis bullosa simplex (EBS) in humans compelled the researchers to investigate the human disorders associated with IFs [68]. Following this, many studies showed the connection between mutations in genes encoding IF proteins and causation or predisposition to a particular human disease. The list of IF family members along with its disease phenotypes is described in Table 2.2 [46]. The peculiar feature about IF is that, the simplest unit of an IF is a tetramer (as described in structure and assembly of IFs section) that consists of either homopolymers (as is seen for desmin, vimentin and some other IF proteins) or obligate heteropolymers (as is seen for keratins). Hence most of the mutations in IF proteins act in a dominant fashion as a result of its normal oligomeric state [69]. The severity of the IF-associated diseases is determined by the location of a mutation within the IF protein backbone [70]. The IF-associated diseases can be

caused due to several genetic alterations like deletions, gene duplications, missense and nonsense mutations etc [69]. However, a majority of them occur as missense mutations. Hotspot mutations are also seen for different IFs, but generally mutations involve many amino acids that are distributed over the entire body of IFs, for instance, Lamin A has about 30% amino acids which are involved in a disease [71]. Certain variants of IFs are also known which show 100% association with specific ethnic backgrounds; like, the K8 Gly434Ser variant is found exclusively in African population [72]. Overall, IFs are associated with more than 80 human tissue-specific diseases; hence it is important to study its functional role in the context of disease biology.

**Table 2.2: Diseases associated with IFs.** Adapted from [46]

<b>Type</b>	<b>Disease associations</b>
<b>I</b>	K14 – epidermolysis bullosa simplex diseases K10, K16, K14 – keratoderma disorders K12 – Meesmann corneal dystrophy K13 – white sponge nevus of cannon K16 – pachyonychia congenital type I K17 – pachyonychia congenital type II
<b>II</b>	K5 – epidermolysis bullosa simplex diseases K1, K9, K2 – keratoderma disorders K3 – Meesmann corneal dystrophy K4 – white sponge nevus of cannon K6a – pachyonychia congenital type I K6b – pachyonychia congenital type II K81 (Hb1), K83 (Hb3), K86 (Hb6) – monilerthrix K85 (Hb5) – pure hair type ectodermal dysplasia
<b>III</b>	Desmin – desmin related myopathy, dilated cardiomyopathy 1I, familial restrictive cardiomyopathy 2 Peripherin – amyotrophic lateral sclerosis GFAP – Alexander disease
<b>IV</b>	NF-L, M and H – amyotrophic lateral sclerosis NF-L – Charcot-Marie-Tooth diseases NF-M – Parkinson disease NF-H – neuronal IF inclusion disease
<b>V</b>	Lamins – large number of disorders including lipodystrophies, muscular dystrophies, neurological disorders and premature aging
<b>Orphan</b>	CP49 – autosomal dominant cataract disease CP115 – autosomal recessive cataract disease

### 2.3.4 Intermediate filament (IF) proteins and cancer

Intermediate filament proteins are expressed in a tissue-specific and differentiation stage specific manner which is why IF typing is used to distinguish and determine the histogenesis of the major tumor groups [73]. Keratins are typically found in keratinizing and nonkeratinizing epithelia; hence they are used to characterize carcinomas. Similarly, desmin filaments, which are usually expressed in sarcomeric, visceral and some type of vascular smooth muscle tissue, are

used to characterize sarcomas of muscle cells. Vimentin filaments classically expressed by endothelial cells, fibroblasts, macrophages, chondrocytes and most but not all lymphatic cells are used to characterize nonmuscle sarcomas. Neurofilaments, which are arranged as neurofilament triplet composed of three different polypeptides, to form the cytoskeletal organization of the central and peripheral neurons, are used to characterize a group of tumors originating from the sympathetic nervous system, e.g., ganglioneuroblastoma, pheochromocytoma, and at least some neuroblastomas. Glial fibrillary acidic protein (GFAP), which is expressed by the normal and reactive astrocytes and also some ependymal cells, is used to characterize gliomas [73, 74]. Increasing evidence suggests the potential of intermediate filaments as prognostic and diagnostic markers in human cancers. For instance, nestin, which is neuroepithelial stem cells specific IF, could be useful as a prognostic and diagnostic marker in case of astrocytomas and malignant melanomas, where its expression is suggestive of a dedifferentiation and advanced phenotype [75]. Aberrant expression of simple epithelial-specific Keratin 8/18 pair was shown to correlate with a poor clinical prognosis, suggesting their potential to be used as prognostic markers for human oral cancer [76]. Aberrant expression of mesenchymal specific protein vimentin was seen in early events of tobacco/areca nut associated oral tumorigenesis. Also in the late events, a significant correlation was seen between vimentin expression and invasive fronts/aggressive phenotype of oral tumours [6]. All this evidence clearly defines the diagnostic and prognostic potential of intermediate filament expression patterns in squamous cell carcinomas of the oral cavity.

### **2.3.5 Vimentin**

Vimentin is a 53 kDa, type III intermediate filament protein (IF), predominantly expressed in cells of mesenchymal origin and in many undifferentiated cells and cultured cells

[5]. Vimentin is encoded by a single-copy gene and is located on chromosome 10p13 [77]. The promoter of vimentin includes elements like TATA box, eight putative GC boxes, Activator protein 1 (AP-1) binding sites, the NF- $\kappa$ B-binding site, and a Smad binding element [5]. In the tumor cell, vimentin expression was shown to be transactivated by  $\beta$ -catenin/ TCF, binding to the putative site 468 bp upstream of the transcription initiation site of vimentin promoter to regulate the invasive potential of the tumor cell [78].

### **2.3.5.1 Structure**

Vimentin protein is comprised of 466 amino acids and its structure resembles any typical IFs with a highly conserved  $\alpha$ -helical “rod” domain that is flanked by non- $\alpha$ -helical N-terminal head domain (77-residues) and C-terminal tail domain (61-residues) [79]. Vimentin forms both homopolymers and heteropolymers (with other type III or IV IFs), through its coiled-coiled alpha-helical domain which helps in the formation of highly stable polymers [5]. The assembly of vimentin filaments is similar to the classical assembly of intermediate filaments.

### **2.3.5.2 Post translational modifications of vimentin**

The head and the tail domains of vimentin serve as a substrate for a number of enzymes which in turn regulates its assembly and functional properties.[5, 80]. For instance, disassembly of vimentin is regulated by its phosphorylation on sites S38 and S72 by protein kinase A (PKA) [81]. Similarly, structural reorganization of vimentin is regulated by p21-activated kinase (PAK) mediated phosphorylation [82]. Also during cytokinetic processes, vimentin filament segregation is regulated by its phosphorylation mediated by Aurora B Kinase [83]. The dynamics of IF, in the interphase of the cell cycle, is also regulated by protein phosphatase 2A (PP2A), which prevents the phosphorylation of vimentin [84]. Vimentin undergoes several other post translational modifications which confer diverse characteristic phenotypes to the cell, for

instance, citrullinated vimentin is seen in macrophages undergoing apoptosis [85]. Similarly, vimentin expressed in glial cells undergoes O-GlcNAcylation which prevents its hyperphosphorylation to finally enable neuronal migration [86], while sumoylation of vimentin is known to regulate the structure and motility of glioblastoma multiforme cells [87]. Moreover, identification of novel post translational modifications on vimentin will provide insights into novel functions executed by vimentin.

### **2.3.5.3 Functions of vimentin**

#### **2.3.5.3.1 Role of vimentin in normal development and differentiation**

The primary function of Vimentin IFs is to maintain cyto-architecture and tissue integrity [88]. Vimentin is partially or completely replaced with their cell type specific IF protein in cells which are committed to undergo terminal differentiation [89]. During mouse embryonic development, vimentin is expressed very early in motile cells like parietal endoderm cells [90]. Surprisingly, functional deletion of vimentin in mice did not result in an obvious phenotype. However, careful examination revealed a certain functional defect in mice lacking vimentin. For example, lymphocytes from vimentin knockout mice showed a decreased capacity for homing to lymph nodes and spleen [91]. Their fibroblasts were unable to bring about migration [92]. Cerebellar defect and an impaired motor coordination were also reported in vimentin null mice [93].

#### **2.3.5.3.2 Role of vimentin in precancerous lesions**

The emerging literature suggests that aberrant expression of vimentin may begin very early in the development of oral tumor. Van der Velden et al., in 1999 had demonstrated the aberrant expression of vimentin in the hyperkeratotic lesions of oral mucosa [94]. Sawant et al. have reported the aberrant expression of vimentin in oral premalignant lesions like leukoplakia

and submucous fibrosis. This expression was found to correlate with the degree of histopathological grade of oral precancerous lesions. Further, they also found a sequential increase in the expression of vimentin, in keratinocytes isolated from carcinoma as compared to dysplasia and hyperplasia [6]. Later to this, Soni et al., observed an increase in aberrant expression of vimentin from early stages (hyperplasia to papilloma), in 4NQO-model of rat lingual carcinogenesis by using quantitative proteomics [7]. These studies indicate that it will be worthwhile to investigate if vimentin is one of the causes or just a consequence of the process of neoplastic development.

### **2.3.5.3.3 Role of vimentin in cancer**

The role of vimentin is increasingly recognized in case of cancer progression. However, it may not play a significant function in the development of cancer as seen in the model of experimental teratocarcinomas. Here, vimentin null or wild-type embryonic stem cells did not alter teratocarcinoma formation or the normal development of experimental tumors [95]. Vimentin expression is seen to be upregulated in many invasive cancers including prostate cancer, gastrointestinal tumors, breast cancer, malignant melanoma and lung cancer [5]. Malignancy is accompanied by a switch in the expression of the type of intermediate filament. Sommers et al., have reported downregulation of keratin and corresponding upregulation of vimentin in malignant breast cancer cells [96]. Lahat et al., have shown that treatment of Withaferin-A (WFA) (a bioactive compound with anticancer properties) specifically targets vimentin-expressing cancer cells to apoptosis [97]. Study on gene expression signatures in breast cancer by Sotiriou et al., has revealed that, vimentin-expressing cancers are of either mesenchymal or Basal B type [98]. Vimentin-expressing breast cancers are known to exhibit undifferentiated, fibroblastic phenotype which increases their likelihood to form distant

metastases to tissues like lung and brain [10]. Coherently, our group along with others has shown a positive correlation of vimentin with the accelerated tumor growth, invasive phenotype, recurrence and poor prognosis [6, 99, 100]. In vitro studies using vimentin knockdown system generated in cancer cell lines; have highlighted the contribution of vimentin in migration [9, 101]. A recent report by Polioudaki has suggested use of vimentin for quantifying protein expression for the characterization of circulating tumor cells (CTCs). This evaluation can be used to generate prognostic information upon diagnosis or during follow-up of patients with breast cancer [102].

#### **2.3.5.3.4 Role of vimentin in Epithelial mesenchymal transition (EMT)**

EMT is a critical event during development wherein at the gastrulation stage; individual cells detach from a layer and migrate to form primitive streak and somites [103]. EMT is also seen in the context with different morphogenetic events like fibrosis, invasion and metastasis of carcinomas [5]. EMT program sets in during tumor metastasis, in which epithelial tumor cells in the primary cancer site are converted into aggressive and metastatic tumor cells. EMT involves series of events which include loss of cell–cell adhesion and gain of a mesenchymal phenotype, followed by the disappearance of basoapical polarization, finally resulting in altered cell-ECM interaction by activation of matrix metalloproteases [104]. Vimentin expression is significantly upregulated while, expression of E-cadherin is downregulated during EMT, which further contributes to tumor metastasis. The mesenchymal-like cells generated as a result of EMT may be transported to metastatic sites, where they may undergo mesenchymal–epithelial transition (MET) by regaining E-cadherin expression to establish itself in a new niche [105]. Therefore, epigenetic regulation appears to be more important than genetic level regulation in maintaining EMT-like phenotype. For instance, Marsit et al. have shown promoter level hypermethylation of

E-cadherin gene in head and neck squamous cell carcinoma [106]. Additionally, EMT process can be epigenetically regulated by microRNAs (miRNAs) as well. Cheng et al., have demonstrated the downregulation of the vimentin expression by miR-30a, leading to inhibition of breast tumor invasiveness and metastasis [107]. Moreover, according to Chaw et al., EMT occurs not only in the late stages of cancer but also at the stage of oral epithelial dysplasia. This indicates that EMT changes may begin much early in the development of OSCC and identification of molecule/mechanism underlying this transition process may serve as a potential target to bring about inhibition of malignant transformation [108]. Furthermore, the role of vimentin is highly reported in the case of cancer cell migration. Hence, a study of the mechanisms underlying vimentin mediated mechanism is important.  $\alpha6\beta4$  integrin, which connects intermediate filaments to the basement membrane has emerged as one of the indirect targets of vimentin, to modulate the migratory ability of the tumor cell.

#### **2.3.5.3.5 Role of vimentin in cell signaling**

Vimentin IFs are seen to interact with many signalling molecules to carry out several cellular functions. Vimentin was shown to bind with activated Erk to prevent its dephosphorylation [109]. In soft-tissue sarcoma cells, phosphorylated vimentin was protected from caspases by AKT1 kinase, in order to promote cell motility and invasion [110]. Phosphorylated vimentin was shown to regulate the availability of 14-3-3 proteins by interacting with it, to prevent its complex formation with other interactors [111]. This thus impacts signalling and cell cycle regulatory pathways. Additionally, vimentin was shown to prevent degradation of Scrib (which is involved in migration), to support directed cell migration of the invasive cells [112]. Similarly, it was known to induce Axl to promote cancer cell migration [10]. Moreover, EMT phenotype induced by Slug and Ras was also dependent on vimentin [10].

Furthermore, a complex interplay between filamin A, an actin binding protein along with vimentin and PKC enable tight regulation of  $\beta 1$  integrin function. This consequently modulates early events in cell adhesion and migration [113]. These reports together highlight the role of vimentin in the regulation of various signalling pathways activated normally and during cancer.

### **2.3.6 Vimentin and $\alpha 6\beta 4$ integrin**

In stratified epithelium,  $\alpha 6\beta 4$  integrin is majorly involved in stabilizing the association of epithelium to its underlying basement membrane. It forms stable adhesion structures by interacting with ECM component laminin-5 [114].  $\alpha 6\beta 4$  integrin loss has been shown to result in epidermis detachment in response to mechanical stress [115]. Also, homozygous in-frame deletion in the  $\beta 4$  integrin gene results in epidermal blistering as seen in the case of humans [116]. It interacts primarily with the keratin intermediate filament system at the cytoplasmic side and laminin-5 at the basement membrane side and gets localized in type I hemidesmosomes in stratified epithelial cells [117]. Along with  $\alpha 6\beta 4$  integrin, type I hemidesmosomes consist of other proteins which include BP180, IFAP300, HD1, plectin and BP230 [118]. The endothelial cells do not express type I hemidesmosomes, but they do express type II hemidesmosomes which consist of only  $\alpha 6\beta 4$  and plectin (lacking BP180, BP230 and electron-dense intracellular plaques) [114].  $\beta 4$  is known to interact with vimentin through HD1/plectin in endothelial cells [14]. Disruption of HD1/plectin or BP230 has been shown to inhibit interactions of basal keratinocytes to its basement membrane [119-121]. Also, the fact that HD1/plectin null mice had very few hemidesmosomes associating with keratin filaments, implied that HD1/plectin may not be indispensable for the linkage of  $\alpha 6\beta 4$  to keratin filaments, but may stabilize this association [121, 122]. A study by Homan et al, has shown that when endothelial cells are grown on laminin 5-rich matrix, recombinant  $\alpha 6\beta 4$  redistributes from the fibrillar structure to type I

hemidesmosome-like structures. This suggests that vimentin may be connected with cell matrix adhesion contact through  $\alpha6\beta4$  integrin, in endothelial cells [114].

### **2.3.6.1 Vimentin and $\alpha6\beta4$ integrin in cancer**

Loss of  $\alpha6\beta4$  at the basal layer was seen in cervical cancer [123]. Similarly, Downer et al., have shown loss of  $\alpha6\beta4$  and its corresponding basement membrane component laminin, in squamous cell carcinomas [124].  $\alpha6\beta4$  integrin has been shown to play a reverse role during cancer progression wherein  $\alpha6\beta4$  integrin has been seen to facilitate cancer cell migration and invasion by regulating multiple signaling pathways, including phosphatidylinositol 3-kinase/Akt and MAPK [125]. In carcinoma derived cells,  $\alpha6\beta4$  integrin can also interact with the actin cytoskeleton in migrating cells [126]. Coherently,  $\beta4$  integrin has been also shown to be capable of activating pivotal kinases involved in carcinogenesis like PKB/Akt and ERK1/2 [127]. Further, activation of  $\beta4$  cytoplasmic domain is seen to recruit adaptor protein Shc to bring about downstream signaling cascade [128]. These observations indicate that the  $\beta4$  integrin signaling component functions to determine the fate of carcinoma cells. Evidence also suggests that  $\alpha6\beta4$  integrin molecules associated with carcinoma cells, bind with the actin cytoskeleton in filopodia and lamellipodia [126, 129]. This collectively indicates that  $\alpha6\beta4$  integrin in normal epithelia functions as adhesion receptor while in cancer plays an anomalous role to enhance migration. Correspondingly, observations by Rabinovitz et al. also suggest that during cancer progression  $\alpha6\beta4$  integrin disappears from the hemidesmosomes to accumulate preferentially in the F-actin rich cell protrusions. This change occurs in response to chemotactic stimulation, to contribute in cancer cell migration [129]. Furthermore, increased turnover of  $\alpha6\beta4$  integrin was seen in a multistep mouse model of skin carcinogenesis [130]. In this context, it is noteworthy that though  $\alpha6\beta4$  integrin was shown to be predominant receptor expressed in carcinomas, its expression was

not polarized but was dissociated and not restricted to the basement membrane [131]. Previously,  $\beta 4$  integrin and E-cadherin loss was seen during EMT of mammary gland cells induced by TGF  $\beta$  due to epigenetic modifications [132]. Also, in a report on kindlin-1 deficient keratinocytes, increase in mesenchymal markers vimentin and fibronectin was seen with a concomitant decrease in epithelial markers like E-cadherin,  $\alpha 6 \beta 4$  integrin, etc., marking the loss of epithelial like phenotype [133]. In this direction, it is noteworthy that cells showing increased levels of vimentin generally exhibit a more dedifferentiated/mesenchymal like phenotype. Therefore, it is worthwhile to investigate, if vimentin is able to modulate the proteins involved in either maintenance or generation of a differentiated epithelial phenotype.

### **2.3.7 Vimentin and differentiation state of cancer cell**

Traditionally, IFs are known to define the tissue origin of poorly differentiated tumors, wherein keratin IFs define epithelial cells while vimentin IFs define mesenchymal cells [4]. In most of the cancers, expression of vimentin is inversely related to the differentiation state of the tumor. For instance, in prostate cancer, its expression has been detected in a poorly differentiated stage of cancer [134]. Though, majority of the reports suggest a strong association of decreased E-cadherin expression and increase mesenchymal differentiation, Nakajima et al found a significant correlation of mesenchymal differentiation with expression of vimentin and N-cadherin but not with expression of E-cadherin in pancreatic carcinoma [135]. In a study by Sommers et al., on breast cancer derived cell lines, expression of vimentin was found to positively correlate with poorly differentiated, fibroblastic phenotype [16].

### **2.3.8 Vimentin and keratins in cancer cell differentiation**

At the advanced stages of cancer progression when tumor cell undergoes EMT, it acquires a characteristic flattened morphology (mesenchymal like) due to loss of cell-cell and cell-substrate

contacts. As reported by Mendez et al., coherently at the same time, there is a dramatic reprogramming of epithelia specific keratins, to now initiate the expression of vimentin [15]. Moll et al., reported a change in keratin composition, associated with a decrease in the degree of differentiation during an injury (inflammation/atrophy), wherein a cell starts expressing more than two keratins/IF proteins, e.g. K7, K17, K19, vimentin etc.[136]. Recent report by Boraas et al. demonstrated cytoskeletal remodeling in case of mouse embryonic fibroblasts, in the course of transition between progenitor and differentiated states [137]. Due to tissue and differentiation state specific expression of keratins, many of them have found wide utility in clinics as diagnostic markers, especially in tumor pathology. Moll et al. have shown a positive correlation of expression patterns of K5, K6, K14, K17, etc. with dedifferentiated and metastatic nature of the squamous cell carcinomas [138]. Alam et al., have shown the contribution of K5/K14 pair in the maintenance of a proliferative and dedifferentiated state of tongue SCC derived cell line AW13516 perhaps in a notch dependent manner [139].

In view of the available literature, the importance of aberrant IFs expression in cancer and their usefulness as diagnostic and prognostic markers is apparent. With the growing evidence of the potential of vimentin in driving the progression of oral cancer, research needs to be focused on understanding overall molecular pathways regulated by vimentin and designing of anticancer agents targeting vimentin expressing carcinomas.

# Chapter 3: Materials and Methods

### 3 Materials and Methods

#### 3.1 List of Cell lines, antibodies and reagents

List of cell lines, reagents and antibodies with their particulars are described in the Table 3.1, 3.2 and 3.3 respectively.

**Table 3.1 List of cell lines with their particulars.**

Cell lines	Source	Media	References
AW13516 and AW8507	SCC of tongue	Complete IMDM	[140]
SCC029B	SCC of buccal mucosa	Complete IMDM	[141]
A431	Epidermal carcinoma of the vulva	Complete DMEM	[142]
HEK-293 cells	Human Embryo Kidney	Complete DMEM	[143]
DOK	Human dysplastic oral mucosa	Complete DMEM with hydrocortisone	[144]
HaCat	Immortal human keratinocyte	Complete DMEM	[145]

**Table 3.2 List of reagents with their particulars.**

Reagents	Catalogue	Company	Country
Accutase	TCL075	Himedia	Mumbai, India
Calcein AM	C1430	Life technologies	Carlsbad, CA, USA
DAPI	D9542	Sigma-Aldrich	USA
Dulbecco's modified eagle's medium (DMEM)	12800-017	Life technologies	Carlsbad, CA, USA
Elite ABC Kit	PK6100	Vector laboratories	USA
Fetal bovine serum (fbs)	SH30071.03	HycloneThermo Scientific	Lafayette, CO

<b>Reagents</b>	<b>Catalogue</b>	<b>Company</b>	<b>Country</b>
FITC-conjugated phalloidin	P5282	Sigma Aldrich	USA
G418	A1720	Sigma-Aldrich	USA
Human Laminin 332	EUV102	Kerafast	USA
Iscove's Modified Dulbecco's Medium (IMDM)	12200-036	Life technologies	Carlsbad, CA, USA
Lipofectamine® 2000 Transfection Reagent	11668030	Life technologies	Carlsbad, CA, USA
Matrigel	354234	BD Biosciences	Franklin lakes, NJ, USA
MG-132	474790	Calbiochem	San Diego, CA, USA
Protease inhibitor cocktail	539131	Calbiochem	San Diego, CA, USA
Protein G-sepharose	P3296	Sigma-Aldrich	USA
Puromycin	P8833	Sigma-Aldrich	USA
PVDF membrane	RPN303F	GE Healthcare	UK
Revert Aid First Strand cDNA synthesis Kit	K1622	ThermoFischer Scientific	USA
SYBR Green Master Mix	4367659	Applied Biosystems	Bedford, MA, USA
TGF-β1	100-21	PeptoTech Inc.	Rocky Hill, USA
TRI reagent	93289-100ml	Sigma-Aldrich	USA
Lipofectamine 2000	11668027	ThermoFischer Scientific	USA
Vectashield mounting medium	H-1000	Vector Laboratories	CA, USA

**Table 3.3 List of antibodies with their particulars.**

<b>Antibody</b>	<b>Dilution</b>	<b>Clone</b>	<b>Company</b>	<b>Catalogue No.</b>
AKT	1:1000 (WB)	Rabbit polyclonal	Cell signaling, USA	9272
Anti-Flag	1:100	Clone M2, Mouse monoclonal	Sigma, USA	F 3165
BP180	1:1000 (WB)	Rabbit polyclonal	Aviva Systems Biology, USA	OAAB05688
CD151	1:2000 (WB)	Clone 11G5a, Mouse monoclonal	Abcam, USA	ab33315
E-cadherin	1:500 (WB)	36/E-cadherin, Mouse monoclonal	BD Transduction Lab	610182
ERK1/2	1: 2000 (WB)	Mouse monoclonal	Abcam, USA	ab36991
Histone H3	1:1000 (WB)	Clone 6.6.2	Millipore, USA	05-499
Involucrin	1:1000 (WB)	Clone SY5, Mouse monoclonal	Serotec, UK	5390-9950
Keratin 17	1:1000 (WB)	Clone D12E5, Rabbit monoclonal	Cell signalling technology, USA	12509
Keratin 5	1:1000 (WB) 1:100 (IF/ IHC)	Clone XM26, Mouse monoclonal	Novocastra, UK	NCL-CK5
Keratin 14	1:10000 (WB) 1:100 (IF/ IHC)	Clone LL002, Mouse monoclonal	Serotec, UK	MCA890
Keratin 8	1:8000 (WB)	Clone M20, Mouse monoclonal	Sigma, USA	C5301
Keratin 18	1:8000 (WB)	Clone CY-90, Mouse monoclonal	Sigma, USA	C 8541
Ki67	1:50 (IF)	Clone MM1, Mouse monoclonal	Novocastra, UK	PA0118
Laminin-5	1:100 (IF)	P3H9-2, Mouse monoclonal	Millipore, USA	MAB1947
NF-κB (p65)	1:1000(WB) 1:30 (IF)	Rabbit polyclonal	Abcam, USA	Ab7970-1
Notch 1 (NICD)	1:1000 (WB)	Rabbit polyclonal	Abcam, USA	Ab8925
p21	1:1000(WB)	Rabbit polyclonal	Santacruz, USA	Sc-471
p27	1:1000(WB)	Rabbit polyclonal	Santacruz, USA	sc-528
p63	1:1000 (WB)	Clone (H-137)	Santacruz, USA	Sc-8343

Antibody	Dilution	Clone	Company	Catalogue No.
PCNA	1:50 (IF)	PC10, Mouse monoclonal	BD Pharmingen, USA	555566
Phospho ERK1/2 (phosphor T185+T202)	1: 1000 (WB)	Rabbit polyclonal	Abcam, USA	ab4819
Plectin	1:500(WB)	Clone 10F6, Mouse monoclonal	AbDSerotec, UK	MCA2741
Vimentin	1:1000 (WB) 1:100 (IF), 1:150(IHC)	Clone V9, Mouse monoclonal	Sigma, USA	V 6630
$\alpha$ tubulin	1:5000(WB)	B-5-1-2, Mouse monoclonal	Sigma, USA	T6074
$\beta$ 1 integrin	1:1000 (WB),	Clone 9EG7	BD Pharmingen, USA	553715
$\beta$ 4 integrin	1:1000 (WB) 1:75 (IF and IHC)	Clone H-101, Rabbit polyclonal	Santa Cruz, USA	sc9090
$\beta$ -actin	1:8000 (WB)	Clone AC-74, Mouse monoclonal	Sigma, USA	A 5316

WB- western blot, IF- immunofluorescence, IHC- immunohistochemistry

### 3.2 Routine maintenance of cell lines

Powdered medium was dissolved in 1l of water. For Dulbecco's Modified Eagle's medium (DMEM), 3.7 g of sodium bicarbonate per liter was added and the pH of medium was adjusted to 6.8. For Iscove's Modified Dulbecco's medium (IMDM), 3.02 g of sodium bicarbonate per liter was added). The media were filtered using Millipore assembly – 0.45  $\mu$ M Membrane filter (Whatman). 1 ml of the filtered medium was added to the sterility test medium and kept at room temperature (RT) for 6 days under observation to ensure the sterility.

### 3.3 Other reagents:

a) Phosphate Buffered Saline (PBS): (150 mM NaCl, 2 mM KCl, 8 mM Na<sub>2</sub>HPO<sub>4</sub>, 1 mM KH<sub>2</sub>PO<sub>4</sub>.) The buffer is autoclaved and used.

b) Trypsin-EDTA: (0.025% Trypsin, 0.2 mM EDTA, 5 mM D-glucose, 5 mM KCL, 0.1 M NaCl and 6 mM NaHCO<sub>3</sub>) The medium was filtered using Millipore assembly – 0.45  $\mu$ M Membrane

filter (Whatman). 1 ml of the filtered trypsin was added to the sterility test medium and kept at RT for 6 days under observation to ensure sterility.

c) Erythrocin B staining solution: 0.4% Erythrocin B in 1X PBS.

d) Freezing medium: 90% Fetal Bovine Serum, 10% DMSO.

e) Complete medium: DMEM or IMDM with 10% FBS and 1% antibiotic solution (Amphotericin B 20 µg/ml, Penicillin 2500 Units/ml, Streptomycin 800 µg/ml in PBS). For culturing DOK cell line, complete DMEM supplemented with 5 µg/ml hydrocortisone was used.

f) Sterility test medium: 14.9 g of Fluid-Thioglycolate was dissolved in approximately 250 ml in water. The volume was made up to 500 ml in measuring flask and boiled. After aliquoting 6 ml of the medium in glass tubes a pinch of Ca<sub>2</sub>CO<sub>3</sub> was added to each tube and autoclaved.

### **3.4 Revival of cells**

A vial was taken out from liquid nitrogen cylinder and placed into a 37°C water bath for thawing. The thawed cell suspension was mixed gently and transferred into a sterile test tube. 5 ml of complete medium was added drop wise with gentle shaking. The thawed cells with medium were further mixed smoothly using glass pipette. The cell suspension obtained was centrifuged for 10' at 1500 rpm at RT. The supernatant was discarded and the pellet was dislodged by finger tapping. 3 ml of complete medium was added drop wise to the test tube with continuous shaking followed by centrifugation at 1500 rpm for 10' at RT. The supernatant was discarded and the pellet was dislodged by tapping and resuspended in 1ml of complete medium. Total cell count and the percent viability were calculated by dye exclusion method using Erythrocin B dye on a haemocytometer in an inverted microscope. The medium was mixed by pipetting and the 100 mm petri plates were seeded with 1 x 10<sup>6</sup> cells. The cells were incubated in a humidified CO<sub>2</sub> (5%) incubator at 37°C and their growth was observed each day under inverted microscope.

### **3.5 Subculture/Trypsinization and transfer of cells:**

The cells were washed with 1X PBS twice and trypsin-EDTA was added to the culture plate. Excess trypsin-EDTA was discarded and the plate was incubated till the cells were partially detached. Complete medium was added to inhibit the trypsin activity into plate containing detached cells, the resulting cell suspension was mixed by pipette to make a single cell suspension. Total cell count was taken and appropriate amount of cells depending upon cell type were seeded in culture plates. The plates were incubated in humidified CO<sub>2</sub> incubator at 37°C.

### **3.6 Freezing and cryopreservation of cells**

Log phase cells were trypsinised and single cell suspension was obtained. After noting the total cell count, the cell suspension was spun at 1500 rpm for 10' at RT. The supernatant was discarded and the pellet was dislodged by tapping. 1 ml of freezing medium was added into the tube drop wise and mixed gently by pipette. The cells suspension was then transferred to freezing vials. The freezing vials were then placed in bio-freezer with 3 rings. First ring was removed after 90', the second ring was removed after 120' and third ring was removed after 150'. The vials were then kept in liquid nitrogen freeze boxes at -196°C for long term storage.

### **3.7 Plasmids and cloning:**

For generation of shRNAs against vimentin, the selected vimentin shRNA sequences (Table 3.4) were cloned into pTU6 PURO vector (a kind gift from Dr. Sorab Dalal, ACTREC, India). For vimentin overexpression, emerald GFP vimentin retroviral construct was used, which was a kind gift from Dr. Robert Goldman (Feinberg School of Medicine, Northwestern University, USA). The emerald GFP vector control was generated by digesting the emerald GFP vimentin retroviral construct with BamH1 followed by self ligation in order to remove the vimentin gene. Vimentin-β4 integrin double knockdown and vector control clones were generated by

transducing beta4integrin shRNA and scrambled shRNA cloned in pCLXSN retroviral vector, a kind gift from Dr.LivioTrusolino, (Department of Oncology, University of Torino School of Medicine, Italy) in vimentin knockdown clone shvim2. Emerald GFP-K14 construct was generated by amplifying K14 gene sequence from K14-pEGFP-N3 construct and subcloned in emerald GFP-pQCXIP vector using single BamHI site. Firstly, emerald GFP-K14 was overexpressed in vimentin knockdown background shvim2 and the positive clones were sorted using FACS Aria based on the GFP fluorescence. Next, the K14 positive clones were used to transduce K5 pLNCX2 retroviral construct (a kind gift from Professor Thomas Magin, TRM & Biology II, University of Leipzig, Germany) and the positive clones were selected using G418 sulphate (400µg/ml). The empty vector backbone of both the constructs was used to generate the vector control clones. For the cloning of  $\Delta$ Np63 $\alpha$ , its cDNA was prepared from HaCat cell line and was cloned in pLNCX2 vector containing N-terminal flag tag sequence using HindIII and Sall restriction enzyme sites. Flag- $\Delta$ Np63 $\alpha$  containing retroviral construct was then transduced in vimentin knockdown clone shvim2 and positive clones were selected using G418 sulphate (400µg/ml). The empty flag pLNCX2 vector backbone served as a vector control.

**Table 3.4 List of vimentin shRNA sequences along with their target site.**

Oligo name	Length	Target site	Sequence (5'-3')
1A	62	971bp-992bp	CCGGAGAAATTGCAGGAGGAGATGAAGTTCT CTCATCTCCTCCTGCAATTTCTCCTTTTTTC
1B			TCGAGAAAAAAGGAGAAATTGCAGGAGGAGA TGAGAGA ACTTCATCTCCTCCTCCTGCAATTTCT
2A	64	1004bp-1026bp	CCGGAAGCCGAAAACACCCCTGCAATAAGTTCT CTATTGCAGGGTGTTTTTCGGCTTCCTTTTTTC
2B			TCGAGAAAAAAGGAAGCCGAAAACACCGTGCA ATAGAGA ACTTATTGCAGGGTGTTTTTCGGCTT

Oligo name	Length	Target site	Sequence (5'-3')
3A	62	1250bp-1271bp	CCGGCTGCCAAGAACCTGCAGGAGAAGTTCT CTCTCCTGCAGGTTCTTGGCAGCCTTTTTTC
3B			TCGAGAAAAAAGGCTGCCAAGAACCTGCAGG AGAGAGAGAACTTCTCCTGCAGGTTCTTGGCAG
4A	62	1416bp-1437bp	CCGGAACCAATGAGTCCCTGGAACAAGTTCT CTGTTCCAGGGACTCATTGGTTCCTTTTTTC
4B			TCGAGAAAAAAGGAACCAATGAGTCCCTGGA ACAGAGAACTTGTTCCAGGGACTCATTGGTT

### 3.8 Validation of shRNA constructs:

To determine the efficacy of RNAi constructs to knockdown the expression of vimentin, 3 µg vimentin shRNA constructs were cotransfected with 1 µg of GFP tagged wild type vimentin expression constructs in HEK293 cells using calcium phosphate precipitation method (Table 3.5) which uses 0.5 M CaCl<sub>2</sub> and 2X BBS (50 mM BES, 1.5 mM Na<sub>2</sub>PO<sub>4</sub> and 250 mM NaCl). pTU6-PURO vector was included in the experiment as a control. 72 h post transfection, fluorescence of GFP was checked by fluorescence microscopy. Further, cells were lysed in SDS lysis buffer and proteins were separated on 10% SDS polyacrylamide gel. For stable selection of knockdown clones, 2 µg of the shRNA construct was transfected into AW13516 using Lipofectamine 2000 transfection reagent, as per manufacturer's instructions. The cells were transfected at a confluency of 30-40%.

**Table 3.5 Calcium phosphate transfection mix.** The table shows the different volumes of the reagents to be mixed for calcium phosphate transfections in different culturedishes.

S. No	Size/diameter of culture dish	Total amount of DNA (in µg)	Autoclaved D/W (in µl)	0.5 M CaCl <sub>2</sub> (in µl)	2X BBS (in µl)	Total volume (in µl)
1	35 mm	5	45	50	100	200
2	60 mm	10	90	100	200	400
3	100 mm	25	225	250	500	1000

### 3.9 Virus production.

HEK293FT cells were cultured in DMEM complete medium containing G418 500 µg/ml in 90mm culture plate to achieve 50% confluency. Co-transfection of expression and packaging vectors was performed, by calcium phosphate precipitation method. Desired amount of DNA was diluted to 260 µl of sterile distilled water in a sterile microcentrifuge tube. Equal volume of 0.5 M CaCl<sub>2</sub> was then added followed by addition of 520 µl of BES Buffered Saline (BBS). The mixture was incubated at RT for 30' and then added to culture dishes dropwise with 50% confluent culture plate of HEK293FT, the plate was gently swirled and incubated for 16 h. After incubation, the medium was replaced with fresh complete DMEM. After 48 h of transfection, viral supernatant was collected in sterile 15 ml tube and centrifuged for 10' at 2500rpm to remove traces of HEK 293FT cells. Supernatant was collected and stored in -80°C or used for transduction

### 3.10 Preparation of whole cell lysates

The cells were grown upto 80-90% confluency in tissue culture dish. They were scraped from the plate and suspended in SDS lysis buffer ((62.5 mM Tris pH 6.8, 2% SDS, protease and phosphatase inhibitor cocktail). The cell suspension was then boiled for 10' followed by

centrifugation at 13000 rpm for 15' to remove cell debris. The supernatant was then aliquoted and stored at -80°C for further use.

### **3.11 Protein estimation by modified Lowry's method**

1 ml of 5 to 25 µg/ml of BSA was taken in test tubes in duplicates as standard along with blank. 5 µl of whole cell lysates were added in test tubes in duplicates and the volume was made up to 1 ml by distilled water. 1 ml of Copper Tartarate Carbonate (CTC) solution (0.1 % copper sulphate(w/v), 0.2 % potassium tartarate (w/v), 10 % Sodium carbonate (w/v), Solution A (Equal volumes of CTC solution, 10 % SDS (w/v), 0.8 N NaOH (w/v) and distilled water (1: 1: 1: 1 proportion)) was added to each test tube and the tubes were vortexed followed by incubation at RT for 10'. 500 µl diluted FC reagent (1 part of FC reagent and 5 parts of distilled water) was added to each tube. The tubes were vortexed and incubated at RT for 30' in dark and absorbance was read at 750 nm using a spectrophotometer. The standard curve was plotted. The protein concentration of the samples was determined using standard curve. The protocol was adapted from [146].

### **3.12 SDS PAGE**

The samples were dissolved in PAGE sample buffer (62.5 mM Tris HCl pH 6.8, 25% Glycerol w/v, 2% SDS, 0.5% Bromophenol blue) and were separated on 6-15% SDS PAGE depending on the molecular weight of the proteins being analyzed with 5% stacking gel. The protocol was adapted from [147].

### **3.13 Western blotting**

After SDS-PAGE, the gel with resolved proteins and the activated PVDF membrane were placed in form of the sandwich and wet electro-blotting using transfer buffer (190 mM Glycine, 20% methanol, 0.05% SDS, 25 mM Tris base) was carried out at 100 V for 1 h. Transfer of proteins

was visualized using Ponceau-S staining (0.2% ponceau stain in 5% acetic acid). The blot was incubated in blocking solution (3% BSA in TBS or 5% Milk in 1X TBS) for 1 h at RT on a rocker. After blocking the blot was incubated with diluted primary antibody for 1 h at RT on the rocker. The blot was then washed thrice with TBST (0.1% TWEEN 20 (v/v), 150 mM NaCl, 10mM Tris HCl pH 8.0) followed by incubation with horseradish peroxidase (HRPO) conjugated secondary antibody for 1 h at RT on the rocker. The secondary antibody was removed and the blot was washed thrice with TBST. Blots were developed using ECL+ chemiluminescence reagent according to the manufacturer's protocol. The protocol was adapted from [148].

### **3.14 Zymography**

To determine the Matrix Metalloproteinase (MMP) activity in conditioned culture medium, gelatin zymography was carried out.  $5 \times 10^5$  cells were seeded in 35 mm tissue culture dish and grown for 24 h at 5% CO<sub>2</sub> at 37°C. The cells were then washed thrice with 1X PBS and grown in serum free medium for 24 h. After 24 h incubation, culture medium was recovered and centrifuged at 13,000 rpm for 15' at 4°C. Cells attached to the plates at the time of the experiment were trypsinized and counted. An equal volume of conditioned medium was mixed with non-reducing Laemmli's sample buffer (62.2 mM Tris-HCl, pH 6.8, 10% SDS, 50% glycerol, 0.025% bromophenol blue) and applied to 10% SDS-PAGE gels polymerized with 1% gelatin. After electrophoresis, the gels were washed three times in a solution containing 2.5% Triton X-100 to eliminate the SDS and to allow reconstitution of the proteins. MMP activity was stimulated by incubating the gels at 37°C for 16 h in reaction buffer (50 mM Tris-HCl, pH 6.8, 150 mM NaCl, 5 mM CaCl<sub>2</sub>, and 0.05% sodium azide). The activity of the MMPs was visualized by staining the gels in Coomassie Brilliant Blue G-250 solution [149].

### **3.15 Co-immunoprecipitation**

The harvested cells were treated for 15' at 4°C with 1X PBS containing 1% Nonidet P-40, 5 mM EDTA, and protease and phosphatase inhibitor mixture followed by centrifugation (13,000rpm for 20' at 4 °C). The supernatant was collected as the Nonidet P-40-soluble fraction (soluble fraction). The resulting insoluble pellet was homogenized in phosphate-buffered saline containing 2% Empigen and incubated for 45' at 4 °C, followed by centrifugation (13,000rpm for 20' at 4 °C). The supernatant was collected as Nonidet P-40-insoluble fraction (filament fraction). The Nonidet P-40 soluble and insoluble fractions were pooled together and then incubated with anti-vimentin/plectin/ $\beta$ 4 integrin antibody bound to protein G-Sepharose beads for overnight at 4°C on slow moving rotor (9 rpm). The beads were washed three times with RIPA buffer (20 mM HEPES, 140 mMNaCl, 5 mM EDTA, and 0.4%Nonidet P-40, pH 7.4). The immune complexes were solubilized in cell lysis buffer, resolved on 10% SDS-PAGE, blotted and probed with respective antibodies. The protocol was adapted from [150].

### **3.16 Protein estimation by RC DC Kit**

The proteins were estimated according to the manufacturer's protocol. Various protein standards (5 to 25  $\mu$ g) and the samples to be estimated were added to the 1.5 ml eppendorf tubes and the volume was made up to 25  $\mu$ l with distilled water. 125  $\mu$ l RC Reagent I was added in each tube, vortexed and incubated for 1' at RT. 125  $\mu$ l RC Reagent II was added in each tube and vortexed. The tubes were then centrifuged at 8000 rpm for 20'. Supernatant was drained completely by inverting the tubes. Reagent A (127  $\mu$ l) was then added to each microfuge tube and vortex. The tubes were incubated at RT for 5', or until precipitate was completely dissolved. The tubes were vortexed and 1 ml of DC Reagent B was added to each tube and vortexed immediately. The tubes were incubated at RT for 15' and absorbance was read at 750 nm.

### 3.17 Two-dimensional polyacrylamide gel electrophoresis (2DE)

The first dimension (IEF) was conducted using IPG strips (pH range 3-10). Samples were dissolved in Urea buffer (8M Urea, 2M Thio urea, 2% CHAPS, 50 mM DTT). After estimation of proteins, 200 µg of protein samples were resuspended in rehydration buffer (8M Urea, 2M Thiourea, 2%CHAPS, 1%DTT, 0.2% Ampholytes, 0.0002%Bromophenol blue) and the resulting solution was placed in the rehydration tray. IPG strip was placed over the sample in the rehydration tray and incubated for 30'. 1 ml of mineral oil was overlaid on the IPG strips to prevent evaporation and the strips were rehydrated overnight (16 h) at RT. The following day, excess mineral oil was discarded and IPG strips were laid on an IEF tray with gel side towards the platinum wires of the tray. Small paper wicks made from Whatman filter paper were wet in distilled water and laid on the platinum wires of the IEF tray to avoid direct contact of gel with wires. The IPG strips were then overlaid with 1.5 ml of mineral oil. The IEF tray was then placed in the Biorad Protean IEF cell and isoelectric focusing was performed using the following automated steps (Table 3.6).

**Table 3.6 Conditions for IEF**

Step	Start voltage	End voltage	Time (min)	Final volt hours	Condition
Step 1	0	250	20	-	Linear
Step 2	250	4000	120	-	Linear
Step 3	4000	4000	-	10000 V-h	Rapid

Further, IPG strips were placed in rehydration tray with the gel side facing upwards and equilibrated with equilibration buffer 1 (6 M Urea, 0.375 M TrisHCl (pH 8.8), 2% SDS, 20% Glycerol, 2% DTT) for 15', followed by equilibration with equilibration buffer 2 (6 M Urea, 0.375 M Tris HCl pH 8.8, 2% SDS, 20% Glycerol, 2.5% Iodoacetamide) for 15' with constant and gentle stirring. The IPG strips were then immersed in electrode buffer and placed on the 10% SDS-PAGE and run on constant 200V for the second-dimension separation.

### **3.18 Coomassie staining**

For coomassie blue staining, the gel was placed in plastic container containing coomassie staining solution (0.25% coomassie brilliant blue R 250, 45% methanol and 10% acetic acid in distilled water) and stained for 2 h. The background of the gel was removed using destainer (45% methanol (v/v) and 10% acetic acid (v/v) in distilled water) and then the gels were stored in distilled water.

### **3.19 In gel tryptic digestion and Mass spectrometry**

After coomassie blue staining, different spots observed on 2DE gel were excised by razor blade and placed in 1.7 ml microfuge tubes. The gel pieces were cut approximately 1-2 mm in size in the tube. The gel pieces were covered with 200  $\mu$ l of MS destainer (200 mM ammonium bicarbonate, 40% acetonitrile) and incubated at 37°C for 30'. The MS destainer in the tube was discarded and the destaining step was repeated once. The gel pieces were dried under vacuum in Speed Vac for 30' and rehydrated by adding appropriate volume (10-20  $\mu$ l) of 20  $\mu$ g/ml trypsin, further incubated for 18 h at 37°C for digestion of proteins. Next day, 50  $\mu$ l of 0.1% TFA was added to the microfuge tubes and placed in sonication bath for 30'. The tubes were centrifuged and supernatant was transferred in another microfuge tube. The remaining gel pieces were again covered with 50  $\mu$ l of 0.1% TFA and placed in sonication bath for 30'. The former step was repeated one more time and the supernatants were pooled in a one microfuge tube and dried in Speed Vac. The dried pellets containing peptides were dissolved in 1% TFA and mixed with equal volume of the CHCA matrix (Cyano Hydroxy Cinnamic acid). This mixture was spotted on 384 well MALDI plate and subjected to Mass Spectrometry, using ultra flex II mass spectrometer from Bruker daltonics.

### **3.20 RNA extraction**

The RNA from cell lines was isolated by Tri reagent as per the manufacturer's instructions. Briefly, the medium was removed and cells were lysed by adding 1 ml/100cm<sup>2</sup> plate of Tri reagent. The lysate was transferred into a 1.5 ml tube and 100 µl of chloroform was added and incubated for 2' at RT. The phase was separated by centrifugation at 12000 rpm and supernatant was transferred to a new tube. RNA was precipitated by adding isopropanol and spun at 12000 rpm. The pellet was washed by 75% ethanol; air dried and dissolved in 50 µl of DEPC treated water. The purity and content of RNA was determined using NanoDrop<sup>TM</sup> Spectrophotometer.

### **3.21 Reverse transcriptase - Polymerase chain reaction (RT-PCR)**

cDNA synthesis was carried out as per the manufacturer's protocol (MBI fermentas). Briefly, 1 µg of total RNA and 0.2 µg (100 pmol of random hexamer/oligo(dT) in a volume of 12 µl were incubated at 70°C for 5' and chilled on ice and centrifuged. Reaction buffer, RiboLock<sup>TM</sup> RNase Inhibitor, dNTP Mix was added to obtain final concentration of 1X, 1 unit/µl and 1 mM each respectively and incubated at 25°C for 5'. RevertAid<sup>TM</sup> H Minus M-MuLV Reverse Transcriptase (200 units) was added and the reaction mixture was incubated at 25°C for 10' followed by 42°C for 1 h. The reaction was terminated by heating at 70°C for 10'. The primer sequences used to amplify target genes and GAPDH (internal control) are listed in Table 3.7. PCR products were run on agarose gel electrophoresis to compare RNA levels.

**Table 3.7 RT-PCR primer sequences**

Sr.No.	Primer Sequence (5'-3')
$\alpha 6$ integrin (F)	CTAACGGAGTCTCACAACCTC
$\alpha 6$ integrin (R)	ACTCTGAAATCAGTCCTCAG
$\beta 4$ integrin (F)	GCGACTATGAGATGAAGGTG
$\beta 4$ integrin (R)	GTGAGTTGTAGTCCCGTGTG
$\Delta$ Np63 isoform (F)	CTAACGGAGTCTCACAACCTC
$\Delta$ Np63 $\alpha$ isoform (R)	TCACTCCCCCTCCTCTTTG
$\Delta$ Np63 $\beta$ isoform (R)	TCAGACTTGCCAGATCCTG
$\Delta$ Np63 $\gamma$ isoform (R)	CTATGGGTACACTGATCGG
Vimentin (F)	GTCAGCAATATGAAAGTGTGGC
Vimentin (R)	GGTAGTTAGCAGCTTCAACGG
GAPDH (F)	GAAGGTGAAGGTCGGAGTC
GAPDH (R)	GAAGATGGTGATGGGATTC

F: Forward primer, R: Reverse primer.

### 3.22 Real-Time Quantitative PCR

cDNA was prepared as described above and used as the template for qRT-PCR (quantitative reverse transcriptase PCR). Master mix SYBR Green (ABI) was used with 200 nM of forward and reverse primers. The primer sequences used to amplify target genes and GAPDH (internal control) are listed in Table 3.8. Real-time quantitative PCR was performed with the ABI PRISM7700 Sequence Detection System. All expression values were normalized against GAPDH. All amplifications were done thrice in triplicates.

**Table 3.8 QRT-PCR primer sequences**

<b>Sr.No.</b>	<b>Primer Sequence (5'-3')</b>
E-cadherin (F)	CTTTGACGCCGAGAGCTACA
E-cadherin (R)	TTTGAATCGGGTGTCTGAGGG
Filaggrin (F)	ATCTGAGGGCACTGAAAGGC
Filaggrin (R)	CACTTCCGTGCTGAGAGTGT
Involucrin (F)	GAAACAGCCAACTCCACTGC
Involucrin (R)	ATTCTTGCTCAGGCAGTCCC
K1 (F)	TGACAAGGTGAGGTTCTCTGG
K1 (R)	GTTGGTCCACTCTCCTTCGG
K14 (F)	CCAGTTCTCCTCTGGATCGCAG
K14 (R)	GATCTTCCAGTGGGATCTGTGTCCA
K5 (F)	GAGGCCAAGGTTGATGCACTG
K5 (R)	GTCCAGGTTGCGGTTGTTGTC
Loricrin (F)	GATCTGCCACCAGACCCAG
Loricrin (R)	CCCCTGGAAAACACCTCAA
Nanog (F)	CTGCAGAGAAGAGTGTCGCA
Nanog (R)	TCTGCTGGAGGCTGAGGTAT
Oct-4 (F)	GCCCGAAAGAGAAAGCGAAC
Oct-4 (R)	AACCACACTCGGACCACATC
Slug (F)	TTCGGACCCACACATTACCT
Slug (R)	TTCTCCCCCGTGTGAGTTCTA
Snail (F)	CCAGTGCCTCGACCACTATG
Snail (R)	CTGCTGGAAGGTAAACTCTGGA
Sox2 (F)	AGGATAAGTACACGCTGCCC
Sox2 (R)	TAACTGTCCATGCGCTGGTT
Twist (F)	TCTACCAGGTCCTCCAGAGC

Sr.No.	Primer Sequence (5'-3')
Twist (R)	CTCCATCCTCCAGACCGAGA
$\alpha$ 6 integrin (F)	TTCGGGAGTACCTTGGTGGA
$\alpha$ 6 integrin (R)	AGAGCGTTTAAAGAATCCCACT
$\beta$ 4 integrin (F)	GAGGTAGGTCCAGGACGGG
$\beta$ 4 integrin (R)	GTTTGCCAAGGTCCCAGAGA
$\Delta$ Np63 (F)	TGTACCTGGAAAACAATGCCCA
$\Delta$ Np63 (R)	GACGAGGAGCCGTTCTGAATCT
Plectin (F)	TACTACCGCGAGAGTGCAGA
Plectin (R)	CTGATCCCGACTGGACCTTG
GAPDH (F)	CTTCTTTTGCCTCGCCAGCC
GAPDH (R)	GAGTTAAAAGCAGCCCTGGTGA

F: Forward primer, R: Reverse primer.

### 3.23 Immunofluorescence

Cells were grown on glass cover slips for 48 h till they reached a confluency of 60-70%. Adhered cells were washed twice with 1X PBS for 10' each. The cells were fixed either with chilled 100% methanol in -20 °C or 4% paraformaldehyde at RT for 10' and 15' respectively. After fixation, coverslips were washed thrice with 1X PBS for 10' each. The cells were then permeabilised using 0.3% Triton X-100 for 90 seconds in case of methanol fixation and 10' in 0.7% Triton X-100 when cells were fixed with paraformaldehyde. The coverslips were again washed thrice with PBS for 5' each. They were then placed in a small humidified chamber and 5% BSA was layered over the cells for blocking and incubated for 1 h. BSA was drained and the cells were layered with 50 $\mu$ l of primary antibody diluted in 5% BSA and incubated for 1h. The coverslips were washed thrice with 1X PBS for 10' each followed by incubation with 100  $\mu$ l of anti-mouse (Alexa Fluor 488) or anti-rabbit (Alexa Fluor 568) conjugated secondary antibody for

1 h and later washed with 1X PBS thrice for 10' each. Coverslips were then mounted using anti-bleaching agent (vectashield) and sealed. Confocal images were obtained using a LSM 780 Carl Zeiss Confocal system. Scatter Plot and Pearson's correlation coefficient(R) for colocalization were obtained using Carl Zeiss (zen 2012 SPI black edition, 64 bit) software.

### **3.24 Immuno-electron microscopy**

Cells were washed with 1X PBS and fixed in 3% Glutaraldehyde followed by secondary fixation in 1% Osmium tetroxide. Ultrathin (70nm) cross-sections were collected on nickel grids and subsequently micro-waved in Heat-induced Antigen Retrieval (HIAR buffer-20mMTris-HCl pH 9.0) for antigen retrieval [151]. After blocking with 5% BSA, the grids were incubated with anti-  $\beta$ 4 integrin antibody (1:20) for 1 h at RT. Following washes with 1X PBS, grids were incubated with goat anti-rabbit gold antibody (cat. no. G7402, Sigma, USA) for 1 h. After thorough washes, the grids were stained with uranyl acetate and lead citrate and viewed under Jeol 1400 plus TEM (Japan) at 120 KV. For analysis, 50 images were acquired, each of vimentin knockdown and vector control cells, at magnification of 20000X and stitched using Multiple Image Alignment tool in integrated iTEM software (Olympus soft imaging solutions, GmbH, Germany).

### **3.25 Induction of EMT and stimulation of $\beta$ 4 integrin signaling**

To induce EMT, AW13516 cells were incubated in serum free media in the presence of Transforming growth factor beta1 i.e. TGF- $\beta$ 1 (5 ng/ml) and kept at 37°C for 48 h. To study  $\beta$ 4 signaling on ligation to laminin-5, cells serum starved for 18 h were harvested using accutase and further washed with plain medium and plated on laminin-5 (2.5  $\mu$ g/ml) coated dishes. For activation of  $\beta$ 4 integrin signaling, vimentin knockdown and vector control clones were serum-

starved for 18 h and then treated with 5 µg/ml of 3E1 antibody (β4 integrin activating antibody). 5 µg/ml mouse-IgG-treated cells were used as control [152]. After treatment, the lysates were made and western blotting was performed.

### **3.26 Cell proliferation/MTT (3-(4, 5-Dimethylthiazol-2-yl)-2, 5-Diphenyltetrazolium Bromide) viability assay**

1000 cells/100 µl were seeded per well, in a 96-well microtitre plate. Proliferation was studied every 24 h up to a period of 4 days. At the desired time points, 100 µl of the medium was replenished from the designated wells and 20 µl MTT solution (5 mg/ml MTT in 1X PBS) was added to each well. Plate was incubated at 37°C in a CO<sub>2</sub> incubator for 4 h, then 100 µl of acidified SDS (10%SDS in 0.01 N HCl) was added to each well and incubated overnight at 37°C. Next day, the absorbance was measured on an ELISA plate reader at 540 nm against a reference wavelength of 690 nm. Growth curve was plotted from three independent experiments. The protocol was adapted from [153].

### **3.27 Adhesion assay**

Ninety-six well microplate was coated with laminin-5 (2.5 µg/ml)/fibronectin (5 µg/ml). Plates were kept overnight at 4°C for polymerization. Unpolymerized substrates were washed with 1X PBS and the plates were blocked with 2% BSA for 2 h at 37°C. The cells were harvested and diluted to a final concentration of 3 x 10<sup>4</sup> cells/ml in IMDM containing 0.1% BSA. 100 µl of the cell suspension was added to each substrate-coated well and cell adhesion was seen for 15'–45' at 37°C. At the end of incubation, non-adherent cells were removed by washing twice with 1X PBS. The adherent cells were quantified using MTT assay. The protocol was adapted from [154].

### **3.28 Live cell spreading assay**

For live cell spreading, cells were detached using accutase and seeded onto laminin-5 (2.5µg/ml)/fibronectin (5 µg/ml) coated surface. Phase-contrast images were captured immediately after the cells were seeded, at every 10' interval, till at least one of the group showed optimum spreading. Images were evaluated for the percentage of well spread cells. Phase-bright and rounded cells were scored as unspread, whereas elongated with visible membrane protrusions were scored as spread cells. 30 cells were counted from three independent experiments.

### **3.29 Colony-forming assay**

200 cells were plated in 60-mm tissue culture plates in triplicates. Cells were grown in complete medium for 14 days, with medium changes every 2–3 days. Cells were first fixed with methanol for 5' at RT and then washed twice with 1X PBS. They were later stained with crystal violet solution (0.5% crystal violet in 20% methanol) for 5' at RT. After washes with distilled water, the images of stained cells were captured using high-resolution Nikon camera. The colonies were counted with Metamorph software.

### **3.30 Soft agar colony forming assay**

The assay was performed in a 35 mm Petri plates. As a first step, 1 ml of the basal layer was made by adding equal volumes of 2X complete IMDM/DMEM and 2% low melting agarose. 1000 cells in complete medium containing 0.4% low melting agarose were seeded over the basal layer. Plates were fed with complete medium on every alternate day and incubated at 37°C in a 5% CO<sub>2</sub> incubator for 15 days. Opaque and dense colonies were observed and counted microscopically on day 15. The assay was carried out in triplicates.

### **3.31 Single cell migration assay**

For single cell migration assay, cells were harvested using accutase, washed with plain IMDM and plated at 30% confluency on laminin-5 (2.5µg/ml)/fibronectin (5 µg/ml) coated dishes. Unspread cells, dividing cells and cells migrating out of the selected field were excluded during analysis. The time lapse data was analysed using the manual tracking plugin of ImageJ (NIH) software. The coordinates obtained were used to plot graph and calculate distance and velocity using chemotaxis and migration tool.

### **3.32 *In vitro* wound healing assay for migration**

The cells were grown in 35 mm plates to 95% confluency. Cells were replaced with fresh IMDM/DMEM with 0.2% serum for 36 h. After incubation, the medium was discarded and wounds were scratched with the help of a sterile 2 µl pipette tip. The cells were fed with fresh IMDM/DMEM with 0.2% serum medium and observed under an Axiovert 200 M Inverted Carl Zeiss microscope fitted with a stage maintained at 37°C and 5% CO<sub>2</sub>. Cells were observed by time lapse microscopy and the images were taken every 20' for 20 h using an AxioCam MRm camera with a 103 phase 1 objective. Migration was measured using the manual tracking plugin of ImageJ (NIH) software.

### **3.33 Boyden chamber cell invasion assay**

The invasiveness of the cells was determined by the Boyden chamber invasion assay. 40 µl Matrigel (1mg/ml) with 140 µl incomplete IMDM/DMEM was applied to 8 µm-pore-size polycarbonate membrane filters and the bottom chamber was filled with 0.6 ml of complete IMDM/DMEM.  $2 \times 10^5$  cells were seeded in the chamber in serum-free medium, and then incubated for 16 h at 37°C. At the 15<sup>th</sup> h, 4 µg/ml calcein AM was added to the lower chamber and incubated for 1 h at 37°C [155]. The cells on the upper surface were carefully removed with

a cotton swab. Fluorescence of the invaded cells was read at wavelengths of 494/517nm (Ex/Em) on a bottom-reading fluorescent plate reader at the 16<sup>th</sup>h. Alternatively, for GFP positive cells, the membranes containing invaded cells were fixed with methanol and stained with 0.5% crystal violet. The invasiveness was quantified by counting 25 random fields under a light microscope. Data obtained from three independent experiments was shown as mean values.

### **3.34 Development of *in vitro* carcinogenesis model**

Cytotoxicity using different concentrations of benzo[a]pyrene was assessed using MTT based cell proliferation assay. Cells were grown in triplicate, in six-well plates at 50-60% confluency, 24 h prior to exposure. Cells were exposed to benzo[a]pyrene at concentrations of 0.5  $\mu$ M as well as DMSO control in a total of 2 ml of media, in triplicate. Cells were incubated with benzo[a]pyrene for 1 h at RT in serum free media. After 1 h exposure, the media was removed, cells were washed twice using 1X PBS, and fresh media was added. After every definite interval cells were tested for their transformation efficiency using soft agar assay and after every exposure freeze stocks were made to preserve cells of that exposure. The carcinogen treatment was stopped after the cells attained transformation and all the assays were performed within 5 passages. The protocol was adapted from [156].

### **3.35 Tumorigenicity assays**

All protocols for animal studies were reviewed and approved by the “Institutional Animal Ethics Committee (IAEC)” constituted under the guidelines of the “Committee for the Purpose of Control and Supervision of Experiments on Animals (CPCSEA)”, Government of India (Approval ID: 19/2014). The tumorigenic potential of vimentin knockdown/vector control and K5/K14 overexpressing/vector control clones was determined by subcutaneous injection in NOD-SCID mice. The cells were suspended in plain medium without serum and  $6 \times 10^6$  cells

were injected sub-cutaneously in the dorsal flank of 6–8 weeks old mice. 6 mice were injected per clone and were observed for tumor formation over a period of approximately 2 months. Tumor volume was determined using a digital vernier caliper and its calculation was carried out by the modified ellipsoidal formula, [Tumor volume =  $1/2(\text{length} \times \text{width}^2)$ ] [157].

### **3.36 Histology and immunohistochemistry**

IHC was performed on the OSCC tissue samples collected from the operation theatre of Tata Memorial Hospital, India. This study was approved by the “Human Ethics Committee”, Tata memorial centre, India (Reg Number: DCGI: ECR/149/Inst/MH/2013) and the written “informed consent” was obtained from all the patients before enrolling them in this study. Similarly for animal studies, mice were euthanized using CO<sub>2</sub> inhalation method. IHC analysis was also performed on the mice tumor tissues originated from vimentin knockdown-vector control and K5/K14 overexpressing-vector control groups. Both human and mice tumor tissues were fixed in 10% formalin buffer and processed for histology. 5 μ sections of formalin fixed and paraffin embedded tissues were stain with haematoxylin/eosin for histology. Immunohistochemical staining was performed according to previously described method [158]. As per the protocol, the tissues were subjected to microwave treatment for antigen retrieval. The sections were then blocked with preimmune horse serum for 30’ at RT followed by incubation in primary and secondary antibody. Signals were detected by an avidin-biotin based immunoperoxidase technique (Elite ABC Kit). Serum from a non-immunized mouse was used as the negative control. The expression of protein in IHC staining was quantified by visual assessment of the microscopic field by counting a total of 100 cells per field and for each section, a total of 3 fields were counted by 2 independent observers. Immunoreactivity was divided into 4 categories and

defined as follows: <5% (no), 6–30% (+/low), 31–50% (++/moderate) and >51% (+++/intense) [159].

### **3.37. Statistical analysis:**

Two groups of data were statistically analyzed by *t test* using Graphpad Prism5 Software. Two way ANOVA using Bonferroni test was performed for two factorial comparisons among multiple groups. A *p* value less than 0.05 was considered statistically significant. The clinico-pathological data and mice tumor volumes were analyzed using Statistical Package, SPSS 16.0 and SPSS 21.0 respectively.

# Chapter 4: Results

## **Results**

### **Objective 1 and 2:**

#### **Part 1**

#### **4.1 Vimentin mediates regulation of cell motility through modulation of $\beta$ 4 integrin protein levels in oral tumor derived cells**

Although, many studies have shown the association of vimentin expression with tumor cell growth, invasion and migration [5], our understanding of the molecular mechanisms underlying vimentin associated phenotype remains limited. Our current study reveals one of the mechanisms adopted by the cancer cell to bring about vimentin mediated migration/invasion.

##### **4.1.1 Downregulation of vimentin decreases in vitro transformation potential and invasiveness of OSCC derived cell line AW13516**

Expression of vimentin at mRNA and protein level (Figure 4.1.1A) was reduced significantly in vimentin knockdown clones (shvim1 and shvim2) as compared to the vector control clone (pTU6vc). Further, confocal analysis showed decreased intensity of vimentin filaments in vimentin knockdown clones (Figure 4.1.1B and C). Vimentin downregulated clones showed a significant reduction in the number of colonies (by ~50%) in soft agar as compared with vector control clones (Figure 4.1.1D and E). They demonstrated significantly decrease in migration as compared to vector control clone (Figure 4.1.1F and G). Also in the invasion assay, shvim1 and shvim2 showed 33% and 50% reduction respectively as compared to vector control clone (Figure

4.1.1H).

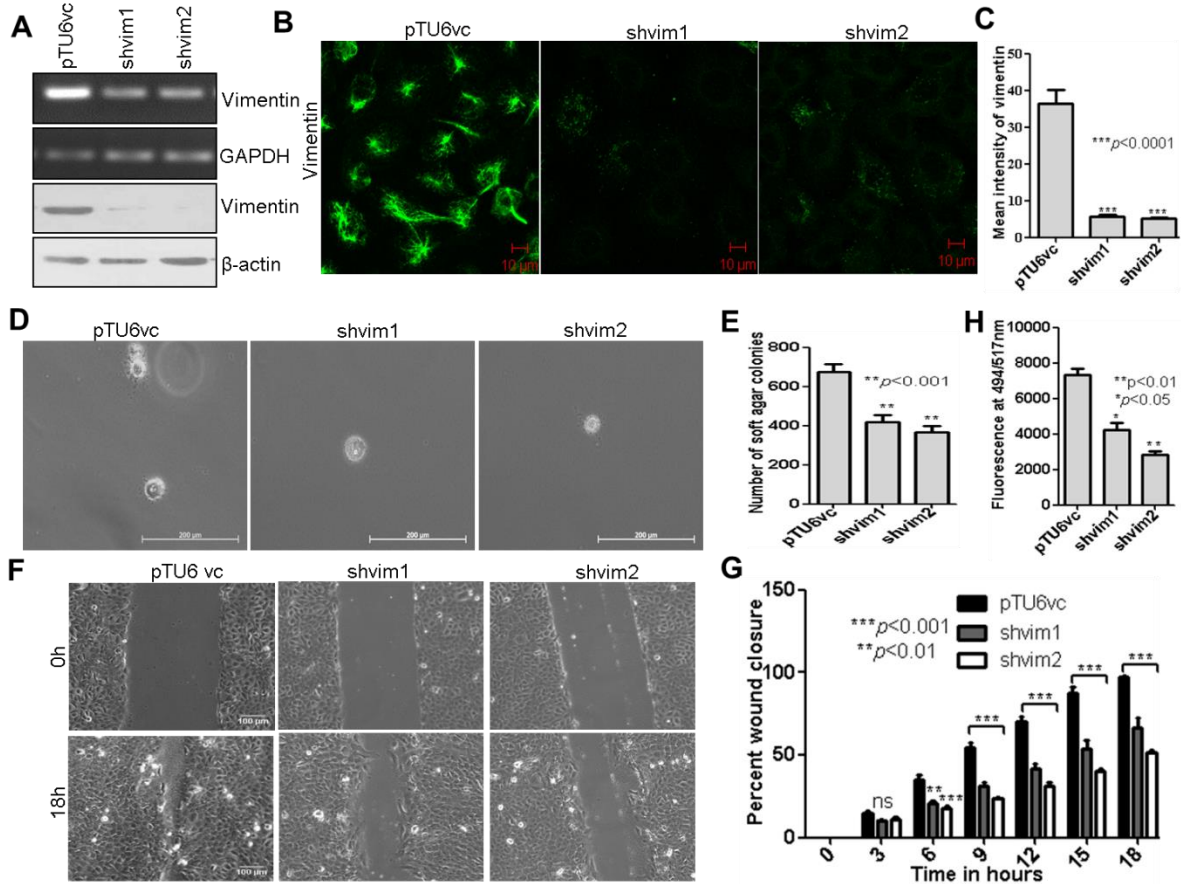


**Figure 4.1.1 Generation of vimentin knockdown clones in oral SCC derived cell line.**

(A) The upper panel shows RT-PCR while the lower panel shows the western blot analysis of vimentin, in vimentin knockdown clones (shvim1, shvim2) and its vector control clone (pTU6vc); (B) Immunofluorescence analysis of vimentin, in vimentin knockdown clones and its vector control clone. (C) The graph shows mean fluorescence intensity of vimentin across clones. (D) Representative images of colonies formed by vimentin knockdown and vector control clones in soft agar. (E) Graphical representation of number of colonies formed in soft agar. (F) Representative time lapse microscopy images showing wound healing. (G) The graph

shows percent wound closure as calculated over 18 h time point. (H) The graph shows fluorescence of invaded cells which is read at wavelengths of 494/517 nm (Ex/Em). For quantification, data represents  $\pm$  standard error mean (SEM) of three independent experiments.

#### 4.1.2 Vimentin downregulation results in a more spread morphology

Vimentin knockdown clones appeared more elongated as compared to the vector control clone (Figure 4.1.2A). Also, vimentin knockdown clones at the wound front showed a more flat, well-spread morphology as compared to the vector control clone (Figure 4.1.2B). The extent of spreading between the clones was assessed by quantifying the area of the cells at the wound edge using Image J software (Figure 4.1.2C).

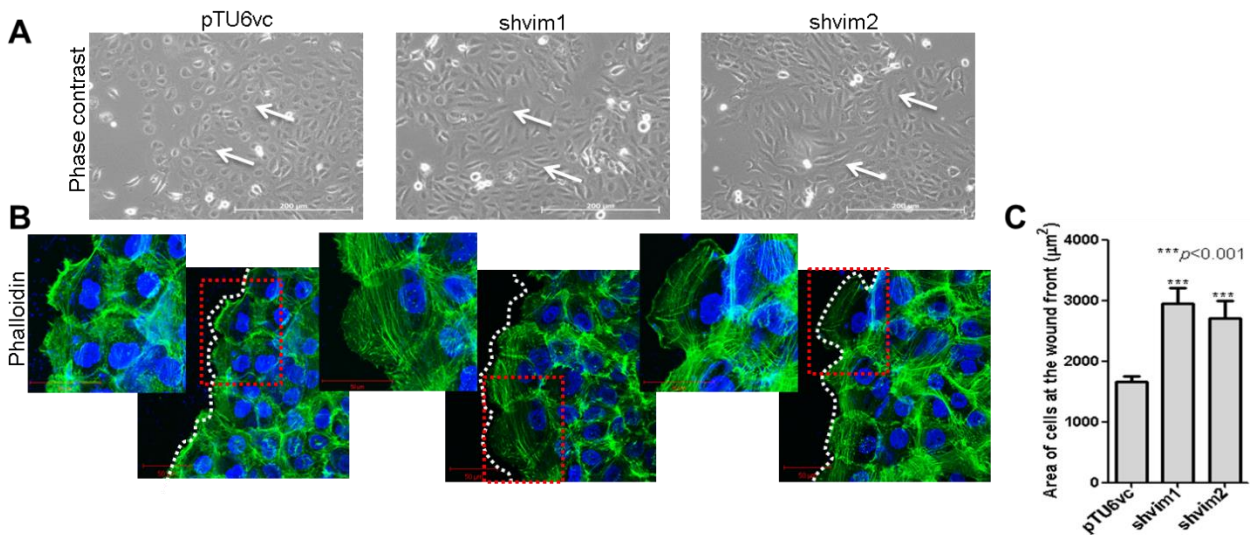


**Figure 4.1.2 Vimentin knockdown cells show elongated morphology.** (A) Representative phase contrast images of vimentin knockdown clones displaying well spread morphology compared to its vector control clone. (B) Immunofluorescence analysis of actin reorganization at the wound edge using phalloidin-FITC staining (Bar: 50μm). The inset shows prominent actin stress fibers in vimentin knockdown clones indicative of a less motile phenotype as compared to vector control clone (Bar: 50μm). (C) The graph shows area of vimentin knockdown and vector control clones at the wound front. At least 30 cells (at the wound edge) from each group were

analyzed per experiment. For quantification, data represents  $\pm$  standard error mean (SEM) of three independent experiments.

#### **4.1.3 Vimentin regulates $\beta$ 4 integrin levels**

Next, to determine the cause of the difference in cell morphology,  $\alpha$ 6 $\beta$ 4 integrin levels (which govern cell spreading) were examined.  $\beta$ 4 integrin levels were found to be upregulated at protein level while its transcript levels stayed unaffected with vimentin downregulation. Both protein and RNA levels of  $\alpha$ 6 integrin remained unaltered (Figure 4.1.3A-E). For further experiments, shvim2 clone was used, which showed higher  $\beta$ 4 integrin levels and more pronounced effects on soft agar/migration/invasion as compared to shvim1.  $\beta$ 1 integrin levels (which are also known to be regulated by vimentin [160]) were found to be downregulated in shvim2 as compared to vector control clone pTU6vc (Figure 4.1.3F). Further, increase in  $\beta$ 4 integrin levels was not coincident with the corresponding increase in its basement membrane ligand laminin-5 (Figure 4.1.3G). Moreover, vimentin knockdown cells showed downregulation of keratin 5/14 pair while keratin 8/18 levels remained unchanged (Figure 4.1.3H and I). This suggests that keratin 8/18 pair is likely to interact with increased  $\beta$ 4 integrin molecules in vimentin knockdown cells.

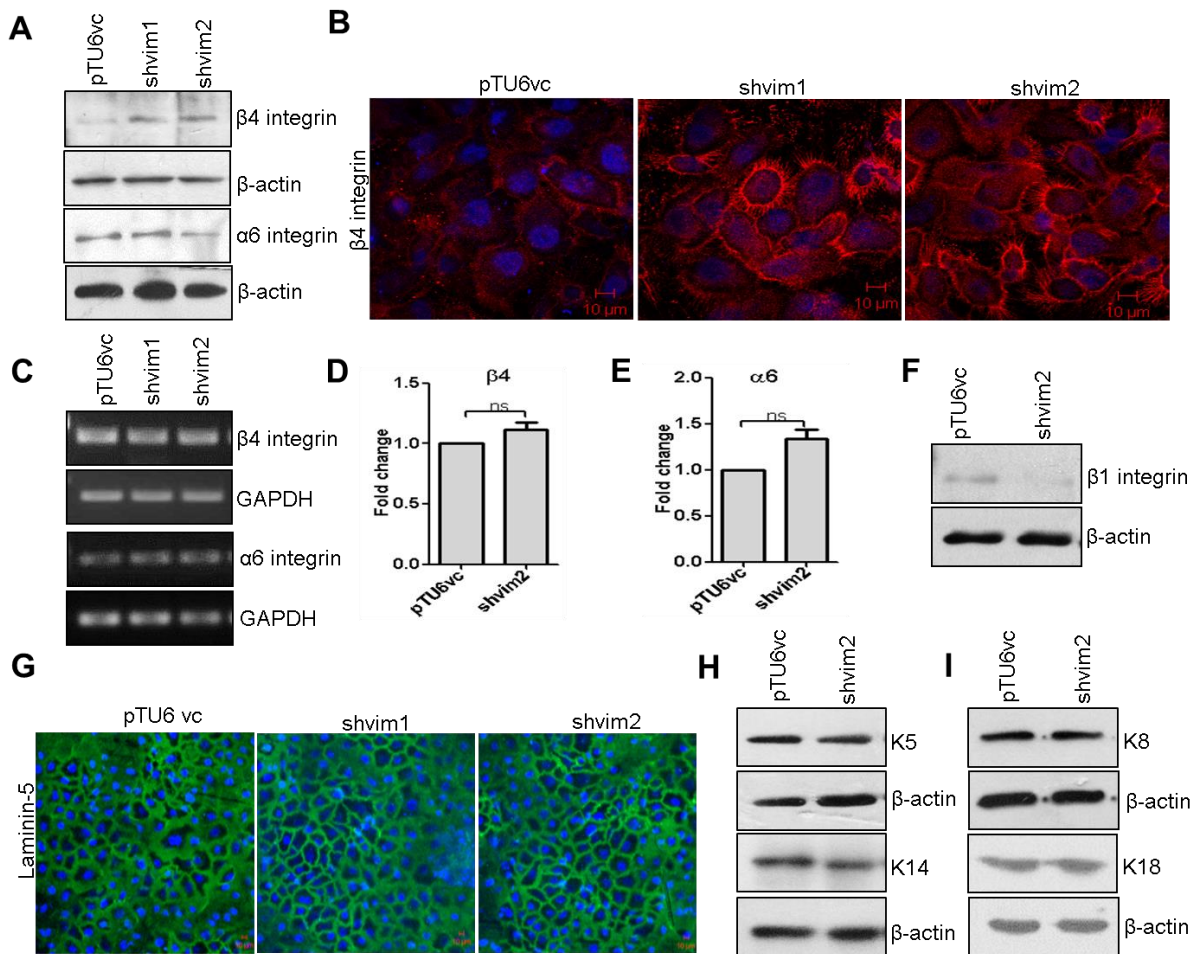


**Figure 4.1.3 Vimentin knockdown cells show upregulation of  $\beta$ 4 integrin protein levels.** (A) Western blot analysis of  $\beta$ 4 and  $\alpha$ 6 integrin in vimentin knockdown and vector control clones. (B) Immunofluorescence staining of  $\beta$ 4 integrin in vimentin knockdown and vector control clones. (C-E) RT-PCR and qRT-PCR analysis of  $\beta$ 4 and  $\alpha$ 6 integrin in vimentin knockdown and vector control clones. For qRT-PCR analysis the relative expression of the target gene was normalized to the GAPDH. (F) Western blot analysis of  $\beta$ 1 integrin levels in the clones. (G) Representative immunofluorescence image of laminin-5 (green) in vimentin knockdown and vector control clones. (H and I) Western blot analysis of K5/14 and K8/18 respectively in

vimentin knockdown and vector control clones.  $\beta$ -actin was used as a loading control. For quantification, data represents  $\pm$  standard error mean (SEM) of three independent experiments.

#### **4.1.4 Changes in vimentin expression directly correlate with the alterations in the levels of $\beta$ 4 integrin in squamous cell carcinoma (SCC) derived cell lines**

TGF- $\beta$ 1 (5ng/ml) exposure induced the expression of vimentin protein and decreased the levels of E-cadherin, marking the acquisition of EMT phenotype in AW13516 cells. Upregulation of vimentin led to the concomitant downregulation in  $\beta$ 4 integrin protein levels (Figure 4.1.4A). Next, other SCC derived cell lines AW13516, AW8507, SCC029B and A431 (Figure 4.1.4B and C) displayed an inverse relation between the status of vimentin and  $\beta$ 4 integrin protein levels. As a proof of principle, exogenous expression of vimentin in A431 demonstrated decrease in  $\beta$ 4 integrin levels compared to the vector control clone A431vc (Figure 4.1.4D). However, forced expression of vimentin in vimentin non-expressing immortalized (HaCaT) and premalignant (DOK) cell lines did not result in any changes in the levels of  $\beta$ 4 integrin (Figure 4.1.4E). Together, these results suggest that, modulation of  $\beta$ 4 integrin protein levels by vimentin is perhaps cancer specific and not cell line specific effect.

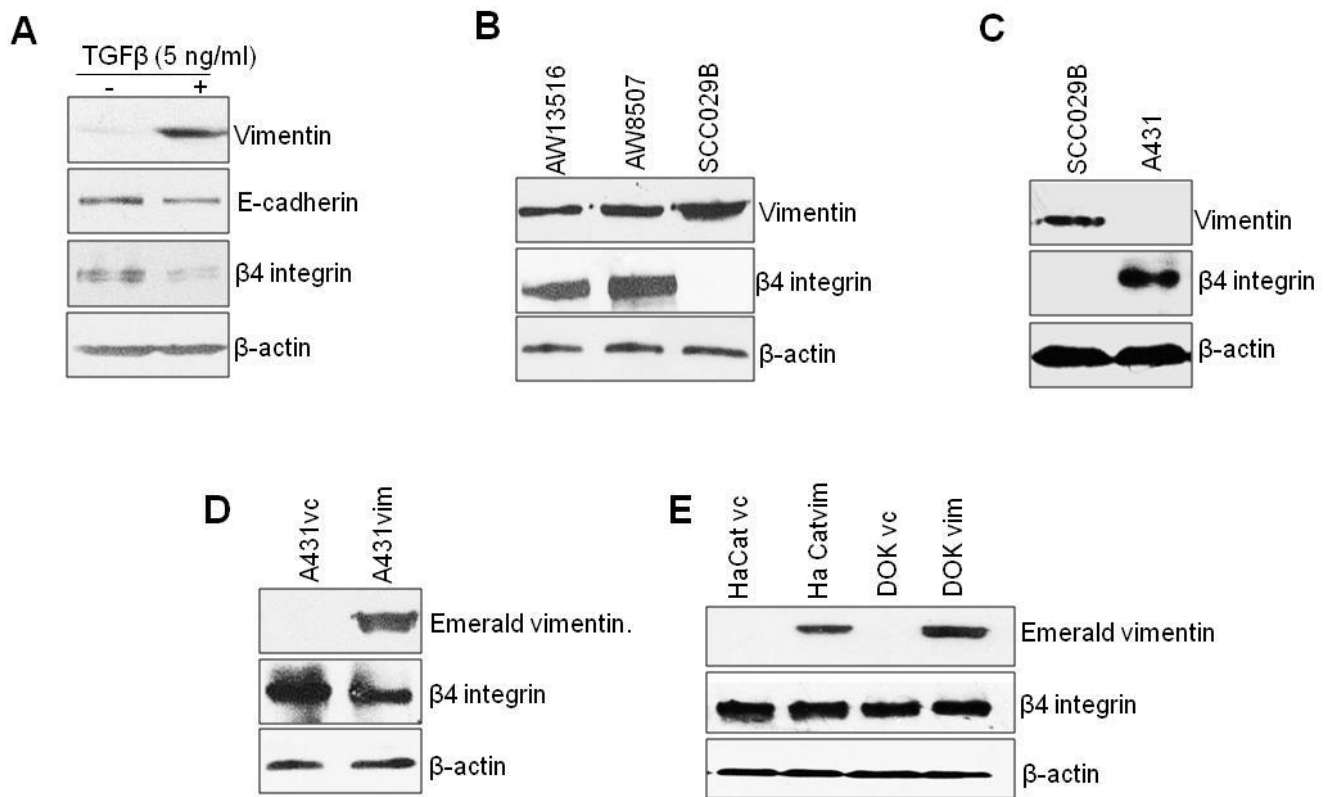


**Figure 4.1.4 Vimentin negatively regulates β4 integrin protein levels in SCC derived cells.**

(A) Protein levels of vimentin, E-cadherin and β4 integrin in TGF-β1 (5 ng/ml) treated AW13516 cells using western blot analysis. (B) Expression levels of vimentin and β4 integrin in 3 oral SCC derived cell lines using western blot analysis. (C) Expression levels of vimentin and β4 integrin in skin SCC derived cell line A431 using western blotting. SCC029B served as a positive control for vimentin expression. (D) Western blot analysis of stable vimentin overexpressing clone (A431vim) and vector control clone (A431vc) derived from the A431 parental cells with antibodies to vimentin and β4 integrin. (E) Western blot analysis of stable vimentin overexpressing clone HaCatvim, DOKvim and vector control clone HaCatvc, DOKvc derived from HaCat and DOK respectively with antibodies to vimentin and β4 integrin. β-actin was used as a loading control in all the western blotting experiments.

#### 4.1.5 Plectin could be a possible linker connecting $\beta 4$ integrin with vimentin intermediate filament protein

Plectin is known to link  $\beta 4$  integrin to the intermediate filament cytoskeleton [122]. Hence, we wanted to check if plectin acted as a linker connecting  $\alpha 6\beta 4$  integrin to vimentin. Co-immunoprecipitation with vimentin was able to pull down both plectin and  $\beta 4$  integrin (Figure 4.1.5A). Further, in vimentin knockdown clones, plectin protein levels were seen to be increased without any change at its transcript levels (Figure 4.1.5B and C). Other hemidesmosomal plaque proteins like CD151 and BP180 remained unaltered (Figure 4.1.5D).

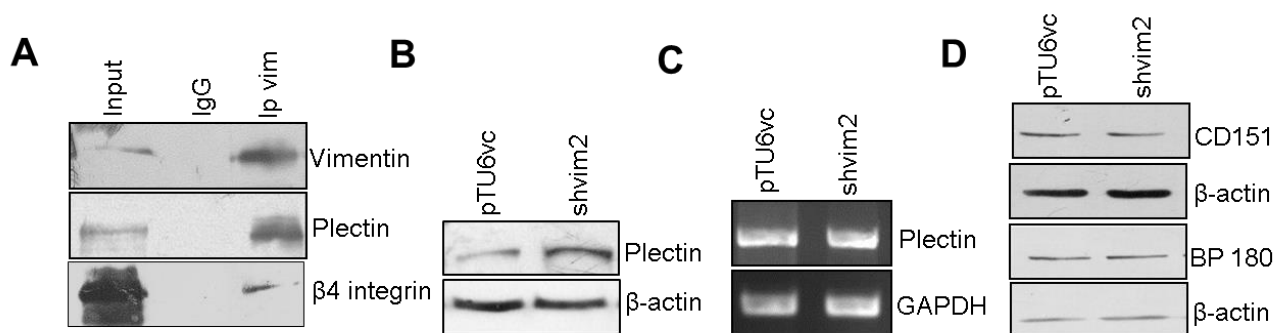


**Figure 4.1.5 Vimentin knockdown cells show upregulation of plectin protein levels.** (A) Endogenous pull down experiment with anti-vimentin antibody performed using cell lysate from AW13516 cells. The immunoprecipitated complex was examined for the presence of vimentin,  $\beta 4$  integrin and plectin. Input represented 10% of cell lysate used in the experiment. (B and C) Western blot and RT-PCR analysis of plectin in vimentin knockdown and vector control clones. (D) Western blot analysis of vimentin knockdown and vector control clones with antibodies against hemidesmosomal complex proteins CD151 and BP180.  $\beta$ -actin was used as a loading control.

#### 4.1.6 Vimentin knockdown results in increased localization of hemidesmosomal proteins ( $\beta 4$ integrin and plectin) at membrane-substrate front

To study the localization of  $\beta 4$  integrin along the site of cell substratum, we performed immunoelectron microscopy. Our results showed extensive localization of  $\beta 4$  integrin at the membrane-substrate front in vimentin knockdown cells as compared to vector control cells (Figure 4.1.6A-C).

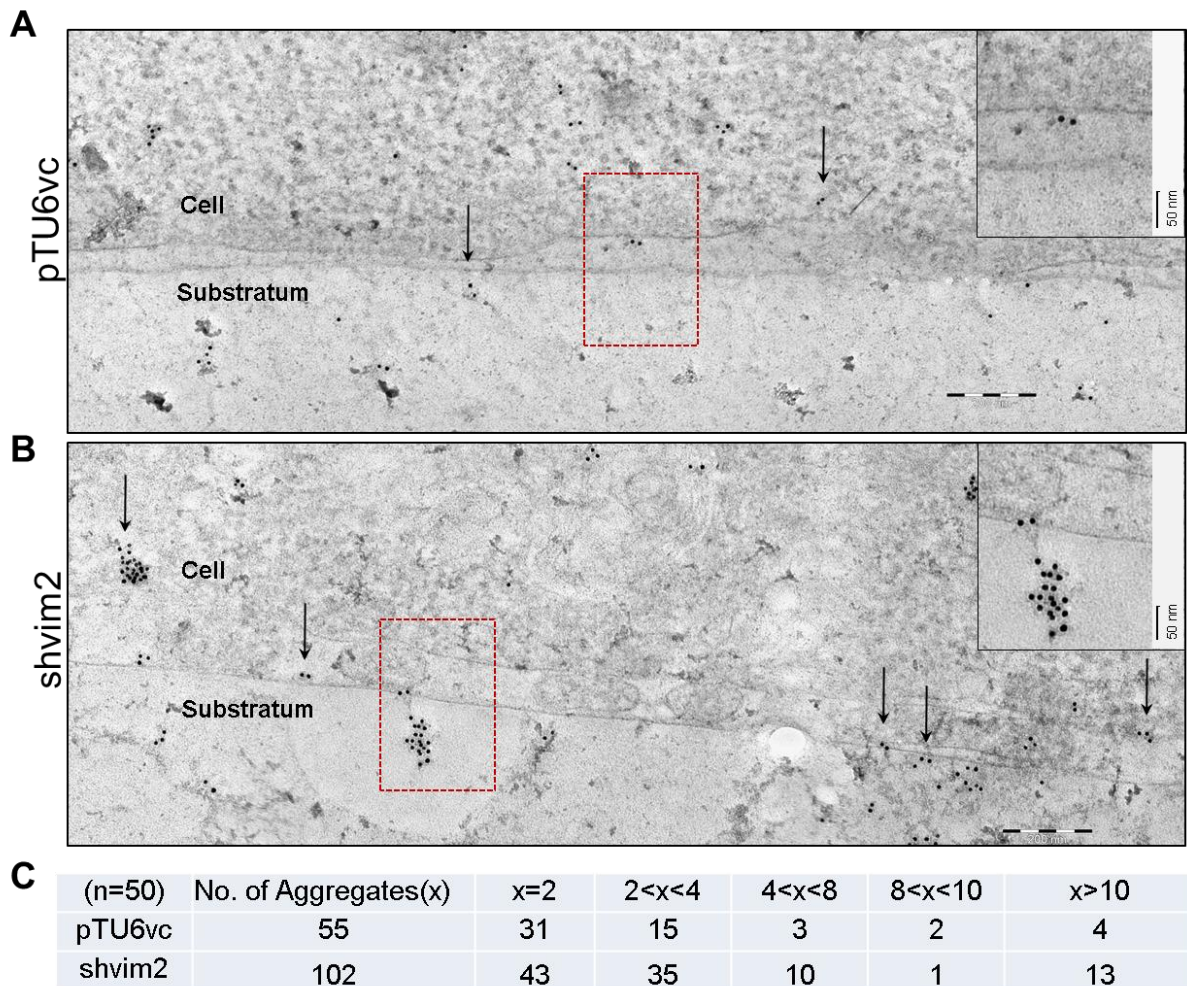


**Figure 4.1.6** Vimentin knockdown cells showed increased localization of  $\beta 4$  integrin at the cell membrane to substratum front. Immunogold staining for  $\beta 4$  integrin was performed on vimentin knockdown and vector control clones (magnification: 20,000X). Cells were grown for

60 h on laminin-5 coated surface and sections were prepared perpendicular to the substratum. Representative images (Bar: 200nm) of immunogold labeling of  $\beta 4$  integrin in (A) vector control and (B) vimentin knockdown cells. Arrows point towards the  $\beta 4$  integrin staining (black grains) along the substratum attached surface of the cell. The region inside the red box is enlarged in the inset. Bar: 50nm. (C) Analysis of  $\beta 4$  integrin (black grains) along the cell membrane-substrate interface for (n=50) images each of vector control and vimentin knockdown cells, using integrated iTEM software (Olympus soft imaging solutions, GmbH, Germany). The table shows number of gold particles in each aggregate, which represents  $\beta 4$  integrin staining.

#### **4.1.7 Vimentin knockdown results in increased colocalization between $\beta 4$ integrin and plectin**

Next we studied the colocalization of  $\beta 4$  integrin and plectin using immunofluorescence. As shown in (Figure 4.1.7A and B), the degree of co-localization of  $\beta 4$  integrin and plectin is higher in vimentin knockdown as compared to vector control clone. Also, at the wound front,  $\beta 4$  integrin and plectin showed higher co-localization in vimentin knockdown as compared to vector control cells (Figure 4.1.7C and D).

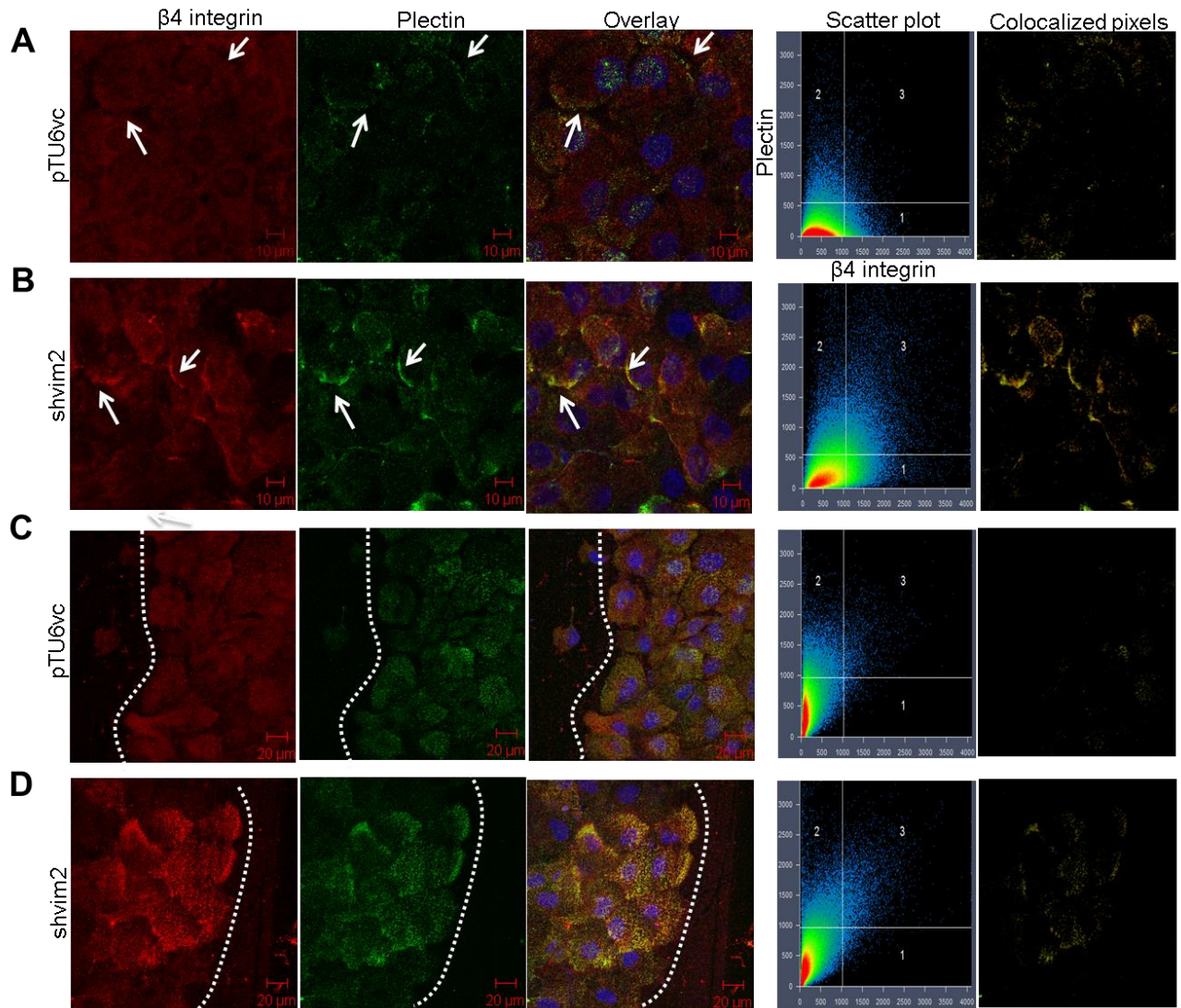


**Figure 4.1.7  $\beta 4$  integrin/plectin colocalize strongly at the membrane upon vimentin knockdown.** (A, B) The degree of colocalization of  $\beta 4$  and plectin is higher in vimentin knockdown (Correlation  $R=0.3422$ ) as compared to vector control clones (Correlation  $R=0.18095$ ). 10 random fields from 3 independent experiments were used for analysis. (C, D) The colocalized regions are prominently seen at the wound front in vimentin knockdown as compared to vector control clone. Scatter plot shows the intensity of  $\beta 4$  (x-axis) and plectin (y-axis) for each pixel. On the right, are the respective pictures of only colocalized pixels.

#### 4.1.8 Vimentin knockdown results in enhanced interaction between $\beta 4$ integrin and plectin

The above results were further confirmed by immunoprecipitation with antibody to plectin or  $\beta 4$  integrin. Both plectin IP and  $\beta 4$  integrin IP fraction showed increased levels of  $\beta 4$  integrin and plectin respectively in vimentin knockdown as compared to vector control clone (Figure 4.1.8A and B). This observation suggests that increased levels of plectin and  $\beta 4$  integrin correspond to an increase in the interaction between the two, in the case of vimentin knockdown clone.

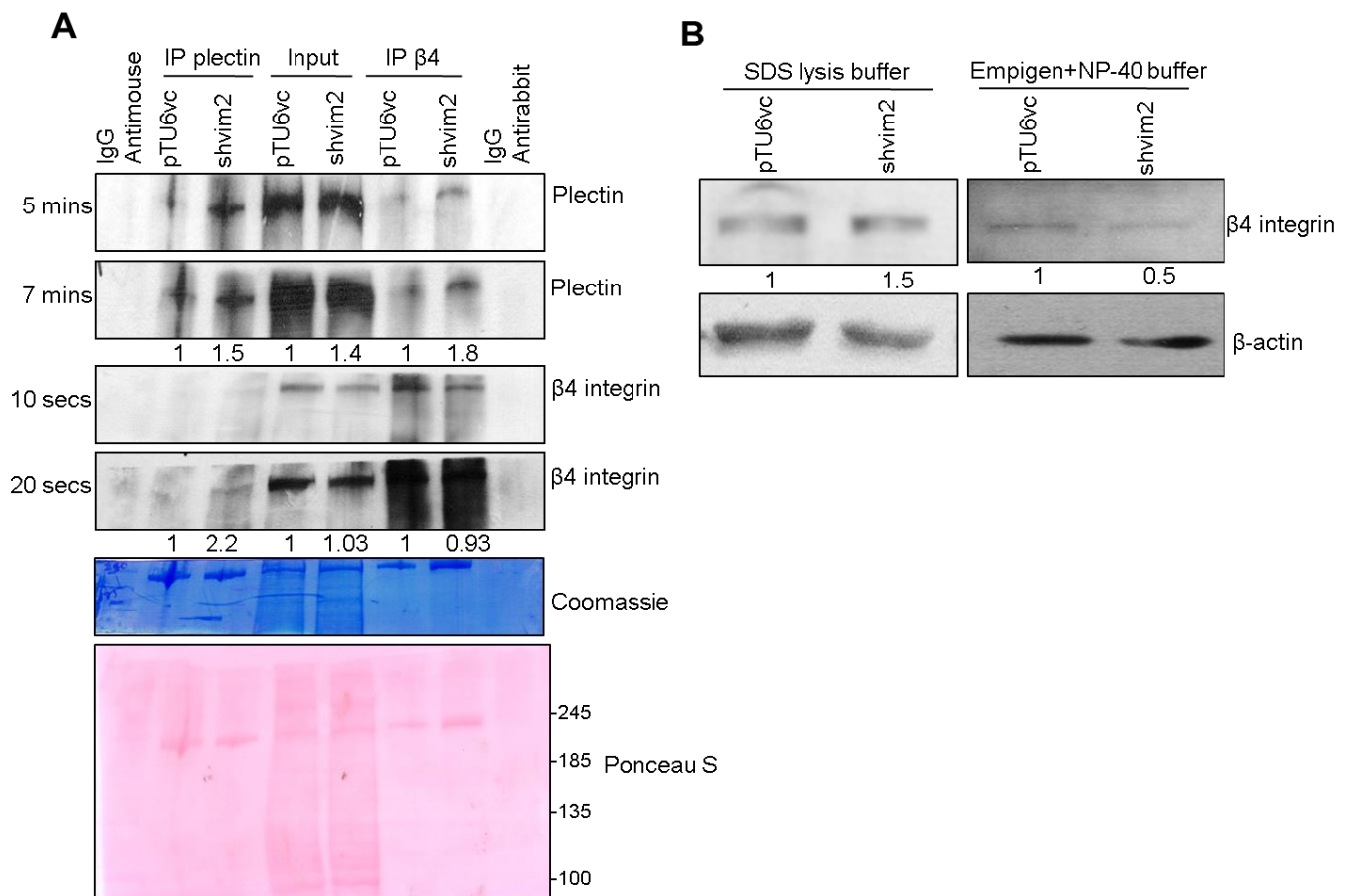


**Figure 4.1.8 Vimentin downregulation results in increased  $\beta 4$  integrin-plectin interaction.**

Cell lysates from vimentin knockdown and vector control clones were incubated with antibody against plectin or  $\beta 4$  integrin. Immunocomplexes formed were bound to protein A beads, and the precipitates were subjected to immunoblotting using  $\beta 4$  integrin or plectin antibody respectively. Input represented 10% of cell lysate used in the experiment. The coomassie stained blot is used

as a loading control. (A) Vimentin knockdown clone showed increased levels of  $\beta 4$  integrin when immunoprecipitated with plectin antibody, correspondingly its immunoprecipitation with  $\beta 4$  integrin antibody showed increased plectin levels as compared to vector control clones. (B) The  $\beta 4$  integrin levels in the input fraction of vimentin knockdown cells are similar to that of vector control as shown in (7A), essentially because the membrane bound fraction of  $\beta 4$  integrin is not extracted as efficiently with the empigen-NP-40 buffer as with SDS lysis buffer.

#### **4.1.9 Functional consequence of $\beta 4$ integrin upregulation in vimentin knockdown cells**

As assessed using cell-ECM adhesion assay, the attachment of vimentin knockdown clone to laminin-5 increased significantly with time as compared to vector control clone (Figure 4.1.9A). Consistent with our results of adhesion assay, vimentin knockdown cells showed more spread morphology on laminin-5 (Figure 4.1.9B and C) while migration on laminin-5 (Figure 4.1.9D-F) was significantly reduced as compared to vector control cells. Since, these assays demonstrated that the vimentin knockdown cells have acquired specific and increased adherence to laminin-5, we hypothesized that, if the interaction between  $\beta 4$  integrin and laminin-5 is inhibited, the cells would be more motile. Treatment with adhesion blocking antibody of  $\beta 4$  integrin (ASC-8), which abrogates laminin-5- $\beta 4$  integrin interaction [161], demonstrated higher in vitro invasive potential in vimentin knockdown as compared to vector control clones (Figure 4.1.9G). Since, vector control clones already exhibit decreased  $\beta 4$  integrin levels; further blocking did not rescue the phenotype to a larger extent.

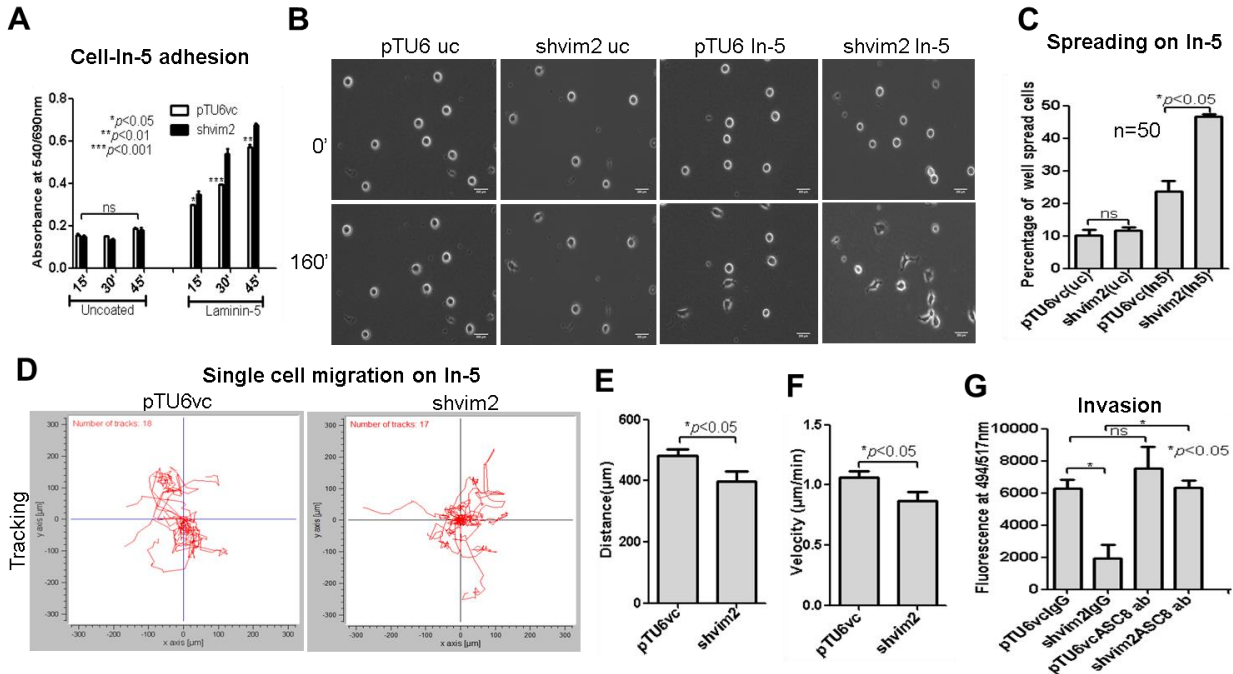


**Figure 4.1.9 Functional consequences of upregulation of  $\beta 4$  integrin in vimentin depleted cells.** (A) Vimentin knockdown and vector control clones were allowed to attach to a 96 well laminin-5 (In5) coated or uncoated (uc) surface. The unadhered cells were removed at different time points, and the number of adhered cells was determined using MTT assay. (B) Representative phase contrast images (20X) of vimentin knockdown and vector control clones at 0' and 160'. Cells were seeded at low density on laminin-5 coated/uncoated surface. Images were recorded after every 10' interval, till 160'. The upper panel shows the cells at 0' and the lower panel shows the cells at 160'. (C) The graph shows percentage of well spread cells on laminin-5 coated or uncoated surface. (D) Single cell migration was performed on laminin-5 coated surface. Each line indicates the migration trace of each cell. pTU6vc (n = 18) and shvim2 (n = 17). (E, F) Graph shows distance and velocity of cell migration respectively. (G) The cells were treated with IgG or ASC-8 antibody ( $\beta 4$  integrin adhesion blocking antibody) and incubated for 1h on ice before proceeding for the invasion assay. The graph shows fluorescence of invaded cells which is read at wavelengths of 494/517nm (Ex/Em).

#### 4.1.10 Vimentin knockdown cells show decreased spreading and migration on fibronectin

Unlike the results with laminin-5, vimentin knockdown cells showed no difference in adhesion to fibronectin (Figure 4.1.10A). Vimentin downregulation resulted in decreased spreading (Figure 4.1.10B and C) and migration (Figure 4.1.10D-F) on fibronectin coated surface. Thus, our results on fibronectin, in turn, indicated that the phenotypic effects seen on vimentin knockdown background, are laminin-5 specific.

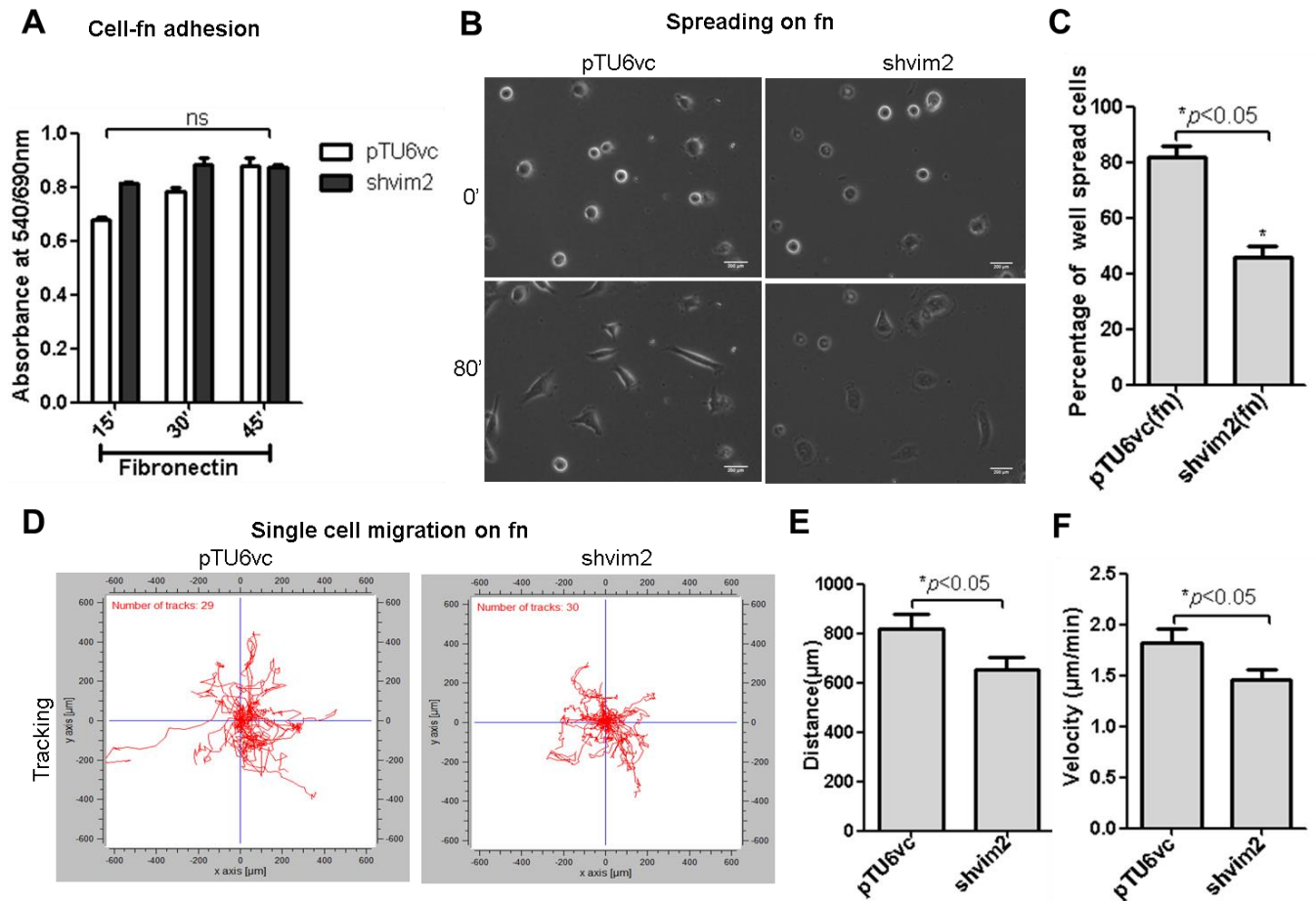


**Figure 4.1.10 Phenotypic effects of vimentin downregulation on fibronectin coated surface.**

(A) Vimentin knockdown and vector control clones were allowed to attach on 96 well fibronectin (fn) coated surface. At different time points the unadhered cells were removed and the number of adhered cells was determined using MTT assay. (B) Representative phase contrast

images (20X) of vimentin knockdown (shvim2) and vector control clones (pTU6vc) at 0' and 80'. Cells were seeded at low density on fibronectin coated surface. Images were recorded after every 10' interval, till 80'. (C) The graph shows percentage of well spread cells on fibronectin coated surface. (D) Single cell migration was performed on fibronectin coated surface. Each line indicates the migration trace of each cell. pTU6vc (n = 29) and shvim2 (n = 30). (E, F) Graph shows distance and velocity of cell migration respectively.

#### **4.1.11 Downstream molecules associated with $\beta$ 4 integrin mediated adhesive phenotype**

Some of the molecules involved in  $\beta$ 4 integrin mediated inside-out and outside-in signaling were tested upon vimentin downregulation. The previous report has shown that ligation of  $\beta$ 4 integrin on non-modified plastic increases cell adhesion which involves activation of PKB/Akt pathway [162]. We found increased phosphorylation of AKT on laminin-5 surface in vimentin knockdown as compared to vector control cells while the uncoated surface did not show any significant difference (Figure 4.1.11A). The outside in signaling of  $\beta$ 4 integrin was assessed by stimulating  $\beta$ 4 integrin with its activating antibody 3E1 and probing for molecules that represent different pathways downstream of  $\beta$ 4 [127]. The activation of ERK remained unaffected while decreased phosphorylation of AKT was seen in vimentin knockdown as compared to vector control clones (Figure 4.1.11B and C). These findings demonstrate that adhesion related signaling predominates upon vimentin downregulation.

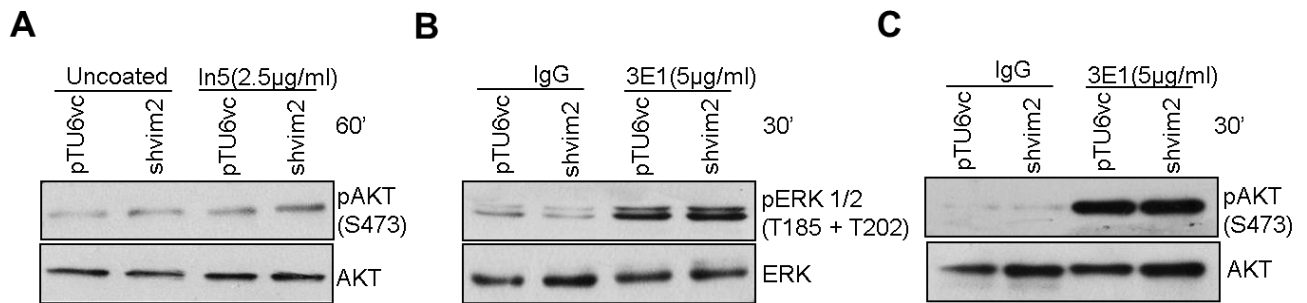


**Figure 4.1.11 Vimentin knockdown cells show increased adhesion associated signaling.** (A)

Vimentin knockdown and vector control cells were serum starved and plated on to laminin-5 coated surface for 1 h. Protein extracts were analyzed for pAKT using western blot analysis. (B, C) The serum starved clones were stimulated with 3E1 or mouse IgG for 30' and protein extracts were analyzed for the activation of ERK1/2 and AKT. Total AKT and ERK1/2 were used as loading controls.

#### **4.1.12 Vimentin knockdown results in decreased protein turnover of $\beta$ 4 integrin and plectin**

The increased expression of  $\beta$ 4 integrin at protein level without any change in its mRNA suggested higher stability of this protein in vimentin deficient background. Upon cycloheximide (CHX; inhibitor of protein biosynthesis) treatment,  $\beta$ 4 integrin levels remained almost unaffected in vimentin knockdown while 40% reduction was observed in the vector control cells (Figure 4.1.12A). The altered turnover rate of  $\beta$ 4 integrin in response to changes in vimentin levels suggested differential regulation by one or more of its known protein degradation modes; which includes, proteasome, lysosome, MMP's and calpain. Blockade of proteasome using MG-132 did not alter the levels of  $\beta$ 4 integrin in vimentin knockdown while vector control clone showed a significant increase (Figure 4.1.12B). Additionally, most of the integrins are internalized through

lysosomal pathway [163] and defective acidification of lysosomes has been shown in vimentin-null cells [164]. Treatment with lysosomal inhibitor chloroquine (CQ) resulted in decrease in  $\beta 4$  integrin protein levels in vimentin knockdown while vector control clone showed 2.7 fold increase (Figure 4.1.12C). Moreover,  $\beta 4$  integrin is also known to be cleaved by matrix metalloproteinase (MMP)-2 and -9 [165]. MMP9 showed upregulation whereas MMP2 was downregulated in vimentin knockdown as compared to vector control clone (Figure 4.1.12D), indicating that it may not have a role in  $\beta 4$  integrin cleavage. Further, plectin followed similar stability trend in vimentin knockdown and vector control clones as observed for  $\beta 4$  integrin (Figure 4.1.12E-G). This indicates decreased targeting of  $\beta 4$  integrin and plectin to proteasomes and lysosomes in vimentin deficient background.

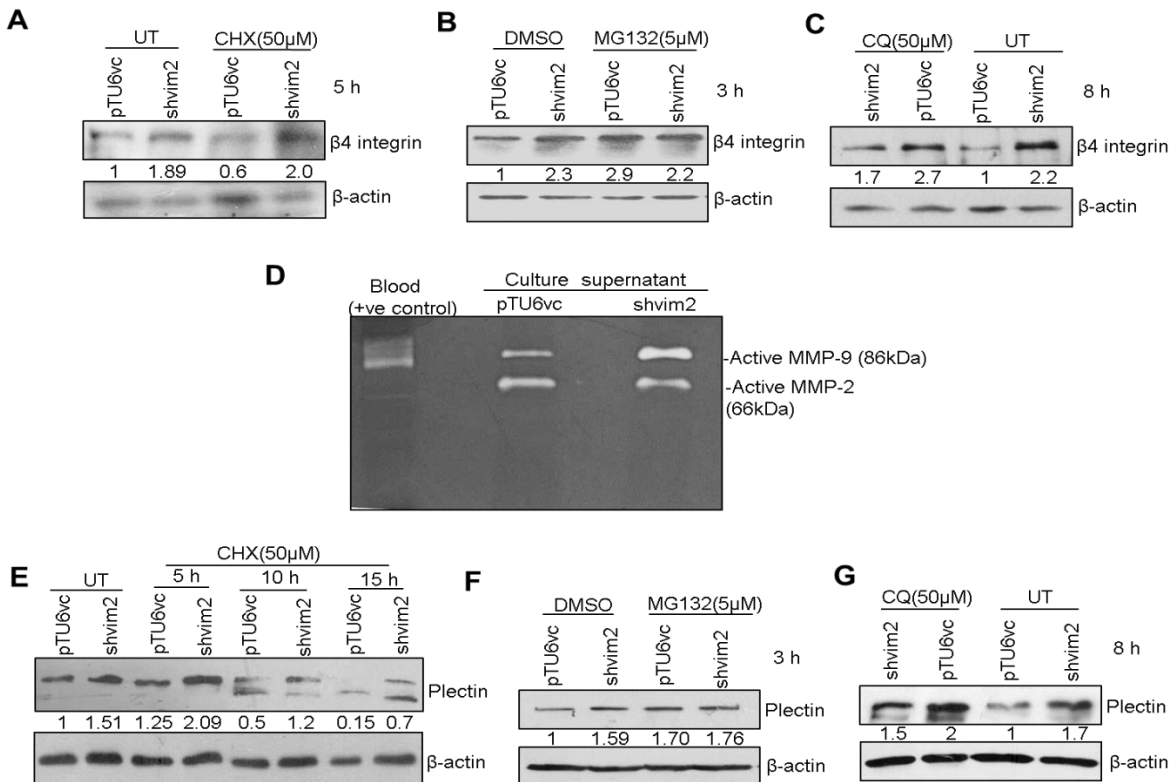


**Figure 4.1.12 Vimentin regulates the turnover of  $\beta 4$  integrin and plectin.** (A-C) Vimentin knockdown and vector control clones were treated with cycloheximide (50  $\mu$ M), MG-132 (5  $\mu$ M)

and chloroquine (50  $\mu$ M) respectively.  $\beta$ 4 integrin levels were assessed after respective treatments using immunoblotting.  $\beta$ -actin was used as a loading control.(D)Gelatin zymography was performed to detect the presence of MMP2 and MMP9 using the culture supernatant from vimentin knockdown and vector control clone. Blood was used as a positive control. (E-G)Vimentin knockdown and vector control clones were treated with cycloheximide (50  $\mu$ M), MG-132 (5  $\mu$ M) and chloroquine (50  $\mu$ M) respectively. Plectin levels were assessed after respective treatments using immunoblotting.  $\beta$ -actin was used as the loading control.

#### **4.1.13 Downregulation of $\beta$ 4 integrin in vimentin knockdown background rescues vimentin knockdown phenotype**

To verify whether the phenotype associated with reduced cell migration in vimentin knockdown cells was due to higher  $\beta$ 4 integrin levels, it was stably downregulated in vimentin knockdown clone shvim2. sh  $\beta$ 4 (shRNA against  $\beta$ 4) showed a reduction in the levels of  $\beta$ 4 integrin and its colocalization with plectin as compared to scr  $\beta$ 4 (scrambled shRNA) (Figure 4.1.13A-D).  $\beta$ 4 integrin knockdown cells demonstrated increased number of colonies in soft agar (Figure 4.1.13E and F). No significant effect was seen in the protein levels of other hemidesmosomal complex proteins like, plectin, CD151 and BP180 respectively (Figure 4.1.13G-I).

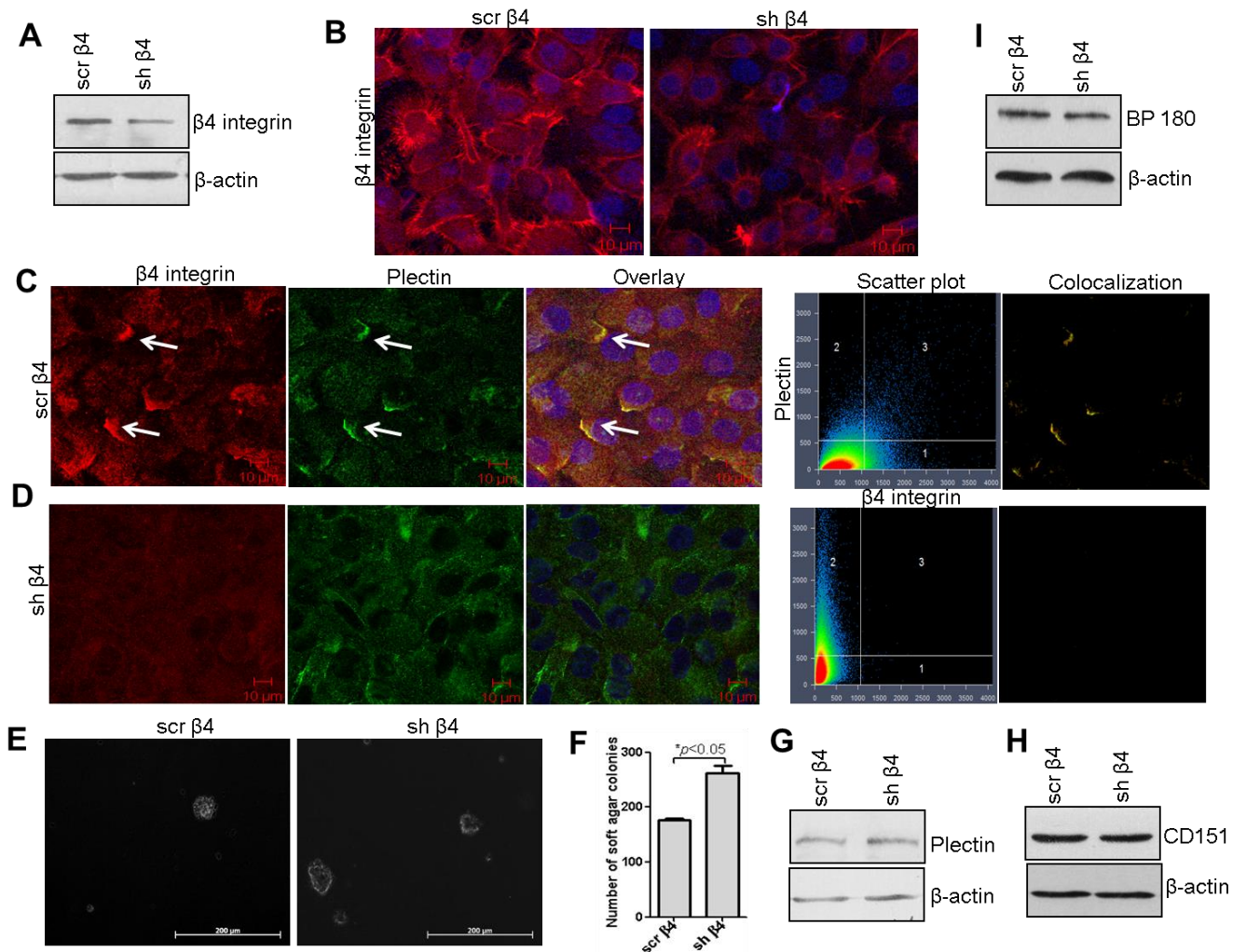


**Figure 4.1.13 Downregulation of  $\beta 4$  integrin in vimentin knockdown background.** (A, B) Western blot and immunofluorescence analysis showing  $\beta 4$  integrin levels in sh  $\beta 4$  (shRNA against  $\beta 4$  integrin) and scr  $\beta 4$  (scrambled vector control) (C, D) Immunofluorescence images of  $\beta 4$  integrin/plectin colocalization in scr  $\beta 4$  (Correlation  $R=0.2490$ ) and sh  $\beta 4$  clones (Correlation  $R=0.188$ ). 10 random fields from 3 independent experiments were used for analysis. (E) Representative images of colonies formed by scr  $\beta 4$  and sh  $\beta 4$  in soft agar. (F) Graphical representation of number of colonies formed in soft agar (G-I) Western blot analysis showing the protein levels of other hemidesmosomal complex proteins plectin, CD151 and BP180 respectively. For quantification, data represents  $\pm$  SEM of three independent experiments.

#### 4.1.14 $\beta 4$ integrin downregulation rescued the vimentin knockdown phenotype

Upon  $\beta 4$  integrin downregulation, a decrease was seen in cell-laminin-5 adhesion (Figure 4.1.14A) and spreading (Figure 4.1.14B and C). A corresponding increase was observed in migration on laminin-5 (Figure 4.1.14D-F) and transwell invasion (Figure 4.1.14G). Activation of AKT on ligation to laminin-5 (Figure 4.1.14H) showed significant decrease. However, only marginal decrease in the phosphorylation of ERK and AKT (Figure 4.1.14I and J) was seen following stimulation with the 3E1 antibody. This was an expected finding since the knockdown of  $\beta 4$  integrin resulted in an overall decrease in the number of available  $\beta 4$  integrin molecules to transmit the signal. Cumulatively, these findings confirm that the more adhesive and less migratory phenotype associated with vimentin knockdown clone is regulated through  $\beta 4$  integrin.

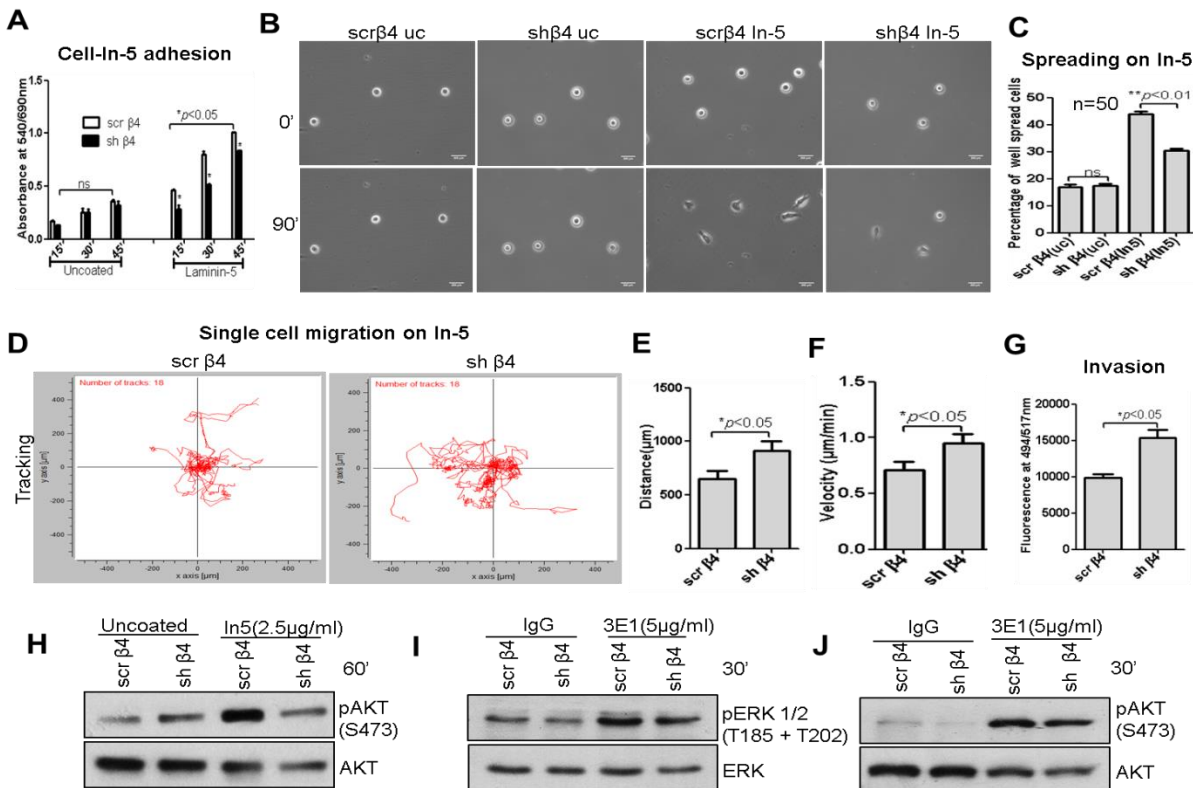


**Figure 4.1.14 Effect of  $\beta 4$  integrin knockdown on its mechanical and signaling function.** (A) sh  $\beta 4$  and scr  $\beta 4$  were allowed to attach on laminin-5 coated or uncoated surface. At different

time points the unadhered cells were removed and the number of adhered cells was determined using MTT assay. (B) Representative phase contrast images (20X) of sh  $\beta 4$  and scr  $\beta 4$  in vimentin knockdown background at 0' and 90'. Cells were seeded at low density on laminin-5 coated/uncoated surface. Images were recorded after every 10' interval, till 90'. The upper panel shows the cells at 0' and the lower panel shows the cells at 90'. (C) The graph shows percentage of well spread cells on laminin-5 coated or uncoated surface. (D) Single cell migration was performed on laminin-5 coated surface. Each line indicates the migration trace of each cell. Scr $\beta 4$  (n = 18) sh  $\beta 4$  (n = 18). (E, F) Graph shows distance and velocity of cell migration respectively. (G) The graph shows fluorescence of invaded cells at 494/517nm (Ex/Em) wavelength ratio. (H-J) Western blots showing signaling of the clones on laminin-5 coated surface (pAKT/AKT) and in response to 3E1 antibody (pERK/ERK and pAKT/AKT) respectively. For quantification, data represents  $\pm$  SEM of three independent experiments.

#### **4.1.15 High vimentin and low $\beta 4$ integrin protein levels are associated with poor survival**

Immunohistochemistry analysis showed an inverse correlation between  $\beta 4$  integrin and vimentin expression (Spearman's nonparametric correlation = -0.200,  $p=0.044$ ,  $n=74$ ) in oral tumor tissues (Figure 4.1.15A), which corroborated with our *in vitro* findings. Interestingly, significant correlation was seen between expression levels of these proteins and some clinical parameters like, stage ( $p = 0.050$ ), tumor size ( $p = 0.037$ ) and node status ( $p = 0.021$ ) (Table 4.1). Kaplan–Meier survival analysis, on the basis of IHC, showed that high vimentin expression was associated with poor survival ( $p = 0.008$ ) (Figure 4.1.15B). Similarly, low  $\beta 4$  integrin expression showed a trend (albeit not significant) for poor prognosis ( $p = 0.238$ ) (Figure 4.1.15C). In addition, combined expression of high vimentin-low  $\beta 4$  integrin was found to strongly correlate

with the poor survival of oral cancer patients ( $p = 0.005$ ) (Figure 4.1.15D). This implies that vimentin and  $\beta 4$  integrin together may be used for prognostication of oral cancer patients.

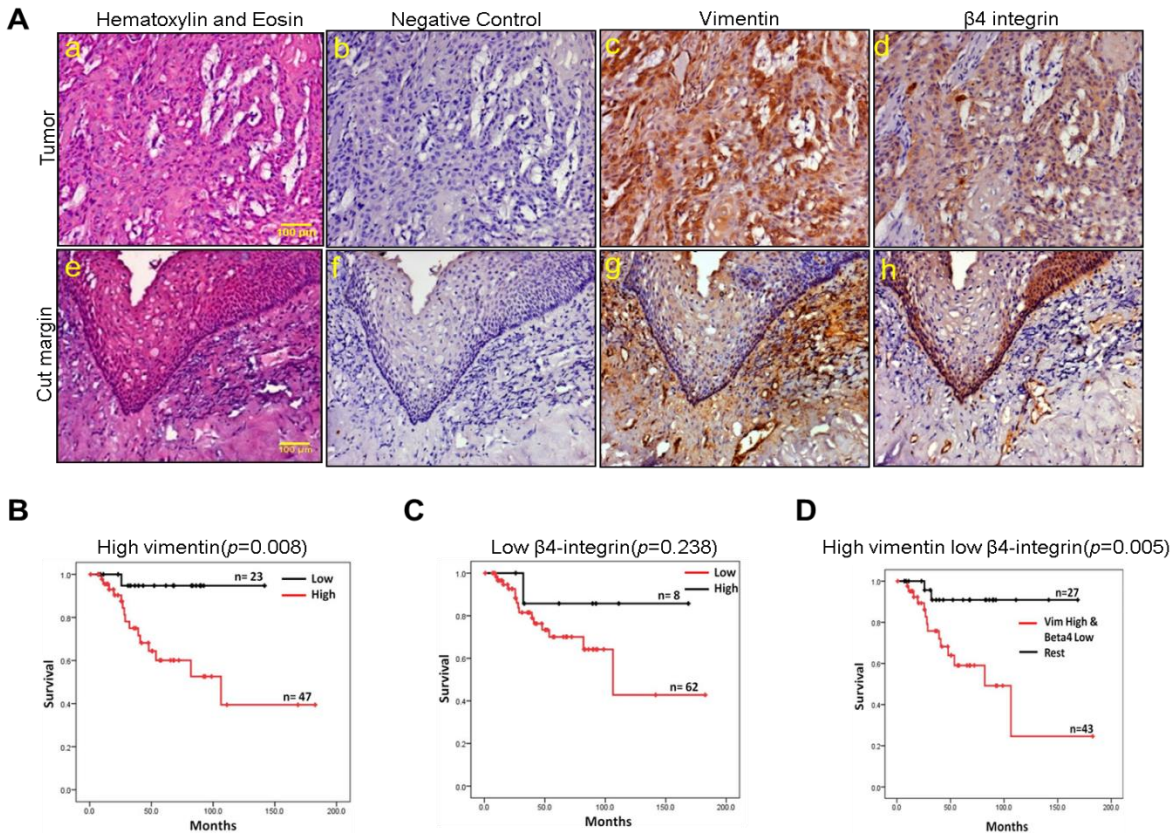


**Figure 4.1.15 High vimentin and low  $\beta 4$  integrin staining intensity together correlates with poor survival in oral SCC patients.** (A) (a-d) The upper panel shows images of haematoxylin and eosin, negative control and IHC staining of vimentin and  $\beta 4$  integrin respectively in tumor tissue while lower panel (e-h) shows images of haematoxylin and eosin, negative control and IHC staining of vimentin and  $\beta 4$  integrin respectively in cut margin tissue. Kaplan-Meier survival analysis (n=70) of (B) High vs. low vimentin expression (C) High vs. low  $\beta 4$  integrin expression and (D) High vimentin/low  $\beta 4$  integrin vs. rest other combinations of vimentin and  $\beta 4$  integrin expression.

**Table 4.1 Correlations of co-expression of vimentin and  $\beta$ 4 integrin with clinico-pathological parameters of the OSCC patients (n=74).**

Clinico-pathological parameter		n = 74	Vimentin (Vim) and $\beta$ 4 integrin ( $\beta$ 4)			
			Expression			p-value
			Vim (High) $\beta$ 4(Low)	Vim (High) $\beta$ 4(High)	Vim (Low) $\beta$ 4(Low/High)	
Age (Years)	<50	41	25	3	13	0.720*
	$\geq$ 50	33	21	1	11	
Sex	Male	60	37	3	20	0.910*
	Female	14	9	1	4	
Site	Tounge	30	19	0	11	0.221*
	BM	44	27	4	13	
Thickness	<2cm	54	35	2	17	0.509*
	$\geq$ 2cm	20	11	2	7	
Stages	< III	20	9	1	10	0.050 <sup>#</sup>
	$\geq$ III	54	37	3	14	
Tumor Size	<T3	27	13	1	13	0.037 <sup>#</sup>
	$\geq$ T3	47	33	3	11	
Node Status	YES	49	34	4	11	0.021*
	NO	25	12	0	13	
Differentiation	Poor/Moderate	67	41	4	22	0.756*
	Well	7	5	0	2	
Bone	Positive	22	13	3	6	0.061*
	Negative	39	27	0	12	
	NA	13				
Perineural Invasion	Yes	18	14	1	3	0.062*
	No	50	30	0	20	
	NA	6				
Perineural Extension	Yes	34	21	3	10	0.205*
	No	33	21	0	12	
	NA	7				

\*Pearson Chi-Square, <sup>#</sup> Spearman Correlation (Ordinal by Ordinal), NA: Data not available.

#### 4.1.16 Summary of part 1

To summarize, vimentin knockdown resulted in increased  $\beta 4$  integrin surface levels leading to strong adhesive contacts. This manifested into decreased motility (Figure 4.1.16). Interestingly, along with  $\beta 4$  integrin, its linker protein plectin was also upregulated with vimentin downregulation probably due to decreased targeting of these molecules to proteasomal and lysosomal machinery. Further, significant correlation was observed between high vimentin- low  $\beta 4$  integrin expression and poor survival of oral cancer patients.

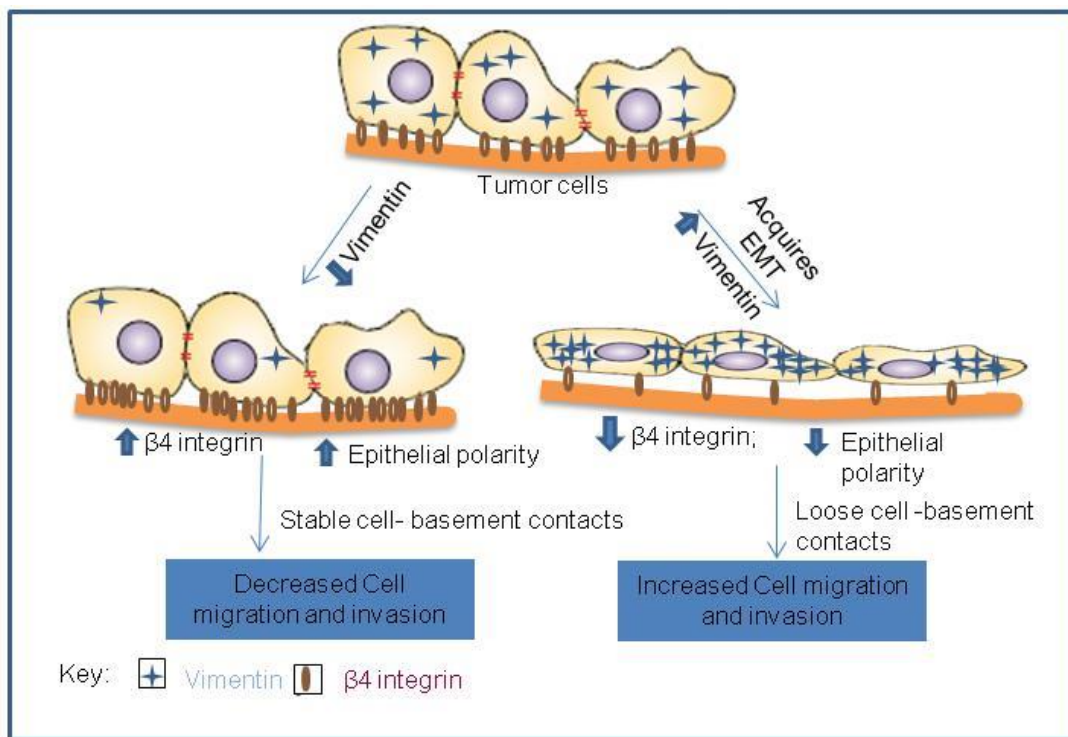


**Figure 4.1.16 Schematic depiction of the role of vimentin in modulating  $\beta 4$  integrin surface levels to regulate migration, in carcinoma derived cells**

## **Part 2**

### **4.2 Vimentin regulates differentiation switch via modulation of Keratin 14 levels and their expression together correlates with poor prognosis in oral cancer patients**

Expression of vimentin is associated with the transition from a more differentiated epithelial phenotype to a dedifferentiated state. Keratins (Ks), being markers and recently perceived as regulators of differentiation in epithelia, it was important to understand whether vimentin modulates differentiation through reprogramming of keratins. Our study demonstrated that, vimentin regulates the differentiation switch via modulation of K5/K14 expression possibly through crosstalk between  $\Delta Np63\alpha$ , notch and NF- $\kappa$ B. Expression of vimentin is strongly associated with the characteristic phenotype of the cells undergoing EMT. Hence, we hypothesized that vimentin may not only be the marker but also the molecular regulator involved in reprogramming the expression of keratins to transit from a differentiated to a more dedifferentiated state.

#### **4.2.1 Downregulation of vimentin results in alteration in the keratin profile of the OSCC derived cell line AW13516**

Expression of vimentin is strongly associated with the characteristic phenotype of the cells undergoing EMT. Hence, we hypothesized that vimentin may not only be the marker but also the molecular regulator involved in reprogramming the expression of keratins to transit from a differentiated to a more dedifferentiated state (Figure 4.2.1A). In order to test this hypothesis we used vimentin knockdown clones generated in OSCC derived cell line AW13516 [159]. Downregulation of vimentin was confirmed by immunofluorescence and western blotting analysis (Figure 4.2.1B-C). To identify the differentially regulated keratins, high salt keratin extraction followed by 2D and MALDI analysis was performed using vimentin knockdown and

vector control clones. K8 was used as a loading control for high salt extracted fractions since its levels did not alter upon vimentin downregulation (Figure 4.2.1D-F). The global keratin profile revealed the identity of the differentially expressed proteins across the clones, one among which was found to be K14, along with the known differentially expressed protein, vimentin (Table 4.2). The appearance of actin (though it is easily soluble in mild buffers) in high-salt extracted fraction could be attributed to its high abundance in the cell.

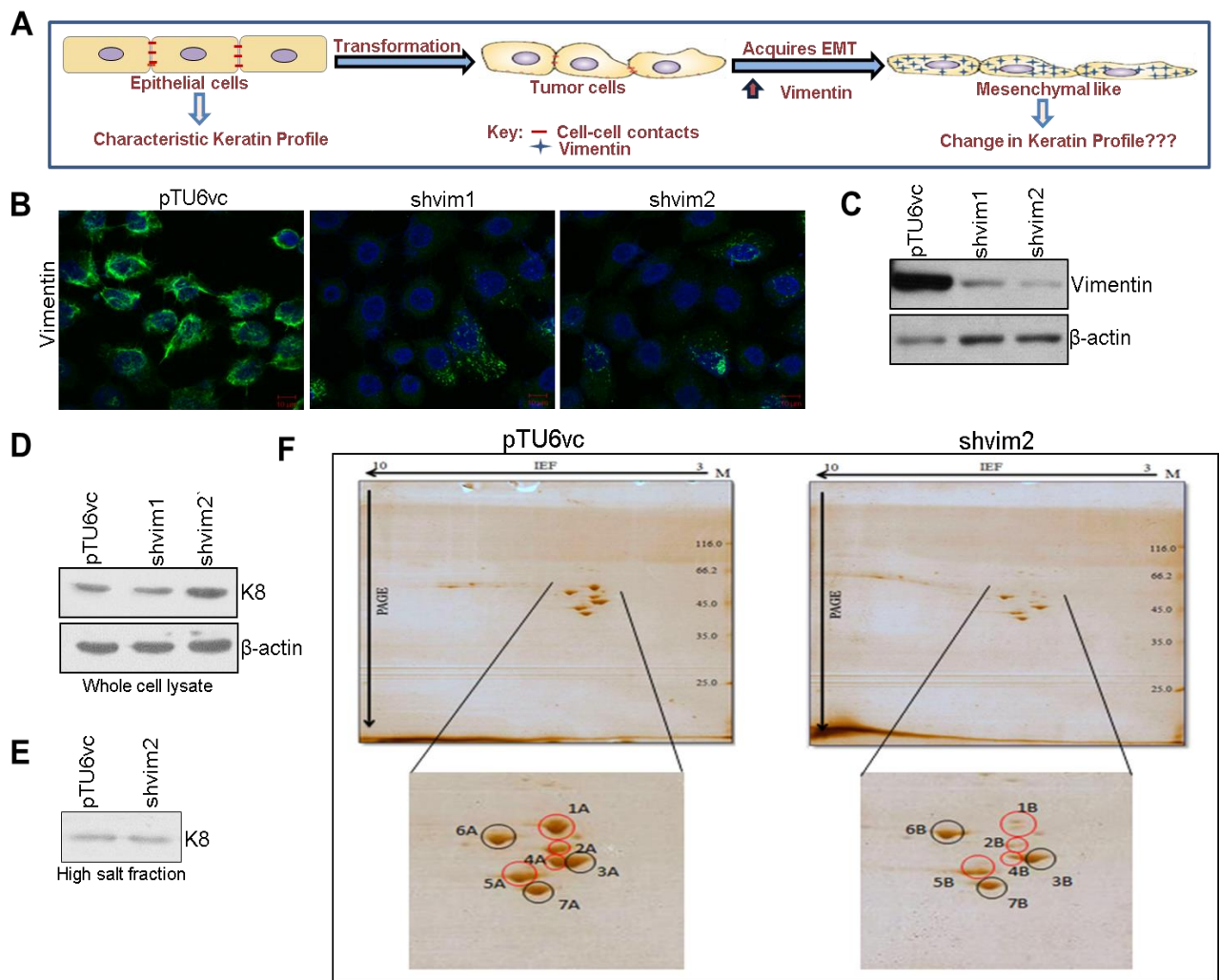


**Figure 4.2.1** Downregulation of vimentin resulted in change in the global keratin profile of the oral SCC derived cell line AW13516. (A) Schematic representation of the hypothesis. As a tumor cell acquires EMT (marked by upregulation of vimentin), it transits from a more epithelial

like to a more mesenchymal like dedifferentiated state. To achieve this transition there could be a vimentin mediated reprogramming of the keratins which distinguishes these states. (B, C) Immunofluorescence (Bar: 10 $\mu$ m) and western blot analysis of vimentin knockdown (shvim1 and shvim2) and its vector control clone (pTU6vc) using antibody against vimentin.  $\beta$ -actin was used as a loading control in the western blotting experiment. (D) K8 levels of vimentin knockdown and its vector control clones were analyzed using western blotting.  $\beta$ -actin was used as a loading control. (E) The expression of K8 did not change upon vimentin downregulation. Thus, K8 was used as a loading control for high salt keratin enriched fraction. (F) Representative images of the 2D-gel, which show changes in keratin expression in high salt keratin enriched fractions of vimentin knockdown and its vector control clones. The black circles indicate similarly expressed while the red circles indicate differentially expressed proteins. All the experiments were repeated independently in triplicates.

**Table 4.2 List of proteins identified using MALDI analysis.**

Spot	Protein	Mass	pI	Score	Matched Peptides	Total Peptides	Protein Sequence Coverage	Expression Status
1A	VIME_HUMAN (Vimentin, OS=Homo sapiens)	53676	4.9	74	8	39	23.6%	Differential
2A	Keratin 14	5172	5.09	52	10	50	23%	Differential
3B	K1C17_HUMAN (Keratin Type 1, Cytoskeletal 17, OS=Homo sapiens)	48361	4.8	156	15	26	50.9%	Similar
4A	Unidentified							Differential
5A	K1C18_HUMAN (Keratin, Type I Cytoskeletal 18 OS=Homo sapiens)	48029	5.2	76	17	60	51.4%	Similar
6A	K2C8_HUMAN (Keratin Type 2, Cytoskeletal 8, OS=Homo sapiens)	53671	Predicted as K8 but with low score					Similar
7A	ACTB_HUMAN (Actin, Cytoplasmic 1 and 2, OS=Homo sapiens)	42052	5.2	75	7	57	38.9%	Similar

MALDI analysis: The resulting data of the keratin spots was analyzed using Flex analysis 3.0 (BruckerDaltonik, Germany) software. The peak list was searched against SwissProt database using MASCOT search engine.

#### **4.2.2 Validation of K14 depletion upon vimentin downregulation**

Downregulation of K14 at protein level was confirmed by western blotting and immunofluorescence analysis. Interestingly, transcript level analysis showed decreased expression of K14 at mRNA level itself (Figure 4.2.2A-C). Further, binding partner of K14, which is K5, was also seen to be downregulated both at protein and mRNA level in vimentin knockdown clones (Figure 4.2.2D-F). This suggests that vimentin may modulate the expression of K5/K14 by, as yet unknown mechanism. The levels of K17 and K18 remained unchanged between the clones, as determined using western blot analysis, which validated the 2D gel observations (Figure 4.2.2G-H). Hereafter, for all the experiments, vimentin knockdown clone shvim2 was used, which showed higher degree of vimentin downregulation as compared to shvim1.

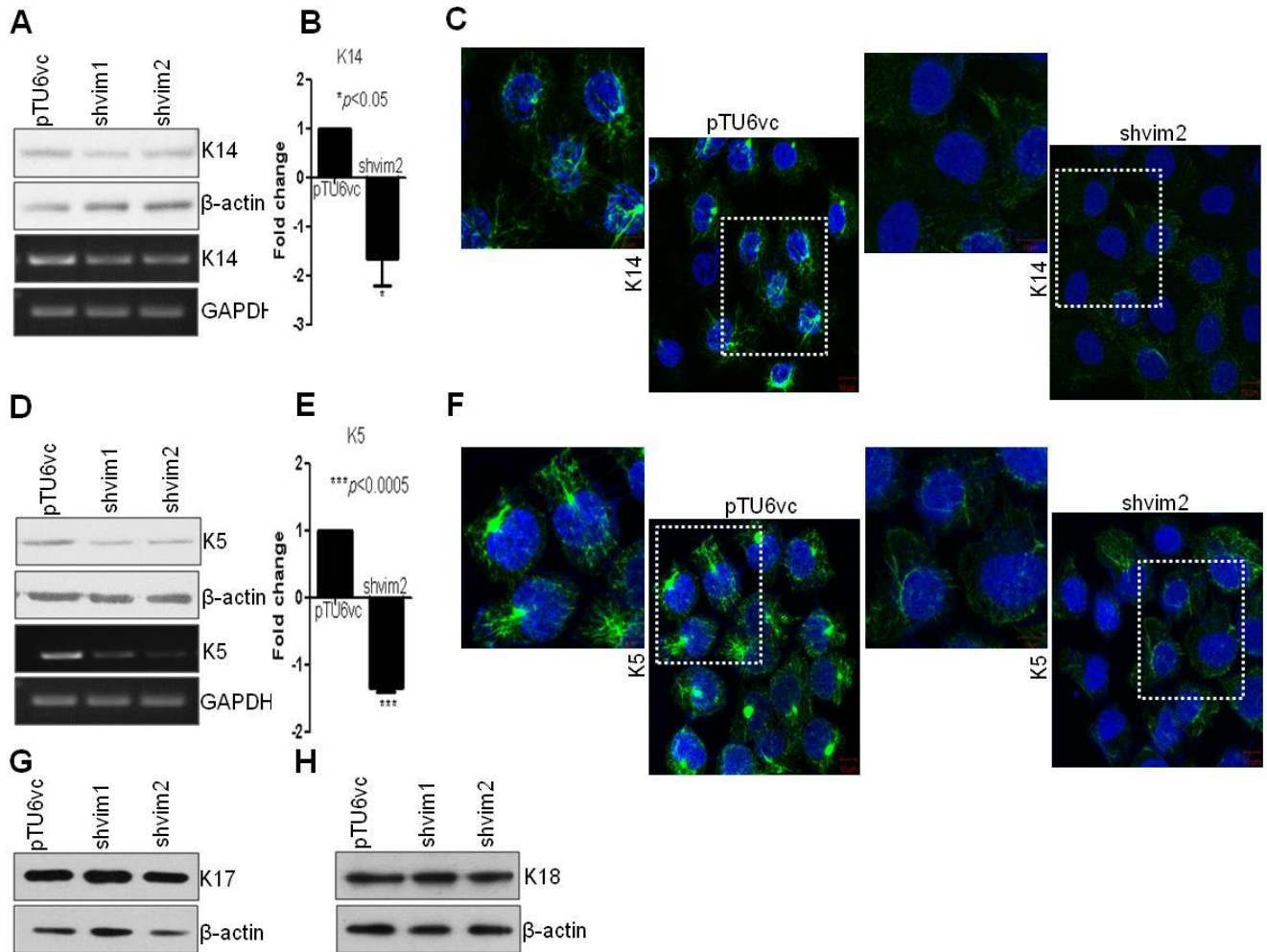


**Figure 4.2.2 Vimentin knockdown cells show downregulation of both K5 and K14 at mRNA as well as protein level.** (A-C) Western blot, RT-PCR, qRT-PCR and immunofluorescence analysis (Bar: 10 $\mu$ m) respectively, of K14 in vimentin knockdown and vector control clones. (D-F) Western blot, RT-PCR, qRT-PCR and immunofluorescence analysis (Bar: 10 $\mu$ m) respectively, of K5 in vimentin knockdown and vector control clones (G and H) Western blot analysis demonstrates unchanged levels of K17 and K18 in vimentin knockdown as compared to vector control clones.  $\beta$ -actin was used as a loading control in all the western blotting experiments. GAPDH was used as a loading control in RT-PCR and for qRT-PCR

experiments; the relative expression of target gene was normalized to the GAPDH. The data represents  $\pm$  standard error mean (SEM) of three independent experiments.

#### **4.2.3 Vimentin modulates the differentiation status of the epithelial cells**

K5/K14 expression is the typical feature of the progenitor basal stem cells of the stratified epithelial origin. Also a previous report from our laboratory has shown direct evidence wherein K5/K14 pair is able to regulate cell proliferation, differentiation and neoplastic progression in the same system AW13516 [139]. Surprisingly, we did not see any obvious differences in the proliferation potential of the vimentin knockdown as compared to the vector control cells using MTT assay (Figure 4.2.3A). In addition, we performed clonogenic assay on vimentin knockdown and vector control clones. Again, no significant difference was seen in the number and size of colonies between the clones which correlated with their similar proliferation rates (Figure 4.2.3B). Further staining with cell proliferation markers, proliferating cell nuclear antigen (PCNA) and Ki67 confirmed our results (Figure 4.2.3C and D). However, during epithelial stratification, as basal cell gets committed to differentiation, it loses the expression of K5/K14 pair and starts expressing involucrin, filaggrin, loricrin and differentiation specific keratins in the upper layers [166]. Vimentin downregulation led to increased expression of K1, involucrin, filaggrin and loricrin respectively (Figure 4.2.3E) while expression of multipotent stem cell marker Oct-4 (Figure 4.2.3F) decreased significantly, as assessed using qRT-PCR. Collectively, these results suggest that vimentin is involved in maintaining a more dedifferentiated state of the cancer cell, perhaps through modulation of K5/K14 expression.

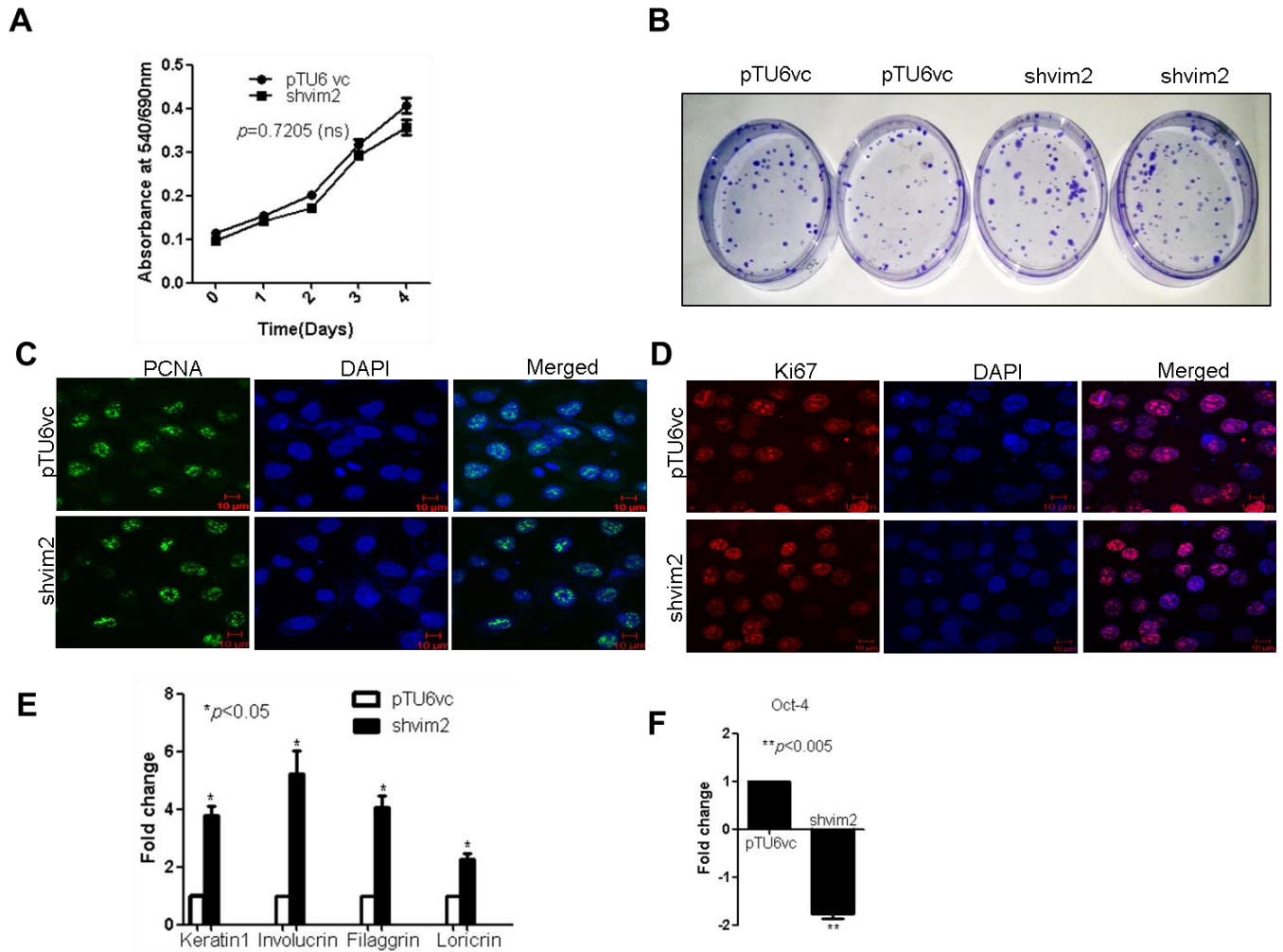


**Figure 4.2.3 Phenotypic alterations associated with K5/K14 downregulation as a consequence of vimentin depletion.** (A) Proliferation curves of vimentin knockdown and its vector control clones over the period of 4 days, using MTT assay. (B) Representative images of clonogenic assay show colonies formed by vimentin knockdown and its vector control clones. (C) Representative immunofluorescence images (Bar: 10 $\mu$ m) of PCNA (green) staining in vimentin knockdown and vector control clones. (D) Representative immunofluorescence images (Bar: 10 $\mu$ m) of Ki67 (red) staining in vimentin knockdown and vector control clones. (E) QRT-PCR analysis of differentiation specific markers K1, involucrin, filaggrin and loricrin respectively. The relative expression of the target gene was normalized to GAPDH. (F) QRT-

PCR analysis of Oct-4 in vimentin knockdown and its vector control clones. The relative expression of the target gene was normalized to GAPDH. For (A, E and F), the data represents  $\pm$  standard error mean (SEM) of three independent experiments.

#### 4.2.4 Vimentin modulates the tumorigenic potential of the epithelial cells

Further, to assess the tumorigenic role of vimentin, vimentin knockdown and vector control cells were injected subcutaneously into NOD-SCID mice (Figure 4.2.4A). Significant reduction was observed in the tumor volume in vimentin knockdown as compared to vector control group (Figure 4.2.4B). Furthermore, IHC analysis confirmed decrease in the expression of K5/K14 in the vimentin depleted tumors (Figure 4.2.4C).

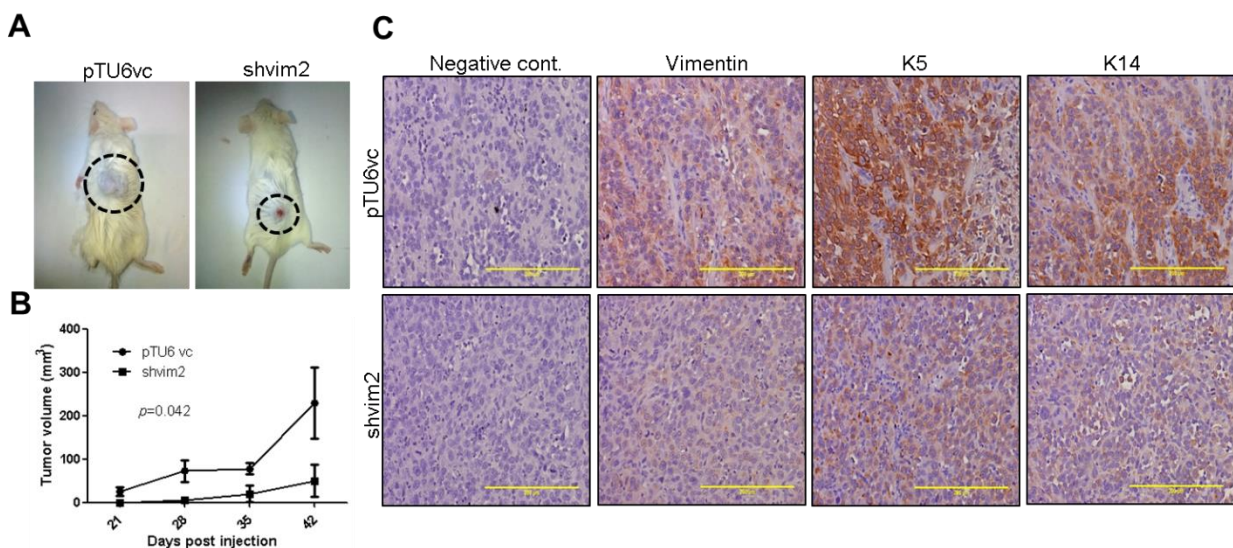


**Figure 4.2.4 Tumorigenic potential of the vimentin knockdown clones.** (A) Representative images of tumorigenicity assays using NOD SCID mice (six animals each) injected with either vimentin knockdown or vector control clones. The tumors are indicated in dotted circles. (B) The tumor measurements were recorded upto 42 days, after which the animals were sacrificed and the tumor tissue was processed for IHC staining. The graph shows tumor volume plotted against time for both the clones. (C) Representative images (Bar: 200 $\mu$ m) of IHC staining for expression

of vimentin, K5 and K14 respectively in mice tumor tissues. The negative control images represent tissue sections incubated with serum from non-immunized mice in place of primary antibodies.

#### **4.2.5 Vimentin positively regulates the expression of K5/K14 pair across different stratified epithelia derived cell lines**

To verify whether the regulation of K5/K14 expression through vimentin is a general mechanism and not a cell line specific phenomenon, it was overexpressed in vimentin lacking, A431 and HaCaT cell lines. Vimentin upregulation in A431 cells led to concomitant increase in the levels of K5, but a marked decrease was seen in the levels of differentiation specific protein, involucrin. However, since A431 cells do not express K14, we checked for the levels of K17, considering the fact that K17 is known to pair with K5 in absence of K14 [167, 168]. We found no change in the levels of K17 upon vimentin overexpression, which further confirmed that the regulation exerted by vimentin on the expression of K5/K14 is highly specific (Figure 4.2.5A). Forced expression of vimentin in HaCaT also showed a marked increase in the expression of K5 while K14 expression was unaffected. The differentiation specific marker involucrin showed a significant decrease in its levels, in response to an increase in vimentin expression (Figure 4.2.5B). Next, we assessed the status of K5/K14 and involucrin with respect to vimentin in some tongue derived cell lines. DOK, (dysplastic lesion derived cell line) which does not express vimentin, displayed reduced protein levels of K5/K14 and increased levels of involucrin as compared to high vimentin expressing AW13516 and AW8507 (both of which are SCC derived cell lines) (Figure 4.2.5C). Additionally, to determine whether K14 also has a similar regulatory effect on vimentin, we assessed the levels of vimentin in the same system AW13516, in K14 knockdown background. Both the protein and mRNA levels of vimentin remained unchanged

(Figure 4.2.5D and E), suggesting that vimentin may be upstream in pathways that regulate the expression of K14.

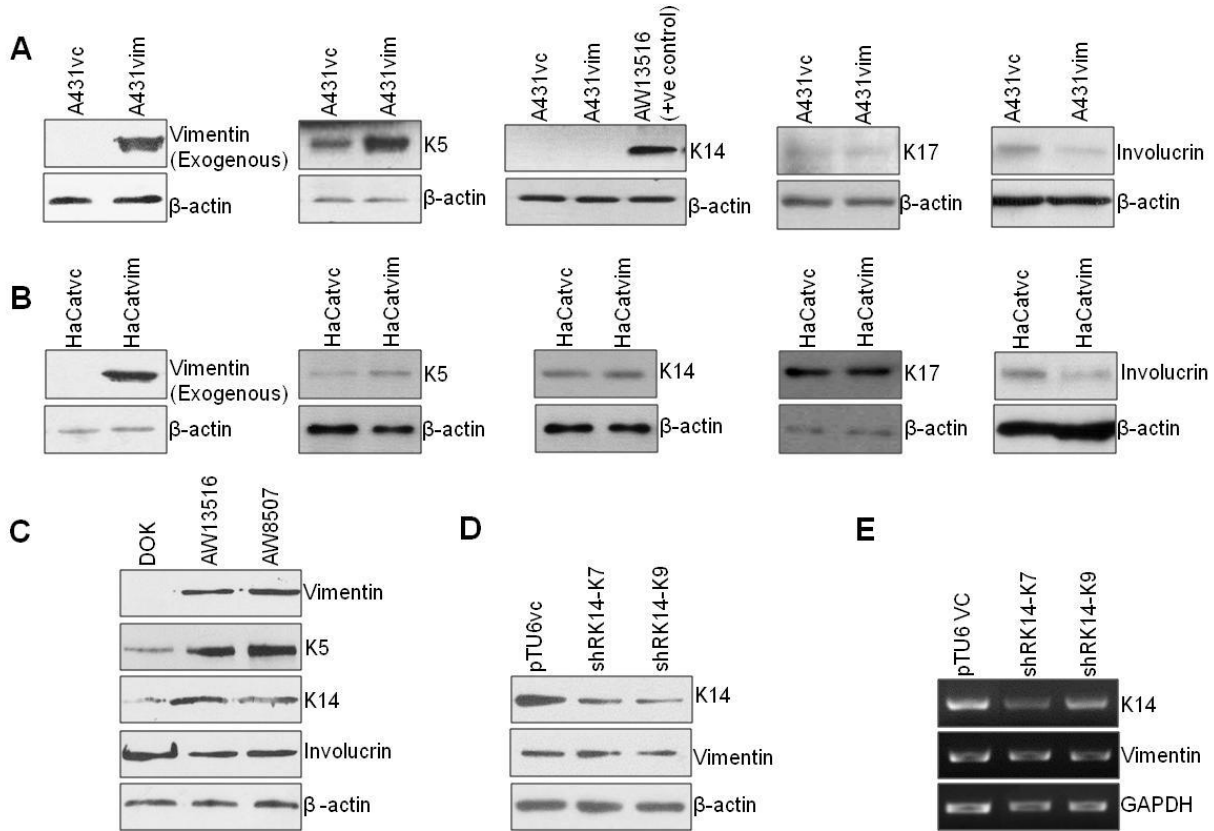


**Figure 4.2.5 Vimentin mediated positive regulation of K5/K14 levels is not a cell line specific phenomenon.** (A and B) Western blot analysis shows expression of vimentin, K5, K14, K17 and involucrin respectively in vimentin overexpressing clones of A431vim and HaCatvim as compared to their respective vector control clones A431vc and HaCatvc. Since A431 does not express K14, whole cell lysate from AW13516 was used as a positive control. (C) Whole cell lysates from DOK, AW13516 and AW8507 cells were probed with antibodies against vimentin, K5, K14 and involucrin respectively using western blotting. (D and E) Western blot and RT-PCR analysis of K14 and vimentin in K14 knockdown (shRK14-K7 and shRK14-K9) and its vector

control clones (pTU6-AW1). GAPDH was used as a loading control in RT-PCR experiment.  $\beta$ -actin was used as the loading control in all western blotting experiments.

#### **4.2.6 Vimentin knockdown phenotype was rescued upon re-expression of K5/K14 pair**

In order to ascertain that the phenotypic changes observed upon vimentin knockdown are brought about by K5/K14 downregulation only and to rule out the possibility of the involvement of other altered molecule/s, we re-expressed K5/K14 pair in vimentin knockdown background shvim2 clone. Immunofluorescence and western blot analysis confirmed overexpression of K5K14 pair in shvim2 clone (Figure 4.2.6A-C). As expected, proliferation and clonogenic potential remained unchanged upon K5/K14 re-expression, which corroborated with that of vimentin knockdown phenotype (Figure 4.2.6D and E). K5/K14 re-expressing clone (K5/K14) showed down-regulation of differentiation specific markers K1, involucrin, filaggrin and loricrin respectively (Figure 4.2.6F) while stemness marker Oct-4 was upregulated (Figure 4.2.6G) as compared to its vector control (vcvc). Tumorigenic potential of K5/K14 re-expressing clones was also significantly higher as reflected by the increased subcutaneous tumor growth in NOD-SCID mice (Figure 4.2.6H-J). This rescue experiment suggests that vimentin mediates the regulation of differentiation switch via reprogramming the expression of basal cell specific K5/K14.

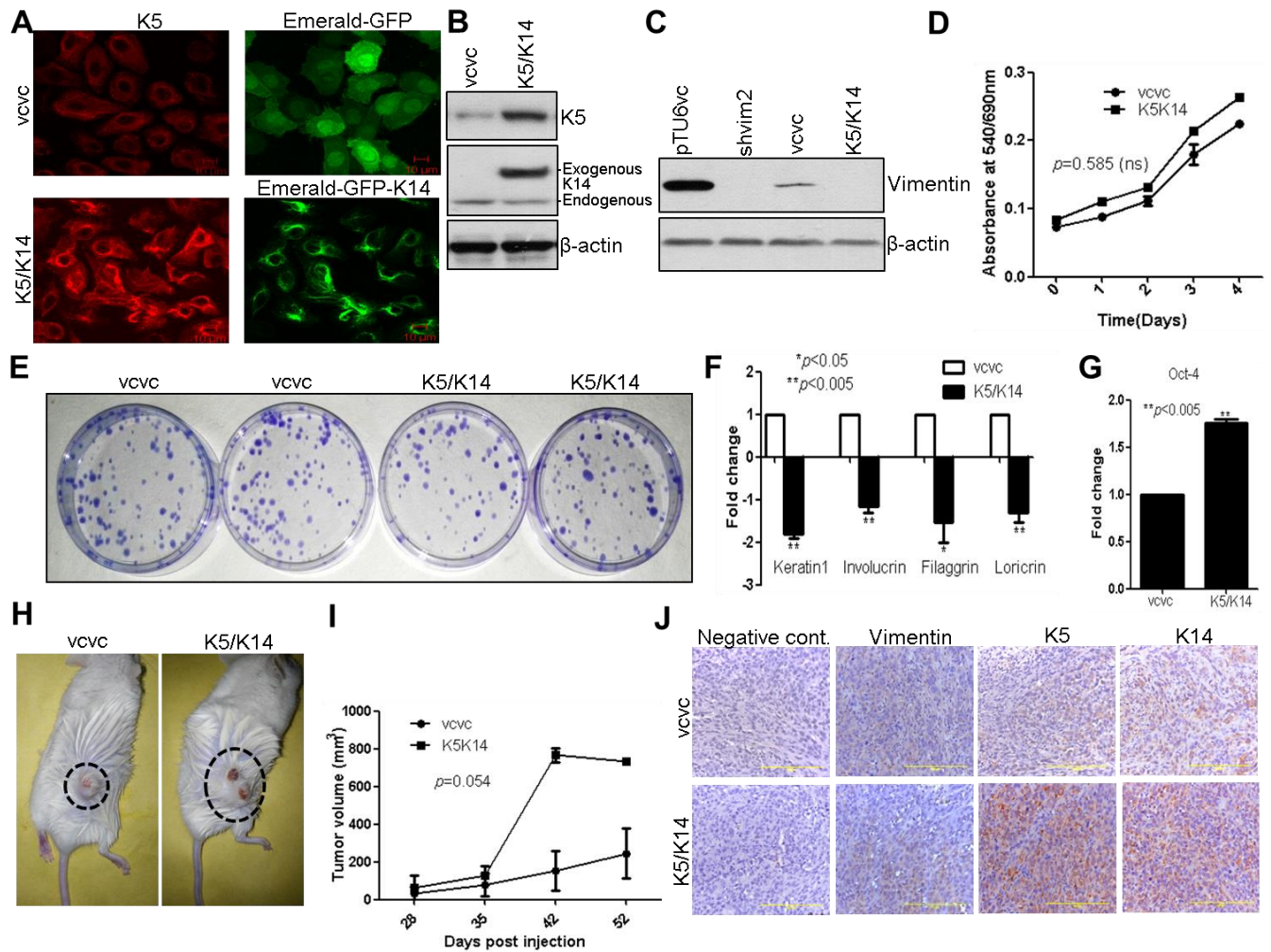


**Figure 4.2.6 Vimentin knockdown phenotype was rescued upon re-expression of K5/K14 together, in vimentin knockdown background.** (A) Confocal microscopy analysis (Bar: 10μm) shows overexpression of emerald GFP-K14 and K5 in K5/K14 (K5 and K14 overexpressing) as compared to its vector control vvcv clones (empty vectors of K5 and K14 together). (B and C) Western blot analysis shows overexpression of emerald GFP-K14 and K5 in K5/K14 overexpressing as compared to its vector control clones. Protein levels of vimentin were tested in vimentin knockdown-vector control and K5/K14 overexpressing-vector control group, to confirm the maintenance of vimentin knockdown background in the second group, using western blotting. (D) Proliferation curves of K5/K14 overexpressing and its vector control clones over

the period of 4 days, using MTT assay. (E) Representative image of clonogenic assay shows colonies formed by K5/K14 overexpressing and its vector control clones. (F) QRT-PCR analysis of differentiation specific markers K1, involucrin, filaggrin and loricrin respectively. The relative expression of target gene was normalized to the GAPDH. (G) QRT-PCR analysis of Oct-4 in K5/K14 overexpressing and its vector control clones. The relative expression of target gene was normalized to the GAPDH. (H) Representative images of tumorigenicity assays using NOD SCID mice (six animals each) injected with either K5/K14 overexpressing or its vector control clones. The tumors are indicated in dotted circles. (I) The tumor measurements were recorded upto 52 days, after which the animals were sacrificed and the tumor tissue was isolated for IHC staining. The graph shows tumor volume plotted against time for both the clones. (J) Representative images (Bar: 200  $\mu\text{m}$ ) of IHC staining for expression of vimentin, K5 and K14 respectively in mice tumor tissues. The negative control images represent tissue sections incubated with serum from non-immunized mice in place of primary antibodies.

#### **4.2.7 $\Delta\text{Np63}$ could be a possible target of vimentin, to bring about the modulation of K5/14 expression**

Next we wanted to investigate the molecular regulator, through which vimentin modulates the expression of K5/K14.  $\Delta\text{Np63}$  is known to directly regulate the expression of K5/K14 pair during the program of keratinocyte stratification [169, 170]. Hence, as a first step we checked its levels in vimentin knockdown background. Western blot and qRT-PCR analysis showed decreased levels of  $\Delta\text{Np63}$ , both at protein and mRNA level respectively (Figure 4.2.7A and B). To functionally characterize the depletion of  $\Delta\text{Np63}$ , we checked for other known molecular alterations associated with  $\Delta\text{Np63}$  loss. Vimentin knockdown clones showed increased levels of p21 and p27, which are typically associated with  $\Delta\text{Np63}\alpha$  downregulation (Figure 4.2.7C).

Further,  $\Delta Np63\alpha$  and  $\Delta Np63\gamma$  isoforms were identified to be downregulated in vimentin knockdown as compared to vector control clones using RT-PCR (Figure 4.2.7D). To verify whether the K5/K14 downregulation seen upon vimentin knockdown is due to reduced  $\Delta Np63$  levels, flag tagged  $\Delta Np63\alpha$  (since  $\Delta Np63\alpha$  is a major isoform expressed in keratinocytes [171]) was stably re-expressed in vimentin knockdown clone shvim2 (Figure 4.2.7E and F).  $\Delta Np63\alpha$  overexpression led to a significant increase in the levels of K14 while K5 expression was only marginally rescued, indicative of the contribution of more than one molecule in the regulation of K5/K14 expression (Figure 4.2.7G and H). The proliferation and clonogenic potential again remained unaffected upon  $\Delta Np63\alpha$  overexpression (Figure 4.2.7I and J). The differentiation status (defined by the expression of differentiation specific markers) remained unchanged (Figure 4.2.7K) while the expression of Oct-4 showed only a marginal increase (not significant) (Figure 4.2.7L) upon  $\Delta Np63\alpha$  upregulation in vimentin knockdown background.

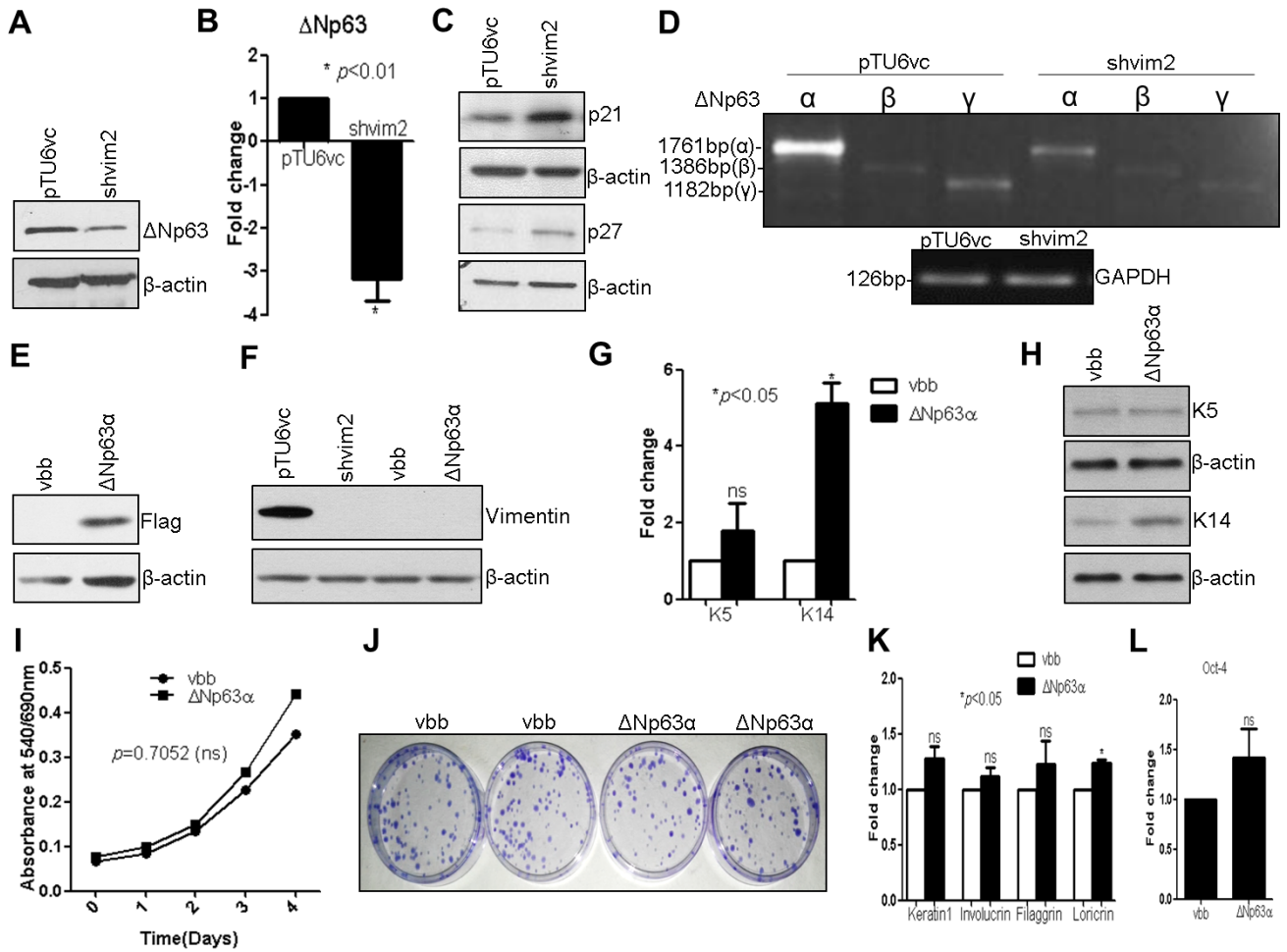


**Figure 4.2.7**  $\Delta Np63\alpha$  may not be the sole regulator of K5/K14 expression in vimentin mediated regulation of differentiation. (A) Western blot analysis shows protein levels of  $\Delta Np63$  from the whole cell lysates of vimentin knockdown and its vector control clones. (B) Fold change in mRNA expression level of  $\Delta Np63$  in vimentin knockdown as compared to vector control clones, using qRT-PCR analysis. (C) Western blot analysis shows protein levels of p21 and p27 from the whole cell lysates of vimentin knockdown and its vector control clones. (D) RT-PCR analysis shows expression of  $\Delta Np63\alpha$ ,  $\beta$  and  $\gamma$  isoforms, between vimentin knockdown and vector control clones. GAPDH was used as a loading control. (E and F) Western blot analysis shows expression of flag in  $\Delta Np63\alpha$  (flag tagged  $\Delta Np63\alpha$  overexpressing) and not in vbb (vector control clone). Protein levels of vimentin were tested in vimentin knockdown-vector

control set and flag- $\Delta$ Np63 $\alpha$ -vector control set, to confirm the maintenance of vimentin knockdown background in the second group, using western blotting. (G and H) QRT-PCR and western blot analysis of K5 and K14 in flag- $\Delta$ Np63 $\alpha$  overexpressing and its vector control group. (I) Proliferation curves of flag- $\Delta$ Np63 $\alpha$  overexpressing and its vector control clones over the period of 4 days, using MTT assay. (J) Representative image of clonogenic assay shows colonies formed by flag- $\Delta$ Np63 $\alpha$  overexpressing and its vector control clones. (K) QRT-PCR analysis of differentiation specific markers K1, involucrin, filaggrin and loricrin. (L) QRT-PCR analysis of Oct-4 in flag- $\Delta$ Np63 $\alpha$  overexpressing and its vector control clones. For all the qRT-PCR experiments, the relative expression of target gene was normalized to the GAPDH and for western blotting experiments;  $\beta$ -actin was used as a loading control. The data represents  $\pm$  standard error mean (SEM) of three independent experiments.

#### **4.2.8 Activation of Notch1 may be a cause or a consequence of $\Delta$ Np63 downregulation in vimentin knockdown background**

$\Delta$ Np63 and notch regulate each other by a negative feedback loop [171]. In order to understand the cause of  $\Delta$ Np63 downregulation we checked for the levels of activated Notch1 upon vimentin downregulation. Vimentin knockdown clone showed increase in activated Notch1 (NICD) levels as compared to vector control clone (Figure 4.2.8A). Correspondingly, its levels showed a significant decrease upon  $\Delta$ Np63 $\alpha$  overexpression (Figure 4.2.8D). The other candidate molecule which may modulate the levels of  $\Delta$ Np63 is nuclear factor-kappaB (NF- $\kappa$ B), since it negatively regulates  $\Delta$ Np63 either through notch or independently as a part of the differentiation program [172]. Increased nuclear localization of NF- $\kappa$ B (p65) was observed upon vimentin downregulation (Figure 4.2.8B and C), while the inverse was seen in  $\Delta$ Np63 $\alpha$  overexpressing clone (Figure 4.2.8E and F). Thus, our preliminary observations suggest the

possibility of the crosstalk between notch (in an NF- $\kappa$ B dependent manner) and  $\Delta$ Np63, to regulate differentiation state in vimentin knockdown cells.

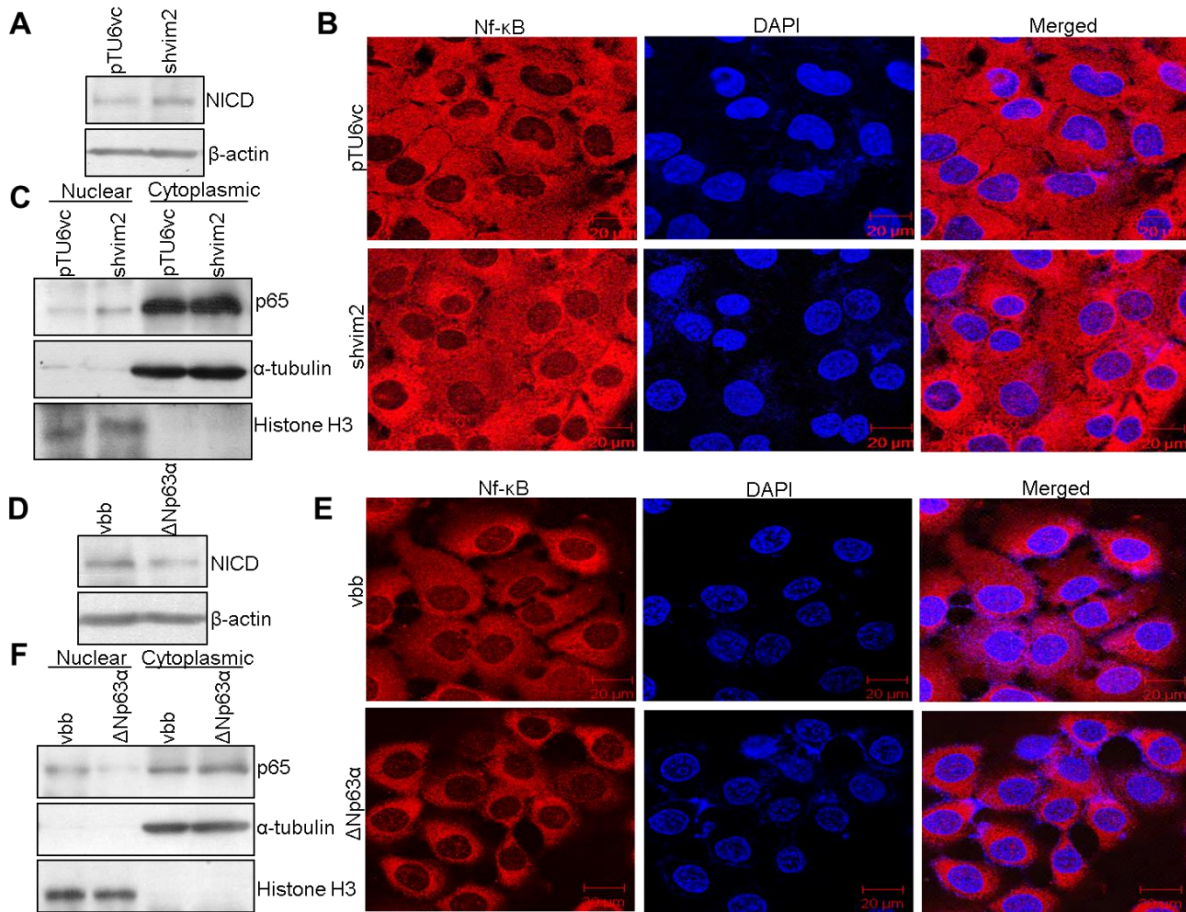


**Figure 4.2.8 Notch1 (independently or through NF- $\kappa$ B) may regulate the expression of  $\Delta$ Np63.** (A and D) Western blot analysis shows the changing trend in the protein levels of notch intracellular domain (NICD) across the whole cell lysates of vimentin knockdown-vector control set and flag- $\Delta$ Np63 $\alpha$ -empty vector backbone set respectively.  $\beta$ -actin was used as a loading control. (B and E) The distribution of NF- $\kappa$ B (p65) (red) in the cytoplasmic vs. nuclear compartment was visualized using confocal microscopy across vimentin knockdown-vector control set and flag- $\Delta$ Np63 $\alpha$ -empty vector backbone set respectively. The nuclei (blue) were stained with DAPI, (Bar: 20  $\mu$ m). (C and F) Subcellular fractionation was carried out to separate

the cytoplasmic and nuclear fractions from vimentin knockdown-vector control set and flag- $\Delta$ Np63 $\alpha$ -empty vector backbone set. Western blot analysis was performed to examine the levels of p65 in these groups.  $\alpha$ -tubulin was included as a loading control for the cytoplasmic fraction while histone H3 protein was included as a loading control for the nuclear fraction. All the experiments were repeated independently in triplicates.

#### **4.2.9 High expression of vimentin-K14 together correlates with recurrence and poor survival of oral cancer patients**

IHC analysis of OSCC tissues showed positive correlation of high vimentin-K14 staining intensity (Figure 4.2.9A) with recurrence ( $p=0.001$ ) (Figure 4.2.9B). In order to determine if the vimentin-K14 status of the tumor has any association with the survival of oral cancer patients, Kaplan-Meier survival analysis based on IHC data was performed on 91 oral tumor samples. The analysis showed a significant correlation between expression status of vimentin-K14 ( $p=0.005$ ) (Figure 4.2.9E) or vimentin alone ( $p=0.007$ ) (Figure 4.2.9C) with poor disease free survival. Expression of K14 alone ( $p=0.397$ ) also showed a trend, although not statistically significant, with poor disease free survival (Figure 4.2.9D). No significant correlation was seen between vimentin-K14 expression and other clinico-pathological parameters, as listed in table 4.3. Collectively, this suggests that the expression of vimentin-K14 together may prove useful for prognostication of human oral cancers.

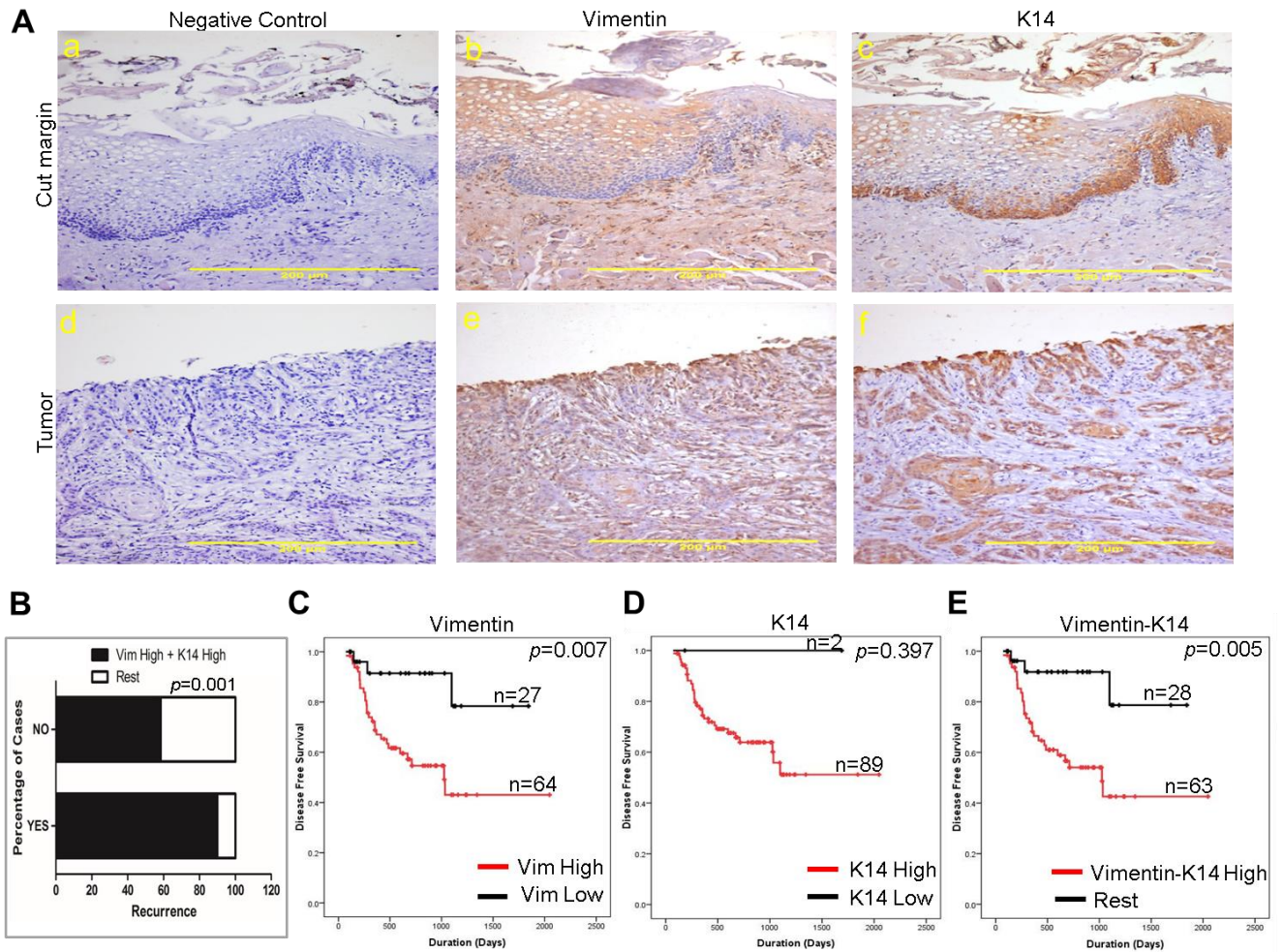


**Figure 4.2.9 High vimentin-K14 expression correlates with poor survival in oral cancer patients.** (A) (a-c) The upper panel shows images (Bar: 200 $\mu$ m) of IHC staining for vimentin and K14 expression in cut margin tissues while lower panel (d-f) shows images (Bar: 200  $\mu$ m) of IHC staining for vimentin and K14 expression in tumor tissues. The negative control images represent tissue sections incubated with serum from non-immunized mice in place of primary antibodies. (B) Graphical representation of recurrence with respect to high vimentin-K14 and rest other combinations of vimentin-K14 expression. Kaplan-Meier survival analysis (n=91) of (C) High vs. low vimentin expression (D) High vs. low K14 expression and (E) High vimentin-K14 vs. rest other combinations of vimentin-K14 expression.

**Table 4.3. Correlations of vimentin-K14 expression with clinico-pathological parameters of the oral cancer patients (n=100).**

Clinico-pathological parameters		n = 100	Data not available	Vimentin and K14 expression		p-value
				Vimentin (High) + K14 (High)	Rest	
Age (Years)	<50	54	0	35	19	0.387*
	≥50	46		32	14	
Sex	Male	81	0	57	24	0.115*
	Female	19		10	9	
Location	Buccal mucosa	52	0	33	19	0.285*
	Tongue	48		34	14	
Thickness	<2cm	42	38	26	16	0.269*
	≥2cm	20		10	10	
Stages	I	4	38	3	1	0.754#
	II	12		6	6	
	III	10		5	5	
	IV	36		22	14	
Tumor Size	T1	8	0	5	3	0.142#
	T2	31		20	11	
	T3	16		12	4	
	T4	45		30	15	
Node Status	NO	41	0	25	16	0.147#
	N1	24		20	4	
	N2	35		22	13	
Differentiation	Poor	30	0	18	12	0.465#
	Moderate	63		45	18	
	Well	7		4	3	
Bone	Positive	26	21	17	9	0.574*
	Negative	53		35	18	
Perineural Invasion	Yes	21	5	14	7	0.567*
	No	74		50	24	
Lympho vascular invasion	Yes	3	8	2	1	0.738*
	No	89		59	30	
Perineural Extension	Yes	37	11	24	13	0.344*
	No	52		37	15	
Cut Margin	Free	56	38	33	23	0.915#
	Closed	4		2	2	
	Invasion	2		1	1	

\*Fisher's exact test, # Pearson Chi-Square

#### 4.2.10 Summary of part 2

To summarise, our data gives insights into the role of vimentin in modulating the expression of K5/K14 pair, partly through  $\Delta$ Np63, to regulate differentiation state of a transformed cell (Figure 4.2.10). Furthermore, vimentin-K14 expression may be clinically relevant for prognostication of the OSCC. Thus, this study depicts the overall vimentin mediated molecular interplay between the key regulators of differentiation to fine tune the differentiation switch in the favor of tumor progression.

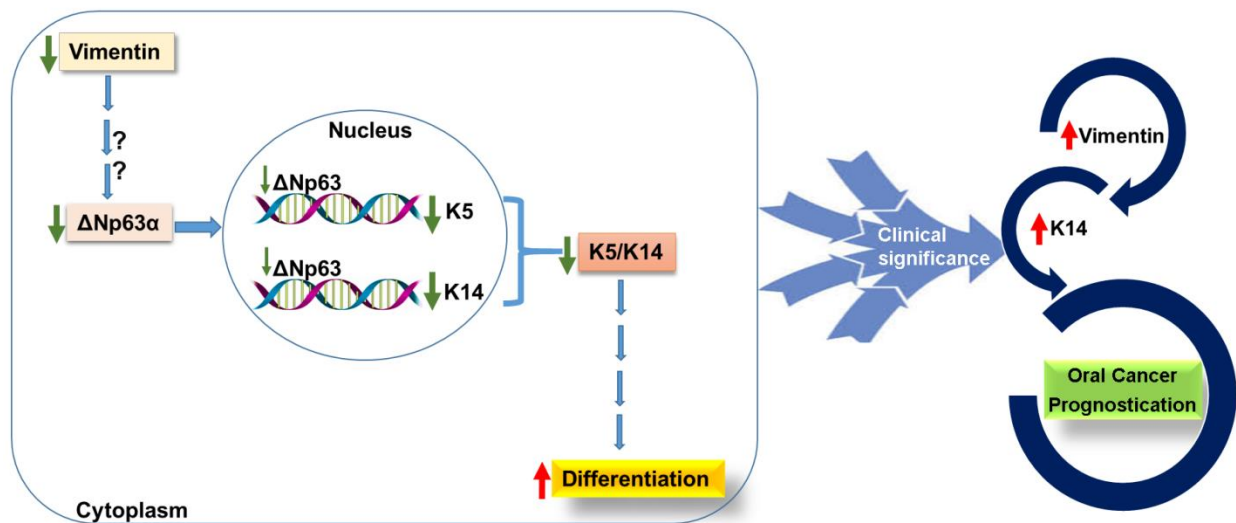


**Figure 4.2.10** Schematic representation depicting role of vimentin in modulating K5/K14 expression to regulate differentiation, in carcinoma derived cells.

### **Objective 3:**

#### **4.3 Evaluation of transformation potential of vimentin in the development of human oral cancer**

In our earlier study, we have shown the expression of vimentin in oral leukoplakia and submucous fibrosis which are known premalignant lesions for human oral cancer [6]. Further, we have reported a sequential increase in aberrant expression of vimentin from early stages in 4NQO-model of rat lingual carcinogenesis [7]. It is still not known whether the presence of vimentin in early events of oral tumorigenesis has any active role to play in bringing about this process. Therefore, the present study was undertaken to understand whether expression of vimentin is one of the causes or consequences of the development of human oral cancer. Additionally, this information can be used to understand if vimentin can be used as a predictive marker for progression of oral precancerous lesions.

##### **4.3.1 Characterization of DOK for vimentin expression**

To check the status of vimentin in oral premalignant lesion derived cell line DOK, RT-PCR, western blotting and confocal microscopy was carried out. Vimentin was not detectable both at RNA and protein level (Figure 4.3.1A and B). Similarly to verify the *in vitro* transformation potential of DOK, soft agar colony formation assay was performed using tongue OSCC derived cell line AW13516, as a positive control and immortalized but non-transformed cell line, HaCat as a negative control. It was confirmed that DOK does not form any soft agar colonies upto two weeks (Figure 4.3.1C).

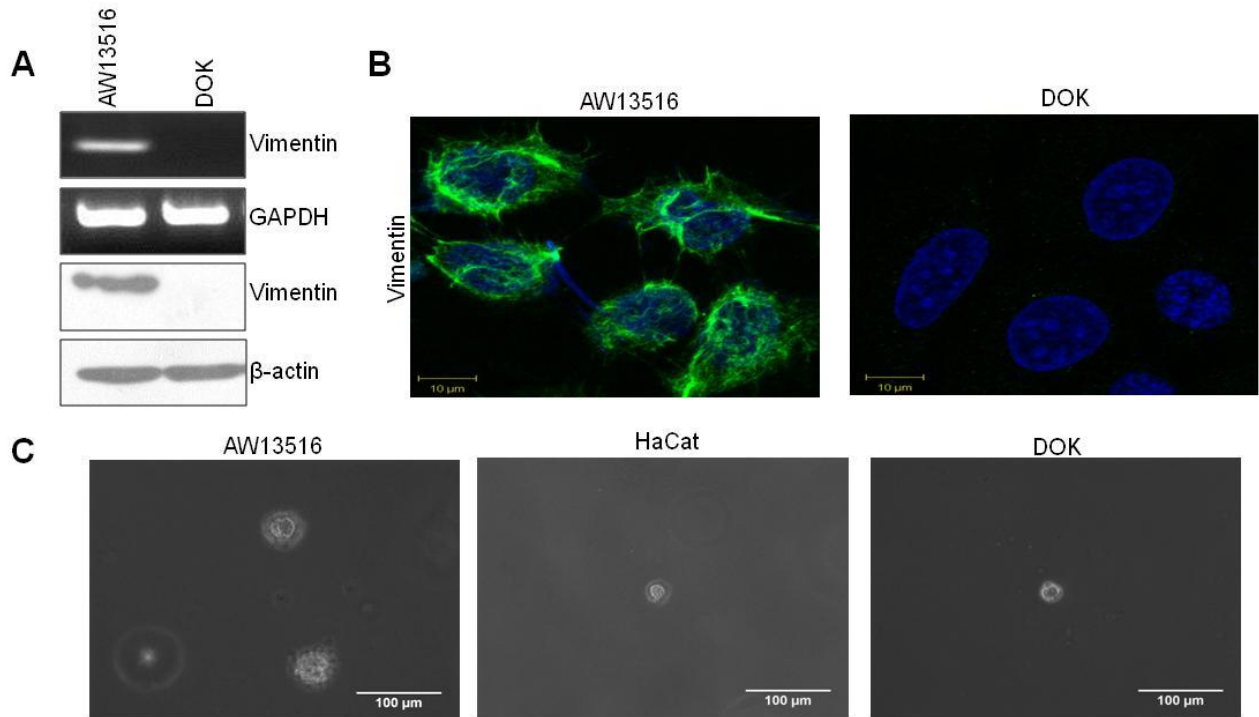


**Figure 4.3.1 Characterization of DOK for vimentin expression and *in vitro* transformation potential.** (A) RT-PCR and western blot analysis did not show presence of vimentin in DOK cells. AW13516 cell line (tongue SCC derived) was used as a positive control. (B) Confocal microscopy analysis (Bar: 10  $\mu$ m) did not show presence of vimentin in DOK cells. AW13516 cell line was used as a positive control. (C) Representative images of colonies formed by DOK cells, in soft agar. AW13516 cell line was used as a positive control while HaCat cell line was used as a negative control.

#### 4.3.2 Overexpression of vimentin in DOK cell line

To answer whether vimentin contributes in the initial events of transformation, the emerald vimentin retroviral construct (a kind gift from Dr. Robert Goldman, Feinberg School of Medicine, Northwestern University, USA) was transduced in premalignant lesion derived DOK cell line (Figure 4.3.2A and B). The vimentin overexpressing clones showed a trend towards increased proliferation (Figure 4.3.2C) and migration (Figure 4.3.2E and F) (albeit not

significant) as compared to the vector control clones. No difference was seen in the soft agar colony formation ability of the cells, upon vimentin overexpression (Figure 4.3.2D). Vimentin being canonical EMT marker, expression of key EMT related regulators was investigated. Vimentin overexpressing clones showed an increase in the expression of EMT regulator twist, while a significant decrease was seen in the expression of epithelial specific marker, E-cadherin (Figure 4.3.2G). Furthermore, Bmi1 being a direct transcriptional target of the EMT regulator Twist1 [173, 174], we also studied the expression of stemness markers. Expression of stemness related marker nanog was found to be upregulated in vimentin overexpressing clones (Figure 4.3.2H). Collectively, these results indicate that vimentin expression alone did not result in transformation of DOK cell line, although initially EMT like signatures were seen. This prompted us to use an additional carcinogenic stimulus and monitor vimentin overexpressing and vector control cells till they showed a transformed phenotype in an *in vitro* transformation assay.

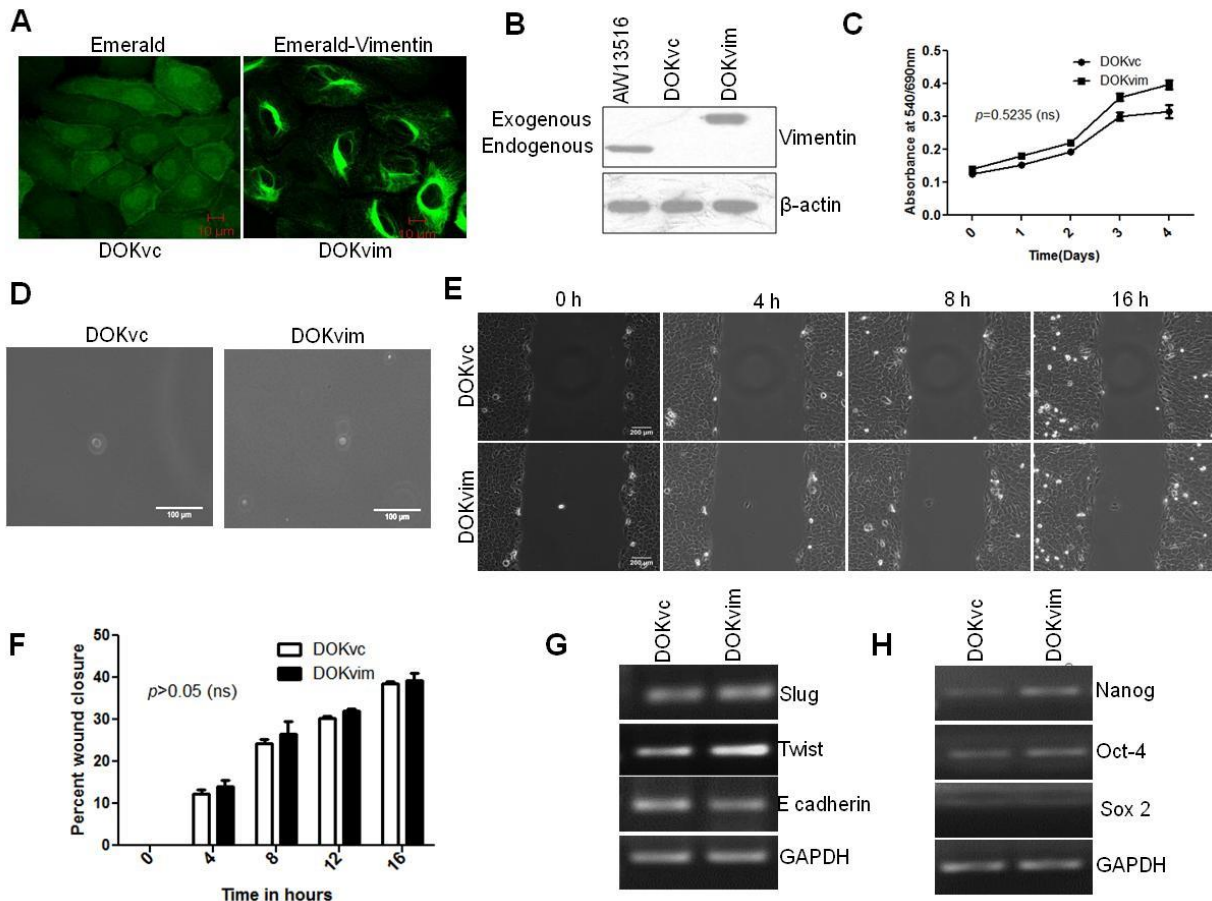


**Figure 4.3.2 Vimentin overexpression did not lead to any transformation related phenotypic alterations.** (A, B) Confocal and western blot analysis showing vimentin levels in DOKvim (vimentin overexpressing) and DOKvc (empty vector control).  $\beta$ -actin was used as a loading control in western blotting experiment. (C) Proliferation curves of vimentin overexpressing and its vector control clones over the period of 4 days, using MTT assay. (D) Representative images of colonies formed by vimentin overexpressing and its vector control clones in soft agar. (E) Representative time lapse microscopy images showing wound healing. (F) The graph shows percent wound closure as calculated over 20 h time point. (G) RT-PCR analysis showing expression of EMT markers (slug, twist, E-cadherin) between vimentin overexpressing and its vector control clones. GAPDH was used as a loading control. (H) RT-

PCR analysis showing expression of stemness related markers (Nanog, Oct-4 and Sox2) between vimentin overexpressing and its vector control clones. GAPDH was used as a loading control.

#### **4.3.3 Development of an *in vitro* carcinogenesis model using benzo[a]pyrene**

Benzo[a]pyrene was used as a procarcinogen to develop an *in vitro* carcinogenesis model in vimentin overexpressing and its vector control cells, after checking for its metabolic competence (Figure 4.3.3A) and cytotoxicity (Figure 4.3.3B). Benzo[a]pyrene treatment was carried out till transformation was reached, as assessed using soft agar colony formation assay. It took 35 weeks of induction for the appearance of visible colonies on soft agar plates (Figure 4.3.3C). The number of colonies was significantly higher in vimentin overexpressing as compared to the vector control clone at the end of 35 weeks of benzo[a]pyrene treatment (Figure 4.3.3D). There was no difference in the proliferation (Figure 4.3.3E) or migratory (Figure 4.3.3F and G) potentials of the benzo[a]pyrene treated vimentin overexpressing and its vector control clones.

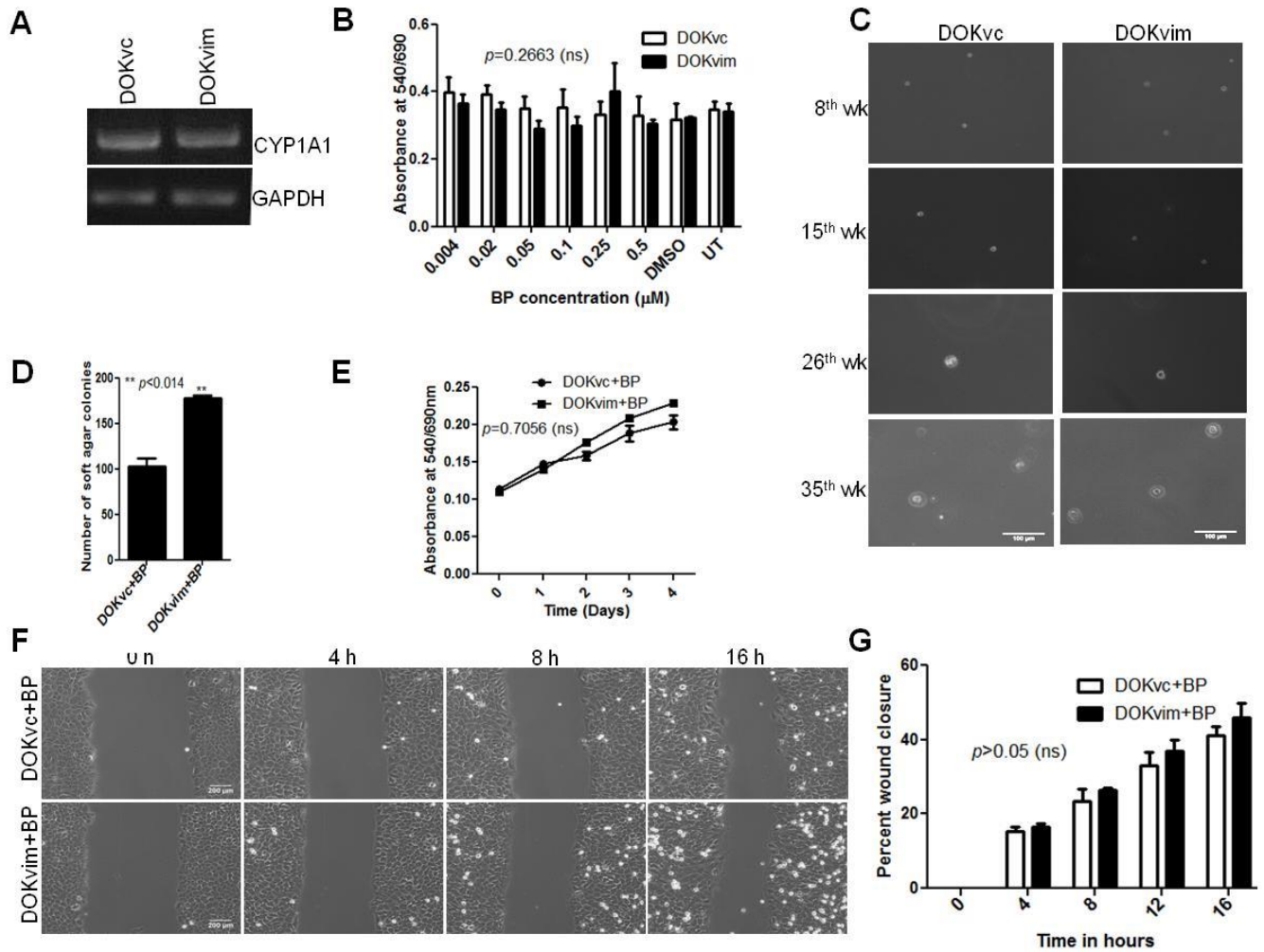


**Figure 4.3.3 Vimentin overexpressing cells showed increased *in vitro* transformation potential in response to benzo[a]pyrene treatment.** (A) RT-PCR analysis showing expression of CYP1A1 in vimentin overexpressing and its vector control clones. GAPDH was used as a loading control. (B) The graphical representation of the dose response of vimentin overexpressing and its vector control clones treated with different concentrations of benzo[a]pyrene for 48 hrs. (C) Representative images of colonies formed by 35 weeks benzo[a]pyrene treated vimentin overexpressing and its vector control clones in soft agar. The soft agar assay was performed at definite weekly intervals in order to monitor the attainment of *in vitro* transformation. (D) Graphical representation of number of colonies formed in soft agar

by 35 weeks benzo[a]pyrene treated vimentin overexpressing and its vector control clones in soft agar. (E) Proliferation curves of 35 weeks benzo[a]pyrene treated vimentin overexpressing and its vector control clones over the period of 4 days, using MTT assay. (F) Representative time lapse microscopy images showing wound healing. (G) The graph shows percent wound closure as calculated over 20 h time point.

#### **4.3.4 Molecular changes associated with the vimentin overexpressing and its vector control cells in response to benzo[a]pyrene treatment**

To understand changes in the levels of EMT and stemness markers as a result of benzo[a]pyrene treatment, we performed RT-PCR analysis of benzo[a]pyrene treated vimentin overexpressing and its vector control clones. mRNA levels of vimentin were verified in order to ensure that the expression of vimentin is not lost, in the course of benzo[a]pyrene treatment (Figure 4.3.4A). Molecular changes associated with transformation like downregulation of p21 and involucrin (Figure 4.3.4E) and upregulation of stemness related markers (Nanog, Sox2, Oct-4) (Figure 4.3.4C), were more prominent in benzo[a]pyrene treated vimentin overexpressing as compared to its vector control clones. While EMT regulators (slug, twist, E-cadherin) (Figure 4.3.4B), known oncogenes (Ras,  $\beta$ -catenin) and oncosuppressors (p53) (Figure 4.3.4D) did not show any change, between vimentin overexpressing and its vector control clones after treatment with benzo[a]pyrene.

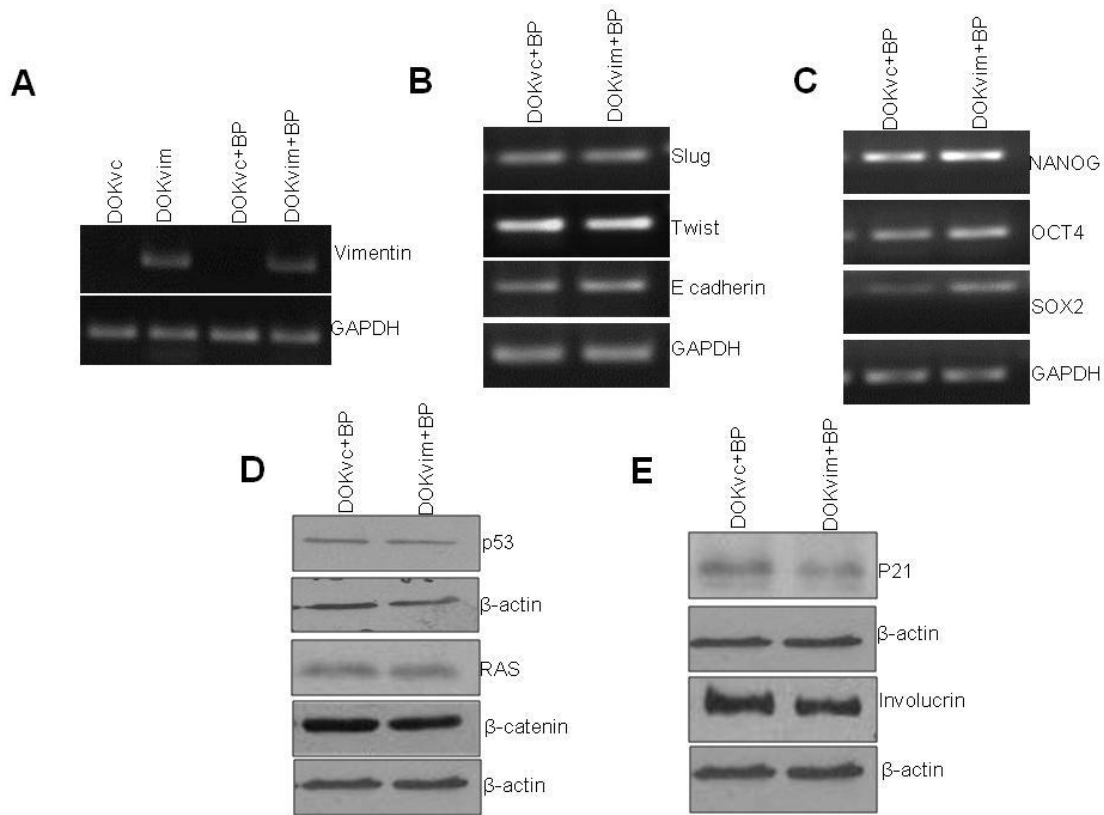


**Figure 4.3.4 Vimentin overexpressing cells treated with benzo[a]pyrene showed transformation related molecular signatures.** (A and B) RT-PCR analysis showing expression of vimentin and other EMT markers (slug, twist, E-cadherin) respectively between 35 weeks benzo[a]pyrene treated vimentin overexpressing and its vector control clones. GAPDH was used as a loading control. (C) RT-PCR analysis showing expression of stemness related markers (Nanog, Oct-4 and Sox2) between 35 weeks benzo[a]pyrene treated vimentin overexpressing and its vector control clones. GAPDH was used as a loading control. (D) Western blot analysis showing protein levels of p53, Ras and  $\beta$ -catenin in benzo[a]pyrene treated vimentin overexpressing and its vector control clones. (E) Western blot analysis showing protein levels of p21 and involucrin in benzo[a]pyrene treated vimentin overexpressing and its vector control clones.  $\beta$ -actin was used as a loading control in western blotting experiments.

### 4.3.5 Summary of objective 3

To summarise, experiments to understand whether expression of vimentin is one of the causes or a consequence of the development of human oral cancers showed that, vimentin overexpression by itself is not enough to bring about transformation. Nevertheless, its forced expression in the initial stage proves to be advantageous to the cell in order to push itself towards transformation in presence of a carcinogenic stimulus (Figure 4.3.5).

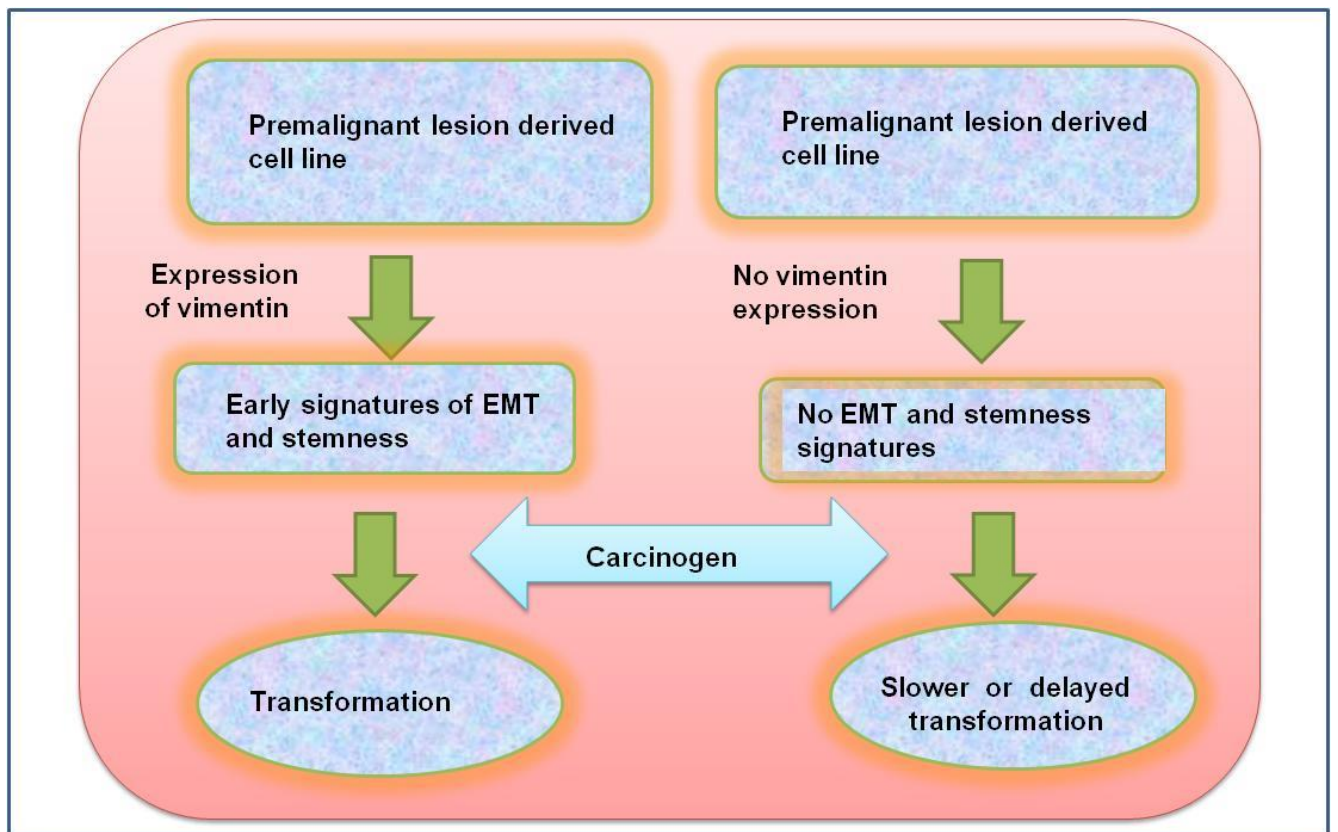


**Figure 4.3.5 Schematic depiction of the possible role of vimentin in early events of transformation.**

# Chapter 5: Discussion

## **Discussion:**

### **Part 1**

Aberrant expression of mesenchymal specific protein vimentin is seen in several cancers including oral cancer, breast cancer, prostate cancer, gastrointestinal tumors, etc. Its overexpression in carcinoma is reported to correlate with various clinico-pathological parameters like tumor growth, invasion and poor prognosis [5]. A previous study from our laboratory has also shown significant association of vimentin expression with invasive fronts and aggressive phenotype of oral tumours [175]. What remains elusive is our understanding of the molecular mechanisms underlying vimentin associated phenotype. In this part of our study, we have attempted to unravel the molecules involved in vimentin mediated cancer cell migration.

To understand the biology associated with aberrant vimentin expression in OSCC derived cells, we downregulated vimentin in tongue oral SCC derived cell line AW13516 using shRNA technology. Reduction in *in vitro* migration and invasion was observed upon vimentin downregulation (Figure 4.1.1). Along with this, a substantial difference was seen in the cell spreading between vimentin knockdown and vector control clones (Figure 4.1.2). As reported by Kim et al., cell spreading is a complex process which involves interactions between the cytoskeleton, matrix adhesion receptors and extracellular matrix (ECM) proteins [176]. In the carcinomas,  $\alpha6\beta4$  and  $\alpha6\beta1$  integrins are majorly involved in the regulation of cancer cell spreading and motility [12]. We found increase in the protein levels of  $\beta4$  integrin upon vimentin depletion. Our subsequent experiments indicated that the reduction in cell motility and invasion observed upon vimentin downregulation could be due to increased adhesive interactions mediated by  $\beta4$  integrin. This was further substantiated by downregulating  $\beta4$  integrin in vimentin knockdown background which thereby resulted in reversal of vimentin knockdown

phenotype. We also observed marked decrease in the protein levels of  $\beta 1$  integrin, which could also contribute to the reduction in migration seen in vimentin knockdown clones [177]. Since, vimentin  $\beta 1$  integrin interaction is well established [178], we decided to decipher the unknown link if any, between vimentin and  $\beta 4$  integrin. To our surprise,  $\alpha 6$  integrin levels remained unaffected in spite of an increase in the level of its binding partner,  $\beta 4$  integrin. This may be because, unlike  $\beta 1$  integrin,  $\beta 4$  integrin heterodimerizes exclusively with  $\alpha 6$  integrin. However,  $\alpha 6$  integrin is known to preferentially dimerize with the  $\beta 4$  subunit [179]. Hence, in our vimentin knockdown system, where  $\beta 1$  integrin levels are low, most of the  $\alpha 6$  subunits which would otherwise pair with  $\beta 1$  are now available to pair with the excess  $\beta 4$  integrin molecules.

$\alpha 6\beta 4$  integrin has contrasting roles in normal and cancerous conditions. Under normal conditions, it is expressed in stratified epithelia, where it forms stable contacts with the underlying basement membrane. However, in carcinomas, it is known to engage in signaling functions to encourage cancer cell migration and invasion [13]. Vimentin knockdown clones showed an increase in adhesion and spreading while a decrease in migration, on laminin-5 coated surfaces (Figure 4.1.9). In contrast, they showed decreased spreading and migration on fibronectin coated surfaces (Figure 4.1.10). This decrease in spreading and migration on fibronectin demonstrated by vimentin knockdown clones may be attributed to the downregulation of  $\beta 1$  integrin which binds to fibronectin in combination with  $\alpha 5$  or  $\alpha v$ . Nevertheless, adhesion on fibronectin is governed by both  $\beta 1$  integrin and  $\beta 3$  integrin, which may be the reason there is no difference in the adhesion on fibronectin, despite a reduction in  $\beta 1$  integrin level [180]. Our observations on both laminin-5 and fibronectin coated surfaces, highlighted the fact that the effects seen in vimentin knockdown cells are laminin-5 specific.

Interaction of vimentin with  $\beta 4$  integrin may not be direct but most probably mediated through a cytolinker like plectin. On these lines, vimentin- $\beta 4$  integrin interaction mediated by plectin has been reported in endothelial cells [14]. In the normal stratified epithelia, the disruption of plectin abrogates the interactions of basal keratinocytes to its basement membrane [119] while in SCCs, as reported by Katada et al., overexpression of plectin was shown to promote migration and invasion [181]. Our immunoprecipitation data suggested that plectin may be a linker connecting vimentin to  $\beta 4$  integrin. Additionally, upregulation of plectin protein levels along with  $\beta 4$  integrin protein levels in vimentin knockdown clones suggested that, plectin may serve to strengthen the cell matrix adhesive contacts in this particular setting. Next, our protein turnover experiments using cycloheximide indicated increased  $\beta 4$  integrin protein stability upon vimentin downregulation. Similar observations were reported in a multistep mouse model of skin carcinogenesis, wherein an increased turnover of  $\alpha 6\beta 4$  integrin was observed in cells derived from carcinoma as compared to those derived from papilloma. [130]. Moreover, a diffused expression of  $\alpha 6\beta 4$  integrin on the membrane was found, resulting in loss of its polarized expression, as seen normally in stratified epithelia [131]. In contrast to its normal function, in carcinomas,  $\alpha 6\beta 4$  integrin is known to stimulate signaling molecules to enhance migration and invasion [13].  $\beta 4$  integrin has been shown to be capable of activating pivotal kinases involved in carcinomas like PKB/Akt and ERK1/2 [127]. Hence we assessed the signaling potential of the  $\beta 4$  cytoplasmic domain in vimentin knockdown clones. Our data showed that the signaling ability of the  $\beta 4$  integrin domain remains unchanged with vimentin downregulation. Nevertheless, signaling associated with adhesive behavior of the cell was increased in vimentin deficient background. Interestingly, non-transformed cells did not exhibit the inverse relationship seen between vimentin and  $\beta 4$  integrin (Figure 4.1.4E), most likely

because expression of vimentin is associated with EMT, which itself is seen very late in the progression of cancer [182]. Hence, the regulation  $\beta$ 4 integrin by vimentin seems to be more of a transformation associated phenomena wherein other transformation associated changes also coexist.

Next, we wanted to investigate the cause of increased protein stability of both  $\beta$ 4 integrin and plectin in vimentin knockdown background. The global cellular protein degradation in eukaryotic systems is carried out by the proteosomal and lysosomal machinery. The proteosomal machinery degrades the cellular unfolded proteins while lysosomal machinery degrades the extracellular/membrane-associated proteins. [164]. Our data indicates involvement of both proteosomal as well as lysosomal machinery in maintaining the turnover of  $\beta$ 4 and plectin. Previously, Micheloni et al. have reported the proteosomal degradation of  $\beta$ 4 integrin in case of junctional epidermolysis bullosa with pyloric atresia [183]. Styers et al. have observed high similarity between AP-3-null and vimentin-null cells with respect to their decreased capacity to acidify the lysosomes. This is likely because interactions between vimentin and the adaptor complex AP-3 are known to be responsible in controlling the positioning, content, and subcellular distribution of selected late endosome/lysosome membrane proteins [164]. All the above reports on the link between vimentin and the proteosomal/lysosomal machinery suggest that perhaps in the absence of vimentin, there is altered targeting of  $\beta$ 4 integrin molecules to proteasome and lysosome, leading to a decrease in its protein turnover. Further studies are required to determine the defect if any, in membrane trafficking through late endosome/lysosome compartments in the vimentin deficient condition. A fraction of  $\beta$ 4 integrin [184] and plectin molecules [185] is shown to be susceptible to proteolytic cleavage by one of the isoforms of the calcium-activated enzyme calpain. Moreover, since MG132 can non-selectively inhibit calpain,

the possibility of involvement of calpain mediated degradation of  $\beta 4$  integrin and plectin molecules cannot be ruled out in our system. Nevertheless, additional experiments are required to understand the actual contribution of each of the degradation machineries.

Vimentin is widely reported as a canonical EMT marker [186]. Hence to understand whether the modulation of  $\beta 4$  integrin levels by vimentin is EMT associated, we treated AW13516 cells with TGF- $\beta 1$  (EMT inducer). TGF- $\beta 1$  mediated induction of EMT resulted in up regulation of vimentin and simultaneous downregulation of  $\beta 4$  integrin levels. Though there are no earlier reports indicating the relation between vimentin and  $\beta 4$  integrin in cancer, there is indirect evidence by Qu et al., who have shown an increase in mesenchymal markers like vimentin and fibronectin with a corresponding decrease in epithelial markers like E-cadherin,  $\alpha 6\beta 4$  integrin, etc. This marked the loss of epithelial like phenotype in kindlin-1 deficient keratinocytes [133]. The above facts suggest that perhaps, during the late stage of tumorigenesis, when EMT sets in, vimentin is overexpressed, leading to depletion of  $\beta 4$  integrin, which in turn, results in weak cell-basement contacts to facilitate migration.

Finally, immunohistochemistry analysis showed an inverse relationship between  $\beta 4$  integrin and vimentin expression, which corroborated with our *in vitro* findings. Vimentin overexpression and its correlation to invasion and metastasis have been shown by several groups [187-189]. Correspondingly, several reports document alterations in the levels of  $\beta 4$  integrin and its effect on the overall outcome of the disease. For example, loss of  $\alpha 6\beta 4$  at the basal layer was seen in cervical cancer [123]. Similarly, Downer et al. have documented the loss of  $\alpha 6\beta 4$  integrin and laminin in squamous cell carcinomas [124]. Our correlative studies of vimentin  $\beta 4$  expression in OSCC tissues with clinico-pathological parameters showed a significant association with the tumor stage, tumor size, node status and patients survival. Remarkably, high

vimentin and low  $\beta 4$  levels correlated with the poor survival as compared to other possible combinations of vimentin and  $\beta 4$  levels in our patients. The results of our *in vitro* data (increased invasion in  $\beta 4$  integrin-vimentin double knockdown) may explain the significant correlation seen between node status and poor survival in tumor samples with high vimentin and low  $\beta 4$  integrin expression. Thus apart from confirming the findings of previous studies, we could also show a hitherto unreported relation between vimentin and  $\beta 4$  integrin. Our data shows an unreported role of vimentin in modulating cancer cell motility by destabilizing  $\beta 4$  integrin mediated adhesive interactions. Further, vimentin- $\beta 4$  integrin could be promising prognostic markers and thus warrant further large scale study on human oral tumors to establish them as prognostic markers.

## **Part 2**

Expression of EMT marker vimentin is usually associated with a more mesenchymal like and dedifferentiated state of the cancer cell [4]. On the other hand, in the case of stratified epithelia, expression of one pair of keratins is specific to one particular differentiation compartment and as the cell moves from one layer to another, the expression pattern of keratins also changes accordingly [190]. This suggests that keratins may also have regulatory role in epithelial differentiation [191]. Hence we wanted to understand whether vimentin modulates a differentiation switch of a transformed cell by modulating the expression of keratins. Our study found the K5/K14 pair to be a novel indirect target of vimentin, through which it is able to confer a dedifferentiated phenotype to the cancer cell.

To understand the overall change in the keratin profile caused due to downregulation of vimentin, we performed a global keratin profile analysis using high salt enriched keratin fraction from vimentin knockdown and vector control cells. Our 2D followed by MALDI analysis identified K14 as one of the differentially expressed proteins upon downregulation of vimentin.

Interestingly its binding partner K5 was also found to be downregulated at the protein level. Further transcript level analysis showed that mRNA levels of both K5 and K14 are downregulated in vimentin knockdown clones.

K5/K14 pair is typically expressed by the basal stem cell layer of the stratified epithelium. As the cell from this layer is committed to differentiation, it replaces the expression of K5/K14 with the expression of one or more differentiation specific keratin pairs e.g. K1 and K10 [190]. A previous study from our laboratory has demonstrated the role of K5/K14 in modulating phosphatidylinositol 3-kinase/Akt-mediated cell proliferation and/or Notch1-dependent cell differentiation, in stratified epithelia derived cells [139]. Our current study showed an increase in the differentiation status of the vimentin knockdown cells, while its proliferation status remained unaffected (Figure 4.2.3). This change in differentiation could be attributed to the decreased levels of K5/K14 since its reversal was seen upon re-expression of K5/K14 in vimentin knockdown background. Proliferation potential of the cells remained unchanged upon vimentin knockdown, perhaps due to remnant levels of K5/K14 or because of an unknown compensatory mechanism operating in this situation.

Progenitor/stem-like and differentiated state are at extreme ends of the differentiation spectrum. Ding et al., have reported the loss of Oct-4 expression during the differentiation of mouse embryonic stem cells [192]. Hence, we were curious to understand if our vimentin knockdown cells, which were more differentiated showed decreased stemness. To verify this, we checked the expression of Oct-4, which is the master regulator of stemness [193]. Our results demonstrated a decrease in the expression of Oct-4 with the decrease in the expression of K5/K14, while re-expression of K5/K14 rescued the decreased levels of Oct-4. This suggests that the expression of Oct-4 is dependent on the levels of K5/K14. What remains

elusive is whether vimentin-K5/K14 axis targets the differentiation programme to lead to increased stemness or it targets stemness related mechanism to suppress differentiation.

Transcription factors like AP1 and NF- $\kappa$ B are implicated in the regulation of basal expression of K5/K14 pair. The activation of these transcription factors is also dependent on extracellular signaling molecules like hormones, vitamins and growth factors [194]. Nevertheless, the role of the epithelial-specific master regulator p63 is well known for its precise control over epithelial cell differentiation [195]. One of the ways in which p63 regulates the differentiation program, is through the maintenance of basal specific and stage specific expression of K5/K14 pair [196]. Vimentin knockdown resulted in downregulation of  $\Delta$ Np63 (a major p63 isoform expressed by undifferentiated keratinocytes), while p21 and p27 levels were found to be upregulated. However, despite the upregulation of cyclin dependent kinase (Cdk) inhibitors, p21 and p27, the proliferation status of vimentin knockdown clone remained unaltered. This is possible because, as shown by Zheng et al., neither p21 nor p27 knockout mice showed any alterations in proliferation of mouse gastrointestinal tract cells [197]. Similarly, some cancer cells are known to proliferate despite CDK2 inhibition [198], suggesting that perhaps under certain conditions, levels of p21 and p27 don't correlate directly with the cell proliferation. Further, analysis of transcript level expression of all the three  $\Delta$ Np63 isoforms revealed downregulation of both  $\Delta$ Np63 $\alpha$  and  $\Delta$ Np63 $\gamma$  and no change in the levels of  $\Delta$ Np63 $\beta$ . Report by Romano et al. suggested a role of  $\Delta$ Np63 $\alpha$  and  $\Delta$ Np63 $\beta$  isoforms in inducing basal markers and stratification [170]. Therefore, to understand if vimentin modulates expression of K5/K14 pair through  $\Delta$ Np63 $\alpha$  isoform, we overexpressed  $\Delta$ Np63 $\alpha$  isoform (since levels of  $\Delta$ Np63 $\beta$  remained unaltered upon vimentin downregulation) in vimentin knockdown background. Overexpression of  $\Delta$ Np63 $\alpha$  resulted in an increase in the expression of K14, while

the expression of K5 remained unaltered. As a result of this, the differentiated state of the cell (marked by the expression of differentiation specific proteins) remained unchanged. This indicated that  $\Delta Np63\gamma$ , may as well, have a role in the regulation of the expression of K5, which was not compensated by the overexpression of  $\Delta Np63\alpha$  isoform alone. The possibility of involvement of some other K5 specific transcription factor/s (enhancer or repressor), downstream of vimentin, cannot be ruled out.

Levels of  $\Delta Np63\alpha$  and notch play a decisive role to either maintain stemness or to proceed towards differentiation [171]. During the stratification process of epidermal tissue, notch suppresses p63 to favor differentiation, as evident by their opposing levels in the basal compartment [172]. Our study showed an increase in the levels of notch1 with decreased  $\Delta Np63$  expression in the vimentin knockdown clone. Correspondingly, a decrease in the level of notch1 was seen upon overexpression of  $\Delta Np63\alpha$  (Figure 4.2.8). This suggests that there may be a reciprocal negative regulatory mechanism between notch and  $\Delta Np63$  in order to govern differentiation in the presence and absence of vimentin. There may be two possibilities in this situation: first being either the deficiency of vimentin relieves the inhibition on notch1 which in turn suppresses the expression of  $\Delta Np63$  or the second possibility is that downregulation of vimentin decreases the expression of  $\Delta Np63$  relieving the negative regulatory effect on notch1 and leading to its activation. Interestingly, while the downregulation of  $\Delta Np63$  has been shown to result in a decrease in the expression of vimentin in esophageal squamous carcinoma [199], we report the reverse here i.e., downregulation of vimentin leads to decreased expression of  $\Delta Np63$ . Evidence of vimentin regulating transcript levels of certain genes is reported previously as well. For instance, Vuoriluoto et al. have shown the role of vimentin in regulating the

expression of several genes associated with EMT and the basal-like phenotype, one of which is Ax1 (a receptor tyrosine kinase) in breast cancer derived cell lines [10].

Factors other than activated notch may also have a significant role to play in the regulation of  $\Delta Np63$ . Along these lines, Flores et al., have shown inhibition of wild-type p53 by  $\Delta Np63$  [200]. Moreover, the parental cell line under study, AW13516 expresses mutant p53 (R273H) [201]. Hence, work in this direction will be required to ascertain if mutant p53 is the cause or consequence of an alteration in  $\Delta Np63\alpha$  expression. Furthermore, specific roles of microRNAs (miRs) [202, 203], Wnt, Hedgehog and EGFR [195] pathways if any, in the regulation of  $\Delta Np63$  expression in vimentin depleted condition, needs to be investigated.

We found a significant correlation between high-vimentin high-K14 expression and recurrence as well as poor survival of oral cancer patients. This finding can be explained by our *in vitro* data using vimentin knockdown system. This showed that vimentin expression promotes events leading to increased dedifferentiation and tumorigenicity, wherein K5/K14 upregulation seems to be an intermediate event. Similar observations were made by Thomas et al., who have reported the association of vimentin-keratin co-expression with poor prognosis and tumor phenotype [204]. Together, this suggests that vimentin aids the aggressiveness of the tumor by contributing to the maintenance of a dedifferentiated state of the tumor cell.

In conclusion, our data sheds light on the modulatory role of vimentin in the expression of K5/K14 pair, to fine tune the differentiation switch in favor of tumor progression. Further, a large scale study on human oral tumors is required to prove the potential of vimentin-K14 as prognostic markers for human oral cancer.

### **Objective 3**

The development of oral cancer is a multistep process. Around 5% to 85% of the oral tumors arise from potentially malignant disorders (PMD) [2]. Although, the oral cavity is accessible for visual examination, the ability of current clinical/histological methods to predict which lesions further progress into malignancy is limited. Hence the development of biological markers which will prove as an adjunct to histo-diagnosis has become essential. In this direction, our laboratory had previously demonstrated aberrant expression of vimentin in oral premalignant lesions and its correlation with the degree of premalignancy [175]. The major limitation of the study was that there was no follow-up data regarding which of these lesions (vimentin expressing or non-expressing) progressed to form a tumor, if any. To address this issue and to ascertain the contribution of vimentin in the early stages of oral tumorigenesis, we overexpressed vimentin in oral premalignant derived cell line DOK. This study demonstrated that vimentin expression alone is not enough to result in transformation of DOK cell line, although initial EMT/stemness related changes were observed. Further, after benzo[a]pyrene treatment (to recapitulate the situation in a chronic smokers), vimentin expressing cells showed increased transformation as compared to non-expressing ones.

We selected DOK cell line for our study, mainly because of two reasons: it was a vimentin negative cell line and was derived from an oral premalignant lesion showing dysplasia [144]. This simulated the situation seen in oral premalignant lesions, wherein the cells are initiated but not yet transformed. After verifying the non-transformed status of DOK by testing for anchorage independence ability, we overexpressed vimentin using viral transduction. Vimentin overexpression in DOK did not cause any phenotypic changes (anchorage independence, migration, proliferation) associated with transformation (Figure 4.3.2). The role of

vimentin is well established in migration and proliferation, for instance, Gilles et al. have reported the association of vimentin expression with the migratory state of the cell, during *in vitro* wound-healing, in the case of human breast cell line MCF10A [60]. Similarly, during lung injury, TGF $\beta$ 1-induced expression of vimentin was shown to result in increased migration, which was independent of proliferation [205]. Furthermore, downregulation of vimentin in breast cancer cell line MDA-MB 231 showed a defect in proliferation and directional migration suggesting its involvement in governing EMT associated cancer cell migration and proliferation [206]. Despite this, vimentin overexpressing cells did not show any difference in migration and proliferation, which may be because vimentin dependent migration is not an isolated event but is tightly coupled either with a physiological need or the transformation process of the cell. Hence, vimentin alone may not be able to regulate migration, in the absence of its other altered interactors or upstream regulators [10, 207]. Nevertheless, some peculiar changes were noticed in the expression of EMT and stemness related regulators. This was an expected observation, since according to recent reports vimentin not only serves as a marker of EMT but also functions to drive the process of EMT [4]. Though direct evidence of vimentin mediated downregulation of the expression of E-cadherin is not known, there are several reports citing an inverse relationship between the expression profiles of vimentin and E-cadherin in many cancers and cancer derived cells [208-210]. This collectively suggested that vimentin alone may not be enough to convert the cell from dysplastic state to transformed state, but can confer some molecular level alterations which may be beneficial for the cell to progress to the next level, if subjected to further carcinogenic trigger.

As an additional carcinogenic trigger to induce transformation, we selected benzo[a]pyrene as a procarcinogen after checking the metabolic competence of the vimentin

overexpressing and its vector control cells. Benzo[a]pyrene was selected because it is mutagenic and carcinogenic in animal models, cell lines and simulates the condition seen in case of chronic smokers [156, 211]. Also, the parental cell line DOK was derived from a heavy smoker [144].

It took 35 weeks of carcinogen exposure to form visible colonies on soft agar, which marked the attainment of an *in vitro* transformed state. Interestingly, benzo[a]pyrene treated vimentin overexpressing cells demonstrated approximately 2-fold increase in the number of colonies formed on soft agar as compared to its treated vector control cells. However, these cells showed no significant difference in the migration and proliferation potential. The increased transformation efficiency seen in benzo[a]pyrene treated vimentin overexpressing cells may be attributed to its pre-acquired molecular level changes in EMT and stemness related regulators (Figure 4.3.3). Our findings corroborated with Tellez et al. data, which showed induction of dedifferentiation program characterized by EMT and stemness related changes, which occurs early in the process of transformation. These changes were shown to contribute to the process of cancer initiation to finally achieve transformation [212]. Although, in this report, the changes in EMT and stemness markers were acquired by an epigenetic mechanism, in our study, vimentin being cytoskeletal protein the likelihood of it exerting direct epigenetic regulation is remote. In this context, we assume the possibility of vimentin targeting some of its interactors or intermediates to subsequently result in transcriptional regulation of EMT and stemness related proteins in the absence of carcinogenic stimulus. Furthermore, after benzo[a]pyrene treatment, the EMT markers did not show any difference while the stemness markers Nanog and Sox2 were overexpressed in vimentin overexpressing as compared to its vector control cells. Thus, it can be speculated that, in the initial stages, EMT regulators drive this process but as it progresses, stemness markers take over to complete the process of transformation and later maintain the

transformed state. Moreover, this hypothesis can be tested by sequential downregulation of EMT and stemness related markers followed by benzo[a]pyrene exposure. Similarly, differential molecular changes like downregulation of involucrin, marking dedifferentiated phenotype and downregulation of p21 marking alteration in cell cycle were noted in benzo[a]pyrene treated vimentin overexpressing cells. These changes are suggestive of a more transformed phenotype although, a decrease in p21 levels did not result in increased proliferation most possibly because in certain instances proliferation may be independent of p21 levels [197]. Surprisingly, neither benzo[a]pyrene treated vimentin overexpressing nor its vector control cells showed endogenous induction of vimentin expression, which suggests that perhaps it occurs very late in the process of transformation and further treatment with benzo[a]pyrene for several weeks, might be required to achieve this stage.

Our study at this preliminary stage supports the potential of vimentin as an early diagnostic marker but additional experiments like nude mice injection with benzo[a]pyrene treated cells and rescue experiments with vimentin knockdown are required to strengthen our hypothesis. The long term goal would be to follow-up the patients presenting with premalignant lesions for 15-20 years and then correlate the status of vimentin in the initial stages with that of the transformation status. Further, our *in vitro* carcinogenesis model may serve as a useful system to screen for vimentin associated molecules and anticancer drugs which specifically target vimentin expressing cancer cells eg. withaferin [97].

In conclusion, our data suggests that forced expression of vimentin in the initial stage proves to be advantageous to the cell in order to push itself towards transformation in presence of an additional carcinogenic trigger.

## 5.1 Overall summary of the role of vimentin deduced in this study

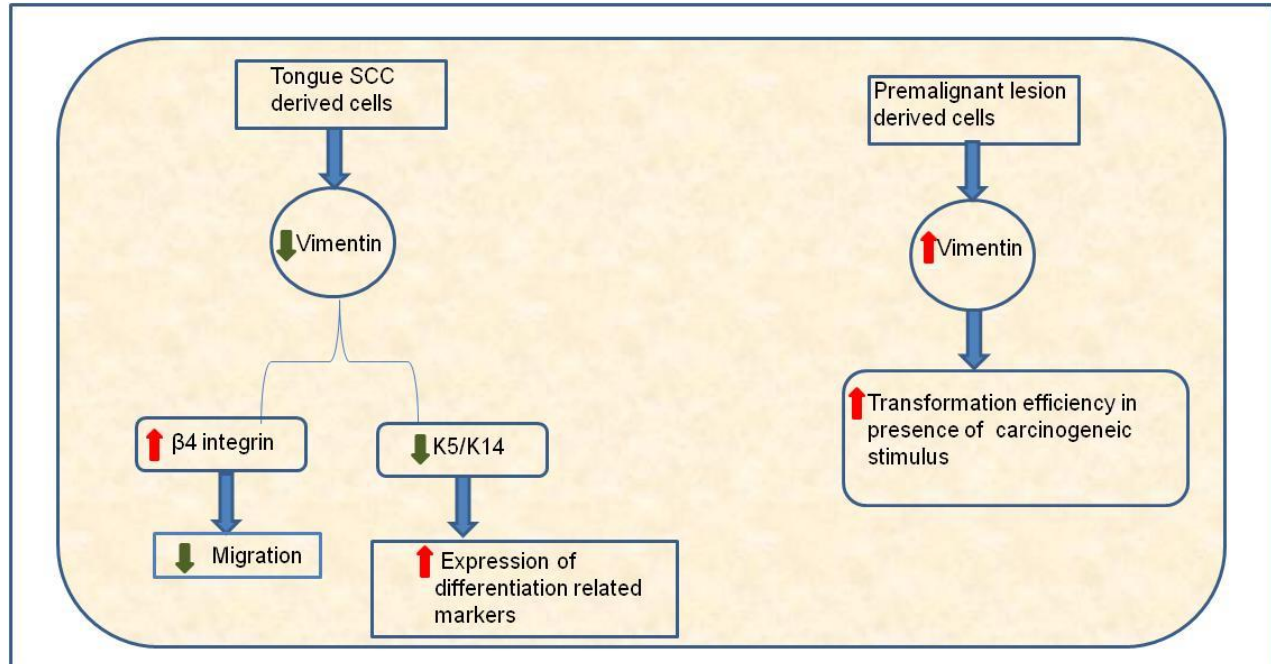


**Figure 5.1 Schematic representation of the role of vimentin in oral precancer and cancer.**

Downregulation of vimentin in tongue SCC derived cells resulted in decreased migration (mediated through upregulation of  $\beta 4$  integrin) and increase in differentiation status (mediated through downregulation of K5/K14). Exogenous expression of vimentin alone, in premalignant lesion derived cells did not result in transformation but led to acquisition of EMT and stemness related signatures. Further, additional carcinogenic trigger promoted the process of transformation, leading to increased transformation efficiency in vimentin overexpressing cells as compared to its control counterpart.

# Chapter 6: Summary and Conclusion

## Summary

Our study deciphers the molecules ( $\beta 4$  integrin and K5/K14) underlying vimentin associated phenotype in oral carcinoma derived cells. Further, our *in vitro* findings using vimentin knockdown cells, corroborated with IHC analysis of human oral tumor samples. Also, our study on early events of oral cancer development indicates that presence of vimentin equips the cell with transformation promoting alterations which renders the cell more prone to transformation upon carcinogenic stimulus.

The highlights of the study are as follows:

- 6.1 Knockdown in tongue SCC derived AW13516 cells resulted in increased  $\beta 4$  integrin surface levels leading to strong adhesive contacts. This manifested into decreased motility. Interestingly, along with  $\beta 4$  integrin, its linker protein plectin was also upregulated in vimentin knockdown clones.
- 6.2 The upregulated levels of  $\beta 4$  integrin and plectin showed a preferential localization at the membrane-substrate front, in vimentin knockdown cells.
- 6.3  $\beta 4$  integrin adhesion blocking antibody (ASC-8) was able to rescue the decreased motility and invasion of vimentin knockdown cells.
- 6.4 Increased  $\beta 4$  integrin level in vimentin knockdown clones was not coupled with the elevated  $\beta 4$  integrin associated intrinsic signaling.
- 6.5 The increased stability of  $\beta 4$  integrin and plectin molecules in vimentin knockdown cells was possibly because of the decreased targeting of these molecules to proteasomal and lysosomal machinery.

- 6.6 Inverse correlation was observed between vimentin and  $\beta 4$  integrin in human oral cancer tissue samples, which correlated with clinico-pathological parameters like stage, tumor size and node status of the OSCC patients.
- 6.7 Vimentin downregulation in AW13516 cells resulted in reduction in the expression of K5/K14 pair.
- 6.8 Vimentin modulates the differentiation status and tumorigenic potential of the carcinoma cells by regulating the expression of basal layer specific K5/K14 pair.
- 6.9 Vimentin may influence Notch1- $\Delta$ Np63 crosstalk to control the expression levels of K5/K14, in order to regulate the differentiation state of a transformed cell.
- 6.10 Furthermore, vimentin-K14 expression may be clinically relevant in order to prognosticate the fate of the OSCC patients.
- 6.11 Overexpression of vimentin in premalignant lesion derived cells did not result in any transformation related phenotypic alterations. Nevertheless, alterations were seen in the expression of key EMT and stemness related regulators.
- 6.12 *In vitro* carcinogenesis model was developed using benzo[a]pyrene for the evaluation of the transformation potential of vimentin in the development of human oral cancer.
- 6.13 Benzo[a]pyrene treated vimentin overexpressing cells showed increased transformation efficiency as compared to its treated vector control cells.

## **Conclusion**

Collectively, vimentin has emerged as one of the drivers of key events, beneficial for tumor progression. High vimentin-high K14-low  $\beta 4$  integrin expression in combination, if validated in more number of samples, may prove useful in prognostication of human oral cancer.

Further studies are required to understand the definitive role of vimentin in initial stages of human oral oncogenesis.

# **Bibliography**

## References

1. Coelho KR. Challenges of the oral cancer burden in India. *Journal of cancer epidemiology*. 2012;2012:701932. doi: 10.1155/2012/701932. PubMed PMID: 23093961; PubMed Central PMCID: PMC3471448.
2. Nair DR, Pruthy R, Pawar U, Chaturvedi P. Oral cancer: Premalignant conditions and screening--an update. *Journal of cancer research and therapeutics*. 2012;8 Suppl 1:S57-66. doi: 10.4103/0973-1482.92217. PubMed PMID: 22322734.
3. da Silva SD, Ferlito A, Takes RP, Brakenhoff RH, Valentin MD, Woolgar JA, et al. Advances and applications of oral cancer basic research. *Oral oncology*. 2011;47(9):783-91. doi: 10.1016/j.oraloncology.2011.07.004. PubMed PMID: 21802978.
4. Kidd ME, Shumaker DK, Ridge KM. The role of vimentin intermediate filaments in the progression of lung cancer. *American journal of respiratory cell and molecular biology*. 2014;50(1):1-6. doi: 10.1165/rcmb.2013-0314TR. PubMed PMID: 23980547; PubMed Central PMCID: PMC3930939.
5. Satelli A, Li S. Vimentin in cancer and its potential as a molecular target for cancer therapy. *Cellular and molecular life sciences : CMLS*. 2011;68(18):3033-46. doi: 10.1007/s00018-011-0735-1. PubMed PMID: 21637948; PubMed Central PMCID: PMC3162105.
6. Sawant SS, Vaidya M, Chaukar DA, Alam H, Dmello C, Gangadaran P, et al. Clinical significance of aberrant vimentin expression in oral premalignant lesions and carcinomas. *Oral diseases*. 2014;20(5):453-65. doi: 10.1111/odi.12151. PubMed PMID: 23865921.
7. Bihari Lal Soni AM, Harsh Pawar, Sharada S. Sawant, Anita Borges,, Ranganathan Kannan AP, Arvind D. Ingle, Hindahally Chandregowda Harsha,, Vaidya MM. Quantitative proteomic analysis of different stages of rat lingual carcinogenesis. *Clinical Communications-Oncology*. 2014;1(1). doi: 10.4103/WKMP-0062.132172.
8. Kang Y, Massague J. Epithelial-mesenchymal transitions: twist in development and metastasis. *Cell*. 2004;118(3):277-9. doi: 10.1016/j.cell.2004.07.011. PubMed PMID: 15294153.
9. Paccione RJ, Miyazaki H, Patel V, Waseem A, Gutkind JS, Zehner ZE, et al. Keratin down-regulation in vimentin-positive cancer cells is reversible by vimentin RNA interference, which inhibits growth and motility. *Molecular cancer therapeutics*. 2008;7(9):2894-903. doi: 10.1158/1535-7163.MCT-08-0450. PubMed PMID: 18790770.
10. Vuoriluoto K, Haugen H, Kiviluoto S, Mpindi JP, Nevo J, Gjerdrum C, et al. Vimentin regulates EMT induction by Slug and oncogenic H-Ras and migration by governing Axl expression in breast cancer. *Oncogene*. 2011;30(12):1436-48. doi: 10.1038/onc.2010.509. PubMed PMID: 21057535.
11. Dong P, Kaneuchi M, Watari H, Hamada J, Sudo S, Ju J, et al. MicroRNA-194 inhibits epithelial to mesenchymal transition of endometrial cancer cells by targeting oncogene BMI-1. *Molecular cancer*. 2011;10:99. doi: 10.1186/1476-4598-10-99. PubMed PMID: 21851624; PubMed Central PMCID: PMC3173388.
12. Cress AE, Rabinovitz I, Zhu W, Nagle RB. The alpha 6 beta 1 and alpha 6 beta 4 integrins in human prostate cancer progression. *Cancer metastasis reviews*. 1995;14(3):219-28. PubMed PMID: 8548870.
13. Mercurio AM, Rabinovitz I, Shaw LM. The alpha 6 beta 4 integrin and epithelial cell migration. *Current opinion in cell biology*. 2001;13(5):541-5. PubMed PMID: 11544021.
14. Homan SM, Martinez R, Benware A, LaFlamme SE. Regulation of the association of alpha 6 beta 4 with vimentin intermediate filaments in endothelial cells. *Experimental cell research*. 2002;281(1):107-14. PubMed PMID: 12441134.
15. Mendez MG, Kojima S, Goldman RD. Vimentin induces changes in cell shape, motility, and adhesion during the epithelial to mesenchymal transition. *FASEB journal : official publication of the*

- Federation of American Societies for Experimental Biology. 2010;24(6):1838-51. doi: 10.1096/fj.09-151639. PubMed PMID: 20097873; PubMed Central PMCID: PMC2874471.
16. Sommers CL, Byers SW, Thompson EW, Torri JA, Gelmann EP. Differentiation state and invasiveness of human breast cancer cell lines. *Breast cancer research and treatment*. 1994;31(2-3):325-35. PubMed PMID: 7881109.
  17. Scully C, Bagan J. Oral squamous cell carcinoma overview. *Oral oncology*. 2009;45(4-5):301-8. doi: 10.1016/j.oraloncology.2009.01.004. PubMed PMID: 19249237.
  18. Holmstrup P, Vedtofte P, Reibel J, Stoltze K. Long-term treatment outcome of oral premalignant lesions. *Oral oncology*. 2006;42(5):461-74. doi: 10.1016/j.oraloncology.2005.08.011. PubMed PMID: 16316774.
  19. Tanaka T, Ishigamori R. Understanding carcinogenesis for fighting oral cancer. *Journal of oncology*. 2011;2011:603740. doi: 10.1155/2011/603740. PubMed PMID: 21772845; PubMed Central PMCID: PMC3136173.
  20. A V. Prevalence of Oral Cancer in India. *J Pharm Sci & Res*. 2015;7(10):4.
  21. Goldenberg D, Lee J, Koch WM, Kim MM, Trink B, Sidransky D, et al. Habitual risk factors for head and neck cancer. *Otolaryngology--head and neck surgery : official journal of American Academy of Otolaryngology-Head and Neck Surgery*. 2004;131(6):986-93. doi: 10.1016/j.otohns.2004.02.035. PubMed PMID: 15577802.
  22. Goldenberg D, Benoit NE, Begum S, Westra WH, Cohen Y, Koch WM, et al. Epstein-Barr virus in head and neck cancer assessed by quantitative polymerase chain reaction. *The Laryngoscope*. 2004;114(6):1027-31. doi: 10.1097/00005537-200406000-00013. PubMed PMID: 15179207.
  23. Shi W, Pataki I, MacMillan C, Pintilie M, Payne D, O'Sullivan B, et al. Molecular pathology parameters in human nasopharyngeal carcinoma. *Cancer*. 2002;94(7):1997-2006. PubMed PMID: 11932902.
  24. Gillison ML. Human papillomavirus-associated head and neck cancer is a distinct epidemiologic, clinical, and molecular entity. *Seminars in oncology*. 2004;31(6):744-54. PubMed PMID: 15599852.
  25. Larsson LG, Sandstrom A, Westling P. Relationship of Plummer-Vinson disease to cancer of the upper alimentary tract in Sweden. *Cancer research*. 1975;35(11 Pt. 2):3308-16. PubMed PMID: 1192404.
  26. Marur S, Forastiere AA. Head and neck cancer: changing epidemiology, diagnosis, and treatment. *Mayo Clinic proceedings*. 2008;83(4):489-501. doi: 10.4065/83.4.489. PubMed PMID: 18380996.
  27. Hayes RB, Gerin M, Raatgever JW, de Bruyn A. Wood-related occupations, wood dust exposure, and sinonasal cancer. *American journal of epidemiology*. 1986;124(4):569-77. PubMed PMID: 3752051.
  28. Hernberg S, Westerholm P, Schultz-Larsen K, Degerth R, Kuosma E, Englund A, et al. Nasal and sinonasal cancer. Connection with occupational exposures in Denmark, Finland and Sweden. *Scandinavian journal of work, environment & health*. 1983;9(4):315-26. PubMed PMID: 6635610.
  29. Sidransky D. Molecular genetics of head and neck cancer. *Current opinion in oncology*. 1995;7(3):229-33. PubMed PMID: 7654824.
  30. Chung CH, Parker J, Levy S, Slebos RJ, Dicker AP, Rodeck U. Gene expression profiles as markers of aggressive disease-EGFR as a factor. *International journal of radiation oncology, biology, physics*. 2007;69(2 Suppl):S102-5. doi: 10.1016/j.ijrobp.2007.05.039. PubMed PMID: 17848272; PubMed Central PMCID: PMC2361130.
  31. Forastiere A, Koch W, Trotti A, Sidransky D. Head and neck cancer. *The New England journal of medicine*. 2001;345(26):1890-900. doi: 10.1056/NEJMra001375. PubMed PMID: 11756581.
  32. Brennan JA, Sidransky D. Molecular staging of head and neck squamous carcinoma. *Cancer metastasis reviews*. 1996;15(1):3-10. PubMed PMID: 8842476.

33. Reed AL, Califano J, Cairns P, Westra WH, Jones RM, Koch W, et al. High frequency of p16 (CDKN2/MTS-1/INK4A) inactivation in head and neck squamous cell carcinoma. *Cancer research*. 1996;56(16):3630-3. PubMed PMID: 8705996.
34. Carnelio S, Rodrigues GS, Shenoy R, Fernandes D. A brief review of common oral premalignant lesions with emphasis on their management and cancer prevention. *The Indian journal of surgery*. 2011;73(4):256-61. doi: 10.1007/s12262-011-0286-6. PubMed PMID: 22851837; PubMed Central PMCID: PMC3144354.
35. Yardimci G, Kutlubay Z, Engin B, Tuzun Y. Precancerous lesions of oral mucosa. *World journal of clinical cases*. 2014;2(12):866-72. doi: 10.12998/wjcc.v2.i12.866. PubMed PMID: 25516862; PubMed Central PMCID: PMC4266835.
36. Au J, Patel D, Campbell JH. Oral lichen planus. *Oral and maxillofacial surgery clinics of North America*. 2013;25(1):93-100, vii. doi: 10.1016/j.coms.2012.11.007. PubMed PMID: 23399399.
37. Fedele S. Diagnostic aids in the screening of oral cancer. *Head & neck oncology*. 2009;1:5. doi: 10.1186/1758-3284-1-5. PubMed PMID: 19284694; PubMed Central PMCID: PMC2654034.
38. Moles DR, Downer MC, Speight PM. Meta-analysis of measures of performance reported in oral cancer and precancer screening studies. *British dental journal*. 2002;192(6):340-4; discussion 32. PubMed PMID: 15552072.
39. McCullough MJ, Prasad G, Farah CS. Oral mucosal malignancy and potentially malignant lesions: an update on the epidemiology, risk factors, diagnosis and management. *Australian dental journal*. 2010;55 Suppl 1:61-5. doi: 10.1111/j.1834-7819.2010.01200.x. PubMed PMID: 20553246.
40. Burzynski NJ, Firriolo FJ, Butters JM, Sorrell CL. Evaluation of oral cancer screening. *Journal of cancer education : the official journal of the American Association for Cancer Education*. 1997;12(2):95-9. doi: 10.1080/08858199709528462. PubMed PMID: 9229272.
41. Bonner JA, Harari PM, Giralt J, Azarnia N, Shin DM, Cohen RB, et al. Radiotherapy plus cetuximab for squamous-cell carcinoma of the head and neck. *The New England journal of medicine*. 2006;354(6):567-78. doi: 10.1056/NEJMoa053422. PubMed PMID: 16467544.
42. Tanaka T. Chemoprevention of human cancer: biology and therapy. *Critical reviews in oncology/hematology*. 1997;25(3):139-74. PubMed PMID: 9177939.
43. Moll R, Franke WW, Schiller DL, Geiger B, Krepler R. The catalog of human cytokeratins: patterns of expression in normal epithelia, tumors and cultured cells. *Cell*. 1982;31(1):11-24. PubMed PMID: 6186379.
44. Strelkov SV, Herrmann H, Aebi U. Molecular architecture of intermediate filaments. *BioEssays : news and reviews in molecular, cellular and developmental biology*. 2003;25(3):243-51. doi: 10.1002/bies.10246. PubMed PMID: 12596228.
45. Lowery J, Kuczmarski ER, Herrmann H, Goldman RD. Intermediate Filaments Play a Pivotal Role in Regulating Cell Architecture and Function. *The Journal of biological chemistry*. 2015;290(28):17145-53. doi: 10.1074/jbc.R115.640359. PubMed PMID: 25957409; PubMed Central PMCID: PMC4498054.
46. Godsel LM, Hobbs RP, Green KJ. Intermediate filament assembly: dynamics to disease. *Trends in cell biology*. 2008;18(1):28-37. doi: 10.1016/j.tcb.2007.11.004. PubMed PMID: 18083519.
47. Fuchs E, Weber K. Intermediate filaments: structure, dynamics, function, and disease. *Annual review of biochemistry*. 1994;63:345-82. doi: 10.1146/annurev.bi.63.070194.002021. PubMed PMID: 7979242.
48. Chang L, Goldman RD. Intermediate filaments mediate cytoskeletal crosstalk. *Nature reviews Molecular cell biology*. 2004;5(8):601-13. doi: 10.1038/nrm1438. PubMed PMID: 15366704.
49. Margiotta A, Bucci C. Role of Intermediate Filaments in Vesicular Traffic. *Cells*. 2016;5(2). doi: 10.3390/cells5020020. PubMed PMID: 27120621; PubMed Central PMCID: PMC4931669.
50. Wang N, Stamenovic D. Contribution of intermediate filaments to cell stiffness, stiffening, and growth. *American journal of physiology Cell physiology*. 2000;279(1):C188-94. PubMed PMID: 10898730.

51. Haudenschild DR, Chen J, Pang N, Steklov N, Grogan SP, Lotz MK, et al. Vimentin contributes to changes in chondrocyte stiffness in osteoarthritis. *Journal of orthopaedic research : official publication of the Orthopaedic Research Society*. 2011;29(1):20-5. doi: 10.1002/jor.21198. PubMed PMID: 20602472; PubMed Central PMCID: PMC2976780.
52. Oriolo AS, Wald FA, Canessa G, Salas PJ. GCP6 binds to intermediate filaments: a novel function of keratins in the organization of microtubules in epithelial cells. *Molecular biology of the cell*. 2007;18(3):781-94. doi: 10.1091/mbc.E06-03-0201. PubMed PMID: 17182859; PubMed Central PMCID: PMC1805110.
53. Conover GM, Gregorio CC. The desmin coil 1B mutation K190A impairs nebulin Z-disc assembly and destabilizes actin thin filaments. *Journal of cell science*. 2011;124(Pt 20):3464-76. doi: 10.1242/jcs.087080. PubMed PMID: 21984811; PubMed Central PMCID: PMC3196858.
54. Cary RB, Klymkowsky MW, Evans RM, Domingo A, Dent JA, Backhus LE. Vimentin's tail interacts with actin-containing structures in vivo. *Journal of cell science*. 1994;107 ( Pt 6):1609-22. PubMed PMID: 7962201.
55. Esue O, Carson AA, Tseng Y, Wirtz D. A direct interaction between actin and vimentin filaments mediated by the tail domain of vimentin. *The Journal of biological chemistry*. 2006;281(41):30393-9. doi: 10.1074/jbc.M605452200. PubMed PMID: 16901892.
56. Virtakoivu R, Mai A, Mattila E, De Franceschi N, Imanishi SY, Corthals G, et al. Vimentin-ERK Signaling Uncouples Slug Gene Regulatory Function. *Cancer research*. 2015;75(11):2349-62. doi: 10.1158/0008-5472.CAN-14-2842. PubMed PMID: 25855378.
57. Toivola DM, Nieminen MI, Hesse M, He T, Baribault H, Magin TM, et al. Disturbances in hepatic cell-cycle regulation in mice with assembly-deficient keratins 8/18. *Hepatology*. 2001;34(6):1174-83. doi: 10.1053/jhep.2001.29374. PubMed PMID: 11732007.
58. Caulin C, Ware CF, Magin TM, Oshima RG. Keratin-dependent, epithelial resistance to tumor necrosis factor-induced apoptosis. *The Journal of cell biology*. 2000;149(1):17-22. PubMed PMID: 10747083; PubMed Central PMCID: PMC2175089.
59. Rao L, Perez D, White E. Lamin proteolysis facilitates nuclear events during apoptosis. *The Journal of cell biology*. 1996;135(6 Pt 1):1441-55. PubMed PMID: 8978814; PubMed Central PMCID: PMC2133948.
60. Gilles C, Polette M, Zahm JM, Tournier JM, Volders L, Foidart JM, et al. Vimentin contributes to human mammary epithelial cell migration. *Journal of cell science*. 1999;112 ( Pt 24):4615-25. PubMed PMID: 10574710.
61. Sutoh Yoneyama M, Hatakeyama S, Habuchi T, Inoue T, Nakamura T, Funyu T, et al. Vimentin intermediate filament and plectin provide a scaffold for invadopodia, facilitating cancer cell invasion and extravasation for metastasis. *European journal of cell biology*. 2014;93(4):157-69. doi: 10.1016/j.ejcb.2014.03.002. PubMed PMID: 24810881.
62. Fortier AM, Asselin E, Cadrin M. Keratin 8 and 18 loss in epithelial cancer cells increases collective cell migration and cisplatin sensitivity through claudin1 up-regulation. *The Journal of biological chemistry*. 2013;288(16):11555-71. doi: 10.1074/jbc.M112.428920. PubMed PMID: 23449973; PubMed Central PMCID: PMC3630871.
63. Narita K, Matsuda Y, Seike M, Naito Z, Gemma A, Ishiwata T. Nestin regulates proliferation, migration, invasion and stemness of lung adenocarcinoma. *International journal of oncology*. 2014;44(4):1118-30. doi: 10.3892/ijo.2014.2278. PubMed PMID: 24481417.
64. Klymkowsky MW, Bachant JB, Domingo A. Functions of intermediate filaments. *Cell motility and the cytoskeleton*. 1989;14(3):309-31. doi: 10.1002/cm.970140302. PubMed PMID: 2684432.
65. Newport JW, Forbes DJ. The nucleus: structure, function, and dynamics. *Annual review of biochemistry*. 1987;56:535-65. doi: 10.1146/annurev.bi.56.070187.002535. PubMed PMID: 3304144.

66. Benavente R, Krohne G. Involvement of nuclear lamins in postmitotic reorganization of chromatin as demonstrated by microinjection of lamin antibodies. *The Journal of cell biology*. 1986;103(5):1847-54. PubMed PMID: 3536954; PubMed Central PMCID: PMC2114394.
67. Hutchison CJ. Lamins: building blocks or regulators of gene expression? *Nature reviews Molecular cell biology*. 2002;3(11):848-58. doi: 10.1038/nrm950. PubMed PMID: 12415302.
68. Herrmann H, Bar H, Kreplak L, Strelkov SV, Aebi U. Intermediate filaments: from cell architecture to nanomechanics. *Nature reviews Molecular cell biology*. 2007;8(7):562-73. doi: 10.1038/nrm2197. PubMed PMID: 17551517.
69. Omary MB. "IF-pathies": a broad spectrum of intermediate filament-associated diseases. *The Journal of clinical investigation*. 2009;119(7):1756-62. doi: 10.1172/JCI39894. PubMed PMID: 19587450; PubMed Central PMCID: PMC2701889.
70. Coulombe PA, Kerns ML, Fuchs E. Epidermolysis bullosa simplex: a paradigm for disorders of tissue fragility. *The Journal of clinical investigation*. 2009;119(7):1784-93. doi: 10.1172/JCI38177. PubMed PMID: 19587453; PubMed Central PMCID: PMC2701872.
71. Szeverenyi I, Cassidy AJ, Chung CW, Lee BT, Common JE, Ogg SC, et al. The Human Intermediate Filament Database: comprehensive information on a gene family involved in many human diseases. *Human mutation*. 2008;29(3):351-60. doi: 10.1002/humu.20652. PubMed PMID: 18033728.
72. Omary MB, Ku NO, Strnad P, Hanada S. Toward unraveling the complexity of simple epithelial keratins in human disease. *The Journal of clinical investigation*. 2009;119(7):1794-805. doi: 10.1172/JCI37762. PubMed PMID: 19587454; PubMed Central PMCID: PMC2701867.
73. Osborn M, Weber K. Tumor diagnosis by intermediate filament typing: a novel tool for surgical pathology. *Laboratory investigation; a journal of technical methods and pathology*. 1983;48(4):372-94. PubMed PMID: 6187996.
74. Altmannsberger M. [Intermediate filament proteins as markers in tumor diagnosis]. *Veröffentlichungen aus der Pathologie*. 1988;127:1-105. PubMed PMID: 3341148.
75. Ehrmann J, Kolar Z, Mokry J. Nestin as a diagnostic and prognostic marker: immunohistochemical analysis of its expression in different tumours. *Journal of clinical pathology*. 2005;58(2):222-3. doi: 10.1136/jcp.2004.021238. PubMed PMID: 15677549; PubMed Central PMCID: PMC1770570.
76. Fillies T, Werkmeister R, Packeisen J, Brandt B, Morin P, Weingart D, et al. Cytokeratin 8/18 expression indicates a poor prognosis in squamous cell carcinomas of the oral cavity. *BMC cancer*. 2006;6:10. doi: 10.1186/1471-2407-6-10. PubMed PMID: 16412231; PubMed Central PMCID: PMC1379654.
77. Rittling SR, Baserga R. Functional analysis and growth factor regulation of the human vimentin promoter. *Molecular and cellular biology*. 1987;7(11):3908-15. PubMed PMID: 3431546; PubMed Central PMCID: PMC368058.
78. Gilles C, Polette M, Mestdagt M, Nawrocki-Raby B, Ruggeri P, Birembaut P, et al. Transactivation of vimentin by beta-catenin in human breast cancer cells. *Cancer research*. 2003;63(10):2658-64. PubMed PMID: 12750294.
79. Goldie KN, Wedig T, Mitra AK, Aebi U, Herrmann H, Hoenger A. Dissecting the 3-D structure of vimentin intermediate filaments by cryo-electron tomography. *Journal of structural biology*. 2007;158(3):378-85. doi: 10.1016/j.jsb.2006.12.007. PubMed PMID: 17289402.
80. Ando S, Tanabe K, Gonda Y, Sato C, Inagaki M. Domain- and sequence-specific phosphorylation of vimentin induces disassembly of the filament structure. *Biochemistry*. 1989;28(7):2974-9. PubMed PMID: 2500966.
81. Eriksson JE, He T, Trejo-Skalli AV, Harmala-Brasken AS, Hellman J, Chou YH, et al. Specific in vivo phosphorylation sites determine the assembly dynamics of vimentin intermediate filaments. *Journal of cell science*. 2004;117(Pt 6):919-32. doi: 10.1242/jcs.00906. PubMed PMID: 14762106.

82. Goto H, Tanabe K, Manser E, Lim L, Yasui Y, Inagaki M. Phosphorylation and reorganization of vimentin by p21-activated kinase (PAK). *Genes to cells : devoted to molecular & cellular mechanisms.* 2002;7(2):91-7. PubMed PMID: 11895474.
83. Goto H, Yasui Y, Kawajiri A, Nigg EA, Terada Y, Tatsuka M, et al. Aurora-B regulates the cleavage furrow-specific vimentin phosphorylation in the cytokinetic process. *The Journal of biological chemistry.* 2003;278(10):8526-30. doi: 10.1074/jbc.M210892200. PubMed PMID: 12458200.
84. Turowski P, Myles T, Hemmings BA, Fernandez A, Lamb NJ. Vimentin dephosphorylation by protein phosphatase 2A is modulated by the targeting subunit B55. *Molecular biology of the cell.* 1999;10(6):1997-2015. PubMed PMID: 10359611; PubMed Central PMCID: PMC25403.
85. Vossenaar ER, Radstake TR, van der Heijden A, van Mansum MA, Dieteren C, de Rooij DJ, et al. Expression and activity of citrullinating peptidylarginine deiminase enzymes in monocytes and macrophages. *Annals of the rheumatic diseases.* 2004;63(4):373-81. PubMed PMID: 15020330; PubMed Central PMCID: PMC1754951.
86. Farach AM, Galileo DS. O-GlcNAc modification of radial glial vimentin filaments in the developing chick brain. *Brain cell biology.* 2008;36(5-6):191-202. doi: 10.1007/s11068-008-9036-5. PubMed PMID: 19132533.
87. Wang L, Zhang J, Banerjee S, Barnes L, Barnes L, Sajja V, et al. Sumoylation of vimentin<sup>354</sup> is associated with PIAS3 inhibition of glioma cell migration. *Oncotarget.* 2010;1(7):620-7. doi: 10.18632/oncotarget.101101. PubMed PMID: 21317457; PubMed Central PMCID: PMC3248133.
88. Franke WW, Grund C, Kuhn C, Jackson BW, Illmensee K. Formation of cytoskeletal elements during mouse embryogenesis. III. Primary mesenchymal cells and the first appearance of vimentin filaments. *Differentiation; research in biological diversity.* 1982;23(1):43-59. PubMed PMID: 6759279.
89. Tapscott SJ, Bennett GS, Toyama Y, Kleinbart F, Holtzer H. Intermediate filament proteins in the developing chick spinal cord. *Developmental biology.* 1981;86(1):40-54. PubMed PMID: 7197239.
90. Lane EB, Hogan BL, Kurkinen M, Garrels JI. Co-expression of vimentin and cytokeratins in parietal endoderm cells of early mouse embryo. *Nature.* 1983;303(5919):701-4. PubMed PMID: 6190091.
91. Nieminen M, Henttinen T, Merinen M, Marttila-Ichihara F, Eriksson JE, Jalkanen S. Vimentin function in lymphocyte adhesion and transcellular migration. *Nature cell biology.* 2006;8(2):156-62. doi: 10.1038/ncb1355. PubMed PMID: 16429129.
92. Eckes B, Colucci-Guyon E, Smola H, Nodder S, Babinet C, Krieg T, et al. Impaired wound healing in embryonic and adult mice lacking vimentin. *Journal of cell science.* 2000;113 ( Pt 13):2455-62. PubMed PMID: 10852824.
93. Colucci-Guyon E, Gimenez YRM, Maurice T, Babinet C, Privat A. Cerebellar defect and impaired motor coordination in mice lacking vimentin. *Glia.* 1999;25(1):33-43. PubMed PMID: 9888296.
94. van der Velden LA, Manni JJ, Ramaekers FC, Kuijpers W. Expression of intermediate filament proteins in benign lesions of the oral mucosa. *European archives of oto-rhino-laryngology : official journal of the European Federation of Oto-Rhino-Laryngological Societies.* 1999;256(10):514-9. PubMed PMID: 10638360.
95. Langa F, Kress C, Colucci-Guyon E, Khun H, Vandormael-Pournin S, Huerre M, et al. Teratocarcinomas induced by embryonic stem (ES) cells lacking vimentin: an approach to study the role of vimentin in tumorigenesis. *Journal of cell science.* 2000;113 Pt 19:3463-72. PubMed PMID: 10984437.
96. Sommers CL, Walker-Jones D, Heckford SE, Worland P, Valverius E, Clark R, et al. Vimentin rather than keratin expression in some hormone-independent breast cancer cell lines and in oncogene-transformed mammary epithelial cells. *Cancer research.* 1989;49(15):4258-63. PubMed PMID: 2472876.
97. Lahat G, Zhu QS, Huang KL, Wang S, Bolshakov S, Liu J, et al. Vimentin is a novel anti-cancer therapeutic target; insights from in vitro and in vivo mice xenograft studies. *PloS one.* 2010;5(4):e10105. doi: 10.1371/journal.pone.0010105. PubMed PMID: 20419128; PubMed Central PMCID: PMC2855704.

98. Sotiriou C, Puzstai L. Gene-expression signatures in breast cancer. *The New England journal of medicine*. 2009;360(8):790-800. doi: 10.1056/NEJMra0801289. PubMed PMID: 19228622.
99. Wei J, Xu G, Wu M, Zhang Y, Li Q, Liu P, et al. Overexpression of vimentin contributes to prostate cancer invasion and metastasis via src regulation. *Anticancer research*. 2008;28(1A):327-34. PubMed PMID: 18383865.
100. Jin H, Morohashi S, Sato F, Kudo Y, Akasaka H, Tsutsumi S, et al. Vimentin expression of esophageal squamous cell carcinoma and its aggressive potential for lymph node metastasis. *Biomedical research*. 2010;31(2):105-12. PubMed PMID: 20460738.
101. McInroy L, Maatta A. Down-regulation of vimentin expression inhibits carcinoma cell migration and adhesion. *Biochemical and biophysical research communications*. 2007;360(1):109-14. doi: 10.1016/j.bbrc.2007.06.036. PubMed PMID: 17585878.
102. Polioudaki H, Agelaki S, Chiotaki R, Politaki E, Mavroudis D, Matikas A, et al. Variable expression levels of keratin and vimentin reveal differential EMT status of circulating tumor cells and correlation with clinical characteristics and outcome of patients with metastatic breast cancer. *BMC cancer*. 2015;15:399. doi: 10.1186/s12885-015-1386-7. PubMed PMID: 25962645; PubMed Central PMCID: PMC4434869.
103. Acloque H, Adams MS, Fishwick K, Bronner-Fraser M, Nieto MA. Epithelial-mesenchymal transitions: the importance of changing cell state in development and disease. *The Journal of clinical investigation*. 2009;119(6):1438-49. doi: 10.1172/JCI38019. PubMed PMID: 19487820; PubMed Central PMCID: PMC2689100.
104. Xu J, Lamouille S, Derynck R. TGF-beta-induced epithelial to mesenchymal transition. *Cell research*. 2009;19(2):156-72. doi: 10.1038/cr.2009.5. PubMed PMID: 19153598; PubMed Central PMCID: PMC4720263.
105. Wells A, Yates C, Shepard CR. E-cadherin as an indicator of mesenchymal to epithelial reverting transitions during the metastatic seeding of disseminated carcinomas. *Clinical & experimental metastasis*. 2008;25(6):621-8. doi: 10.1007/s10585-008-9167-1. PubMed PMID: 18600305; PubMed Central PMCID: PMC2929356.
106. Marsit CJ, Posner MR, McClean MD, Kelsey KT. Hypermethylation of E-cadherin is an independent predictor of improved survival in head and neck squamous cell carcinoma. *Cancer*. 2008;113(7):1566-71. doi: 10.1002/cncr.23770. PubMed PMID: 18711702; PubMed Central PMCID: PMC3645304.
107. Cheng CW, Wang HW, Chang CW, Chu HW, Chen CY, Yu JC, et al. MicroRNA-30a inhibits cell migration and invasion by downregulating vimentin expression and is a potential prognostic marker in breast cancer. *Breast cancer research and treatment*. 2012;134(3):1081-93. doi: 10.1007/s10549-012-2034-4. PubMed PMID: 22476851.
108. Chaw SY, Majeed AA, Dalley AJ, Chan A, Stein S, Farah CS. Epithelial to mesenchymal transition (EMT) biomarkers--E-cadherin, beta-catenin, APC and Vimentin--in oral squamous cell carcinogenesis and transformation. *Oral oncology*. 2012;48(10):997-1006. doi: 10.1016/j.oraloncology.2012.05.011. PubMed PMID: 22704062.
109. Perlson E, Michaelievski I, Kowalsman N, Ben-Yaakov K, Shaked M, Seger R, et al. Vimentin binding to phosphorylated Erk sterically hinders enzymatic dephosphorylation of the kinase. *Journal of molecular biology*. 2006;364(5):938-44. doi: 10.1016/j.jmb.2006.09.056. PubMed PMID: 17046786.
110. Zhu QS, Rosenblatt K, Huang KL, Lahat G, Brobey R, Bolshakov S, et al. Vimentin is a novel AKT1 target mediating motility and invasion. *Oncogene*. 2011;30(4):457-70. doi: 10.1038/onc.2010.421. PubMed PMID: 20856200; PubMed Central PMCID: PMC3010301.
111. Tzivion G, Luo ZJ, Avruch J. Calyculin A-induced vimentin phosphorylation sequesters 14-3-3 and displaces other 14-3-3 partners in vivo. *The Journal of biological chemistry*. 2000;275(38):29772-8. doi: 10.1074/jbc.M001207200. PubMed PMID: 10887173.

112. Phua DC, Humbert PO, Hunziker W. Vimentin regulates scribble activity by protecting it from proteasomal degradation. *Molecular biology of the cell*. 2009;20(12):2841-55. doi: 10.1091/mbc.E08-02-0199. PubMed PMID: 19386766; PubMed Central PMCID: PMC2695792.
113. Kim H, Nakamura F, Lee W, Shifrin Y, Arora P, McCulloch CA. Filamin A is required for vimentin-mediated cell adhesion and spreading. *American journal of physiology Cell physiology*. 2010;298(2):C221-36. doi: 10.1152/ajpcell.00323.2009. PubMed PMID: 19776392; PubMed Central PMCID: PMC4380480.
114. Homan SM, Mercurio AM, LaFlamme SE. Endothelial cells assemble two distinct alpha6beta4-containing vimentin-associated structures: roles for ligand binding and the beta4 cytoplasmic tail. *Journal of cell science*. 1998;111 ( Pt 18):2717-28. PubMed PMID: 9718365.
115. DiPersio CM, van der Neut R, Georges-Labouesse E, Kreidberg JA, Sonnenberg A, Hynes RO. alpha3beta1 and alpha6beta4 integrin receptors for laminin-5 are not essential for epidermal morphogenesis and homeostasis during skin development. *Journal of cell science*. 2000;113 ( Pt 17):3051-62. PubMed PMID: 10934043.
116. Vidal F, Aberdam D, Miquel C, Christiano AM, Pulkkinen L, Uitto J, et al. Integrin beta 4 mutations associated with junctional epidermolysis bullosa with pyloric atresia. *Nature genetics*. 1995;10(2):229-34. doi: 10.1038/ng0695-229. PubMed PMID: 7545057.
117. Stepp MA, Spurr-Michaud S, Tisdale A, Elwell J, Gipson IK. Alpha 6 beta 4 integrin heterodimer is a component of hemidesmosomes. *Proceedings of the National Academy of Sciences of the United States of America*. 1990;87(22):8970-4. PubMed PMID: 2247472; PubMed Central PMCID: PMC55082.
118. Green KJ, Jones JC. Desmosomes and hemidesmosomes: structure and function of molecular components. *FASEB journal : official publication of the Federation of American Societies for Experimental Biology*. 1996;10(8):871-81. PubMed PMID: 8666164.
119. McLean WH, Pulkkinen L, Smith FJ, Rugg EL, Lane EB, Bullrich F, et al. Loss of plectin causes epidermolysis bullosa with muscular dystrophy: cDNA cloning and genomic organization. *Genes & development*. 1996;10(14):1724-35. PubMed PMID: 8698233.
120. Guo L, Degenstein L, Dowling J, Yu QC, Wollmann R, Perman B, et al. Gene targeting of BPAG1: abnormalities in mechanical strength and cell migration in stratified epithelia and neurologic degeneration. *Cell*. 1995;81(2):233-43. PubMed PMID: 7736575.
121. Andra K, Lassmann H, Bittner R, Shorny S, Fassler R, Propst F, et al. Targeted inactivation of plectin reveals essential function in maintaining the integrity of skin, muscle, and heart cytoarchitecture. *Genes & development*. 1997;11(23):3143-56. PubMed PMID: 9389647; PubMed Central PMCID: PMC316746.
122. Rezniczek GA, de Pereda JM, Reipert S, Wiche G. Linking integrin alpha6beta4-based cell adhesion to the intermediate filament cytoskeleton: direct interaction between the beta4 subunit and plectin at multiple molecular sites. *The Journal of cell biology*. 1998;141(1):209-25. PubMed PMID: 9531560; PubMed Central PMCID: PMC2132717.
123. Carico E, French D, Bucci B, Falcioni R, Vecchione A, Mariani-Costantini R. Integrin beta 4 expression in the neoplastic progression of cervical epithelium. *Gynecologic oncology*. 1993;49(1):61-6. doi: 10.1006/gyno.1993.1087. PubMed PMID: 7683305.
124. Downer CS, Watt FM, Speight PM. Loss of alpha 6 and beta 4 integrin subunits coincides with loss of basement membrane components in oral squamous cell carcinomas. *The Journal of pathology*. 1993;171(3):183-90. doi: 10.1002/path.1711710306. PubMed PMID: 8277367.
125. Lipscomb EA, Mercurio AM. Mobilization and activation of a signaling competent alpha6beta4 integrin underlies its contribution to carcinoma progression. *Cancer metastasis reviews*. 2005;24(3):413-23. doi: 10.1007/s10555-005-5133-4. PubMed PMID: 16258729.
126. Rabinovitz I, Mercurio AM. The integrin alpha6beta4 functions in carcinoma cell migration on laminin-1 by mediating the formation and stabilization of actin-containing motility structures. *The*

Journal of cell biology. 1997;139(7):1873-84. PubMed PMID: 9412479; PubMed Central PMCID: PMC2132643.

127. Kippenberger S, Hofmann M, Zoller N, Thaci D, Muller J, Kaufmann R, et al. Ligation of beta4 integrins activates PKB/Akt and ERK1/2 by distinct pathways-relevance of the keratin filament. *Biochimica et biophysica acta*. 2010;1803(8):940-50. doi: 10.1016/j.bbamcr.2010.03.009. PubMed PMID: 20307589.

128. Di Guglielmo GM, Baass PC, Ou WJ, Posner BI, Bergeron JJ. Compartmentalization of SHC, GRB2 and mSOS, and hyperphosphorylation of Raf-1 by EGF but not insulin in liver parenchyma. *The EMBO journal*. 1994;13(18):4269-77. PubMed PMID: 7925272; PubMed Central PMCID: PMC395354.

129. Rabinovitz I, Toker A, Mercurio AM. Protein kinase C-dependent mobilization of the alpha6beta4 integrin from hemidesmosomes and its association with actin-rich cell protrusions drive the chemotactic migration of carcinoma cells. *The Journal of cell biology*. 1999;146(5):1147-60. PubMed PMID: 10477766; PubMed Central PMCID: PMC2169473.

130. Witkowski CM, Bowden GT, Nagle RB, Cress AE. Altered surface expression and increased turnover of the alpha6beta4 integrin in an undifferentiated carcinoma. *Carcinogenesis*. 2000;21(2):325-30. PubMed PMID: 10657977.

131. Tennenbaum T, Yuspa SH, Grover A, Castronovo V, Sobel ME, Yamada Y, et al. Extracellular matrix receptors and mouse skin carcinogenesis: altered expression linked to appearance of early markers of tumor progression. *Cancer research*. 1992;52(10):2966-76. PubMed PMID: 1533815.

132. Yang X, Pursell B, Lu S, Chang TK, Mercurio AM. Regulation of beta 4-integrin expression by epigenetic modifications in the mammary gland and during the epithelial-to-mesenchymal transition. *Journal of cell science*. 2009;122(Pt 14):2473-80. doi: 10.1242/jcs.049148. PubMed PMID: 19549682; PubMed Central PMCID: PMC2704882.

133. Qu H, Wen T, Pesch M, Aumailley M. Partial loss of epithelial phenotype in kindlin-1-deficient keratinocytes. *The American journal of pathology*. 2012;180(4):1581-92. doi: 10.1016/j.ajpath.2012.01.005. PubMed PMID: 22326752.

134. Zhao Y, Yan Q, Long X, Chen X, Wang Y. Vimentin affects the mobility and invasiveness of prostate cancer cells. *Cell biochemistry and function*. 2008;26(5):571-7. doi: 10.1002/cbf.1478. PubMed PMID: 18464297.

135. Nakajima S, Doi R, Toyoda E, Tsuji S, Wada M, Koizumi M, et al. N-cadherin expression and epithelial-mesenchymal transition in pancreatic carcinoma. *Clinical cancer research : an official journal of the American Association for Cancer Research*. 2004;10(12 Pt 1):4125-33. doi: 10.1158/1078-0432.CCR-0578-03. PubMed PMID: 15217949.

136. Moll R, Hage C, Thoenes W. Expression of intermediate filament proteins in fetal and adult human kidney: modulations of intermediate filament patterns during development and in damaged tissue. *Laboratory investigation; a journal of technical methods and pathology*. 1991;65(1):74-86. PubMed PMID: 1712875.

137. Boraas LC, Guidry JB, Pineda ET, Ahsan T. Cytoskeletal Expression and Remodeling in Pluripotent Stem Cells. *PloS one*. 2016;11(1):e0145084. doi: 10.1371/journal.pone.0145084. PubMed PMID: 26771179.

138. Moll R, Divo M, Langbein L. The human keratins: biology and pathology. *Histochemistry and cell biology*. 2008;129(6):705-33. doi: 10.1007/s00418-008-0435-6. PubMed PMID: 18461349; PubMed Central PMCID: PMC2386534.

139. Alam H, Sehgal L, Kundu ST, Dalal SN, Vaidya MM. Novel function of keratins 5 and 14 in proliferation and differentiation of stratified epithelial cells. *Molecular biology of the cell*. 2011;22(21):4068-78. doi: 10.1091/mbc.E10-08-0703. PubMed PMID: 21900500; PubMed Central PMCID: PMC3204069.

140. Tataka RJ, Rajaram N, Damle RN, Balsara B, Bhisey AN, Gangal SG. Establishment and characterization of four new squamous cell carcinoma cell lines derived from oral tumors. *Journal of cancer research and clinical oncology*. 1990;116(2):179-86. PubMed PMID: 1691185.
141. Martin CL, Reshmi SC, Ried T, Gottberg W, Wilson JW, Reddy JK, et al. Chromosomal imbalances in oral squamous cell carcinoma: examination of 31 cell lines and review of the literature. *Oral oncology*. 2008;44(4):369-82. doi: 10.1016/j.oraloncology.2007.05.003. PubMed PMID: 17681875; PubMed Central PMCID: PMC2362065.
142. Giard DJ, Aaronson SA, Todaro GJ, Arnstein P, Kersey JH, Dosik H, et al. In vitro cultivation of human tumors: establishment of cell lines derived from a series of solid tumors. *Journal of the National Cancer Institute*. 1973;51(5):1417-23. PubMed PMID: 4357758.
143. Graham FL, Smiley J, Russell WC, Nairn R. Characteristics of a human cell line transformed by DNA from human adenovirus type 5. *The Journal of general virology*. 1977;36(1):59-74. doi: 10.1099/0022-1317-36-1-59. PubMed PMID: 886304.
144. Chang SE, Foster S, Betts D, Marnock WE. DOK, a cell line established from human dysplastic oral mucosa, shows a partially transformed non-malignant phenotype. *International journal of cancer Journal international du cancer*. 1992;52(6):896-902. PubMed PMID: 1459732.
145. Boukamp P, Petrussevska RT, Breitkreutz D, Hornung J, Markham A, Fusenig NE. Normal keratinization in a spontaneously immortalized aneuploid human keratinocyte cell line. *The Journal of cell biology*. 1988;106(3):761-71. PubMed PMID: 2450098; PubMed Central PMCID: PMC2115116.
146. Peterson GL. A simplification of the protein assay method of Lowry et al. which is more generally applicable. *Analytical biochemistry*. 1977;83(2):346-56. PubMed PMID: 603028.
147. Laemmli UK. Cleavage of structural proteins during the assembly of the head of bacteriophage T4. *Nature*. 1970;227(5259):680-5. PubMed PMID: 5432063.
148. Towbin H, Staehelin T, Gordon J. Electrophoretic transfer of proteins from polyacrylamide gels to nitrocellulose sheets: procedure and some applications. *Proceedings of the National Academy of Sciences of the United States of America*. 1979;76(9):4350-4. PubMed PMID: 388439; PubMed Central PMCID: PMC411572.
149. Dange MC, Agarwal AK, Kalraiya RD. Extracellular galectin-3 induces MMP9 expression by activating p38 MAPK pathway via lysosome-associated membrane protein-1 (LAMP1). *Molecular and cellular biochemistry*. 2015;404(1-2):79-86. doi: 10.1007/s11010-015-2367-5. PubMed PMID: 25739356.
150. Srikanth B, Vaidya MM, Kalraiya RD. O-GlcNAcylation determines the solubility, filament organization, and stability of keratins 8 and 18. *The Journal of biological chemistry*. 2010;285(44):34062-71. doi: 10.1074/jbc.M109.098996. PubMed PMID: 20729549; PubMed Central PMCID: PMC2962505.
151. Yamashita S, Okada Y. Heat-induced Antigen Retrieval in Conventionally Processed Epon-embedded Specimens: Procedures and Mechanisms. *The journal of histochemistry and cytochemistry : official journal of the Histochemistry Society*. 2014;62(8):584-97. doi: 10.1369/0022155414537899. PubMed PMID: 24850662.
152. Alam H, Kundu ST, Dalal SN, Vaidya MM. Loss of keratins 8 and 18 leads to alterations in alpha6beta4-integrin-mediated signalling and decreased neoplastic progression in an oral-tumour-derived cell line. *Journal of cell science*. 2011;124(Pt 12):2096-106. doi: 10.1242/jcs.073585. PubMed PMID: 21610092.
153. Mosmann T. Rapid colorimetric assay for cellular growth and survival: application to proliferation and cytotoxicity assays. *Journal of immunological methods*. 1983;65(1-2):55-63. PubMed PMID: 6606682.
154. Dua P, Ingle A, Gude RP. Suramin augments the antitumor and antimetastatic activity of pentoxifylline in B16F10 melanoma. *International journal of cancer Journal international du cancer*. 2007;121(7):1600-8. doi: 10.1002/ijc.22843. PubMed PMID: 17582610.

155. Partridge J, Flaherty P. An in vitro FluoroBlok tumor invasion assay. *Journal of visualized experiments : JoVE*. 2009;(29). doi: 10.3791/1475. PubMed PMID: 19620957; PubMed Central PMCID: PMC3148933.
156. Damiani LA, Yingling CM, Leng S, Romo PE, Nakamura J, Belinsky SA. Carcinogen-induced gene promoter hypermethylation is mediated by DNMT1 and causal for transformation of immortalized bronchial epithelial cells. *Cancer research*. 2008;68(21):9005-14. doi: 10.1158/0008-5472.CAN-08-1276. PubMed PMID: 18974146.
157. Jensen MM, Jorgensen JT, Binderup T, Kjaer A. Tumor volume in subcutaneous mouse xenografts measured by microCT is more accurate and reproducible than determined by 18F-FDG-microPET or external caliper. *BMC medical imaging*. 2008;8:16. doi: 10.1186/1471-2342-8-16. PubMed PMID: 18925932; PubMed Central PMCID: PMC2575188.
158. Ranganathan K, Kavitha R, Sawant SS, Vaidya MM. Cytokeratin expression in oral submucous fibrosis--an immunohistochemical study. *Journal of oral pathology & medicine : official publication of the International Association of Oral Pathologists and the American Academy of Oral Pathology*. 2006;35(1):25-32. doi: 10.1111/j.1600-0714.2005.00366.x. PubMed PMID: 16393250.
159. Dmello C, Sawant S, Alam H, Gangadaran P, Tiwari R, Dongre H, et al. Vimentin mediated regulation of cell motility through modulation of beta4 integrin protein levels in oral tumor derived cells. *The international journal of biochemistry & cell biology*. 2015. doi: 10.1016/j.biocel.2015.11.015. PubMed PMID: 26646105.
160. Kim H, Nakamura F, Lee W, Hong C, Perez-Sala D, McCulloch CA. Regulation of cell adhesion to collagen via beta1 integrins is dependent on interactions of filamin A with vimentin and protein kinase C epsilon. *Experimental cell research*. 2010;316(11):1829-44. doi: 10.1016/j.yexcr.2010.02.007. PubMed PMID: 20171211.
161. Egles C, Huet HA, Dogan F, Cho S, Dong S, Smith A, et al. Integrin-blocking antibodies delay keratinocyte re-epithelialization in a human three-dimensional wound healing model. *PloS one*. 2010;5(5):e10528. doi: 10.1371/journal.pone.0010528. PubMed PMID: 20502640; PubMed Central PMCID: PMC2873945.
162. Kippenberger S, Loitsch S, Muller J, Guschel M, Kaufmann R, Bernd A. Ligation of the beta4 integrin triggers adhesion behavior of human keratinocytes by an "inside-out" mechanism. *The Journal of investigative dermatology*. 2004;123(3):444-51. doi: 10.1111/j.0022-202X.2004.23323.x. PubMed PMID: 15304080.
163. Dozynkiewicz MA, Jamieson NB, Macpherson I, Grindlay J, van den Berghe PV, von Thun A, et al. Rab25 and CLIC3 collaborate to promote integrin recycling from late endosomes/lysosomes and drive cancer progression. *Developmental cell*. 2012;22(1):131-45. doi: 10.1016/j.devcel.2011.11.008. PubMed PMID: 22197222; PubMed Central PMCID: PMC3507630.
164. Styers ML, Salazar G, Love R, Peden AA, Kowalczyk AP, Faundez V. The endo-lysosomal sorting machinery interacts with the intermediate filament cytoskeleton. *Molecular biology of the cell*. 2004;15(12):5369-82. doi: 10.1091/mbc.E04-03-0272. PubMed PMID: 15456899; PubMed Central PMCID: PMC532017.
165. Pal-Ghosh S, Blanco T, Tadvalkar G, Pajoohesh-Ganji A, Parthasarathy A, Zieske JD, et al. MMP9 cleavage of the beta4 integrin ectodomain leads to recurrent epithelial erosions in mice. *Journal of cell science*. 2011;124(Pt 15):2666-75. doi: 10.1242/jcs.085480. PubMed PMID: 21750188; PubMed Central PMCID: PMC3138707.
166. Truong AB, Kretz M, Ridky TW, Kimmel R, Khavari PA. p63 regulates proliferation and differentiation of developmentally mature keratinocytes. *Genes & development*. 2006;20(22):3185-97. doi: 10.1101/gad.1463206. PubMed PMID: 17114587; PubMed Central PMCID: PMC1635152.
167. Troy TC, Turksen K. In vitro characteristics of early epidermal progenitors isolated from keratin 14 (K14)-deficient mice: insights into the role of keratin 17 in mouse keratinocytes. *Journal of cellular*

- physiology. 1999;180(3):409-21. doi: 10.1002/(SICI)1097-4652(199909)180:3<409::AID-JCP12>3.0.CO;2-V. PubMed PMID: 10430181.
168. Wawersik M, Paladini RD, Noensie E, Coulombe PA. A proline residue in the alpha-helical rod domain of type I keratin 16 destabilizes keratin heterotetramers. *The Journal of biological chemistry*. 1997;272(51):32557-65. PubMed PMID: 9405470.
169. Romano RA, Birkaya B, Sinha S. A functional enhancer of keratin14 is a direct transcriptional target of deltaNp63. *The Journal of investigative dermatology*. 2007;127(5):1175-86. doi: 10.1038/sj.jid.5700652. PubMed PMID: 17159913.
170. Romano RA, Ortt K, Birkaya B, Smalley K, Sinha S. An active role of the DeltaN isoform of p63 in regulating basal keratin genes K5 and K14 and directing epidermal cell fate. *PloS one*. 2009;4(5):e5623. doi: 10.1371/journal.pone.0005623. PubMed PMID: 19461998; PubMed Central PMCID: PMC2680039.
171. Nguyen BC, Lefort K, Mandinova A, Antonini D, Devgan V, Della Gatta G, et al. Cross-regulation between Notch and p63 in keratinocyte commitment to differentiation. *Genes & development*. 2006;20(8):1028-42. doi: 10.1101/gad.1406006. PubMed PMID: 16618808; PubMed Central PMCID: PMC1472299.
172. Dotto GP. Crosstalk of Notch with p53 and p63 in cancer growth control. *Nature reviews Cancer*. 2009;9(8):587-95. doi: 10.1038/nrc2675. PubMed PMID: 19609265.
173. Wu KJ. Direct activation of Bmi1 by Twist1: implications in cancer stemness, epithelial-mesenchymal transition, and clinical significance. *Chang Gung medical journal*. 2011;34(3):229-38. PubMed PMID: 21733352.
174. Wu KJ, Yang MH. Epithelial-mesenchymal transition and cancer stemness: the Twist1-Bmi1 connection. *Bioscience reports*. 2011;31(6):449-55. doi: 10.1042/BSR20100114. PubMed PMID: 21919891.
175. Sawant S, Vaidya M, Chaukar D, Alam H, Dmello C, Gangadaran P, et al. Clinical significance of aberrant vimentin expression in oral premalignant lesions and carcinomas. *Oral diseases*. 2014;20(5):453-65. doi: 10.1111/odi.12151. PubMed PMID: 23865921.
176. Kim H, McCulloch CA. Filamin A mediates interactions between cytoskeletal proteins that control cell adhesion. *FEBS letters*. 2011;585(1):18-22. doi: 10.1016/j.febslet.2010.11.033. PubMed PMID: 21095189.
177. Brockbank EC, Bridges J, Marshall CJ, Sahai E. Integrin beta1 is required for the invasive behaviour but not proliferation of squamous cell carcinoma cells in vivo. *British journal of cancer*. 2005;92(1):102-12. doi: 10.1038/sj.bjc.6602255. PubMed PMID: 15597106; PubMed Central PMCID: PMC2361733.
178. Ivaska J, Vuoriluoto K, Huovinen T, Izawa I, Inagaki M, Parker PJ. PKCepsilon-mediated phosphorylation of vimentin controls integrin recycling and motility. *The EMBO journal*. 2005;24(22):3834-45. doi: 10.1038/sj.emboj.7600847. PubMed PMID: 16270034; PubMed Central PMCID: PMC1283946.
179. Basora N, Herring-Gillam FE, Boudreau F, Perreault N, Pageot LP, Simoneau M, et al. Expression of functionally distinct variants of the beta(4)A integrin subunit in relation to the differentiation state in human intestinal cells. *The Journal of biological chemistry*. 1999;274(42):29819-25. PubMed PMID: 10514460.
180. Lin GL, Cohen DM, Desai RA, Breckenridge MT, Gao L, Humphries MJ, et al. Activation of beta 1 but not beta 3 integrin increases cell traction forces. *FEBS letters*. 2013;587(6):763-9. doi: 10.1016/j.febslet.2013.01.068. PubMed PMID: 23395612; PubMed Central PMCID: PMC3966909.
181. Katada K, Tomonaga T, Satoh M, Matsushita K, Tonoike Y, Koderu Y, et al. Plectin promotes migration and invasion of cancer cells and is a novel prognostic marker for head and neck squamous cell carcinoma. *Journal of proteomics*. 2012;75(6):1803-15. doi: 10.1016/j.jprot.2011.12.018. PubMed PMID: 22245045.

182. Kalluri R, Weinberg RA. The basics of epithelial-mesenchymal transition. *The Journal of clinical investigation*. 2009;119(6):1420-8. doi: 10.1172/JCI39104. PubMed PMID: 19487818; PubMed Central PMCID: PMC2689101.
183. Micheloni A, De Luca N, Tadini G, Zambruno G, D'Alessio M. Intracellular degradation of beta4 integrin in lethal junctional epidermolysis bullosa with pyloric atresia. *The British journal of dermatology*. 2004;151(4):796-802. doi: 10.1111/j.1365-2133.2004.06206.x. PubMed PMID: 15491419.
184. Giancotti FG, Stepp MA, Suzuki S, Engvall E, Ruoslahti E. Proteolytic processing of endogenous and recombinant beta 4 integrin subunit. *The Journal of cell biology*. 1992;118(4):951-9. PubMed PMID: 1500432; PubMed Central PMCID: PMC2289563.
185. Walko G, Vukasinovic N, Gross K, Fischer I, Sibitz S, Fuchs P, et al. Targeted proteolysis of plectin isoform 1a accounts for hemidesmosome dysfunction in mice mimicking the dominant skin blistering disease EBS-Ogna. *PLoS genetics*. 2011;7(12):e1002396. doi: 10.1371/journal.pgen.1002396. PubMed PMID: 22144912; PubMed Central PMCID: PMC3228830.
186. Ivaska J. Vimentin: Central hub in EMT induction? *Small GTPases*. 2011;2(1):51-3. doi: 10.4161/sgtp.2.1.15114. PubMed PMID: 21686283; PubMed Central PMCID: PMC3116616.
187. Takemura K, Hirayama R, Hirokawa K, Inagaki M, Tsujimura K, Esaki Y, et al. Expression of vimentin in gastric cancer: a possible indicator for prognosis. *Pathobiology : journal of immunopathology, molecular and cellular biology*. 1994;62(3):149-54. PubMed PMID: 7945921.
188. Gilles C, Polette M, Piette J, Delvigne AC, Thompson EW, Foidart JM, et al. Vimentin expression in cervical carcinomas: association with invasive and migratory potential. *The Journal of pathology*. 1996;180(2):175-80. doi: 10.1002/(SICI)1096-9896(199610)180:2<175::AID-PATH630>3.0.CO;2-G. PubMed PMID: 8976877.
189. Al-Saad S, Al-Shibli K, Donnem T, Persson M, Bremnes RM, Busund LT. The prognostic impact of NF-kappaB p105, vimentin, E-cadherin and Par6 expression in epithelial and stromal compartment in non-small-cell lung cancer. *British journal of cancer*. 2008;99(9):1476-83. doi: 10.1038/sj.bjc.6604713. PubMed PMID: 18854838; PubMed Central PMCID: PMC2579693.
190. Hsu YC, Li L, Fuchs E. Emerging interactions between skin stem cells and their niches. *Nature medicine*. 2014;20(8):847-56. doi: 10.1038/nm.3643. PubMed PMID: 25100530; PubMed Central PMCID: PMC4358898.
191. Vaidya MM, Kanojia D. Keratins: markers of cell differentiation or regulators of cell differentiation? *Journal of biosciences*. 2007;32(4):629-34. PubMed PMID: 17762135.
192. Ding L, Paszkowski-Rogacz M, Nitsche A, Slabicki MM, Heninger AK, de Vries I, et al. A genome-scale RNAi screen for Oct4 modulators defines a role of the Paf1 complex for embryonic stem cell identity. *Cell stem cell*. 2009;4(5):403-15. doi: 10.1016/j.stem.2009.03.009. PubMed PMID: 19345177.
193. Zeineddine D, Hammoud AA, Mortada M, Boeuf H. The Oct4 protein: more than a magic stemness marker. *American journal of stem cells*. 2014;3(2):74-82. PubMed PMID: 25232507; PubMed Central PMCID: PMC4163606.
194. Ma S, Rao L, Freedberg IM, Blumenberg M. Transcriptional control of K5, K6, K14, and K17 keratin genes by AP-1 and NF-kappaB family members. *Gene expression*. 1997;6(6):361-70. PubMed PMID: 9495317.
195. Yoh K, Prywes R. Pathway Regulation of p63, a Director of Epithelial Cell Fate. *Frontiers in endocrinology*. 2015;6:51. doi: 10.3389/fendo.2015.00051. PubMed PMID: 25972840; PubMed Central PMCID: PMC4412127.
196. Medawar A, Virolle T, Rostagno P, de la Forest-Divonne S, Gambaro K, Rouleau M, et al. DeltaNp63 is essential for epidermal commitment of embryonic stem cells. *PloS one*. 2008;3(10):e3441. doi: 10.1371/journal.pone.0003441. PubMed PMID: 18927616; PubMed Central PMCID: PMC2562986.

197. Zheng Y, Bie W, Yang R, Perekatt AO, Poole AJ, Tyner AL. Functions of p21 and p27 in the regenerating epithelial linings of the mouse small and large intestine. *Cancer biology & therapy*. 2008;7(6):873-9. PubMed PMID: 18344686; PubMed Central PMCID: PMC3005242.
198. Tetsu O, McCormick F. Proliferation of cancer cells despite CDK2 inhibition. *Cancer cell*. 2003;3(3):233-45. PubMed PMID: 12676582.
199. Lee KB, Ye S, Park MH, Park BH, Lee JS, Kim SM. p63-Mediated activation of the beta-catenin/c-Myc signaling pathway stimulates esophageal squamous carcinoma cell invasion and metastasis. *Cancer letters*. 2014;353(1):124-32. doi: 10.1016/j.canlet.2014.07.016. PubMed PMID: 25045846.
200. Flores ER. The roles of p63 in cancer. *Cell cycle*. 2007;6(3):300-4. PubMed PMID: 17264676.
201. Mishra R, Palve V, Kannan S, Pawar S, Teni T. High expression of survivin and its splice variants survivin DeltaEx3 and survivin 2 B in oral cancers. *Oral surgery, oral medicine, oral pathology and oral radiology*. 2015;120(4):497-507. doi: 10.1016/j.oooo.2015.06.027. PubMed PMID: 26346910.
202. Candi E, Amelio I, Agostini M, Melino G. MicroRNAs and p63 in epithelial stemness. *Cell death and differentiation*. 2015;22(1):12-21. doi: 10.1038/cdd.2014.113. PubMed PMID: 25168241; PubMed Central PMCID: PMC4262770.
203. Manni I, Artuso S, Careccia S, Rizzo MG, Baserga R, Piaggio G, et al. The microRNA miR-92 increases proliferation of myeloid cells and by targeting p63 modulates the abundance of its isoforms. *FASEB journal : official publication of the Federation of American Societies for Experimental Biology*. 2009;23(11):3957-66. doi: 10.1096/fj.09-131847. PubMed PMID: 19608627.
204. Thomas PA, Kirschmann DA, Cerhan JR, Folberg R, Seftor EA, Sellers TA, et al. Association between keratin and vimentin expression, malignant phenotype, and survival in postmenopausal breast cancer patients. *Clinical cancer research : an official journal of the American Association for Cancer Research*. 1999;5(10):2698-703. PubMed PMID: 10537332.
205. Rogel MR, Soni PN, Troken JR, Sitikov A, Trejo HE, Ridge KM. Vimentin is sufficient and required for wound repair and remodeling in alveolar epithelial cells. *FASEB journal : official publication of the Federation of American Societies for Experimental Biology*. 2011;25(11):3873-83. doi: 10.1096/fj.10-170795. PubMed PMID: 21803859; PubMed Central PMCID: PMC3205840.
206. Liu CY, Lin HH, Tang MJ, Wang YK. Vimentin contributes to epithelial-mesenchymal transition cancer cell mechanics by mediating cytoskeletal organization and focal adhesion maturation. *Oncotarget*. 2015;6(18):15966-83. doi: 10.18632/oncotarget.3862. PubMed PMID: 25965826; PubMed Central PMCID: PMC4599250.
207. Lanier MH, Kim T, Cooper JA. CARMIL2 is a novel molecular connection between vimentin and actin essential for cell migration and invadopodia formation. *Molecular biology of the cell*. 2015;26(25):4577-88. doi: 10.1091/mbc.E15-08-0552. PubMed PMID: 26466680; PubMed Central PMCID: PMC4678016.
208. Xiong H, Hong J, Du W, Lin YW, Ren LL, Wang YC, et al. Roles of STAT3 and ZEB1 proteins in E-cadherin down-regulation and human colorectal cancer epithelial-mesenchymal transition. *The Journal of biological chemistry*. 2012;287(8):5819-32. doi: 10.1074/jbc.M111.295964. PubMed PMID: 22205702; PubMed Central PMCID: PMC3285352.
209. Liu LK, Jiang XY, Zhou XX, Wang DM, Song XL, Jiang HB. Upregulation of vimentin and aberrant expression of E-cadherin/beta-catenin complex in oral squamous cell carcinomas: correlation with the clinicopathological features and patient outcome. *Modern pathology : an official journal of the United States and Canadian Academy of Pathology, Inc*. 2010;23(2):213-24. doi: 10.1038/modpathol.2009.160. PubMed PMID: 19915524.
210. Zhang X, Miao Y, Yu X, Zhang Y, Jiang G, Liu Y, et al. C6orf106 enhances NSCLC cell invasion by upregulating vimentin, and downregulating E-cadherin and P120ctn. *Tumour biology : the journal of the International Society for Oncodevelopmental Biology and Medicine*. 2015;36(8):5979-85. doi: 10.1007/s13277-015-3274-9. PubMed PMID: 25736925.

211. Balmain A, Harris CC. Carcinogenesis in mouse and human cells: parallels and paradoxes. *Carcinogenesis*. 2000;21(3):371-7. PubMed PMID: 10688857.
212. Tellez CS, Juri DE, Do K, Bernauer AM, Thomas CL, Damiani LA, et al. EMT and stem cell-like properties associated with miR-205 and miR-200 epigenetic silencing are early manifestations during carcinogen-induced transformation of human lung epithelial cells. *Cancer research*. 2011;71(8):3087-97. doi: 10.1158/0008-5472.CAN-10-3035. PubMed PMID: 21363915; PubMed Central PMCID: PMC3078195.

# Publications



## Vimentin-mediated regulation of cell motility through modulation of beta4 integrin protein levels in oral tumor derived cells

Crismita Dmello<sup>a</sup>, Sharada Sawant<sup>a</sup>, Hunain Alam<sup>a,1</sup>, Prakash Gangadaran<sup>a,2</sup>, Richa Tiwari<sup>a</sup>, Harsh Dongre<sup>a</sup>, Neha Rana<sup>a</sup>, Sai Barve<sup>a</sup>, Daniela Elena Costea<sup>b,c</sup>, Davendra Chaukar<sup>d</sup>, Shubhada Kane<sup>e</sup>, Harish Pant<sup>f</sup>, Milind Vaidya<sup>a,\*</sup>

<sup>a</sup> Cancer Research Institute (CRI), Advanced Centre for Treatment, Research and Education in Cancer (ACTREC), Tata Memorial Centre (TMC), Kharghar, Navi Mumbai, India

<sup>b</sup> Gade Laboratory for Pathology, Institute of Clinical Medicine, University of Bergen, Norway

<sup>c</sup> Department of Pathology, Haukeland University Hospital, Bergen, Norway

<sup>d</sup> Surgical Oncology, Head and Neck Unit, Tata Memorial Hospital (TMH), Parel, Mumbai, India

<sup>e</sup> Department of Pathology, Tata Memorial Hospital (TMH), Parel, Mumbai, India

<sup>f</sup> Laboratory of Neurochemistry, National Institute of Neurological Disorders and Stroke, National Institutes of Health, Bethesda, MD 20892, USA

### ARTICLE INFO

#### Article history:

Received 20 August 2015

Received in revised form

10 November 2015

Accepted 26 November 2015

Available online 29 November 2015

#### Keywords:

Vimentin  
OSCC  
β4 integrin  
Cell adhesion  
Migration

### ABSTRACT

Vimentin expression correlates well with migratory and invasive potential of the carcinoma cells. The molecular mechanism by which vimentin regulates cell motility is not yet clear. Here, we addressed this issue by depleting vimentin in oral squamous cell carcinoma derived cell line. Vimentin knockdown cells showed enhanced adhesion and spreading to laminin-5. However, we found that they were less invasive as compared to the vector control cells. In addition, signaling associated with adhesion behavior of the cell was increased in vimentin knockdown clones. These findings suggest that the normal function of β4 integrin as mechanical adhesive device is enhanced upon vimentin downregulation. As a proof of principle, the compromised invasive potential of vimentin depleted cells could be rescued upon blocking with β4 integrin adhesion-blocking (ASC-8) antibody or downregulation of β4 integrin in vimentin knockdown background. Interestingly, plectin which associates with α6β4 integrin in the hemidesmosomes, was also found to be upregulated in vimentin knockdown clones. Furthermore, experiments on lysosome and proteasome inhibition revealed that perhaps vimentin regulates the turnover of β4 integrin and plectin. Moreover, an inverse association was observed between vimentin expression and β4 integrin in oral squamous cell carcinoma (OSCC). Collectively, our results show a novel role of vimentin in modulating cell motility by destabilizing β4 integrin-mediated adhesive interactions. Further, vimentin-β4 integrin together may prove to be useful markers for prognostication of human oral cancer.

© 2015 Elsevier Ltd. All rights reserved.

**Abbreviations:** TGF-β1, Transforming growth factor beta1; RT-PCR, Reverse transcriptase polymerase chain reaction; IP, immunoprecipitation; IHC, Immunohistochemistry; EMT, Epithelial mesenchymal transition; MET, Mesenchymal epithelial transition; ns, non-significant; MMP, Matrix-metalloproteinase; cq, Chloroquine; chx, Cycloheximide; OSCC, Oral squamous cell carcinoma; SCC, Squamous cell carcinoma; SEM, Standard error mean; IF, Intermediate filament; Ex/Em, Extension/emission; ECM, Extracellular matrix; In5, laminin-5; fn, fibronectin; uc, Uncoated.

\* Corresponding author. Tel.: +91 22 27405055; fax: +91 22 2705085.

E-mail address: [mvaitya@actrec.gov.in](mailto:mvaitya@actrec.gov.in) (M. Vaidya).

<sup>1</sup> Current Address: Department of Molecular and Cellular Oncology, MD Anderson Cancer Centre, University of Texas, Houston, Texas, United States of America.

<sup>2</sup> Current Address: Department of Nuclear Medicine, Kyunpook National University school of Medicine, N101, Dongin-Dong, Jung-Gu, Daegu, Republic of Korea.

### 1. Introduction

Vimentin is a type III intermediate filament protein (IF), predominantly expressed in mesenchymal cells, many undifferentiated cells and cultured cells (Lazarides, 1982). It is partially or completely replaced with their cell type specific IF protein in cells which are committed to undergo terminal differentiation (Tapscott et al., 1981). Functional deletion of vimentin in mice resulted in decreased capacity of lymphocytes for homing to lymph nodes and spleen (Niemenen et al., 2006). Also, their fibroblasts were unable to bring about migration. Contribution of vimentin in pathological or physiological processes has been described in human keratinocytes involved in the outgrowth of keratinocyte sheets (Biddle and Spandau, 1996) and also in normal human bronchial cells studied in an *in vitro* wound healing model (Buisson et al., 1996).

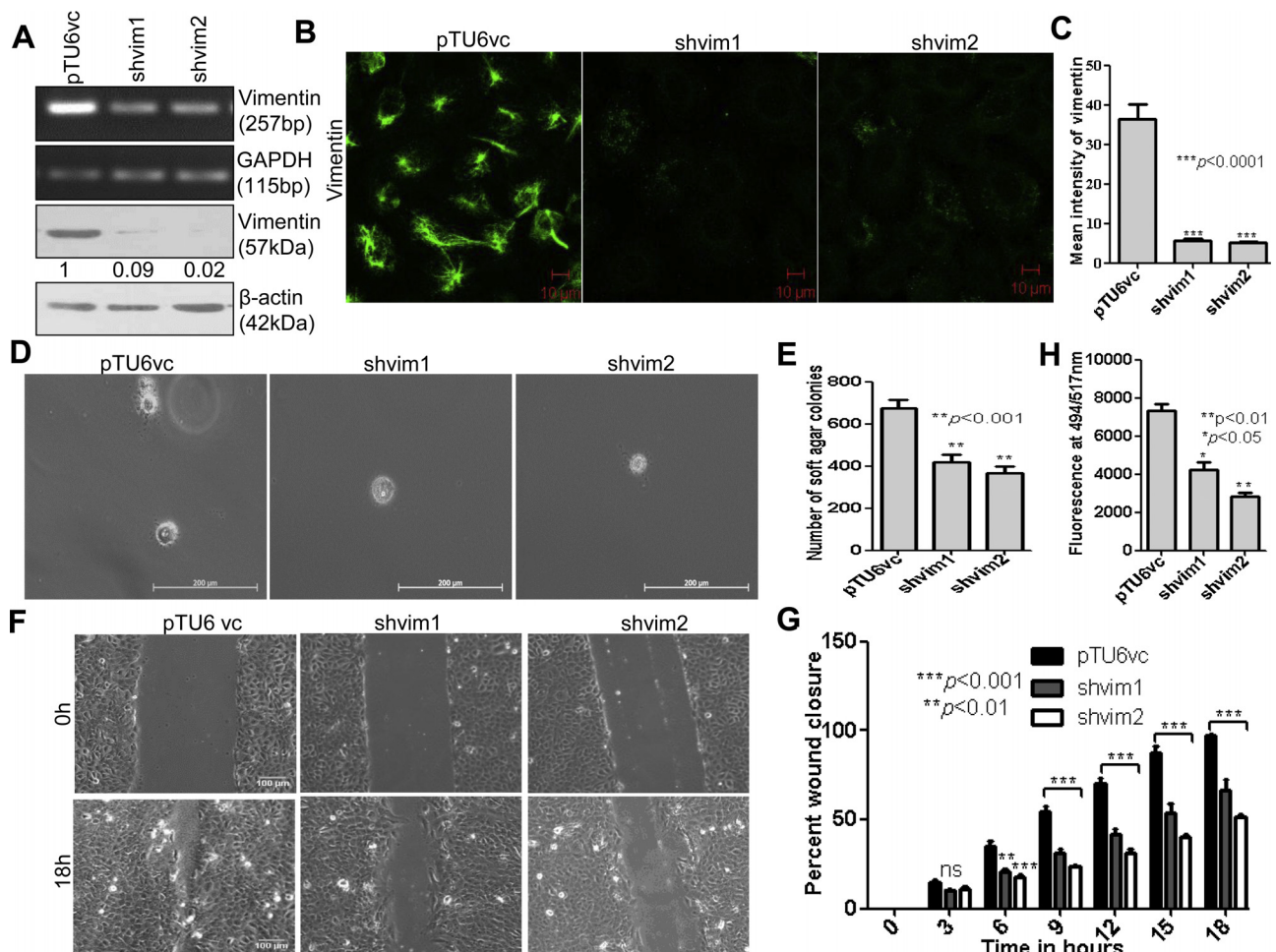


**Fig. 1.** Generation of vimentin knockdown clones in oral SCC derived cell line. (A, B) RT-PCR, western blot and immunofluorescence analysis of vimentin, in vimentin knockdown clones (shvim1, shvim2) and its vector control clone (pTU6vc). (C) The graph shows mean fluorescence intensity of vimentin across clones. (D) Representative images of colonies formed by vimentin knockdown and vector control clones in soft agar. (E) Graphical representation of number of colonies formed in soft agar. (F, G) Representative time lapse microscopy images showing wound healing. The graph shows percent wound closure as calculated over 18 h time point. (H) The graph shows fluorescence of invaded cells which is read at wavelengths of 494/517 nm (Ex/Em). Note: The numbers labeled below each blot represent relative intensity of the bands using densitometric analysis. For quantification, data represents  $\pm$  standard error mean (SEM) of three independent experiments.

These studies together emphasize upon the role of vimentin in normal body development.

Role of vimentin is increasingly recognized in case of cancer progression. However, it may not play a significant function in the development of cancer (Langa et al., 2000). Vimentin expression is seen to be upregulated in many invasive cancers (Satelli and Li, 2011). *In vitro* studies have indicated role of vimentin in migration (Paccione et al., 2008). It has been shown that vimentin might play a functional role in epithelial cell migration associated with stress or pathological situations (Gilles et al., 1999). Recent reports give some insights into the probable mechanism by which vimentin contributes in cell migration. For example, regulation of cell adhesion and motility by vimentin phosphorylation was shown in HMT-3522 epithelial cells. Vimentin phosphorylation by protein kinase C $\epsilon$  (pkc $\epsilon$ ) mediates  $\beta$ 1 integrin recycling to the surface, thus contributing in cell motility (Ivaska et al., 2005). Vimentin is also shown to regulate receptor tyrosine kinase Axl, to bring about cell migration during epithelial mesenchymal transition (EMT) (Vuoriluoto et al., 2011). Conversely, in mesenchymal epithelial transition (MET) vimentin levels decrease leading to reduced motility (Chaffer et al., 2006). Though the contribution of vimentin in cancer cell migration and invasion is well established, the role of regulatory molecules/signaling pathways involved are not yet well defined.

Previous report from our laboratory has shown aberrant expression of vimentin in oral dysplastic and fibrotic tissues. In addition, its expression in OSCC showed significant correlation with aggressive phenotype and survival of the patients (Sawant et al., 2014). These preliminary observations prompted us to investigate the downstream molecules involved in vimentin-mediated migration and invasion.

In the present study, vimentin knockdown resulted in increased  $\beta$ 4 integrin surface levels leading to strong adhesive contacts. This manifested into decreased motility. Interestingly, along with  $\beta$ 4 integrin, its linker protein plectin was also upregulated with vimentin downregulation probably due to decreased targeting of these molecules to proteasomal and lysosomal machinery. Similar inverse correlation was observed between vimentin and  $\beta$ 4 integrin in human oral cancer tissue samples.

## 2. Materials and methods

### 2.1. Ethics statement

This study was approved by the “Human Ethics Committee”, Tata memorial centre, India (Reg Number: DCGI:

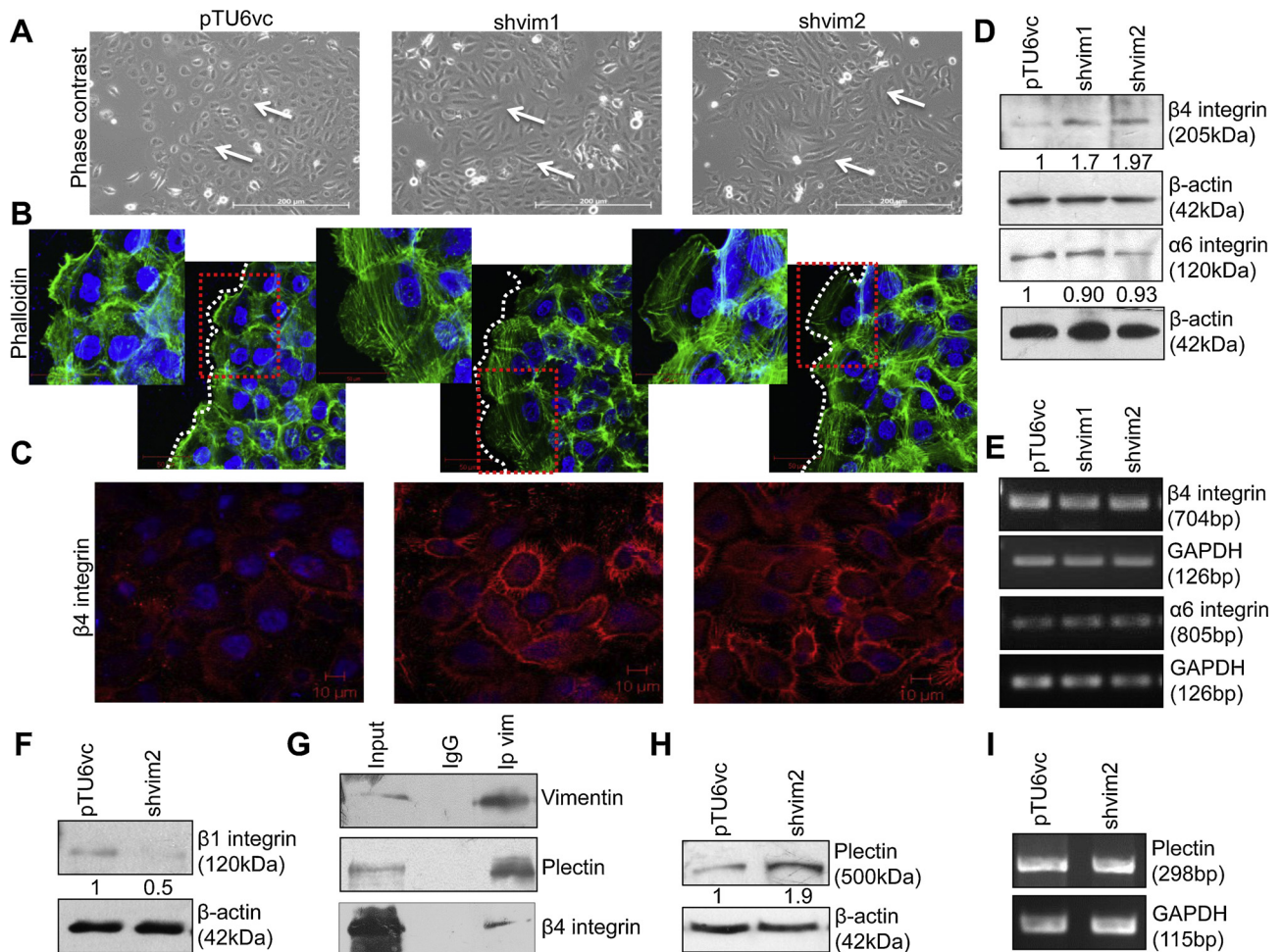


**Fig. 2.** Vimentin knockdown cells show upregulation of both  $\beta 4$  integrin and plectin protein levels. (A) Representative phase contrast images of vimentin knockdown clones displaying well-spread morphology compared to its vector control clone. (B) Immunofluorescence analysis of actin reorganization at the wound edge using phalloidin-FITC staining (Bar: 50  $\mu\text{m}$ ). The inset shows prominent actin stress fibers in vimentin knockdown clones indicative of a less motile phenotype as compared to vector control clone (Bar: 50  $\mu\text{m}$ ). (C) Immunofluorescence staining of  $\beta 4$  integrin in vimentin knockdown and vector control clones. (D–E) Western blot and RT-PCR analysis of  $\beta 4$  and  $\alpha 6$  integrin in vimentin knockdown and vector control clones. (F) Western blot analysis of  $\beta 1$  integrin levels in the clones. (G) Endogenous pull down experiment with anti-vimentin antibody performed using cell lysate from AW13516 cells. The immunoprecipitated complex was examined for the presence of vimentin,  $\beta 4$  integrin and plectin. Input represented 10% of cell lysate used in the experiment. (H, I) Western blot and RT-PCR analysis of plectin in vimentin knockdown and vector control clone. For quantification, data represents  $\pm$  SEM of three independent experiments.

ECR/149/Inst/MH/2013). The written “informed consent form” was obtained from the patients before enrolling them.

## 2.2. Cell lines, antibodies and reagents

List of cell lines, antibodies and reagents with their particulars are described in the Supplementary table S1, S2 and S3, respectively.

## 2.3. Plasmids and retroviral constructs

The selected vimentin shRNA sequences (Supplementary table S4) were cloned into pTU6 PURO vector (a kind gift from Dr. Sorab) and validated in HEK293 by co-transfecting them with GFP tagged vimentin as described previously (Kundu et al., 2008). Effective shRNA sequences vim3A and vim3B were transfected using lipofectamine 2000 to generate vimentin knockdown clone in AW13516 cells. For vimentin overexpression, emerald GFP vimentin retroviral construct (a kind gift from Professor Robert Goldman) was used. Vimentin- $\beta 4$  integrin double knockdown and vector control clones were generated by transducing  $\beta 4$  integrin shRNA and scrambled shRNA cloned in pCLXSN retroviral vector (a kind gift from Dr. Livio

Trusolino) in vimentin knockdown clone shvim2. Virus production was done as described previously (Helfand et al., 2011).

## 2.4. Real-time quantitative PCR/reverse transcriptase PCR (RT-PCR)

Real-time quantitative PCR/RT-PCR was performed as described previously (Alam et al., 2011). The primers and PCR conditions are shown in Supplementary table S5. RT-PCR primer sequences for  $\beta 4$  integrin were obtained from (Lo et al., 2001).

## 2.5. Western blotting, immunoprecipitation (IP), scratch wound migration assay, soft agar assay and zymography

Cell lysates for western blotting were prepared in SDS lysis buffer (62.5 mM Tris and 2% SDS, pH 6.8). For immunoprecipitation, cell lysates were made by pooling both NP-40 (1%) and Empigen (2%) fractions as described previously (Srikanth et al., 2010). Scratch wound migration assay, soft agar assay (Iyer et al., 2013) and gelatin zymography (Dange et al., 2015) were performed as described previously.

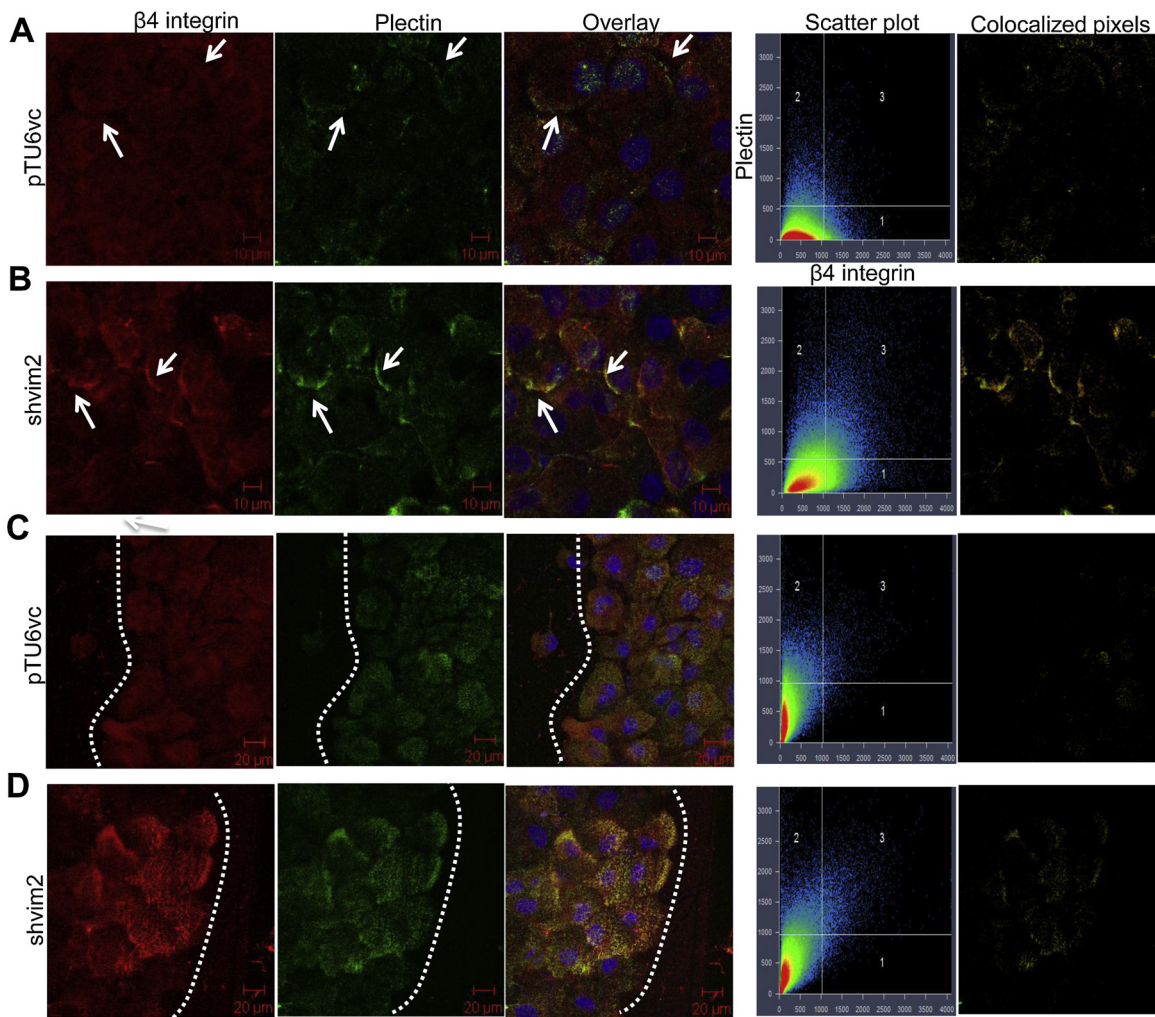


**Fig. 3.**  $\beta 4$  integrin/plectin colocalize strongly at the membrane upon vimentin knockdown. (A, B) The degree of colocalization of  $\beta 4$  and plectin is higher in vimentin knockdown (Correlation  $R = 0.3422$ ) as compared to vector control clones (Correlation  $R = 0.18095$ ). 10 random fields from 3 independent experiments were used for analysis. (C, D) The colocalized regions are prominently seen at the wound front in vimentin knockdown as compared to vector control clone. Scatter plot shows the intensity of  $\beta 4$  ( $x$ -axis) and plectin ( $y$ -axis) for each pixel. On the right, are the respective pictures of only colocalized pixels.

## 2.6. Immunofluorescence

Immunofluorescence staining was performed as previously described (Raul et al., 2004). Scatter Plot and Pearson's correlation coefficient ( $R$ ) for colocalization were obtained using Carl Zeiss (zen 2012 SPI black edition, 64 bit) software.

## 2.7. Cell adhesion, migration, invasion and spreading assays

Cell-laminin-5 (2.5  $\mu\text{g/ml}$ )/fibronectin (5  $\mu\text{g/ml}$ ) adhesion assays were performed as described previously (Alam et al., 2011). For invasion assays, the insert was coated with 40  $\mu\text{l}$  of matrigel (1 mg/ml). The cells were then treated with IgG or ASC-8 antibody ( $\beta 4$  integrin adhesion blocking antibody) and incubated for 1 h on ice. Cells were seeded on the coated inserts (8  $\mu\text{m}$  pore size) and incubated for 16 h. At the 15th h, 4  $\mu\text{g/ml}$  calcein AM was added to the lower chamber and incubated for 1 h at 37  $^{\circ}\text{C}$  (Partridge and Flaherty, 2009). Fluorescence of invaded cells was read at wavelengths of 494/517 nm (Ex/Em) on a bottom-reading fluorescent plate reader at 16th h. For live cell spreading, cells were detached using accutase and seeded onto laminin-5 (2.5  $\mu\text{g/ml}$ )/fibronectin (5  $\mu\text{g/ml}$ ) coated surface. Phase-contrast images were captured just after the cells were seeded, at every 10' interval, till at least one of the group showed optimum spreading. Images were

evaluated for the percentage of well spread cells. Unspread cells were described as phase-bright and rounded, whereas spread cells were elongated with visible membrane protrusions. 30 cells each were counted from three independent experiments. For single cell migration assay, cells were harvested using accutase, washed with plain IMDM (Iscove's Modified Dulbecco's Medium) and plated at 30% confluency on laminin-5 (2.5  $\mu\text{g/ml}$ )/fibronectin (5  $\mu\text{g/ml}$ ) coated dishes. Unspread cells, dividing cells and cells migrating out of the selected field were excluded during analysis. The time lapse data was analyzed using ImageJ (NIH) manual tracking plugin. The coordinates obtained were used to plot graph and calculate distance and velocity using chemotaxis and migration tool.

## 2.8. Induction of EMT and stimulation of $\beta 4$ integrin signaling

To induce EMT, AW13516 cells were incubated in serum free media in the presence of transforming growth factor beta1, *i.e.*, TGF- $\beta 1$  (5 ng/ml) and kept at 37  $^{\circ}\text{C}$  for 48 h. To study  $\beta 4$  signaling on ligation to laminin-5, 18 h serum starved cells were harvested using accutase and further washed with plain medium and plated on laminin-5 (2.5  $\mu\text{g/ml}$ ) coated dishes. For activation of  $\beta 4$  integrin signaling, vimentin knockdown and vector control clones were serum-starved for 18 h and then treated with 5  $\mu\text{g/ml}$  of 3E1

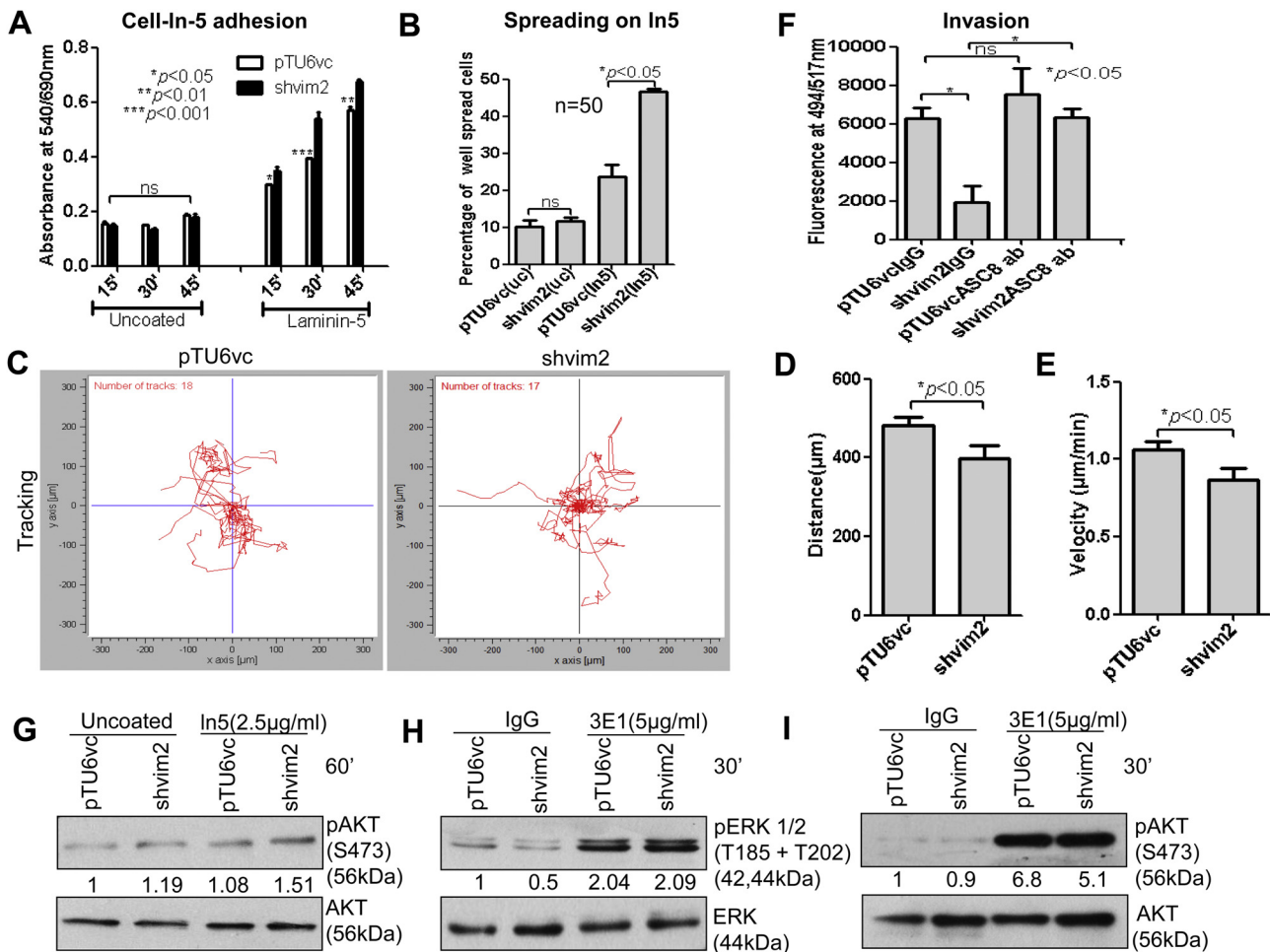


**Fig. 4.** Functional consequences of upregulation of  $\beta 4$  integrin in vimentin depleted cells. (A) Vimentin knockdown and vector control clones were allowed to attach on 96 well laminin-5 (In5) coated or uncoated (uc) surface. The unadhered cells were removed at different time points, and the number of adhered cells was determined using MTT assay. (B) The graph shows percentage of well spread cells on laminin-5 coated or uncoated surface. (C) Single cell migration was performed on laminin-5 coated surface. Each line indicates the migration trace of each cell. pTU6vc ( $n = 18$ ) and shvim2 ( $n = 17$ ). (D, E) Graph shows distance and velocity of cell migration respectively. (F) The graph shows fluorescence of invaded cells which is read at wavelengths of 494/517 nm (Ex/Em). Invasion assay was performed in the presence of IgG or ASC-8 antibody. (G) Vimentin knockdown and vector control cells were serum starved and plated on to laminin-5 coated surface for 1 h. Protein extracts were analyzed for pAKT using western blot analysis. (H, I) The serum starved clones were stimulated with 3E1 or mouse IgG for 30' and protein extracts were analyzed for the activation of ERK1/2 and AKT. Total AKT and ERK1/2 were used as loading controls. For quantification, data represents  $\pm$  SEM of three independent experiments.

antibody ( $\beta 4$  integrin activating antibody). 5  $\mu$ g/ml mouse-IgG-treated cells were used as control. After treatment, the lysates were made and western blotting was performed.

### 2.9. Immuno-electron microscopy

Cells were washed with 1XPBS and fixed in 3% Glutaraldehyde followed by secondary fixation in 1% Osmium tetroxide. Ultrathin (70 nm) cross-sections were collected on nickel grids and subsequently micro-waved in Heat-induced Antigen Retrieval (HIAR) buffer-20mMTris-HCl pH 9.0) for antigen retrieval (Yamashita and Okada, 2014). After blocking with 5% BSA, the grids were incubated with anti-  $\beta 4$  integrin antibody (1:20) for 1 h at room temperature. Following washes with 1XPBS, grids were incubated with goat anti-rabbit gold antibody (cat. no. G7402, Sigma, USA) for 1 h. After thorough washes, the grids were stained with uranyl acetate and lead citrate and viewed under Jeol 1400 plus TEM (Japan) at 120 kV. For analysis, we acquired 50 images, each of vimentin knockdown and vector control cells, at magnification of 20000X and stitched using Multiple Image Alignment tool in integrated iTEM software (Olympus soft imaging solutions, GmbH, Germany). Quantification of number of gold conjugates at the cell-substratum front was done.

### 2.10. Immunohistochemistry (IHC) and statistical analysis

Tissue samples were collected from the operation theatre of Tata Memorial Hospital, India. IHC was carried out as described previously (Sawant et al., 2014)

### 2.11. Statistical analysis

Statistical analysis was carried out as described previously (Iyer et al., 2013). Two way ANOVA using Bonferroni test was performed for two factorial comparisons among multiple groups. A  $p$  value of less than 0.05 was considered statistically significant.

## 3. Results

### 3.1. Downregulation of vimentin decreases in vitro transformation potential and invasiveness of OSCC derived cell line AW13516

Expression of vimentin at mRNA and protein level (Fig. 1A) was reduced significantly in vimentin knockdown clones (shvim1 and shvim2) as compared to the vector control clone (pTU6vc). Further,

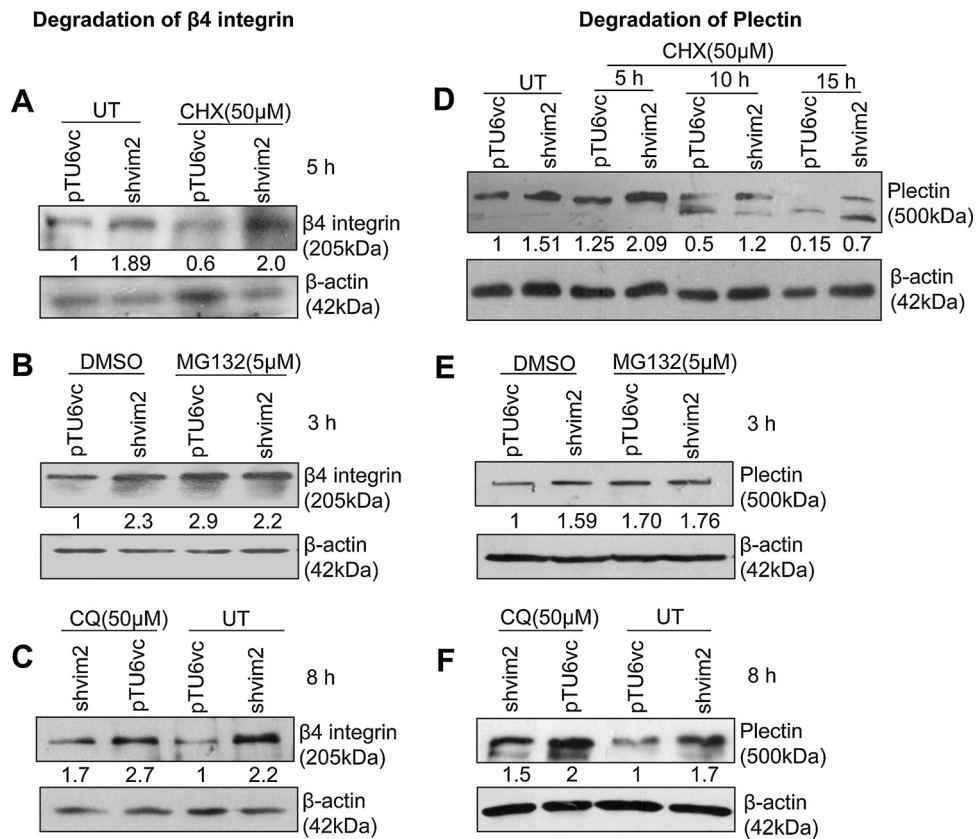


**Fig. 5.** Vimentin regulates the turnover of  $\beta 4$  integrin and plectin. (A, D) Vimentin knockdown and vector control clones were treated with cycloheximide at 50  $\mu$ M. (B, E) Clones were treated with MG-132 at 5  $\mu$ M. 0.1% DMSO was used as a vehicle control. (C, F) Clones were treated with chloroquine at 50  $\mu$ M.  $\beta 4$  integrin/plectin levels were assessed after respective treatments using immunoblotting.  $\beta$ -actin was used as a loading control.

confocal analysis showed decreased intensity of vimentin filaments in vimentin knockdown clones (Fig. 1B and C). Vimentin downregulated clones showed a significant reduction in number of colonies (by ~50%) in soft agar as compared with vector control clones (Fig. 1D and E). They demonstrated significantly decreased migration as compared to vector control clone (Fig. 1F and G). Also in the invasion assay, shvim1 and shvim2 showed 33% and 50% reduction respectively as compared to vector control clone (Fig. 1H).

### 3.2. Vimentin regulates $\beta 4$ integrin levels

Vimentin knockdown clones appeared more elongated (Fig. 2A) and at the wound edge showed flat, well-spread morphology (Fig. 2B) as compared to vector control cells. The extent of spreading between the clones was assessed by quantifying the area of the cells at the wound edge using Image J software (Supplementary Fig. 1). Next, to determine the cause of difference in cell morphology;  $\alpha 6\beta 4$  integrin levels (which govern cell spreading) were examined.  $\beta 4$  integrin levels were found to be upregulated at protein level while its transcript levels stayed unaffected with vimentin downregulation. Both protein and RNA levels of  $\alpha 6$  integrin remained unaltered (Fig. 2C–E and Supplementary Fig. 2A and B). For further experiments, shvim2 clone was used, which showed higher  $\beta 4$  integrin levels and more pronounced effects on soft agar/migration/invasion as compared to shvim1.  $\beta 1$  integrin levels (which are also known to be regulated by vimentin (Kim et al., 2010)) were found to be downregulated in shvim2 as compared to vector control clone pTU6vc (Fig. 2F). Further, increase in  $\beta 4$  integrin levels was not coincident with the corresponding increase in its basement membrane ligand laminin-5 (Supplementary Fig. 2C). Moreover, vimentin knockdown cells showed downregulation of

keratin 5/14 pair while keratin 8/18 levels remained unchanged (Supplementary Fig. 3). This suggests that keratin 8/18 pair is likely to interact with increased  $\beta 4$  integrin molecules in vimentin knockdown cells.

### 3.3. Changes in vimentin expression directly correlate with the alterations in the levels of $\beta 4$ integrin in squamous cell carcinoma (SCC) derived cell lines

TGF- $\beta 1$  (5 ng/ml) exposure induced the expression of vimentin protein and decreased the levels of E-cadherin, marking the acquisition of EMT phenotype in AW13516 cells. Upregulation of vimentin led to concomitant downregulation in  $\beta 4$  integrin protein levels (Supplementary Fig. 4A). Next, other SCC derived cell lines AW13516, AW8507, SCC29B and A431 (Supplementary Fig. 4B and C) displayed inverse relation between the status of vimentin and  $\beta 4$  integrin protein levels. As a proof of principle, exogenous expression of vimentin in A431 demonstrated decrease in  $\beta 4$  integrin levels compared to the vector control clone A431vc (Supplementary Fig. 4D). However, forced expression of vimentin in vimentin nonexpressing immortalized/premalignant cell lines like HaCaT and DOK did not result in any changes in the levels of  $\beta 4$  integrin (Supplementary Fig. 4E). Together, these results suggest that, modulation of  $\beta 4$  integrin protein levels by vimentin is perhaps cancer specific and not cell line specific effect.

### 3.4. Plectin could be a possible linker connecting $\beta 4$ integrin with vimentin intermediate filament protein

Plectin is known to link  $\beta 4$  integrin to the intermediate filament cytoskeleton (Reznicek et al., 1998). Hence, we wanted to check

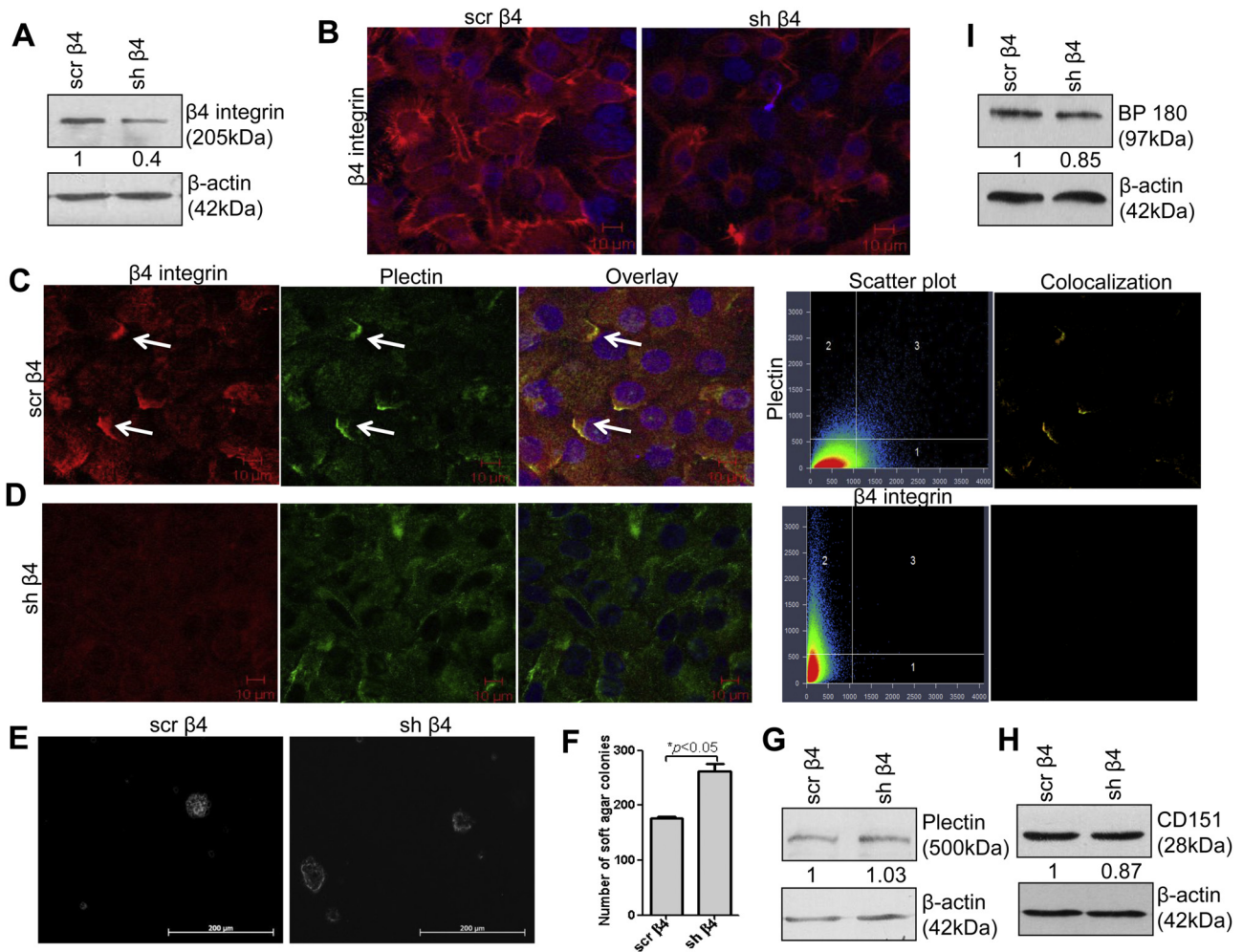


**Fig. 6.** Downregulation of  $\beta 4$  integrin in vimentin knockdown background. (A, B) Western blot and immunofluorescence analysis showing  $\beta 4$  integrin levels in sh  $\beta 4$  (shRNA against  $\beta 4$  integrin) and scr  $\beta 4$  (scrambled vector control). (C, D) Immunofluorescence images of  $\beta 4$  integrin/plectin colocalization in scr  $\beta 4$  (Correlation  $R = 0.2490$ ) and sh  $\beta 4$  clones (Correlation  $R = 0.188$ ). 10 random fields from 3 independent experiments were used for analysis. (E) Representative images of colonies formed by scr  $\beta 4$  and sh  $\beta 4$  in soft agar. (F) Graphical representation of number of colonies formed in soft agar (G–I) Western blot analysis showing protein levels of other hemidesmosomal complex proteins plectin, CD151 and BP180 respectively. For quantification, data represents  $\pm$  SEM of three independent experiments.

if plectin acted as a linker connecting  $\alpha 6\beta 4$  integrin to vimentin. Co-immunoprecipitation with vimentin was able to pull down both plectin and  $\beta 4$  integrin (Fig. 2G). Further, in vimentin knockdown clones, plectin protein levels were seen to be increased without any change at its transcript levels (Fig. 2H and I). Other hemidesmosomal plaque proteins like CD151 and BP180 remained unaltered (Supplementary Fig. 5A and B).

### 3.5. Vimentin knockdown results in increased localization of hemidesmosomal proteins ( $\beta 4$ integrin and plectin) at membrane-substrate front

To study the localization of  $\beta 4$  integrin along the site of cell substratum, we performed immuno-electron microscopy. Our results showed extensive localization of  $\beta 4$  integrin at the membrane-substrate front in vimentin knockdown cells as compared to vector control cells (Supplementary Fig. 6A–C). Next we studied colocalization of  $\beta 4$  integrin and plectin using immunofluorescence. As shown in Fig. 3A and B, the degree of co-localization of  $\beta 4$  integrin and plectin is higher in vimentin knockdown as compared to vector control clone. Also, at the wound front,  $\beta 4$  integrin and plectin showed higher co-localization in vimentin knockdown as compared to vector control cells (Fig. 3C and D). These results were further confirmed by immunoprecipitation with antibody to

plectin or  $\beta 4$  integrin. Both plectin IP and  $\beta 4$  integrin IP fraction showed increased levels of  $\beta 4$  integrin and plectin respectively in vimentin knockdown as compared to vector control clone (Supplementary Fig. 7A and B). This observation suggests that increased levels of plectin and  $\beta 4$  integrin correspond to increase in interaction between the two as well, in case of vimentin knockdown clone.

### 3.6. Functional consequence of $\beta 4$ integrin upregulation in vimentin knockdown cells

As assessed using cell-ECM adhesion assay, the attachment of vimentin knockdown clone to laminin-5 increased significantly with time as compared to vector control clone (Fig. 4A). Consistent with our results of adhesion assay, vimentin knockdown cells showed more spread morphology on laminin-5 (Fig. 4B, Supplementary Fig. 8) while migration on laminin-5 (Fig. 4C–E, Supplementary movie 1 and 2) was significantly reduced as compared to vector control cells. Unlike the results with laminin-5, vimentin knockdown cells showed decreased spreading and migration on fibronectin while its adhesion remained unaltered (Supplementary Fig. 9, Supplementary movie 5 and 6). Since, these assays demonstrated that the vimentin knockdown cells have acquired specific and increased adherence to laminin-5, we

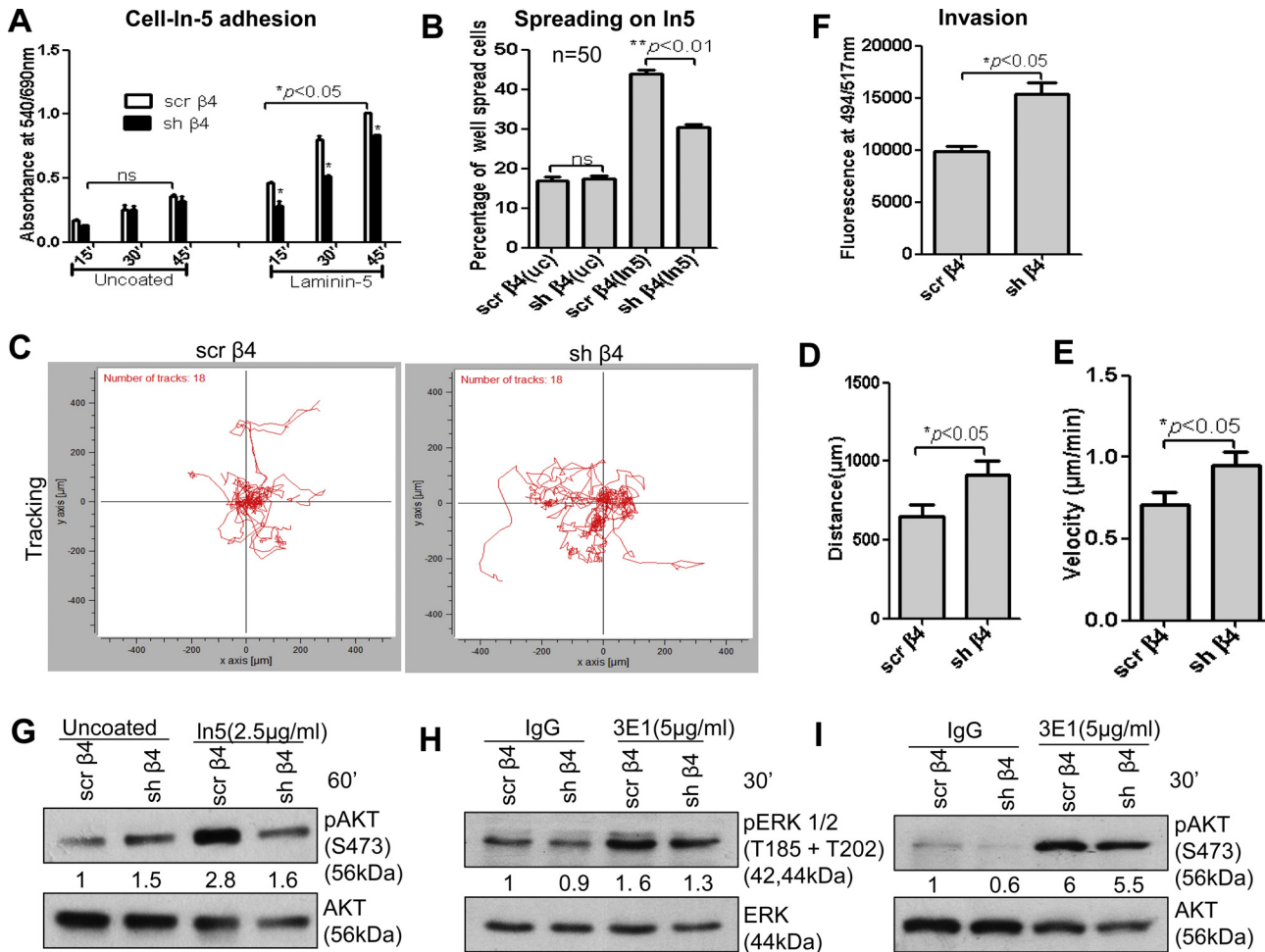


**Fig. 7.** Effect of  $\beta 4$  integrin knockdown on its mechanical and signaling function. (A) sh  $\beta 4$  and scr  $\beta 4$  were allowed to attach on laminin-5 coated or uncoated surface. At different time points, the unadhered cells were removed and the number of adhered cells was determined using MTT assay. (B) The graph shows percentage of well spread cells on laminin-5 coated or uncoated surface. (C) Single cell migration was performed on laminin-5 coated surface. Each line indicates the migration trace of each cell. scr  $\beta 4$  ( $n = 18$ ) sh  $\beta 4$  ( $n = 18$ ). (D, E) Graph shows distance and velocity of cell migration respectively. (F) The graph shows fluorescence of invaded cells which is read at wavelengths of 494/517 nm (Ex/Em). (G–I) Western blots showing signaling of the clones on laminin-5 coated surface (pAKT/AKT) and in response to 3E1 antibody (pERK/ERK and pAKT/AKT) respectively. For quantification, data represents  $\pm$  SEM of three independent experiments.

hypothesized that, if the interaction between  $\beta 4$  integrin and laminin-5 is inhibited, the cells would be more motile. Treatment with adhesion blocking antibody of  $\beta 4$  integrin (ASC-8), which abrogates laminin-5- $\beta 4$  integrin interaction (Egles et al., 2010), demonstrated higher *in vitro* invasive potential in vimentin knockdown as compared to vector control clones (Fig. 4F). Since, vector control clones already exhibit decreased  $\beta 4$  integrin levels; further blocking did not rescue the phenotype to a larger extent.

### 3.7. Downstream molecules associated with $\beta 4$ integrin-mediated adhesive phenotype

Some of the molecules involved in  $\beta 4$  integrin-mediated inside-out and outside-in signaling were tested upon vimentin downregulation. The previous report has shown that ligation of  $\beta 4$  integrin on non-modified plastic increases cell adhesion which involves activation of PKB/Akt pathway (Kippenberger et al., 2004). We found increased phosphorylation of AKT on laminin-5 surface in vimentin knockdown as compared to vector control cells while the uncoated surface did not show any significant difference (Fig. 4G). The outside in signaling of  $\beta 4$  integrin was assessed by stimulating  $\beta 4$  integrin with its activating antibody 3E1 and probing for molecules that represent different pathways downstream of  $\beta 4$  (Kippenberger et al., 2010). The activation of ERK remained

unaffected while decreased phosphorylation of AKT was seen in vimentin knockdown as compared to vector control clones (Fig. 4H and I). These findings demonstrate that adhesion related signaling predominates upon vimentin downregulation.

### 3.8. Vimentin knockdown results in decreased protein turnover of $\beta 4$ integrin and plectin.

The increased expression of  $\beta 4$  integrin at protein level without any change in its mRNA suggested higher stability of this protein in vimentin deficient background. Upon cycloheximide (CHX; inhibitor of protein biosynthesis) treatment,  $\beta 4$  integrin levels remained almost unaffected in vimentin knockdown while 40% reduction was observed in the vector control cells (Fig. 5A). The altered turnover rate of  $\beta 4$  integrin in response to changes in vimentin levels suggested differential regulation by one or more of its known protein degradation modes; which includes, proteasome, lysosome, MMP's and calpain. Blockade of proteasome using MG-132 did not alter the levels of  $\beta 4$  integrin in vimentin knockdown while vector control clone showed significant increase (Fig. 5B). Additionally, most of the integrins are internalized through lysosomal pathway (Dozykiewicz et al., 2012) and defective acidification of lysosomes has been shown in vimentin-null cells (Styers et al., 2004). Treatment with lysosomal inhibitor

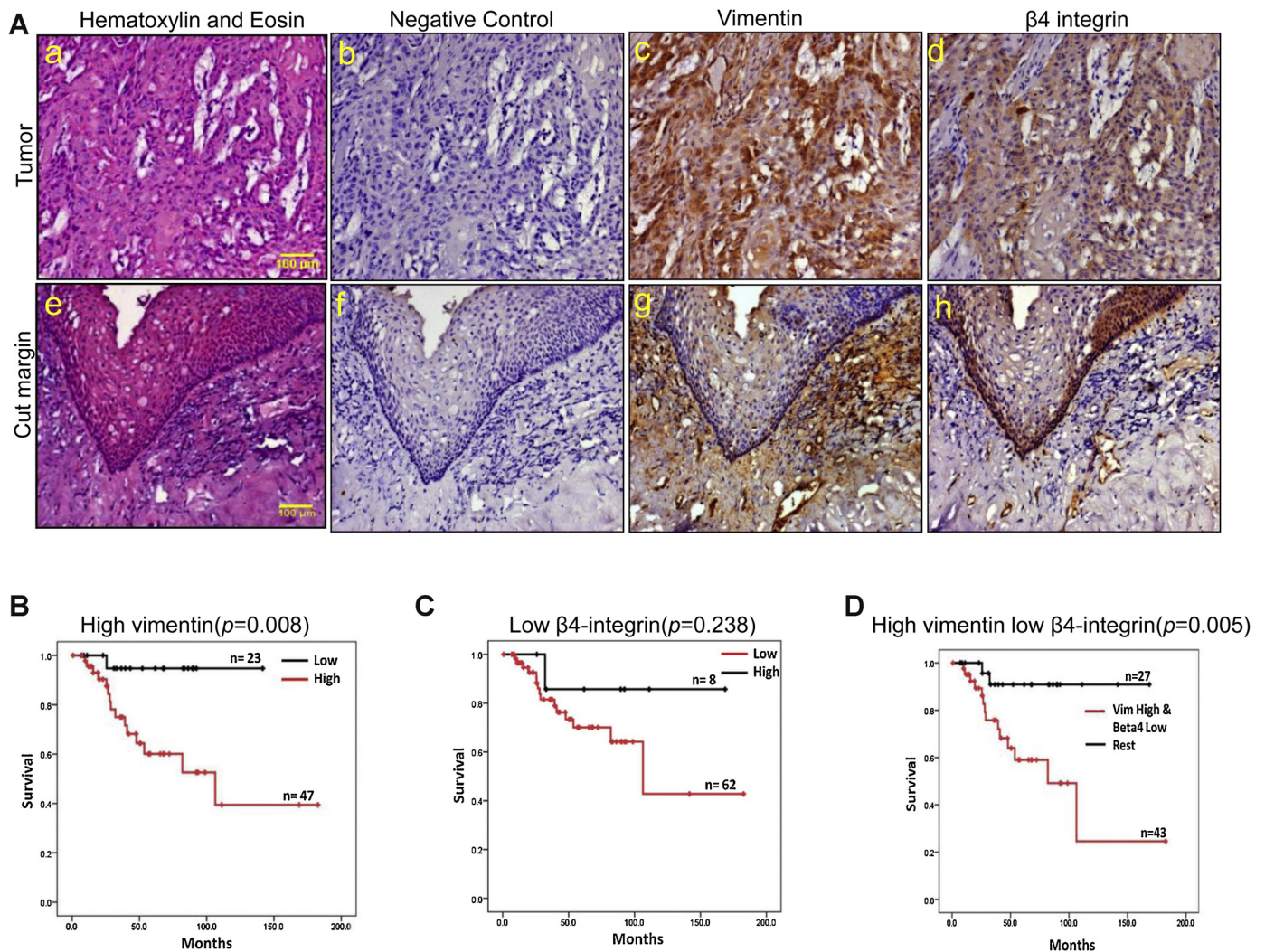


**Fig. 8.** High vimentin and low  $\beta 4$  integrin staining intensity together correlates with poor survival in oral SCC patients. (A) (a–d) The upper panel shows images of haematoxylin and eosin, negative control and IHC staining of vimentin and  $\beta 4$  integrin respectively in tumor tissue while lower panel (e–h) shows images of haematoxylin and eosin, negative control and IHC staining of vimentin and  $\beta 4$  integrin respectively in cut margin tissue. Kaplan–Meier survival analysis ( $n = 70$ ) of (B) High vs. low vimentin expression, (C) High vs. low  $\beta 4$  integrin expression and (D) High vimentin/low  $\beta 4$  integrin vs. rest other combinations of vimentin and  $\beta 4$  integrin expression.

chloroquine (CQ) resulted in decrease in  $\beta 4$  integrin protein levels in vimentin knockdown while vector control clone showed 2.7-fold increase (Fig. 5C). Moreover,  $\beta 4$  integrin is also known to be cleaved by matrix metalloproteinase (MMP)-2 and -9 (Pal-Ghosh et al., 2011). MMP9 showed upregulation whereas MMP2 was downregulated in vimentin knockdown as compared to vector control clone (Supplementary Fig. 10), indicating that it may not have a role in  $\beta 4$  integrin cleavage. Further, plectin followed similar stability trend in vimentin knockdown and vector control clones as observed for  $\beta 4$  integrin (Fig. 5D–F). This indicates decreased targeting of  $\beta 4$  integrin and plectin to proteasomes and lysosomes in vimentin deficient background.

### 3.9. $\beta 4$ integrin downregulation rescued the vimentin knockdown phenotype.

To verify whether the phenotype associated with reduced cell migration in vimentin knockdown cells was due to higher  $\beta 4$  integrin levels, it was stably downregulated in vimentin knockdown clone shvim2. sh  $\beta 4$  (shRNA against  $\beta 4$ ) showed reduction in the levels of  $\beta 4$  integrin and its colocalization with plectin as compared to scr  $\beta 4$  (scrambled shRNA) (Fig. 6A–D).  $\beta 4$  integrin knockdown cells demonstrated increased number of colonies in soft agar

(Fig. 6E and F). No significant effect was seen on the expression of other hemidesmosomal complex proteins like, plectin, CD151 and BP180 respectively (Fig. 6G–I). Upon  $\beta 4$  integrin downregulation, a decrease was seen in cell-laminin-5 adhesion (Fig. 7A) and spreading (Fig. 7B, Supplementary Fig. 11). A corresponding increase was observed in migration on laminin-5 (Fig. 7C–E, Supplementary movie 3 and 4) and transwell invasion (Fig. 7F). Activation of AKT on ligation to laminin-5 (Fig. 7G) showed significant decrease. However, only marginal decrease in the phosphorylation of ERK and AKT (Fig. 7H and I) was seen following stimulation with 3E1 antibody. This was an expected finding since the knockdown of  $\beta 4$  integrin resulted in overall decrease in the number of available  $\beta 4$  integrin molecules to transmit the signal. Cumulatively, these findings confirm that the more adhesive and less migratory phenotype associated with vimentin knockdown clone is regulated through  $\beta 4$  integrin.

### 3.10. High vimentin and low $\beta 4$ integrin protein levels are associated with poor survival

Immunohistochemistry analysis showed negative relationship between  $\beta 4$  integrin and vimentin expression (Spearman's non-parametric correlation =  $-0.200$ ,  $p = 0.044$ ,  $n = 74$ ) in oral tumor

**Table 1**  
Correlations of co-expression of vimentin and  $\beta 4$  integrin with clinico-pathological parameters of the OSCC patients ( $n = 74$ ).

Clinico-pathological parameter		n (74)	Vimentin (Vim) and Beta4 integrin ( $\beta 4$ )			p-value
			Expression			
			Vim (high) $\beta 4$ (low)	Vim (high) $\beta 4$ (high)	Vim (low) $\beta 4$ (low/high)	
<b>Age (years)</b>	<50	41	25	3	13	<b>0.720<sup>a</sup></b>
	$\geq 50$	33	21	1	11	
<b>Sex</b>	Male	60	37	3	20	<b>0.910<sup>a</sup></b>
	Female	14	9	1	4	
<b>Thickness</b>	2cm	54	35	2	17	<b>0.509<sup>a</sup></b>
	$\geq 2$ cm	20	11	2	7	
<b>Stages</b>	<III	20	9	1	10	<b>0.050<sup>b</sup></b>
	$\geq$ III	54	37	3	14	
<b>Tumor size</b>	<T3	27	13	1	13	<b>0.037<sup>b</sup></b>
	$\geq$ T3	47	33	3	11	
<b>Node status</b>	Yes	49	34	4	11	<b>0.021<sup>a</sup></b>
	No	25	12	0	13	
<b>Differentiation</b>	Poor/moderate	67	41	4	22	<b>0.756<sup>a</sup></b>
	Well	7	5	0	2	
<b>Bone</b>	Positive	22	13	3	6	<b>0.061<sup>a</sup></b>
	Negative	39	27	0	12	
	NA	13				
<b>Perineural invasion</b>	Yes	18	14	1	3	<b>0.062<sup>a</sup></b>
	No	50	30	0	20	
	NA	6				
<b>Perineural extension</b>	Yes	34	21	3	10	<b>0.205<sup>a</sup></b>
	No	33	21	0	12	
	NA	7				

NA: Data not available.

<sup>a</sup> Pearson chi-Square.

<sup>b</sup> Spearman correlation (ordinal by ordinal)

tissues (Fig. 8A), which corroborated with our *in vitro* findings. Interestingly, significant correlation was seen between expression levels of these proteins and some clinical parameters like, stage ( $p = 0.050$ ), tumor size ( $p = 0.037$ ) and node status ( $p = 0.021$ ) (Table 1). Kaplan–Meier survival analysis, on the basis of IHC, showed that high vimentin expression was associated with poor survival ( $p = 0.008$ ) (Fig. 8B). Similarly, low  $\beta 4$  integrin expression showed a trend (albeit not significant) for poor prognosis ( $p = 0.238$ ) (Fig. 8C). In addition, our combinatorial survival analysis demonstrated significant correlation between high vimentin-low  $\beta 4$  integrin expression and poor patient survival ( $p = 0.005$ ) (Fig. 8D). This implies that, vimentin and  $\beta 4$  integrin together may be used for prognostication of oral cancer patients.

#### 4. Discussion

Our understanding of the molecular mechanisms underlying vimentin associated phenotype remains limited. Although in many studies vimentin expression is associated with tumor cell growth, invasion and migration (Satelli and Li, 2011), we show here a previously unidentified negative regulation of  $\beta 4$  integrin expression by vimentin to facilitate cell migration by compromising adhesion function of  $\beta 4$  integrin.

As a first step, we generated vimentin knockdown system and found reduction in *in vitro* migration and invasion in vimentin deficient state. Interestingly, we found substantial difference in the cell spreading between vimentin knockdown and vector control clones. Cell spreading takes place by complex interactions between the cytoskeleton, matrix adhesion receptors and extracellular matrix

(ECM) proteins (Kim and McCulloch, 2011). In case of carcinomas,  $\alpha 6\beta 4$  and  $\alpha 6\beta 1$  integrins are known to majorly contribute towards cell spreading and motility (Cress et al., 1995). We found reduction in cell motility and invasion with vimentin depletion as a result of increased adhesive interaction mediated by  $\beta 4$  integrin. Moreover, decreased  $\beta 1$  integrin levels may also contribute to reduction in migration (Brockbank et al., 2005) in vimentin knockdown cells but since vimentin  $\beta 1$  integrin interaction is well established (Ivaska et al., 2005), we went ahead to decipher the unknown link if any, between vimentin and  $\beta 4$  integrin. Surprisingly  $\alpha 6$  integrin, which heterodimerizes with  $\beta 4$  integrin remained unchanged probably because  $\beta 1$  integrin levels are down, hence most of the  $\alpha 6$  subunits which would otherwise pair with  $\beta 1$  are now available to pair with the excess  $\beta 4$  integrin molecules.

The primary function of  $\alpha 6\beta 4$  integrin in stratified epithelia is to form stable contacts with underlying basement membrane. Contrasting to its normal function, in carcinomas,  $\alpha 6\beta 4$  integrin is known to stimulate signaling molecules to enhance migration and invasion (Mercurio et al., 2001). Our data shows an increase in adhesion and spreading leading to reduction in motility on laminin-5, while significant decrease was seen in spreading and migration on fibronectin. This may be due to downregulation of  $\beta 1$  integrin (which binds to fibronectin in combination with  $\alpha 5$  or  $\alpha v$ ) upon vimentin knockdown. Interestingly, adhesion on fibronectin did not alter between the clones, even after  $\beta 1$  integrin downregulation, most likely due to engagement of  $\beta 3$  integrin with fibronectin to mediate adhesion (Lin et al., 2013). Thus our results on fibronectin in turn indicate that the effects seen in vimentin knockdown cells are laminin-5 specific.

Vimentin is not known to directly interact with  $\beta 4$ . However,  $\beta 4$  is shown to interact with vimentin through plectin in endothelial cells (Homan et al., 2002). In the normal scenario, disruption of plectin has been shown to inhibit interactions of basal keratinocytes to its basement membrane (McLean et al., 1996). Conversely, in malignancies, overexpression of plectin is shown to promote migration and invasion (Katada et al., 2012). Here, we demonstrate that plectin interacts with vimentin/ $\beta 4$  integrin and shows upregulation concomitant to  $\beta 4$  integrin increase, in vimentin downregulated cells. This suggests that, cytoskeletal linker plectin may perhaps contribute in strengthening of cell matrix adhesion mediated by  $\alpha 6\beta 4$  integrin. Also increasing reports provide evidence about its expression, localization and function in cancer cells which is opposing to its normal role. Consistent with our results, increased turnover of  $\alpha 6\beta 4$  integrin was seen in multistep mouse model of skin carcinogenesis (Witkowski et al., 2000). In this context, it is noteworthy that though  $\alpha 6\beta 4$  integrin was shown to be predominant receptor expressed in carcinomas, its expression was not polarized but was dissociated and not restricted to the basement membrane (Tennenbaum et al., 1992). In our study, non-cancerous cells, upon vimentin overexpression, did not show alterations in  $\beta 4$  integrin levels perhaps because vimentin expression in carcinomas begins as a part of EMT program, where the cell prepares itself for invasion (Kalluri and Weinberg, 2009). Hence, along with an aberrant vimentin expression, other transformation related changes also accompany in a transformed cell which are not seen in a non-transformed cell.

Next, we wanted to understand the cause of increased protein levels of  $\beta 4$  integrin/plectin concomitant with vimentin downregulation. Two major systems; proteasome complex which degrades most of the cellular unfolded proteins and the lysosomal apparatus involved in the degradation of extracellular/membrane-associated proteins, control the protein turnover in eukaryotic cells (Styers et al., 2004). We see contribution of both proteasome and lysosome in degradation of  $\beta 4$  and plectin. Previously, degradation of  $\beta 4$  integrin via proteasome has been demonstrated in junctional epidermolysis bullosa with pyloric atresia (Michelsoni et al., 2004). Interactions between vimentin and the adaptor complex AP-3 are seen to control the positioning, content, and subcellular distribution of selected late endosome/lysosome membrane proteins. As a result, AP-3-null and vimentin-null cells are seen to have decreased capacity to acidify their lysosomes (Styers et al., 2004). In this context, our observations lead to the hypothesis that the upregulation of  $\beta 4$  and plectin levels seen in absence of vimentin could be a consequence of reduced degradation due to altered targeting to proteasomal and lysosomal machinery. Additionally, plectin (Walko et al., 2011) and  $\beta 4$  molecules (Giancotti et al., 1992) are shown to be susceptible to proteolytic cleavage by calcium-activated enzyme calpain. Furthermore, MG132, a proteasome inhibitor can also inhibit calpain. Hence the possibility of involvement of calpains in degradation of plectin and  $\beta 4$  integrin cannot be ruled out.

Recent literature suggest, role of vimentin in regulation of EMT (Ivaska, 2011). In an earlier report on kindlin-1 deficient keratinocytes, increase in mesenchymal markers like vimentin and fibronectin was seen with concomitant decrease in epithelial markers like E-cadherin,  $\alpha 6\beta 4$  integrin, etc., marking the loss of epithelial like phenotype (Qu et al., 2012). This is in line with our study where we find up regulation of vimentin with downregulation of  $\beta 4$  integrin during TGF- $\beta 1$  induced EMT. This result raises the hypothesis that, during the late stage of tumorigenesis, vimentin is induced in response to EMT, causing depletion of  $\beta 4$  integrin, which in turn, facilitates detachment of cell from basement membrane and promotes migration.

Finally, we wanted to see if our *in vitro* findings corroborate with clinical data. Vimentin overexpression and its correlation to

invasion and metastasis has been shown (Satelli and Li, 2011). Correspondingly, several reports document alterations in the levels of  $\beta 4$  and its effect on the overall outcome of the disease. For example, loss of  $\alpha 6\beta 4$  at the basal layer was seen in cervical cancer (Carico et al., 1993). Similarly, loss of  $\alpha 6\beta 4$  and its corresponding basement membrane component laminin-5 was seen in squamous cell carcinomas (Downer et al., 1993). Interestingly, high vimentin and low  $\beta 4$  expression correlated with the poor survival as compared to other possible combinations of vimentin and  $\beta 4$  expression in our patients. Correlation to node status and poor survival in high vimentin and low  $\beta 4$  samples could be explained on the basis of our *in vitro* findings. Thus, apart from confirming the findings of previous studies, we could also show a hitherto unreported relation between vimentin and  $\beta 4$  integrin.

## 5. Conclusion

Our current study provides insights into the role of vimentin in mediating tumor cell migration by modulation of  $\beta 4$  integrin levels. Further, vimentin and  $\beta 4$  integrin together may be used to predict the biology of oral cancer progression.

## 6. Authors contributions

Conceived and designed the experiments: CD, MMV. Performed the experiments: CD, HA, PG, HD and SB. Analyzed the data: CD, SSS, PG, RT, NR and SK. Contributed reagents/materials/analysis tools: HA, DC, DAC and HP. CD and MMV wrote the manuscript. All authors read and approved the final manuscript.

## 7. Conflict of interest

The authors have declared that they have no potential conflicts of interest.

## Acknowledgments

We thank Professor Robert Goldman (Feinberg School of Medicine, Northwestern University, USA) for his generous gift of the emerald vimentin retroviral construct. We thank Dr. Livio Trusolino (Department of Oncology, University of Torino School of Medicine, Italy) for his generous gift of  $\beta 4$  integrin shRNA and scrambled shRNA construct. We thank following people from ACTREC, TMC, India for their kind help. Dr. Sorab Dalal for his generous gift of pTU6 PURO vector. Pratik Chaudhari for critically reviewing the manuscript. Indrajit Sahu, Shyam More, Manohar Dange for their valuable experimental suggestions. We are thankful to Mrs. Tejaswinin Modak (Online trainer and instructor for English Writing Skills, Centre for e-learning and Training) for english spelling and grammar. This work was supported by grant from Department of Biotechnology (Grant no. 102/IFD/SAN/947). CD was supported by fellowship from ACTREC, TMC.

## Appendix A. Supplementary data

Supplementary data associated with this article can be found, in the online version, at <http://dx.doi.org/10.1016/j.biocel.2015.11.015>.

## References

- Alam, H., Sehgal, L., Kundu, S.T., Dalal, S.N., Vaidya, M.M., 2011. Novel function of keratins 5 and 14 in proliferation and differentiation of stratified epithelial cells. *Mol. Biol. Cell* 22, 4068–4078.
- Biddle, D., Spandau, D.F., 1996. Expression of vimentin in cultured human keratinocytes is associated with cell–extracellular matrix junctions. *Arch. Dermatol. Res.* 288, 621–624.

- Brockbank, E.C., Bridges, J., Marshall, C.J., Sahai, E., 2005. Integrin beta1 is required for the invasive behaviour but not proliferation of squamous cell carcinoma cells *in vivo*. *Br. J. Cancer* 92, 102–112.
- Buisson, A.C., Gilles, C., Polette, M., Zahm, J.M., Birembaut, P., Tournier, J.M., 1996. Wound repair-induced expression of a stromelysins is associated with the acquisition of a mesenchymal phenotype in human respiratory epithelial cells. *Lab. Invest.*; *J. Tech. Methods Pathol.* 74, 658–669.
- Carico, E., French, D., Bucci, B., Falcioni, R., Vecchione, A., Mariani-Costantini, R., 1993. Integrin beta4 expression in the neoplastic progression of cervical epithelium. *Gynecol. Oncol.* 49, 61–66.
- Chaffer, C.L., Brennan, J.P., Slavin, J.L., Blick, T., Thompson, E.W., Williams, E.D., 2006. Mesenchymal-to-epithelial transition facilitates bladder cancer metastasis: role of fibroblast growth factor receptor-2. *Cancer Res.* 66, 11271–11278.
- Cress, A.E., Rabinovitz, I., Zhu, W., Nagle, R.B., 1995. The alpha 6 beta 1 and alpha 6 beta 4 integrins in human prostate cancer progression. *Cancer Metastasis Rev.* 14, 219–228.
- Dange, M.C., Agarwal, A.K., Kalraiy, R.D., 2015. Extracellular galectin-3 induces MMP9 expression by activating p38 MAPK pathway via lysosome-associated membrane protein-1 (LAMP1). *Mol. Cell. Biochem.* 404, 79–86.
- Downer, C.S., Watt, F.M., Speight, P.M., 1993. Loss of alpha 6 and beta 4 integrin subunits coincides with loss of basement membrane components in oral squamous cell carcinomas. *J. Pathol.* 171, 183–190.
- Dozynkiewicz, M.A., Jamieson, N.B., Macpherson, I., Grindlay, J., van den Berghe, P.V., von Thun, A., et al., 2012. Rab25 and CLIC3 collaborate to promote integrin recycling from late endosomes/lysosomes and drive cancer progression. *Dev. Cell* 22, 131–145.
- Egles, C., Huet, H.A., Dogan, F., Cho, S., Dong, S., Smith, A., et al., 2010. Integrin-blocking antibodies delay keratinocyte re-epithelialization in a human three-dimensional wound healing model. *PLoS One* 5, e10528.
- Giancotti, F.G., Stepp, M.A., Suzuki, S., Engvall, E., Ruoslahti, E., 1992. Proteolytic processing of endogenous and recombinant beta 4 integrin subunit. *J. Cell Biol.* 118, 951–959.
- Gilles, C., Polette, M., Zahm, J.M., Tournier, J.M., Volders, L., Foidart, J.M., et al., 1999. Vimentin contributes to human mammary epithelial cell migration. *J. Cell Sci.* 112 (Pt 24), 4615–4625.
- Helfand, B.T., Mendez, M.G., Murthy, S.N., Shumaker, D.K., Grin, B., Mohammad, S., et al., 2011. Vimentin organization modulates the formation of lamellipodia. *Mol. Biol. Cell* 22, 1274–1289.
- Homan, S.M., Martinez, R., Benware, A., LaFlamme, S.E., 2002. Regulation of the association of alpha 6 beta 4 with vimentin intermediate filaments in endothelial cells. *Exp. Cell Res.* 281, 107–114.
- Ivaska, J., 2011. Vimentin: central hub in EMT induction? *Small GTPases* 2, 51–53.
- Ivaska, J., Vuoriluoto, K., Huovinen, T., Izawa, I., Inagaki, M., Parker, P.J., 2005. PKCepsilon-mediated phosphorylation of vimentin controls integrin recycling and motility. *EMBO J.* 24, 3834–3845.
- Iyer, S.V., Dange, P.P., Alam, H., Sawant, S.S., Ingle, A.D., Borges, A.M., et al., 2013. Understanding the role of keratins 8 and 18 in neoplastic potential of breast cancer derived cell lines. *PLoS One* 8, e53532.
- Kalluri, R., Weinberg, R.A., 2009. The basics of epithelial-mesenchymal transition. *J. Clin. Invest.* 119, 1420–1428.
- Katada, K., Tomonaga, T., Satoh, M., Matsushita, K., Tonoike, Y., Koder, Y., et al., 2012. Plectin promotes migration and invasion of cancer cells and is a novel prognostic marker for head and neck squamous cell carcinoma. *J. Proteom.* 75, 1803–1815.
- Kim, H., McCulloch, C.A., 2011. Filamin A mediates interactions between cytoskeletal proteins that control cell adhesion. *FEBS Lett.* 585, 18–22.
- Kim, H., Nakamura, F., Lee, W., Hong, C., Perez-Sala, D., McCulloch, C.A., 2010. Regulation of cell adhesion to collagen via beta1 integrins is dependent on interactions of filamin A with vimentin and protein kinase C epsilon. *Exp. Cell Res.* 316, 1829–1844.
- Kippenberger, S., Hofmann, M., Zoller, N., Thaci, D., Muller, J., Kaufmann, R., et al., 2010. Ligation of beta4 integrins activates PKB/Akt and ERK1/2 by distinct pathways-relevance of the keratin filament. *Biochim. Biophys. Acta* 1803, 940–950.
- Kippenberger, S., Loitsch, S., Muller, J., Guschel, M., Kaufmann, R., Bernd, A., 2004. Ligation of the beta4 integrin triggers adhesion behavior of human keratinocytes by an “inside-out” mechanism. *J. Invest. Dermatol.* 123, 444–451.
- Kundu, S.T., Gosavi, P., Khapare, N., Patel, R., Hosing, A.S., Maru, G.B., et al., 2008. Plakophilin3 downregulation leads to a decrease in cell adhesion and promotes metastasis. *Int. J. Cancer J. Int. Cancer* 123, 2303–2314.
- Langa, F., Kress, C., Colucci-Guyon, E., Khun, H., Vandormael-Pourmin, S., Huerre, M., et al., 2000. Teratocarcinomas induced by embryonic stem (ES) cells lacking vimentin: an approach to study the role of vimentin in tumorigenesis. *J. Cell Sci.* 113 (Pt 19), 3463–3472.
- Lazarides, E., 1982. Intermediate filaments: a chemically heterogeneous, developmentally regulated class of proteins. *Annu. Rev. Biochem.* 51, 219–250.
- Lin, G.L., Cohen, D.M., Desai, R.A., Breckenridge, M.T., Gao, L., Humphries, M.J., et al., 2013. Activation of beta 1 but not beta 3 integrin increases cell traction forces. *FEBS Lett.* 587, 763–769.
- Lo, A.K., Yuen, P.W., Liu, Y., Wang, X.H., Cheung, A.L., Wong, Y.C., et al., 2001. Downregulation of hemidesmosomal proteins in nasopharyngeal carcinoma cells. *Cancer Lett.* 163, 117–123.
- McLean, W.H., Pulkkinen, L., Smith, F.J., Rugg, E.L., Lane, E.B., Bullrich, F., et al., 1996. Loss of plectin causes epidermolysis bullosa with muscular dystrophy: cDNA cloning and genomic organization. *Genes Dev.* 10, 1724–1735.
- Mercurio, A.M., Rabinovitz, I., Shaw, L.M., 2001. The alpha 6 beta 4 integrin and epithelial cell migration. *Curr. Opin. Cell Biol.* 13, 541–545.
- Michelson, A., De Luca, N., Tadini, G., Zambruno, G., D'Alessio, M., 2004. Intracellular degradation of beta4 integrin in lethal junctional epidermolysis bullosa with pyloric atresia. *Br. J. Dermatol.* 151, 796–802.
- Nieminen, M., Henttinen, T., Merinen, M., Marttila-Ichihara, F., Eriksson, J.E., Jalkanen, S., 2006. Vimentin function in lymphocyte adhesion and transcellular migration. *Nat. Cell Biol.* 8, 156–162.
- Paccione, R.J., Miyazaki, H., Patel, V., Waseem, A., Gutkind, J.S., Zehner, Z.E., et al., 2008. Keratin down-regulation in vimentin-positive cancer cells is reversible by vimentin RNA interference, which inhibits growth and motility. *Mol. Cancer Ther.* 7, 2894–2903.
- Pal-Ghosh, S., Blanco, T., Tadvalkar, G., Pajoohesh-Ganji, A., Parthasarathy, A., Zieske, J.D., et al., 2011. MMP9 cleavage of the beta4 integrin ectodomain leads to recurrent epithelial erosions in mice. *J. Cell Sci.* 124, 2666–2675.
- Partridge, J., Flaherty, P., 2009. An *in vitro* FluoroBlok tumor invasion assay. *J. Vis. Exp.* 29, <http://dx.doi.org/10.3791/1475>, e1475.
- Qu, H., Wen, T., Pesch, M., Aumailley, M., 2012. Partial loss of epithelial phenotype in kindlin-1-deficient keratinocytes. *Am. J. Pathol.* 180, 1581–1592.
- Raul, U., Sawant, S., Dange, P., Kalraiy, R., Ingle, A., Vaidya, M., 2004. Implications of cyokeratin 8/18 filament formation in stratified epithelial cells: induction of transformed phenotype. *Int. J. Cancer J. Int. Cancer* 111, 662–668.
- Reznicek, G.A., de Pereda, J.M., Reipert, S., Wiche, G., 1998. Linking integrin alpha6beta4-based cell adhesion to the intermediate filament cytoskeleton: direct interaction between the beta4 subunit and plectin at multiple molecular sites. *J. Cell Biol.* 141, 209–225.
- Satelli, A., Li, S., 2011. Vimentin in cancer and its potential as a molecular target for cancer therapy. *Cell. Mol. Life Sci.* CMLS 68, 3033–3046.
- Sawant, S., Vaidya, M., Chaukar, D., Alam, H., Dmello, C., Gangadharan, P., et al., 2014. Clinical significance of aberrant vimentin expression in oral premalignant lesions and carcinomas. *Oral Dis.* 20, 453–465.
- Srikanth, B., Vaidya, M.M., Kalraiy, R.D., 2010. O-GlcNAcylation determines the solubility, filament organization, and stability of keratins 8 and 18. *J. Biol. Chem.* 285, 34062–34071.
- Styers, M.L., Salazar, G., Love, R., Peden, A.A., Kowalczyk, A.P., Faundez, V., 2004. The endo-lysosomal sorting machinery interacts with the intermediate filament cytoskeleton. *Mol. Biol. Cell* 15, 5369–5382.
- Tapscott, S.J., Bennett, G.S., Toyama, Y., Kleinbart, F., Holtzer, H., 1981. Intermediate filament proteins in the developing chick spinal cord. *Dev. Biol.* 86, 40–54.
- Tennenbaum, T., Yuspa, S.H., Grover, A., Castronovo, V., Sobel, M.E., Yamada, Y., et al., 1992. Extracellular matrix receptors and mouse skin carcinogenesis: altered expression linked to appearance of early markers of tumor progression. *Cancer Res.* 52, 2966–2976.
- Vuoriluoto, K., Haugen, H., Kiviluoto, S., Mpindi, J.P., Nevo, J., Gjerdrum, C., et al., 2011. Vimentin regulates EMT induction by Slug and oncogenic H-Ras and migration by governing Axl expression in breast cancer. *Oncogene* 30, 1436–1448.
- Walko, G., Vukasinovic, N., Gross, K., Fischer, I., Sibitz, S., Fuchs, P., et al., 2011. Targeted proteolysis of plectin isoform 1a accounts for hemidesmosome dysfunction in mice mimicking the dominant skin blistering disease EBS-Ogna. *PLoS Genet.* 7, e1002396.
- Witkowski, C.M., Bowden, G.T., Nagle, R.B., Cress, A.E., 2000. Altered surface expression and increased turnover of the alpha6beta4 integrin in an undifferentiated carcinoma. *Carcinogenesis* 21, 325–330.
- Yamashita, S., Okada, Y., 2014. Heat-induced antigen retrieval in conventionally processed EPON-embedded specimens: procedures and mechanisms. *J. Histochem. Cytochem.: Off. J. Histochem. Soc.* 62, 584–597.

RESEARCH ARTICLE

# Vimentin regulates differentiation switch via modulation of keratin 14 levels and their expression together correlates with poor prognosis in oral cancer patients

Crismita Dmello<sup>1,2</sup>, Sharada Sawant<sup>1,2</sup>, Hunain Alam<sup>1<sup>aa</sup></sup>, Prakash Gangadaran<sup>1<sup>ab</sup></sup>, Saie Mogre<sup>1</sup>, Richa Tiwari<sup>1,2</sup>, Zinia D'Souza<sup>1</sup>, Manish Narkar<sup>1</sup>, Rahul Thorat<sup>1</sup>, Komal Patil<sup>1</sup>, Devendra Chaukar<sup>2,3</sup>, Shubhada Kane<sup>2,4</sup>, Milind Vaidya<sup>1,2\*</sup>

**1** Cancer Research Institute (CRI), Advanced Centre for Treatment, Research and Education in Cancer (ACTREC), Tata Memorial Centre (TMC), Kharghar, Navi Mumbai, India, **2** Homi Bhabha National Institute, Training school complex, Anushakti Nagar, Mumbai, India, **3** Surgical Oncology, Head and Neck Unit, Tata Memorial Hospital (TMH), Parel, Mumbai, India, **4** Department of Pathology, Tata Memorial Hospital (TMH), Parel, Mumbai, India

<sup>aa</sup> Current address: Department of Molecular and Cellular Oncology, MD Anderson Cancer Centre, University of Texas, Houston, Texas, United States of America

<sup>ab</sup> Current address: Department of Nuclear Medicine, Kyunpook National University school of Medicine, N101, Dongin-Dong, Jung-Gu, Daegu, Republic of Korea

\* [mvoidya@actrec.gov.in](mailto:mvoidya@actrec.gov.in)



**OPEN ACCESS**

**Citation:** Dmello C, Sawant S, Alam H, Gangadaran P, Mogre S, Tiwari R, et al. (2017) Vimentin regulates differentiation switch via modulation of keratin 14 levels and their expression together correlates with poor prognosis in oral cancer patients. PLoS ONE 12(2): e0172559. doi:10.1371/journal.pone.0172559

**Editor:** Pavel Strnad, Medizinische Fakultät der RWTH Aachen, GERMANY

**Received:** September 7, 2016

**Accepted:** February 7, 2017

**Published:** February 22, 2017

**Copyright:** © 2017 Dmello et al. This is an open access article distributed under the terms of the [Creative Commons Attribution License](https://creativecommons.org/licenses/by/4.0/), which permits unrestricted use, distribution, and reproduction in any medium, provided the original author and source are credited.

**Data Availability Statement:** All relevant data are within the paper and its Supporting Information files.

**Funding:** Support was provided by the Department of Biotechnology, grant number: 102/IFD/SAN/947 [<http://www.dbtindia.nic.in/>] to SS. The funders had no role in study design, data collection and analysis, decision to publish, or preparation of the manuscript.

## Abstract

Vimentin is an intermediate filament protein, predominantly expressed in cells of mesenchymal origin, although its aberrant expression is seen in many carcinomas during epithelial mesenchymal transition. In cancer, vimentin expression is associated with the transition from a more differentiated epithelial phenotype to a dedifferentiated state. In view of the perceived role of keratins (Ks) as regulators of differentiation in epithelia, it was important to understand whether vimentin modulates differentiation through the reprogramming of keratins, in transformed cells. To address this, vimentin was stably downregulated in oral cancer derived cells. Further, global keratin profiling was performed after high salt keratin extraction. K5/K14 pair was found to be significantly downregulated, both at protein and mRNA levels upon vimentin downregulation. The previous study from our laboratory has shown a role of the K5/K14 pair in proliferation and differentiation of squamous epithelial cells. Vimentin depleted cells showed an increase in the differentiation state, marked by an increase in the levels of differentiation specific markers K1, involucrin, filaggrin and loricrin while its proliferation status remained unchanged. Rescue experiments with the K5/K14 pair overexpressed in vimentin knockdown background resulted in decreased differentiation state. ΔNp63 emerged as one of the indirect targets of vimentin, through which it modulates the expression levels of K5/K14. Further, immunohistochemistry showed a significant correlation between high vimentin-K14 expression and recurrence/poor survival in oral cancer patients. Thus, in conclusion, vimentin regulates the differentiation switch via modulation of K5/K14 expression. Moreover, vimentin-K14 together may prove to be the novel markers for the prognostication of human oral cancer.

**Competing interests:** The authors have declared that no competing interests exist.

## Introduction

Vimentin is normally a mesenchymal-specific, type III intermediate filament (IF) protein. Traditionally, vimentin has been known to maintain cellular integrity and provide resistance to stress [1]. Studies on mouse embryos have shown that, during embryogenesis, synthesis of vimentin takes place for the first time exclusively in the primary mesenchymal cells at the primitive streak stage [2]. Moreover, vimentin is replaced partially or completely with their cell type specific IF protein in the terminally differentiating neuroepithelial cells [3]. Also, transgenic mice overexpressing the vimentin gene showed an inhibition in the normal differentiation of lens fibers [4]. Even in the liver development, expression of vimentin is associated with an undifferentiated status of liver cells [5]. Consistent with this, vimentin has been shown to impede osteoblast terminal differentiation by inhibiting the transactivation function of activating transcription factor 4 (ATF4) [6]. Furthermore, vimentin expression was found to correlate well with the poorly-differentiated and fibroblastic phenotype of breast cancer cell lines [7]. The above evidence suggests the ability of vimentin to retain dedifferentiation, most likely by restricting differentiation.

Vimentin expression has recently gained importance from the point of view of identifying the mesenchymal origin of a cell, as a prognostic marker to predict the biology of the tumor and to detect micro-metastasis [8]. Overexpression of vimentin is seen in various carcinomas like prostate, gastrointestinal, breast, lung and also melanomas [9]. Our laboratory along with others has shown a correlation of aberrant vimentin expression with lymph node metastasis, recurrence and also poor survival [10–12]. Vimentin is now being perceived not only as a canonical marker but also as a driver of epithelial–mesenchymal transition (EMT) [8]. During the process of EMT, the cell acquires a characteristic flattened morphology (mesenchymal-like) due to loss of cell-cell and cell-substrate contact. At the same time, there is a dramatic reprogramming of epithelia-specific keratins, to initiate the expression of mesenchyme-specific protein vimentin [13]. Such a change in keratin composition, associated with a reduction in the degree of differentiation, is also seen during an injury (inflammation/atrophy) wherein a cell starts expressing more than two keratins/IF proteins, e.g. K7, K17, K19, vimentin etc. [14]. Recent evidence of cytoskeletal remodeling was seen in the case of mouse embryonic fibroblasts, in the course of transition between progenitor and differentiated states [15]. Due to tissue and differentiation state-specific expression of keratins, many of them have found wide utility in clinics as diagnostic markers especially in tumor pathology. Expression patterns of K5, K6, K14, K17, etc. have been shown to positively correlate with the dedifferentiated and metastatic nature of squamous cell carcinomas [16]. Our group has shown aberrant expression of K8/K18 and its functional/molecular role in the progression of oral squamous cell carcinoma (OSCC) [17, 18].

Previous work from our laboratory has shown the contribution of K5/K14 pair in the maintenance of a proliferative and dedifferentiated state of the tongue squamous cell carcinoma (SCC) derived cell line AW13516 [19]. In the current study, we found a reduction in the expression of K5/K14 pair upon vimentin downregulation, perhaps mediated through  $\Delta$ Np63, resulting in a more differentiated phenotype of the tumor cell. Thus, this study depicts the modulatory role of vimentin to fine tune the differentiation switch to favor tumor progression.

## Materials and methods

### Ethics statement

This study was approved by the “Human Ethics Committee”, Tata memorial centre, India (Reg Number: DCGI: ECR/149/Inst/MH/2013) and the written “informed consent” was

obtained from all the patients before enrolling them in this study. All protocols for animal studies were reviewed and approved by the “Institutional Animal Ethics Committee (IAEC)” constituted under the guidelines of the “Committee for the Purpose of Control and Supervision of Experiments on Animals (CPCSEA)”, Government of India (Approval ID: 19/2014).

## Housing and monitoring of experimental animals

NOD-SCID mice used in the present study were procured from Charles River Laboratory UK Ltd. Mice were maintained under strict specific pathogen-free (SPF) conditions and all animals used for this study were healthy. Animals were housed in Individually Ventilated Caging system (M/S Citizen Industries, Ahmedabad, Gujrat, India) and provided with commercially available corn cob bedding material from ATNT Laboratories, Mumbai MS, India. Overall dimensions of the IVC cage are L 369 mm x W 156 mm x H 182 mm; cage floor area is 360 cm<sup>2</sup>. The animals were housed in a controlled environment under 23±2°C, 40–70% relative humidity and the dark-light cycle of 12 h each. The animals received sterile water *ad libitum* and autoclaved balanced diet prepared in-house from natural ingredients like wheat, roasted Bengal gram, casein, milk powder, ground nut oil, vitamins and mineral supplements which provide approximately 21% crude protein. As a quality control program, CD4, CD8 and CD19 status of NOD-SCID animals are checked, using flow cytometry. This is performed twice a year with randomly selected animals from the expansion colony. Periodically, the microbiological and clinico-pathological status of animals is also tested. Prior to the injection of tumor cells, no anesthetics or analgesics were given to the animals, in order to alleviate momentary pain. Also, the animals were not euthanized prior to the injection of tumor cells. During the injections, the mice were handled by a trained, certified animal technician and the cells were injected into the dorsal flank region by the in-house attending veterinarian (FELASA certified), ensuring minimum distress. After 42–52 days post injection, the animals were sacrificed so that the mean tumor diameter did not exceed 1.2 cm, as described in the AAALAC guidelines for animal welfare in cancer research [20]. Animal injury/illness or mortality was not seen during the course of this study. Every investigator follows the institute’s protocol (displayed on the institute’s intranet) to set humane endpoints prior to the sanction by the IAEC. For euthanasia, the mice were kept in a chamber (which was vented out before the next euthanasia) for 2’–3’ and then CO<sub>2</sub> was introduced from the cylinder supply valve into the chamber at an optimal flow rate of 20% of the chamber volume. After verifying the cessation of respiration and heart beats, cervical dislocation was performed by skilled personnel to confirm the death.

## Cell lines, antibodies and reagents

The establishment and characterization details of AW13516, AW8507 [21], DOK [22], HaCat [23] and A431 [24] are as described previously. Lists of cell lines, antibodies and reagents with their particulars are given in the S1–S3 Tables respectively.

## Plasmids and retroviral constructs

The details of the generation of vimentin knockdown and vector control clones are as described previously [25]. For vimentin overexpression, emerald GFP-vimentin retroviral construct (a kind gift from Professor Robert Goldman) was used. Emerald GFP-K14 construct was generated by amplifying K14 gene sequence from K14-pEGFP-N3 construct and subcloned into emerald GFP-pQCXIP vector using the single BamHI site. Firstly, emerald GFP-K14 was overexpressed in vimentin knockdown background shvim2 and the positive clones were sorted using FACSaria based on the GFP fluorescence. Next, the K14 positive clones were used to transduce K5 pLNCX2 retroviral construct (a kind gift from Professor Thomas Magin) and the positive clones were

selected using G418 sulphate (400 $\mu$ g/ml). The empty vector backbone of both the constructs was used to generate the vector control clones. For the cloning of  $\Delta$ Np63 $\alpha$ , its cDNA was prepared from HaCat cell line and was cloned into the pLNCX2 vector containing N-terminal flag tag sequence using HindIII and Sall restriction enzyme sites. Flag- $\Delta$ Np63 $\alpha$  containing retroviral construct was then transduced into vimentin knockdown clone shvim2 and positive clones were selected using G418 sulphate (400 $\mu$ g/ml). The empty flag pLNCX2 vector backbone served as a vector control.

### Quantitative Real-Time PCR (qRT-PCR) and Reverse Transcriptase PCR (RT-PCR)

RNA was isolated with the TRI reagent and cDNA was prepared using Revert Aid First Strand cDNA synthesis Kit according to the manufacturer's protocol. qRT-PCR and RT-PCR were performed as described previously [26]. The list of qRT-PCR and RT-PCR primer sequences is given in the [S4 Table](#). Primer sequences used for the detection of  $\Delta$ Np63 isoforms were adapted from a report by Sniezek et al. [27].

### Western blotting, high salt keratin extraction, two-dimensional (2D) gel electrophoresis and mass spectroscopy

Western blotting was performed as described previously [17]. Briefly, whole-cell lysates were prepared in SDS lysis buffer (62.5 mM Tris (pH 6.8), 2% SDS, 0.1% BME ( $\beta$ -Mercaptoethanol) and 10% glycerol). A protease inhibitor cocktail was added to the lysis buffer. An equal amount of protein was loaded and resolved on SDS-PAGE gels followed by western blotting. Keratin enrichment was done using a high salt extraction protocol described previously [28]. This high salt keratin-rich fraction was subjected to 2D gel electrophoresis using IPG strips (pH 3–10). The gel was then stained with coomassie brilliant blue and differentially expressed spots were excised and processed for matrix-assisted laser desorption ionization (MALDI) analysis as previously described [18].

### Preparation of cytoplasmic and nuclear fractions

The cytoplasmic fraction was separated using 1X hypotonic cell lysis buffer (along with protease and phosphatase inhibitors). The hypotonic cell lysis buffer was prepared as per the composition given in the manual of CelLytic NuCLEAR Extraction Kit (Sigma, product code NXTRACT). The cytoplasmic fraction was separated and the nuclear pellet was resuspended in SDS lysis buffer, vortexed, boiled for 5' and centrifuged at 13,000 rpm for 20'. The supernatant obtained was used as the nuclear fraction.

### Immunofluorescence

For immunofluorescence, cells were grown on coverslips for 48 h and treated with 0.03% Triton X-100 in chilled methanol for 90 seconds. Permeabilized cells were then fixed in chilled methanol for 10' at -20°C. Further, the procedure followed is as described previously [17]. All confocal images were acquired using Zeiss LSM 780 microscope.

### Cell proliferation and clonogenic assays

Cell proliferation using MTT (3-(4,5-dimethylthiazol-2-yl)-2,5-diphenyltetrazolium bromide) assay was performed as per the previously described protocol [19]. Accordingly, 1000 Cells were seeded per well in triplicates and monitored over a period of 4 days. The absorbance of the well was considered as a measure of cell density to study the proliferation capacity of the

clones. For the clonogenic assay, 200 cells of each clone were seeded in 60mm dishes and monitored for 10 days till visible colonies were formed. The colonies were then fixed in methanol for 5' and stained with 0.5% crystal violet (prepared in 20% methanol) for 5'.

### Tumorigenicity assays

The tumorigenic potential of vimentin knockdown/vector control and K5/K14 overexpressing/vector control clones was determined by subcutaneous injection into NOD-SCID mice. Six mice were injected per clone ( $6 \times 10^6$  cells each) and were observed for tumor formation over a period of approximately two months. Tumor dimensions were determined using a vernier caliper and its volume was calculated according to the modified ellipsoidal formula, [Tumor volume =  $1/2(\text{length} \times \text{width}^2)$ ] [29].

### Immunohistochemistry (IHC) and statistical analysis

IHC was performed on the OSCC tissue samples (48 SCCs of the tongue and 52 SCCs of the buccal mucosa) collected from the operation theatre of Tata Memorial Hospital, India. IHC analysis was also performed on mice tumor tissues that originated from vimentin knockdown-vector control and K5/K14 overexpressing-vector control groups. Statistical analysis was carried out as described previously [26]. A *p* value less than 0.05 was considered statistically significant. The clinico-pathological data and mice tumor volumes were analyzed using Statistical Package, SPSS 16.0 and SPSS 21.0 respectively.

## Results

### Downregulation of vimentin results in an alteration in the keratin profile of the OSCC derived cell line AW13516

Expression of vimentin is strongly associated with the characteristic phenotype of the cells undergoing EMT. Hence, we hypothesized that vimentin may not only be a marker but also a molecular regulator involved in reprogramming the expression of keratins to transit from a differentiated to a more dedifferentiated state (Fig 1A). In order to test this hypothesis, we used vimentin knockdown clones generated in the OSCC derived cell line AW13516 [25]. Downregulation of vimentin was confirmed by immunofluorescence and western blotting analysis (Fig 1B and 1C) and (S1 Fig). To identify differentially regulated keratins, high salt keratin extraction followed by 2D and MALDI analysis was performed using vimentin knockdown and vector control clones. K8 was used as the loading control for high salt extracted fractions since its levels did not alter upon vimentin downregulation (Fig 1D–1F) and (S1 Fig). The global keratin profile revealed the identity of differentially expressed proteins across the clones, one among which was found to be K14, along with the known differentially expressed protein, vimentin (Table 1). The appearance of actin (though it is easily soluble in mild buffers) in the high-salt extracted fraction could be attributed to its high abundance in the cell. Downregulation of K14 at the protein level was confirmed by western blotting and immunofluorescence analysis. Interestingly, transcript level analysis showed decreased expression of K14 at the mRNA level itself (Fig 2A–2C and S2 Fig). Furthermore, the binding partner of K14, which is K5, was also found to be downregulated both at the protein and mRNA level in vimentin knockdown clones (Fig 2D–2F and S2 Fig). This suggests that vimentin may modulate the expression of K5/K14 by unknown mechanism/s. However, since the downregulation of K5/K14 pair was at the transcript level itself, the possibility of altered solubility was excluded. The levels of K17 and K18 remained unchanged between the clones, as determined using western blot analysis, which validated the 2D gel observations (Fig 2G and 2H and S2 Fig). Hereafter, for all the experiments,

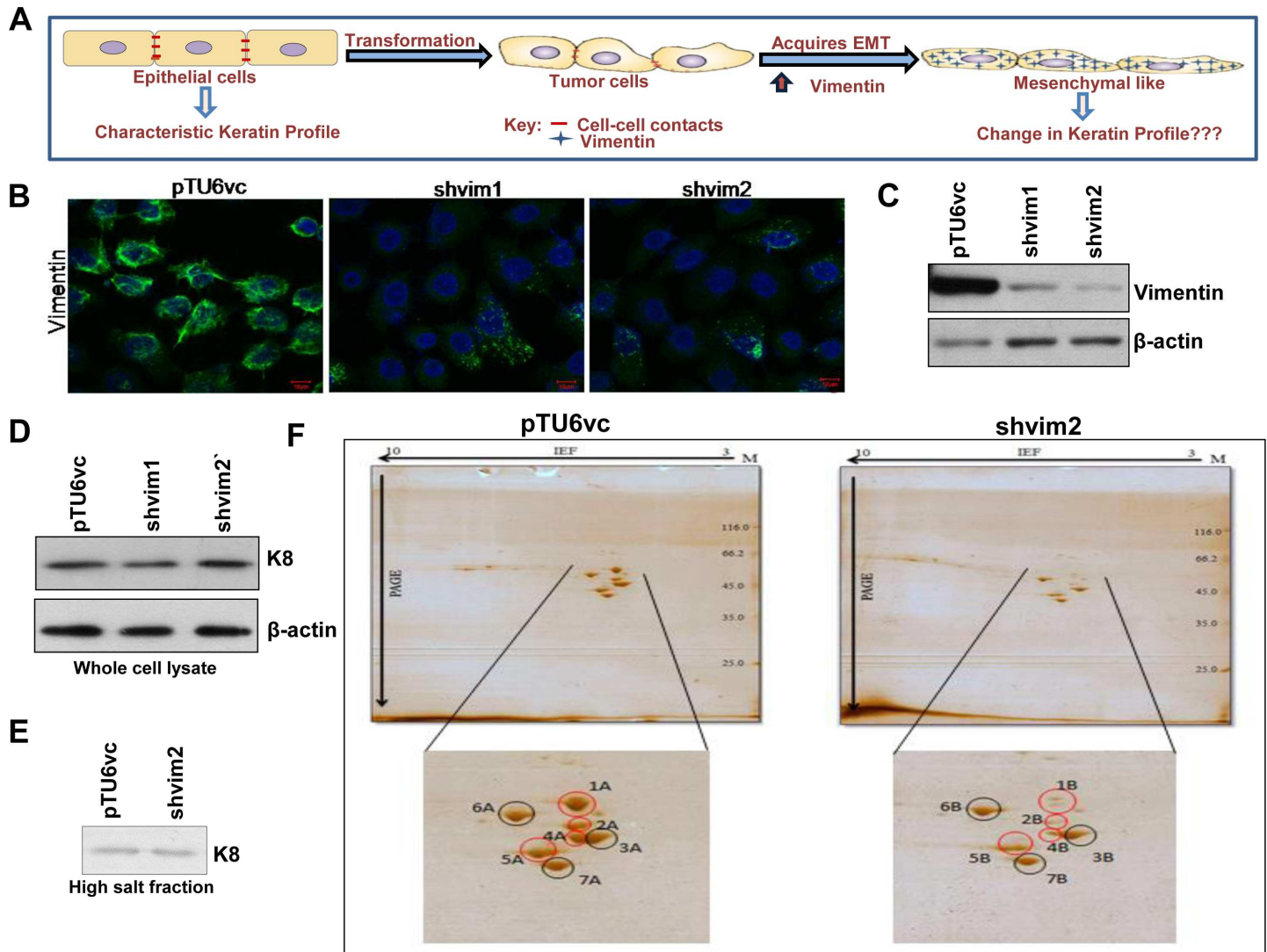


**Fig 1. Downregulation of vimentin resulted in a change in the global keratin profile of the oral SCC derived cell line AW13516.** (A) Schematic representation of the hypothesis. As a tumor cell acquires EMT (marked by upregulation of vimentin), it undergoes transition from a more epithelial-like to a more mesenchymal-like dedifferentiated state. To achieve this transition, there could be a vimentin mediated reprogramming of the keratins which distinguish these states. (B and C) Immunofluorescence (Bar: 10  $\mu$ m) and western blot analysis of vimentin knockdown (shvim1 and shvim2) and its vector control clone (pTU6vc) using an antibody against vimentin.  $\beta$ -actin was used as the loading control in the western blotting experiment. (D) K8 levels of vimentin knockdown and its vector control clones were analyzed using western blotting.  $\beta$ -actin was used as a loading control. (E) The expression of K8 does not change upon vimentin downregulation. Thus, K8 was used as the loading control for high salt keratin enriched fraction. (F) Representative images of the 2D-gel, which show changes in keratin expression in the high salt keratin enriched fractions of vimentin knockdown and its vector control clones. The black circles indicate similarly expressed while the red circles indicate differentially expressed proteins. All the experiments were repeated independently in triplicates. For all the western blot experiments, the numbers below each blot represent the relative intensity of the bands determined using densitometry.

doi:10.1371/journal.pone.0172559.g001

vimentin knockdown clone shvim2 was used, which showed a higher degree of vimentin down-regulation as compared to shvim1.

### Vimentin modulates the differentiation status and tumorigenic potential of epithelial cells

The K5/K14 expression is a typical feature of progenitor basal stem cells of stratified epithelial origin. Also, a previous report from our laboratory has shown direct evidence wherein the

**Table 1. List of proteins identified using MALDI analysis.**

Spot	Protein	Mass	pI	Score	Matched Peptides	Total Peptides	Protein Sequence Coverage	Expression status of proteins in vimentin knockdown as compared to vector control clone	
1A	VIME_HUMAN (Vimentin, OS = Homo sapiens)	53676	4.9	74	8	39	23.6%	Downregulated	
2A	Keratin 14	51872	5.09	52	10	50	23%	Downregulated	
3B	K1C17_HUMAN (Keratin Type 1, Cytoskeletal 17, OS = Homo sapiens)	48361	4.8	156	15	26	50.9%	Unchanged	
4A	Unidentified							Downregulated	
5A	K1C18_HUMAN (Keratin, Type I Cytoskeletal 18 OS = Homo sapiens)	48029	5.2	76	17	60	51.4%	Unchanged	
6A	K2C8_HUMAN (Keratin Type 2, Cytoskeletal 8, OS = Homo sapiens)	53671	Predicted as K8 but with low score						Unchanged
7A	ACTB_HUMAN (Actin, Cytoplasmic 1 and 2, OS = Homo sapiens)	42052	5.2	75	7	57	38.9%	Unchanged	

MALDI analysis: The resulting data of the keratin spots was analyzed using Flex analysis 3.0 (BruckerDaltonik, Germany) software. The peak list was searched against SwissProt database using MASCOT search engine. The last column shows the expression status of proteins in vimentin knockdown as compared to its vector control clone after validating the spots identified by MALDI, with western blotting.

doi:10.1371/journal.pone.0172559.t001

K5/K14 pair is able to regulate cell proliferation, differentiation and neoplastic progression in the same system AW13516 [19]. Surprisingly, MTT assay did not show any obvious difference in the proliferation potential of vimentin knockdown as compared to its vector control cells (Fig 3A). In addition, we performed a clonogenic assay on vimentin knockdown and vector control clones. Again, no significant difference was seen in the number and size of colonies between the clones which correlated with their similar proliferation rates (Fig 3B). Further staining with cell proliferation markers, proliferating cell nuclear antigen (PCNA) and Ki67 confirmed our results (S3A and S3B Fig). However, during epithelial stratification, as a basal cell gets committed to differentiation, it loses the expression of K5/K14 pair and starts expressing involucrin, filaggrin, loricrin and differentiation specific keratins in the upper layers [30]. Vimentin downregulation led to an increased expression of K1, involucrin, filaggrin and loricrin respectively (Fig 3C) and involucrin protein levels (S4 Fig) as determined using qRT-PCR and western blotting. However, transcript levels of multipotent stem cell marker Oct-4 (S5 Fig) decreased significantly. Further, to assess the tumorigenic role of vimentin, vimentin knockdown and vector control cells were injected subcutaneously into NOD-SCID mice (Fig 3D). A significant reduction was observed in the tumor volume in vimentin knockdown as compared its vector control group (Fig 3E). Furthermore, IHC analysis confirmed the decrease in the expression of K5/K14 (Fig 3F) and increase in the expression of involucrin (S6 Fig) in tumors formed in mice from vimentin knockdown cells. Moreover, expression of PCNA did not show any difference among the two groups (S6 Fig). Collectively, these results suggest that vimentin is involved in maintaining a more dedifferentiated state of the cancer cell, perhaps through modulation of K5/K14 expression.

### Vimentin positively regulates the expression of K5/K14 pair across different stratified epithelial-derived cell lines

To verify whether the regulation of K5/K14 expression by vimentin is not a cell line specific phenomenon or an off-target effect of the shRNA associated vimentin downregulation, it was overexpressed in vimentin lacking, A431 and HaCaT cell lines. Vimentin upregulation in A431 cells led to a concomitant increase in the levels of K5, but a marked decrease was seen in

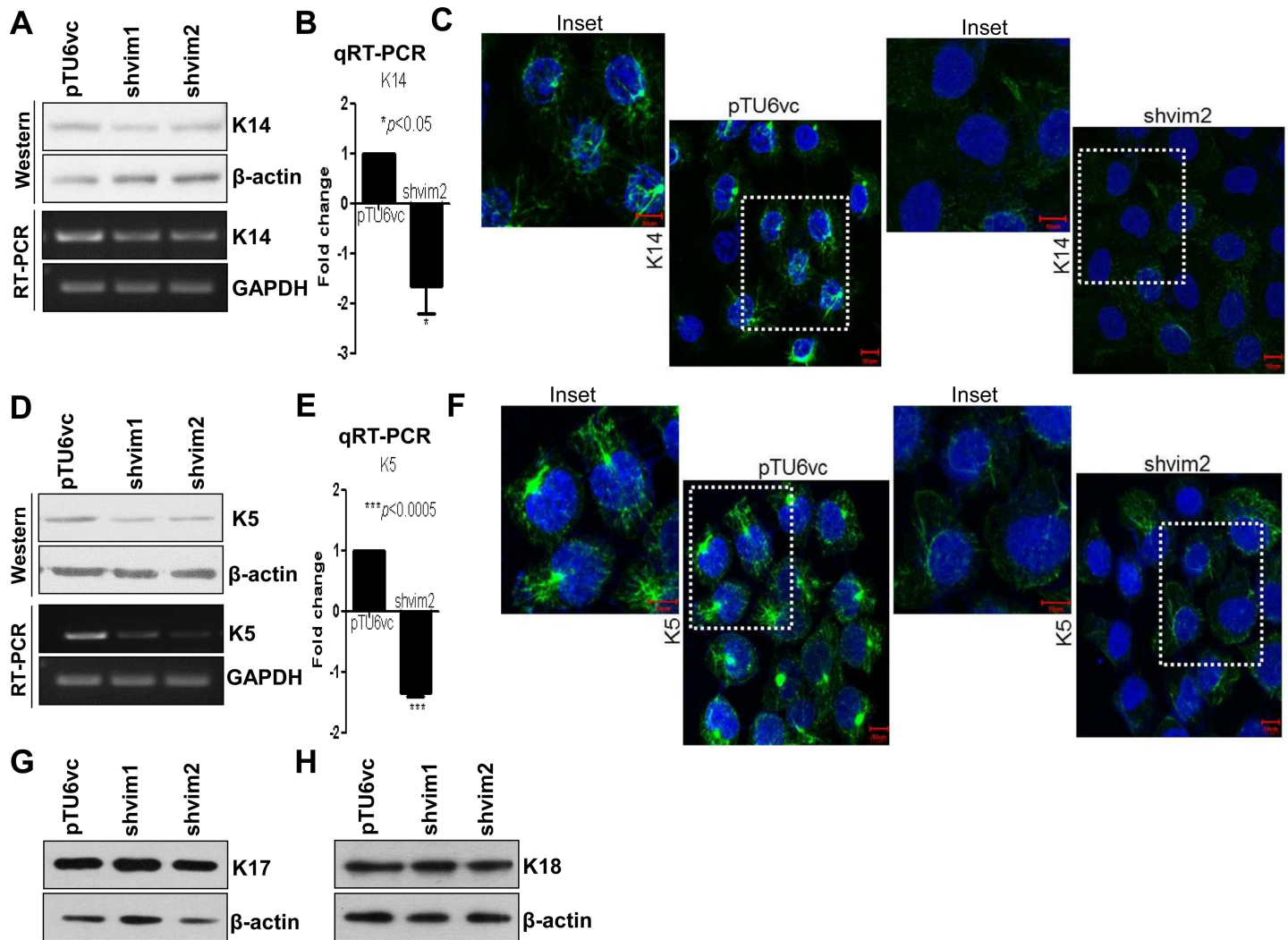


**Fig 2. Vimentin knockdown cells show downregulation of both K5 and K14 at the mRNA as well as protein level.** (A and B) Western blot, RT-PCR and qRT-PCR respectively of K14, in vimentin knockdown and vector control clones. (C) Immunofluorescence analysis (Bar: 10  $\mu$ m) of the K14 levels in the indicated clones. Insets display magnification of the K14 filaments (in the adjacent figure of the one marked by the dotted white boxes). (D and E) Western blot, RT-PCR and qRT-PCR respectively of K5, in vimentin knockdown and vector control clones. (F) Immunofluorescence analysis (Bar: 10  $\mu$ m) of the K5 levels in the indicated clones. Insets display magnification of the K5 filaments (in the adjacent figure of the one marked by the dotted white boxes). (G and H) Western blot analysis demonstrates unchanged levels of K17 and K18 in vimentin knockdown as compared to vector control clones.  $\beta$ -actin was used as the loading control in all the western blotting experiments. GAPDH was used as the loading control in RT-PCR. For qRT-PCR experiments; the relative expression of the target genes was normalized to GAPDH. The graphical data represents  $\pm$  standard error mean (SEM) of three independent experiments.

doi:10.1371/journal.pone.0172559.g002

the levels of differentiation specific protein, involucrin [31]. However, since A431 cells do not express K14, we checked for the levels of K17, considering the fact that K17 is known to pair with K5 in the absence of K14 [32, 33]. We found no change in the levels of K17 upon vimentin overexpression, which further confirmed that the regulation exerted by vimentin on the expression of K5/K14 is highly specific (Fig 4A and S7A Fig). Forced expression of vimentin in HaCaT also showed a marked increase in the expression of K5 while K14 expression was unaffected. The differentiation specific marker involucrin showed a significant decrease in its levels, in response to an increase in the expression of vimentin (Fig 4B and S7B Fig). Next, we assessed the status of K5/K14 and involucrin with respect to vimentin in some tongue derived

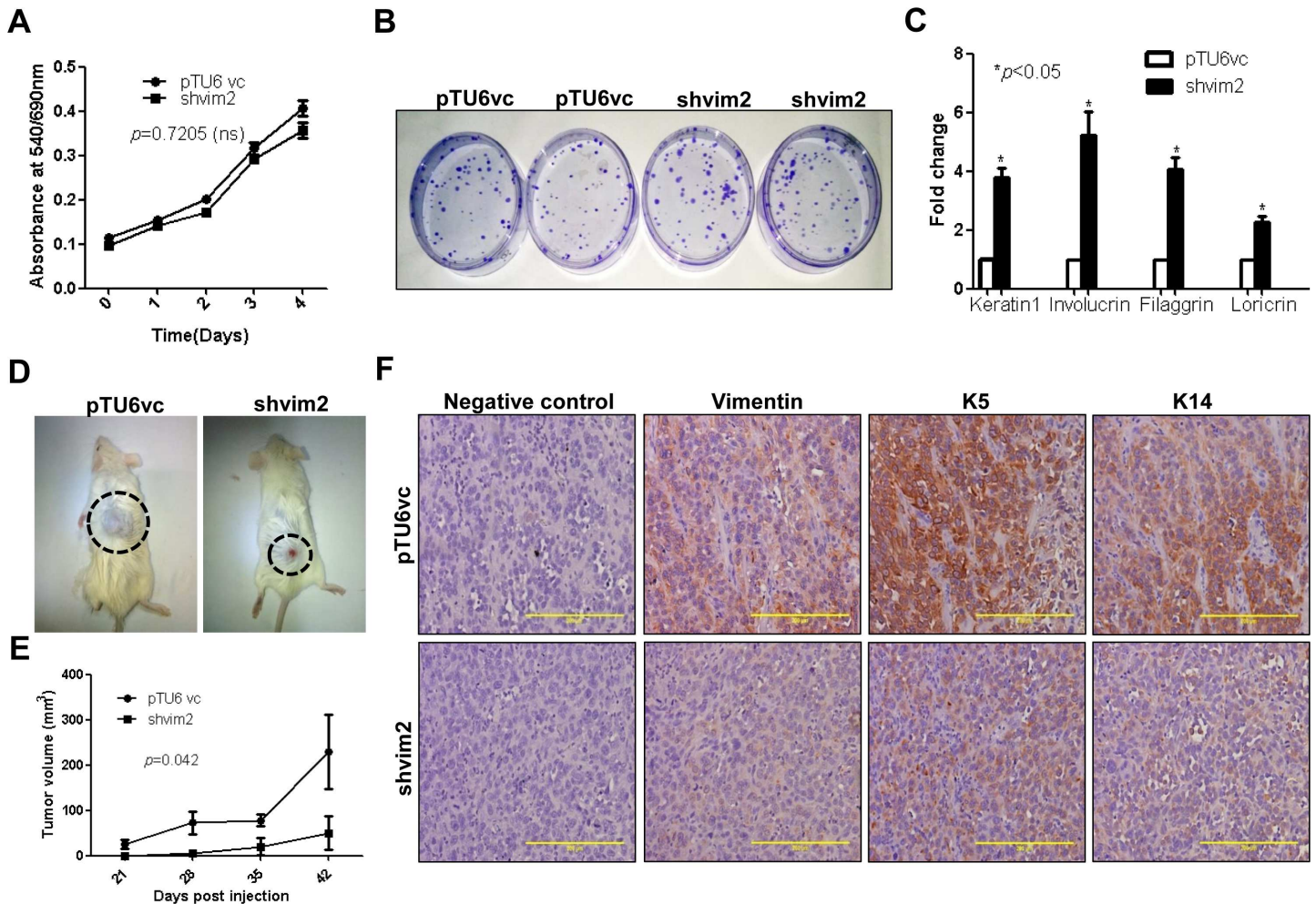


**Fig 3. Phenotypic alterations associated with K5/K14 downregulation as a consequence of vimentin depletion.** (A) Proliferation curves of vimentin knockdown and its vector control clones over a period of 4 days, using MTT assay. (B) Representative image of the clonogenic assay shows colonies formed by vimentin knockdown and its vector control clones. (C) qRT-PCR analysis of differentiation specific markers K1, involucrin, filaggrin and loricrin respectively. The relative expression of the target gene was normalized to GAPDH. For (A and C), the graphical data represents  $\pm$  SEM of three independent experiments. (D) Representative images of tumorigenicity assays using NOD-SCID mice (6 animals each) injected with either vimentin knockdown or vector control clones. The tumors are indicated by dotted circles. (E) The tumor measurements were recorded up to 42 days, after which the animals were sacrificed and the tumor tissue was isolated for IHC staining. The graph shows the tumor volume plotted against time for both the clones. (F) Representative images (Bar: 200 $\mu$ m) of IHC staining for expression of vimentin, K5 and K14 respectively in mice tumor tissues. The negative control images represent tissue sections incubated with serum from non-immunized mice in place of primary antibodies.

doi:10.1371/journal.pone.0172559.g003

cell lines. High vimentin expressing AW13516 and AW8507 cells (both of which are SCC derived cell lines) displayed elevated protein levels of K5/K14 and decreased levels of involucrin as compared to DOK cells (dysplastic lesion derived cell line), which does not express vimentin (Fig 4C and S7C Fig). Additionally, to determine whether K14 also has a similar regulatory effect on vimentin, we assessed the levels of vimentin in the same system AW13516, with the K14 knockdown background. Both the protein and mRNA levels of vimentin remained unchanged (Fig 4D and 4E and S7D Fig), suggesting that vimentin may be upstream in pathway/s that regulates the expression of K14.

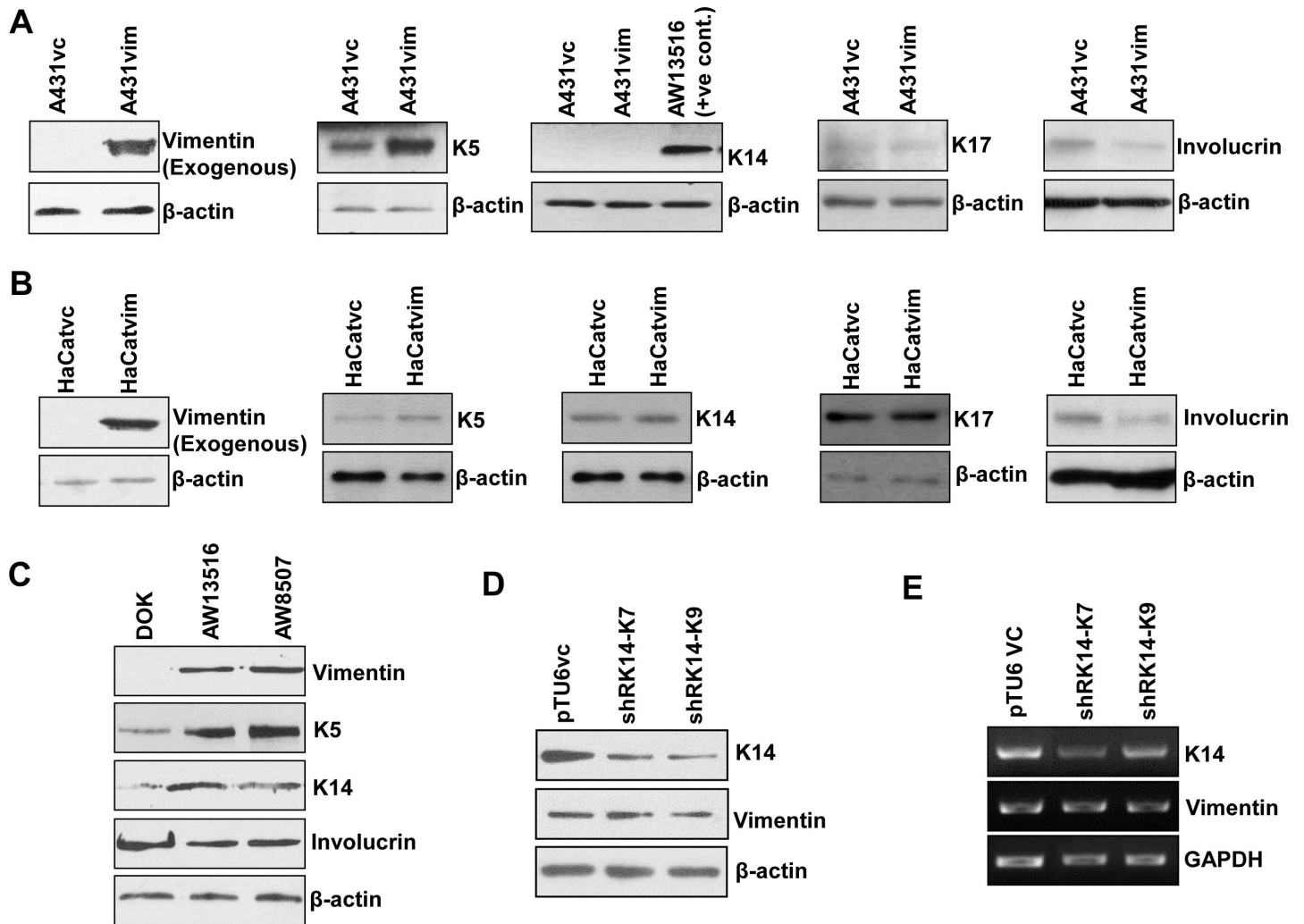


**Fig 4. Vimentin mediated positive regulation of K5/K14 levels is not a cell line specific phenomenon.** (A and B) Western blot analysis shows protein level of vimentin, K5, K14, K17 and involucrin in vimentin overexpressing clones of A431vim and HaCatvim as compared to its respective vector control clones A431vc and HaCatvc. Since A431 does not express K14, whole cell lysate from AW13516 was used as a positive control. (C) Whole cell lysates from DOK, AW13516 and AW8507 cells were probed with antibodies against vimentin, K5, K14 and involucrin respectively using western blotting. (D and E) Western blot and RT-PCR analysis of K14 and vimentin in K14 knockdown (shRK14-K7 and shRK14-K9) and its vector control clones (pTU6-AW1). GAPDH was used as the loading control in RT-PCR experiment.  $\beta$ -actin was used as the loading control in western blotting experiments. Western blotting experiments were done thrice with three independent sets of samples.

doi:10.1371/journal.pone.0172559.g004

### Vimentin knockdown phenotype was rescued upon re-expression of K5/K14 pair

Next, we re-expressed the K5/K14 pair in vimentin knockdown background because of two reasons: 1. to verify if the changes associated with vimentin knockdown are specifically due to K5/K14 downregulation and 2. To exclude the possibility of involvement of other altered molecule/s. Western blot (Fig 5A and 5B, S8A–S8C Fig) and immunofluorescence analysis (S9A and S9B Fig) confirmed the overexpression of K5/K14 pair in the shvim2 clone (shvim2-vimentin knockdown clone was used, since it showed a higher degree of vimentin downregulation as compared to shvim1 clone). As expected, proliferation and clonogenic potential remained unchanged upon K5/K14 re-expression, which corroborated with that of the vimentin knockdown phenotype (Fig 5C and 5D). K5/K14 re-expressing clone (“K5/K14”-shvim2 transduced

with emerald GFP-K14-pQCXIP and K5-pLNCX2 overexpressing vectors) showed a decrease in the expression of differentiation specific markers K1, involucrin, filaggrin and loricrin (Fig 5E) and in the involucrin protein levels (S10 Fig) as determined using qRT-PCR and western blotting respectively. However, stemness marker Oct-4 was upregulated (S11 Fig) in K5/K14 re-expressing clone as compared to its vector control (“vcvc”-shvim2 transduced with emerald GFP-pQCXIP and pLNCX2 empty vectors). Interestingly, no significant change was observed

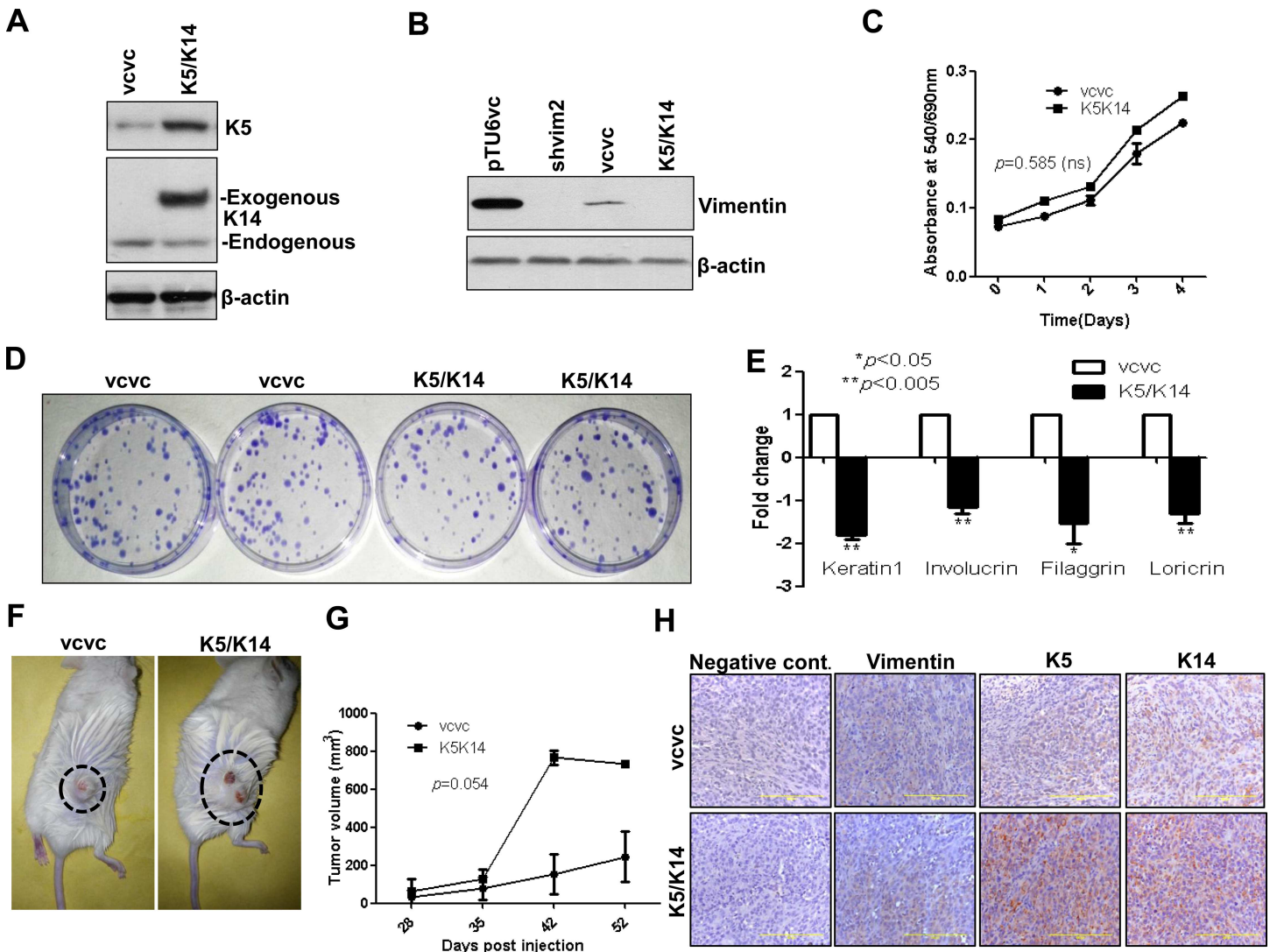


**Fig 5. Vimentin knockdown phenotype was rescued upon re-expression of K5/K14 together, in vimentin knockdown background.** (A and B) Western blot analysis shows overexpression of emerald GFP-K14 and K5 in K5/K14 overexpressing clone (“K5/K14”-shvim2 transduced with emerald GFP-K14-pQCXIP and K5-pLNCX2 overexpressing vectors) as compared to its vector control clone (“vcvc”-shvim2 transduced with emerald GFP-pQCXIP and pLNCX2 empty vectors). Protein levels of vimentin were tested in vimentin knockdown-vector control and K5/K14 overexpressing-vector control groups to confirm the maintenance of vimentin knockdown background in the second group, using western blotting. (C) Proliferation curves of K5/K14 overexpressing and its vector control clones over the period of 4 days, using MTT assay. (D) Representative image of clonogenic assay shows colonies formed by K5/K14 overexpressing and its vector control clones. (E) qRT-PCR analysis of differentiation specific markers K1, involucrin, filaggrin and loricrin respectively. The relative expression of the target gene was normalized to GAPDH. (F) Representative images of tumorigenicity assays using NOD-SCID mice (6 animals each) injected with either K5/K14 overexpressing or its vector control clones. The tumors are indicated by dotted circles. (G) The tumor measurements were recorded up to 52 days, after which the animals were sacrificed and the tumor tissue was isolated for IHC staining. The graph shows tumor volume plotted against time for both the clones. (H) Representative images (Bar: 200 μm) of IHC staining for expression of vimentin, K5 and K14 respectively in mice tumor tissues. The negative control images represent tissue sections incubated with serum from non-immunized mice in place of primary antibodies.

doi:10.1371/journal.pone.0172559.g005

in the levels of involucrin upon either K5 (S12 Fig) or K14 (S13 Fig) overexpression alone, indicating that perhaps both are required for conferring a more de-differentiated phenotype to the tumor cell. Tumorigenic potential of K5/K14 re-expressing clones was also significantly higher as reflected by the increased subcutaneous tumor growth in NOD-SCID mice (Fig 5F–5H). Further, tumors formed in mice from K5/K14 re-expressing clones showed a decrease in the expression of involucrin while no change was observed in the expression of PCNA (S14 Fig). This rescue experiment suggests that vimentin mediates regulation of the differentiation switch via the reprogramming of basal cell specific K5/K14 expression.

### $\Delta$ Np63 could be a possible target of vimentin, to bring about the modulation of K5/14 expression

Next, we wanted to investigate the molecular regulator, through which vimentin modulates the expression of K5/K14.  $\Delta$ Np63 is known to directly regulate the expression of both K5 and K14, during the program of keratinocyte stratification [34, 35]. Hence, as a first step, we checked its levels in the vimentin knockdown background. Western blot and qRT-PCR analysis showed decreased levels of  $\Delta$ Np63, both at protein and mRNA levels respectively (Fig 6A and 6B and S15A Fig). The antibody used for detection of  $\Delta$ Np63 is a pan-p63 antibody (SC-8343), which recognizes  $\alpha$ ,  $\beta$  and  $\gamma$  isoforms of p63. Since the expression of  $\Delta$ Np63 $\alpha$  isoform is very abundant, it is very likely that the single band seen in western blot is of  $\Delta$ Np63 $\alpha$  [36]. To functionally characterize depletion of  $\Delta$ Np63, we checked for other known molecular alterations associated with  $\Delta$ Np63 loss. Vimentin knockdown clones showed increased levels of p21 and p27 (Fig 6C and S15A Fig), which are typically associated with  $\Delta$ Np63 $\alpha$  downregulation [37, 38]. Further, RT-PCR analysis showed downregulation of both  $\Delta$ Np63 $\alpha$  and  $\Delta$ Np63 $\gamma$  isoforms in vimentin knockdown as compared to its vector control clones (Fig 6D). To verify whether the K5/K14 downregulation seen upon vimentin knockdown is due to reduced  $\Delta$ Np63 levels, flag-tagged  $\Delta$ Np63 $\alpha$  (since  $\Delta$ Np63 $\alpha$  is a major isoform expressed in keratinocytes [37]) was stably re-expressed in vimentin knockdown clone shvim2 (Fig 6E and 6F and S15B and S15C Fig).  $\Delta$ Np63 $\alpha$  overexpression led to a significant increase in the levels of K14 while K5 expression was only marginally rescued, indicative of the contribution of more than one molecule in the regulation of K5/K14 expression (Fig 6G and 6H and S15D Fig). Nevertheless, K14 formed filaments despite the lesser levels of its partner K5 (S16A and S16B Fig), most likely due to the presence of K8 in AW13516 cells [39]. The proliferation and clonogenic potential remained unaffected upon  $\Delta$ Np63 $\alpha$  overexpression (Fig 6I and 6J). The differentiation status (defined by the expression of differentiation specific markers) remained unchanged (Fig 6K) while the expression of Oct-4 showed only a marginal increase (not significant) (S17 Fig) upon  $\Delta$ Np63 $\alpha$  upregulation in the vimentin knockdown background.

### Notch1- $\Delta$ Np63 crosstalk may be involved in the vimentin mediated modulation of the differentiation switch

$\Delta$ Np63 and notch regulate each other by a negative feedback loop [37]. In order to understand the cause of  $\Delta$ Np63 downregulation, we checked for the levels of activated Notch1 upon vimentin knockdown. Vimentin knockdown clone showed increase in activated Notch1 (notch intracellular domain (NICD)) levels as compared to the vector control clone (S18A Fig and S19A Fig). The other candidate molecule which may modulate the levels of  $\Delta$ Np63 is nuclear factor-kappaB (NF- $\kappa$ B), since it negatively regulates  $\Delta$ Np63 either through the notch or independently as a part of the differentiation program [40]. Increased nuclear localization of NF- $\kappa$ B (p65) was observed in vimentin knockdown cells (S18B and S18C Fig and S19B Fig). On the other hand, these molecular changes showed reversal (decrease in activated Notch1 levels and in nuclear

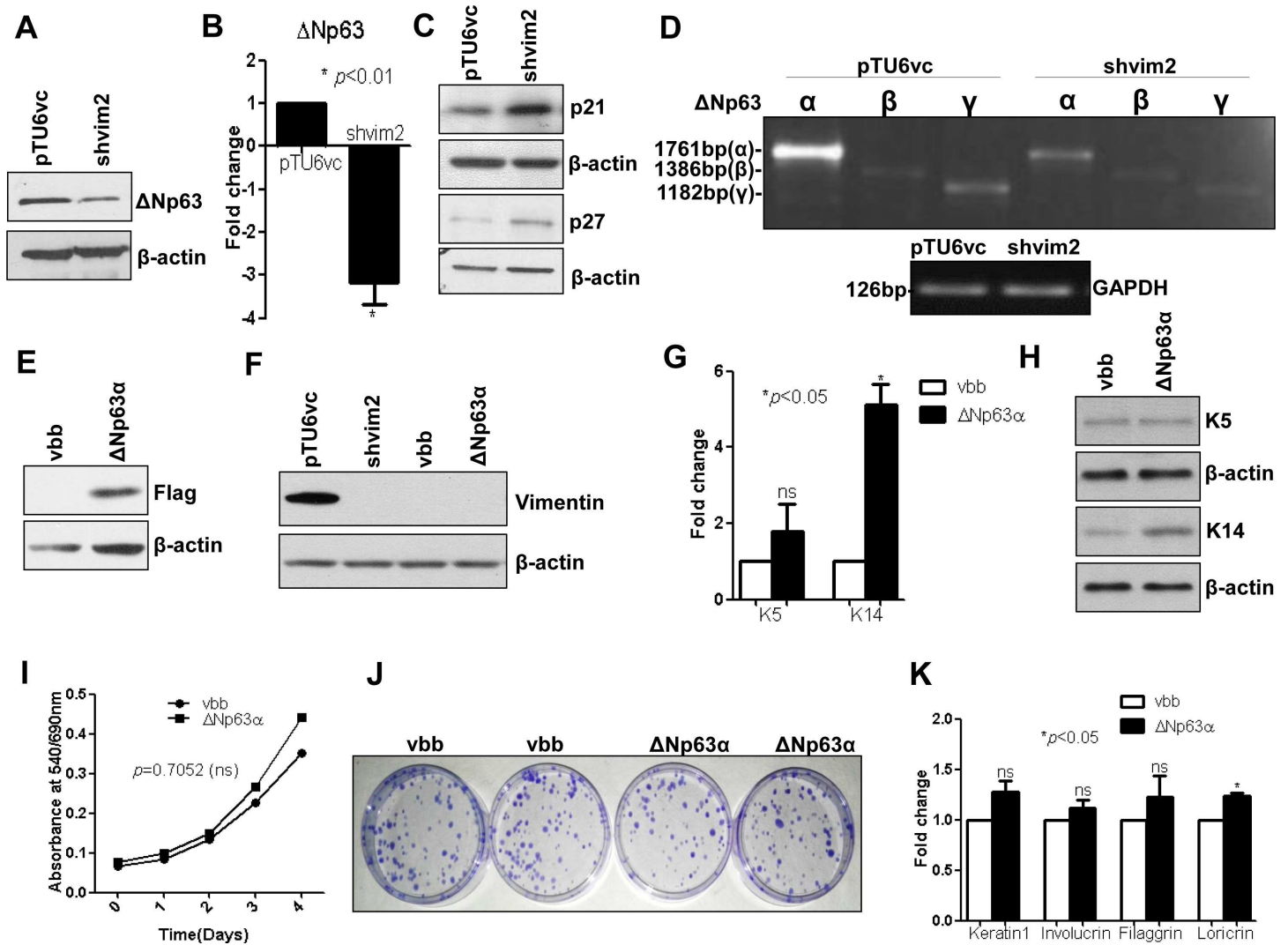


**Fig 6. Vimentin knockdown phenotype was partially rescued upon re-expression of  $\Delta$ Np63 $\alpha$  in vimentin knockdown background.** (A) Western blot analysis shows protein levels of  $\Delta$ Np63 from whole cell lysates of vimentin knockdown and its vector control clones. (B) Fold change in mRNA expression level of  $\Delta$ Np63 in vimentin knockdown as compared to vector control clones, using qRT-PCR analysis. (C) Western blot analysis shows protein levels of p21 and p27 from the whole cell lysates of vimentin knockdown and its vector control clones. (D) RT-PCR analysis shows expression of  $\Delta$ Np63 $\alpha$ ,  $\beta$  and  $\gamma$  isoforms, between vimentin knockdown and vector control clones. GAPDH was used as a loading control. (E) Western blot analysis using anti-flag antibody confirmed the overexpression of flag-tagged  $\Delta$ Np63 $\alpha$ . (F) The protein level of vimentin was tested by western blotting in vimentin knockdown-vector control set and flag- $\Delta$ Np63 $\alpha$ -vector control set, to confirm the maintenance of vimentin knockdown background in the second group. (G and H) qRT-PCR and western blot analysis of K5 and K14 in flag- $\Delta$ Np63 $\alpha$  overexpressing and its vector control group. (I) Proliferation curves of flag- $\Delta$ Np63 $\alpha$  overexpressing and its vector control clones over the period of 4 days, using MTT assay. (J) Representative image of clonogenic assay shows colonies formed by flag- $\Delta$ Np63 $\alpha$  overexpressing and its vector control clones. (K) QRT-PCR analysis of differentiation specific markers K1, involucrin, filaggrin and loricrin. For all the qRT-PCR experiments, the relative expression of the target gene was normalized to the GAPDH. For all western blotting experiments,  $\beta$ -actin was used as a loading control. The graphical data represents  $\pm$  SEM of three independent experiments.

doi:10.1371/journal.pone.0172559.g006

localization of NF- $\kappa$ B) upon  $\Delta$ Np63 $\alpha$  overexpression in vimentin knockdown background (S18D–S18F Fig and S19A and S19B Fig). Further, qRT-PCR analysis for Hes1 (which is a known Notch dependent target gene [41, 42]) suggested increase in notch activity upon vimentin depletion while the reverse was seen upon  $\Delta$ Np63 $\alpha$  overexpression in vimentin knockdown background (S19C Fig). Also, qRT-PCR analysis of I $\kappa$ B $\alpha$  (which is a known NF- $\kappa$ B dependent target gene [43, 44]) suggested increase in p65 activity upon vimentin depletion while the reverse was

seen upon  $\Delta Np63\alpha$  overexpression in vimentin knockdown background (S19D Fig). Thus, our preliminary observations speculate the possibility of the crosstalk between notch (perhaps in an NF- $\kappa$ B dependent manner) and  $\Delta Np63$ , to regulate differentiation state in vimentin knockdown cells.

## High expression of vimentin-K14 together correlates with recurrence and poor survival of oral cancer patients

Statistical correlation between clinico-pathological parameters and vimentin-K14 expression is listed in S5 Table. IHC analysis of OSCC tissues showed a positive correlation between high vimentin-K14 staining intensity (Fig 7A) and recurrence ( $p = 0.001$ ) (Fig 7B). In order to determine if the vimentin-K14 status of the tumor has any association with the survival of the oral cancer patients, Kaplan-Meier survival analysis based on IHC data was performed on 91 oral tumor samples. The analysis showed a significant correlation between high vimentin ( $p = 0.007$ ) and poor disease-free survival (Fig 7C). High K14 expression ( $p = 0.397$ ) did not show a significant correlation with the disease-free survival (Fig 7D). This could be because of only 2 cases showing low expression of K14. On the other hand, a significant correlation was seen between high vimentin-K14 expression ( $p = 0.005$ ) and poor disease free survival (Fig 7E). Collectively, this suggests that the expression of vimentin-K14 together may prove useful for the prognostication of human oral cancer. Additionally, we performed IHC for the expression of K5 and differentiation specific marker K1, on the same tumor samples whose vimentin and K14 expression was determined previously. Immunohistochemistry analysis (S20A Fig) showed positive correlation between K5/K14 and vimentin expression (Spearman's non-parametric correlation = 0.500,  $p = 0.001$ ,  $n = 100$ ) in oral tumor tissues while no significant correlation was seen between the expression of K1 and vimentin (Spearman's non-parametric correlation = -0.044,  $p = 0.663$ ,  $n = 100$ ) in oral tumor tissues. Further, Kaplan-Meier survival analysis showed a trend (albeit not significant) between high vimentin-K5-K14-low K1 expression and poor disease free survival ( $p = 0.966$ ) (S20B Fig). Also, significant correlation was found between high vimentin-K5-K14-low K1 expression and thickness ( $p = 0.019$ ) of the tumor mass (S6 Table).

## Discussion

Expression of EMT marker vimentin is usually associated with a more mesenchymal-like and dedifferentiated state of the cancer cell [8]. On the other hand, in the case of stratified epithelia, expression of one pair of keratins is specific to one particular differentiation compartment and as the cell moves from one layer to another, the expression pattern of keratins also changes accordingly [45]. This suggests that keratins may have a regulatory role in epithelial differentiation as well [46]. Hence, we wanted to understand whether vimentin modulates a differentiation switch of a transformed cell by modulating the expression of keratins. Our study found the K5/K14 pair to be a novel indirect target of vimentin, through which it is able to confer a dedifferentiated phenotype to the cancer cell.

To understand the overall change in the keratin profile caused due to downregulation of vimentin, we performed a global keratin profile analysis using high salt enriched keratin fraction from vimentin knockdown and vector control cells. Our 2D followed by MALDI analysis identified K14 as one of the differentially expressed proteins upon downregulation of vimentin. Interestingly, its binding partner K5 was also found to be downregulated at the protein level. Further, transcript level analysis showed that mRNA levels of both K5 and K14 are downregulated in vimentin knockdown clones.

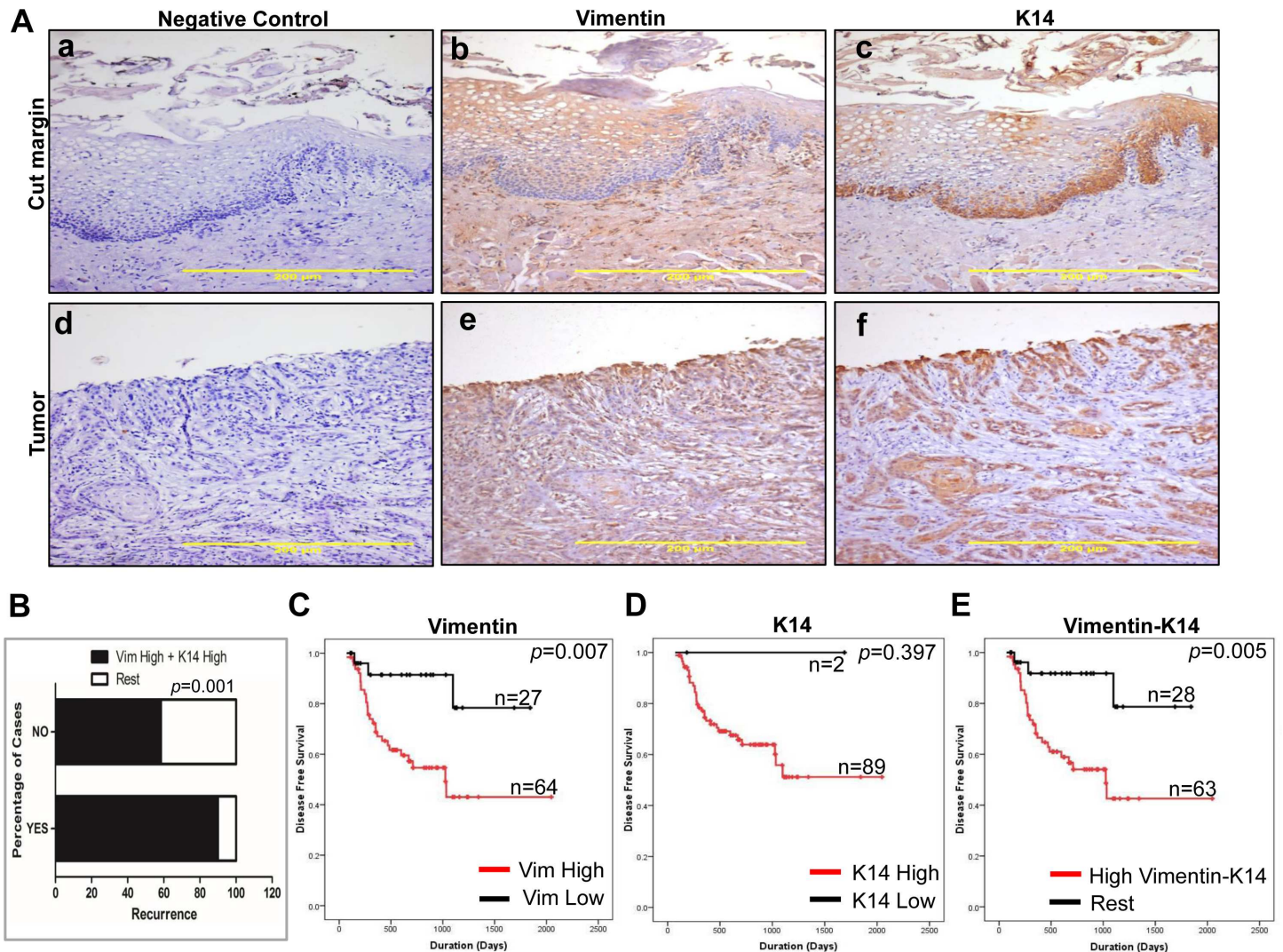


**Fig 7. High vimentin-K14 expression correlates with poor survival in oral cancer patients.** (A) (a-c) The upper panel show images (Bar: 200 $\mu$ m) of IHC staining for vimentin and K14 expression in cut margin tissues while lower panel (d-f) show images (Bar: 200 $\mu$ m) of IHC staining for vimentin and K14 expression in tumor tissues. The negative control images represent tissue sections incubated with serum from non-immunized mice in place of primary antibodies. (B) The graphical representation shows recurrence with respect to high vimentin-K14 expression and recurrence with respect to the other combinations of vimentin-K14 expression. Kaplan-Meier survival analysis (n = 91) of (C) High vs. low vimentin expression (D) High vs. low K14 expression and (E) High vimentin-K14 vs. the other combinations of vimentin-K14 expression.

doi:10.1371/journal.pone.0172559.g007

K5/K14 pair is typically expressed by the basal stem cell layer of the stratified epithelium. As the cell from this layer is committed to differentiation, it replaces the expression of K5/K14 with the expression of one or more differentiation specific keratin pairs e.g., K1 and K10 [45]. A previous study from our laboratory has demonstrated the role of K5/K14 in modulating phosphatidylinositol 3-kinase/Akt-mediated cell proliferation and/or Notch1-dependent cell differentiation, in stratified epithelia derived cells [19]. Our current study showed an increase in the differentiation status of the vimentin knockdown cells, while its proliferation status remained unaffected. This change in differentiation could be attributed to the decreased levels of K5/K14 since its reversal was seen upon re-expression of K5/K14 in vimentin knockdown background. Proliferation potential of the cells remained unchanged upon vimentin knockdown, perhaps due to

remnant levels of K5/K14 or because of an unknown compensatory mechanism operating in this situation.

Progenitor/stem-like and differentiated state are at extreme ends of the differentiation spectrum. Ding et al. have reported the loss of Oct-4 expression during the differentiation of mouse embryonic stem cells [47]. Hence, we were curious to understand if our vimentin knockdown cells, which were more differentiated showed any indications of somatic cell reprogramming. To verify this, we checked the expression of Oct-4, which is the master regulator of stemness [48]. Our results demonstrated a decrease in the expression of Oct-4 with the decrease in the expression of K5/K14, while re-expression of K5/K14 rescued the decreased levels of Oct-4. Nevertheless, additional experiments involving study of Oct-4 dependent target genes will help to elucidate if decrease in Oct-4 transcript levels has any functional impact in vimentin knockdown background. Transcription factors like AP1 and NF- $\kappa$ B are implicated in the regulation of basal expression of K5/K14 pair. The activation of these transcription factors is also dependent on extracellular signaling molecules like hormones, vitamins and growth factors [49]. Nevertheless, the role of the epithelial-specific master regulator p63 is well known for its precise control over epithelial cell differentiation [50]. One of the ways in which p63 regulates the differentiation program is through the maintenance of basal specific and stage specific expression of K5/K14 pair [51]. p63 is expressed as the isoform with a transactivation domain called as TA isoform and as a isoform lacking this domain, which is known as the  $\Delta$ N isoform [52].  $\Delta$ Np63 isoform has been shown to act as a dominant negative regulator of TAp63 and p53 [53], which also suggest its oncogenic potential.  $\Delta$ Np63 (which is the highly expressed isoform of p63 in the basal layer of epithelial tissues) is known to transcriptionally activate genes such as suppressor of fused homologue (SUFU), homeobox C4 (HOXC4) and myelin protein zero-like 2 (MPZL2; also known as EVA1) along with K5/K14 genes [52]. In our study, vimentin knockdown resulted in downregulation of  $\Delta$ Np63, while p21 and p27 levels were found to be upregulated. However, despite the upregulation of cyclin-dependent kinase (Cdk) inhibitors, p21 and p27, the proliferation status of vimentin knockdown clone remained unaltered. Similar observations were also reported by Zheng et al., wherein neither p21 nor p27 knockout mice showed any alterations in the proliferation of mouse gastrointestinal tract cells [54]. Similarly, some cancer cells are known to proliferate despite CDK2 inhibition [55], suggesting that perhaps correlation between p21 and p27 with the cell proliferation is context dependent. Further, analysis of transcript level expression of all the three  $\Delta$ Np63 isoforms revealed downregulation of both  $\Delta$ Np63 $\alpha$  and  $\Delta$ Np63 $\gamma$  and no change in the levels of  $\Delta$ Np63 $\beta$ . Report by Romano et al. suggested a role of  $\Delta$ Np63 $\alpha$  and  $\Delta$ Np63 $\beta$  isoforms in inducing basal markers and stratification [35]. Therefore, to understand if vimentin modulates expression of K5/K14 pair through  $\Delta$ Np63 $\alpha$  isoform, we overexpressed  $\Delta$ Np63 $\alpha$  isoform (since levels of  $\Delta$ Np63 $\beta$  remained unaltered upon vimentin downregulation) in vimentin knockdown background. Overexpression of  $\Delta$ Np63 $\alpha$  resulted in an increase in the expression of K14, while the expression of K5 remained unaltered. As a result of this, the differentiated state of the cell (marked by the expression of differentiation specific proteins) remained unchanged. This indicated that  $\Delta$ Np63 $\gamma$ , may as well, have a role in the regulation of the expression of K5, which was not compensated by the overexpression of  $\Delta$ Np63 $\alpha$  isoform alone. The possibility of the involvement of some other K5 specific transcription factor/s (enhancer or repressor), downstream of vimentin, cannot be ruled out.

Levels of  $\Delta$ Np63 $\alpha$  and notch play a decisive role to either maintain stemness or to proceed towards differentiation [37]. During the stratification process of epidermal tissue, notch suppresses p63 to favor differentiation, as evident by their opposing levels in the basal compartment [40]. Our study showed an increase in the levels of notch1 with decreased  $\Delta$ Np63 expression in the vimentin knockdown clone. Correspondingly, a decrease in the level of notch1 was seen upon overexpression of  $\Delta$ Np63 $\alpha$ . This suggests that there may be a reciprocal

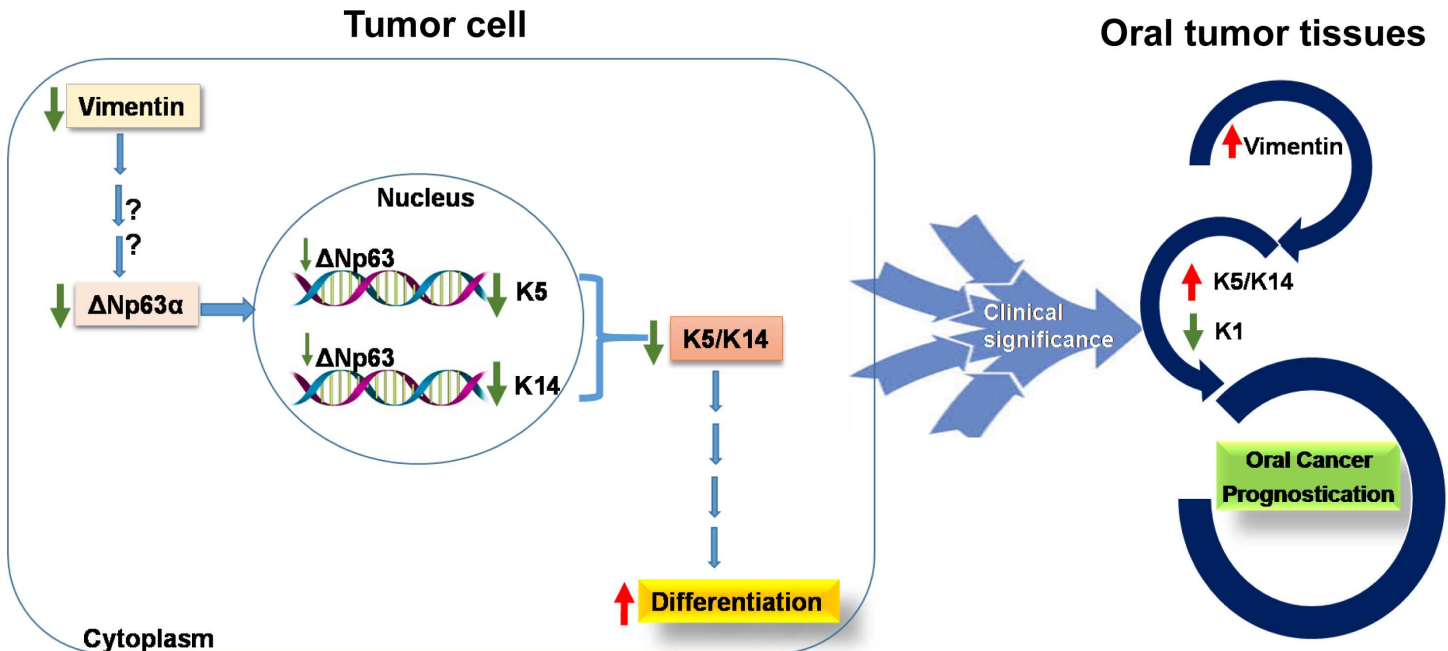


**Fig 8. Schematic representation depicting the role of vimentin in modulation of K5/K14 expression, to regulate differentiation in carcinoma-derived cells.** The model shows the regulation of K5/14 expression by vimentin, perhaps through  $\Delta Np63$ . Determination of vimentin-K14 status in oral tumor tissues may have clinical implications.

doi:10.1371/journal.pone.0172559.g008

negative regulatory mechanism between notch and  $\Delta Np63$  in order to govern differentiation in the presence and absence of vimentin. There may be two possibilities in this situation: first being either the deficiency of vimentin relieves the inhibition on notch1 which in turn suppresses the expression of  $\Delta Np63$  or the second possibility is that downregulation of vimentin decreases the expression of  $\Delta Np63$  relieving the negative regulatory effect on notch1 and leading to its activation. Interestingly, while the downregulation of  $\Delta Np63$  has been shown to result in a decrease in the expression of vimentin in esophageal squamous carcinoma [56], we report the reverse here i.e., downregulation of vimentin leads to decreased expression of  $\Delta Np63$ . There are reports of vimentin regulating transcript levels of certain genes in the literature. For instance, Vuoriluoto et al. have shown the role of vimentin in regulating the expression of several genes associated with EMT and the basal-like phenotype, one of which is Axl (a receptor tyrosine kinase) in breast cancer-derived cell lines [57]. Nevertheless, both the possibilities need to be tested experimentally to ascertain the directionality of the crosstalk between  $\Delta Np63$  and notch1 in vimentin knockdown background.

Factors other than activated notch may also have a significant role to play in the regulation of  $\Delta Np63$ . Along these lines, Flores et al., have shown inhibition of wild-type p53 by  $\Delta Np63$  [58]. Moreover, the parental cell line under study, AW13516 expresses mutant p53 (R273H) [59]. Hence, work in this direction will be required to ascertain if mutant p53 is the cause or consequence of an alteration in  $\Delta Np63\alpha$  expression. Furthermore, specific roles of microRNAs (miRs) [60, 61], Wnt, Hedgehog and EGFR [50] pathways if any, in the regulation of  $\Delta Np63$  expression in vimentin depleted condition, needs to be investigated.

We found a significant correlation between high vimentin-K14 expression and recurrence as well as the poor survival of oral cancer patients. This finding can be explained by our *in vitro* data using vimentin knockdown system. This showed that vimentin expression promotes events leading to increased dedifferentiation and tumorigenicity, wherein K5/K14

upregulation seems to be an intermediate event. Similar observations were made by Thomas et al., who have reported the association of vimentin-keratin co-expression with poor prognosis and tumor phenotype [62]. Together, this suggests that vimentin aids the aggressiveness of the tumor by contributing to the maintenance of a dedifferentiated state of the tumor cell.

In conclusion, our data sheds light on the modulatory role of vimentin in the expression of K5/K14 pair, to fine tune the differentiation switch in favor of tumor progression. Further, a large-scale study on human oral tumors is required to prove the potential of vimentin-K14 as prognostic markers for human oral cancer (Fig 8).

## Supporting information

**S1 Fig. Graph showing fold change in the protein level of vimentin and K8 upon vimentin downregulation.** Graph shows quantitation of western blots using densitometry. Fold-change in vimentin and K8 protein level in vimentin knockdown clones is shown relative to that of its vector control clone. Error bars denote  $\pm$  SEM. from three independent experiments.

(TIF)

**S2 Fig. Graph showing fold change in the protein level of K14, K5, K17 and K18 upon vimentin downregulation.** Graph shows quantitation of western blots using densitometry. Fold-change in K14, K5, K17 and K18 protein level in vimentin knockdown clones is shown relative to that of its vector control clone. Error bars denote  $\pm$ S.E.M. from three independent experiments.

(TIF)

**S3 Fig. Proliferation-related markers like PCNA and Ki67 remained unchanged upon vimentin downregulation.** (A) Representative immunofluorescence images (Bar: 10 $\mu$ m) of PCNA (green) staining in vimentin knockdown and vector control clones. (B) Representative immunofluorescence images (Bar: 10 $\mu$ m) of Ki67 (red) staining in vimentin knockdown and vector control clones.

(TIF)

**S4 Fig. Vimentin downregulation led to a significant increase in the protein level of differentiation specific marker involucrin.** (A) Western blot analysis shows protein level of involucrin from whole cell lysates of vimentin knockdown and its vector control clones. (B) Graph shows quantitation of western blot using densitometry. Fold-change in involucrin protein level in vimentin knockdown clone is shown relative to that of its vector control clone. Error bars denote  $\pm$  SEM. from three independent experiments.

(TIF)

**S5 Fig. Oct-4 mRNA levels decreased significantly upon vimentin downregulation.**

QRT-PCR analysis of Oct-4 in vimentin knockdown and its vector control clones.

(TIF)

**S6 Fig. Tumors formed in mice from vimentin knockdown cells showed an increase in the expression of involucrin.** Representative images (Bar: 200 $\mu$ m) of IHC staining for expression of involucrin and PCNA in tumor tissues of mice, injected with either vimentin knockdown or vector control clones. The negative control images represent tissue sections incubated with serum from non-immunized mice in place of primary antibodies.

(TIF)

**S7 Fig. Graphs showing fold change in the protein level of vimentin, K5, K14 and involucrin across different cell lines.** Graphs show quantitation of western blots using densitometry.

(A and B) Fold-change in vimentin, K5, K14, K17 and involucrin protein level in vimentin overexpressing clones of A431vim and HaCatvim is shown relative to its respective vector control clones A431vc and HaCatvc. (C) Fold-change in vimentin, K5, K14, K17 and involucrin protein level in AW13516 and AW8507 cells is shown relative to that of DOK cells. (D) Fold-change in K14 and vimentin protein level in K14 knockdown clones is shown relative to its respective vector control clone. Error bars denote  $\pm$  SEM from three independent experiments.

(TIF)

**S8 Fig. Graphs showing fold change in the protein level of K5, K14 and vimentin upon K5/K14 re-expression in vimentin knockdown background.** Graphs show quantitation of western blots using densitometry. (A and B) Fold-change in K5 and K14 protein level in K5/K14 overexpressing clone is shown relative to that of its vector control clone. (C) Fold-change in vimentin protein level in vimentin knockdown (shvim2), K5/K14 overexpressing clone (K5/K14) and its vector control clone (vcvc) is shown relative to that of vector control clone (pTU6vc). Error bars denote  $\pm$  SEM from three independent experiments.

(TIF)

**S9 Fig. Confocal images showing filament organization of K5 and K14, after their re-expression in vimentin knockdown background.** (A and B) Confocal microscopy analysis (Bar: 10 $\mu$ m) shows levels and filament networks of K5 and K14 respectively in K5/K14 (K5 and K14 overexpressing) as compared to its vector control vcvc clones (empty vectors of K5 and K14 together).

(TIF)

**S10 Fig. K5/K14 re-expression in vimentin knockdown background led to a significant decrease in the protein level of differentiation specific marker involucrin.** (A) Western blot analysis shows protein level of involucrin from whole cell lysates of K5/K14 overexpressing as compared to its vector control clones. (B) Graph shows quantitation of western blot using densitometry. Fold-change in involucrin protein level in K5/K14 overexpressing clone is shown relative to that of its vector control clone. Error bars denote  $\pm$  SEM from three independent experiments.

(TIF)

**S11 Fig. Oct-4 mRNA levels increased significantly upon K5/K14 re-expression in vimentin knockdown background.** qRT-PCR analysis of Oct-4 in K5/K14 overexpressing and its vector control clones.

(TIF)

**S12 Fig. K5 re-expression alone in vimentin knockdown background failed to rescue the protein level of differentiation specific marker involucrin.** (A) Immunofluorescence (Bar: 10  $\mu$ m) images of K5 overexpressing (K5) and its vector control clone (K5vc) using antibodies against K5 and K14. (B) Western blot analysis shows protein level of K5, K14 and involucrin in K5 overexpressing and its vector control clones.  $\beta$ -actin was used as the loading control in the western blotting experiment. (C) Graph shows quantitation of western blot using densitometry. Fold-change in K5, K14 and involucrin protein level in K5 overexpressing clone is shown relative to that of its vector control clone. Error bars denote  $\pm$  SEM from three independent experiments.

(TIF)

**S13 Fig. K14 re-expression alone in vimentin knockdown background failed to rescue the protein level of differentiation specific marker involucrin.** (A) Immunofluorescence (Bar:

10  $\mu\text{m}$ ) images shows K14 overexpression in overexpressing (K14) and its vector control clone (K14vc). K5 levels remained unchanged between the clones. (B) Western blot analysis shows protein level of K14, K5 and involucrin in K14 overexpressing and its vector control clones.  $\beta$ -actin was used as the loading control in the western blotting experiment. (C) Graph shows quantitation of western blot using densitometry. Fold-change in K14, K5 and involucrin protein level in K14 overexpressing clone is shown relative to that of its vector control clone. Error bars denote  $\pm$  SEM from three independent experiments. (TIF)

**S14 Fig. Tumors formed in mice from K5/K14 overexpressing cells showed a decrease in the expression of involucrin.** Representative images (Bar: 200 $\mu\text{m}$ ) of IHC staining for expression of involucrin and PCNA in tumor tissues of mice, injected with either K5/K14 overexpressing or its vector control clones. The negative control images represent tissue sections incubated with serum from non-immunized mice in place of primary antibodies. (TIF)

**S15 Fig. Graphs showing fold change in the protein level of  $\Delta\text{Np63}$  and its related molecules.** Graphs show quantitation of western blots using densitometry. (A) Fold-change in  $\Delta\text{Np63}$ , p21 and p27 protein level in vimentin knockdown clones is shown relative to that of its vector control clone. (B) Fold-change in flag-tagged  $\Delta\text{Np63}\alpha$  protein level in flag- $\Delta\text{Np63}\alpha$  overexpressing clone is shown relative to that of its vector control clone. (C) Fold-change in vimentin protein level in vimentin knockdown (shvim2), flag- $\Delta\text{Np63}\alpha$  overexpressing ( $\Delta\text{Np63}\alpha$ ) and its vector control clone (vbb) is shown relative to that of vector control clone (pTU6vc). (D) Fold-change in K5 and K14 protein level in flag- $\Delta\text{Np63}\alpha$  overexpressing clone is shown relative to that of its vector control clone. Error bars denote  $\pm$  SEM from three independent experiments. (TIF)

**S16 Fig. Confocal images showing filament organization of K5 and K14, upon re-expression of  $\Delta\text{Np63}\alpha$  in vimentin knockdown cells.** (A and B) Confocal microscopy analysis (Bar: 10 $\mu\text{m}$ ) shows levels and filament networks of K5 and K14 respectively in  $\Delta\text{Np63}\alpha$  (flag tagged  $\Delta\text{Np63}\alpha$  overexpressing) as compared to vbb (vector control clone). (TIF)

**S17 Fig. Oct-4 mRNA levels did not change significantly upon  $\Delta\text{Np63}\alpha$  re-expression.** qRT-PCR analysis of Oct-4 in flag- $\Delta\text{Np63}\alpha$  overexpressing and its vector control clones. (TIF)

**S18 Fig. Notch1 (independently or through NF- $\kappa\text{B}$ ) may regulate the expression of  $\Delta\text{Np63}$ .** (A) Western blot analysis shows the protein levels of notch intracellular domain (NICD) in vimentin knockdown and its vector control cells. (B) The confocal images (Bar: 20 $\mu\text{m}$ ) show the distribution of NF- $\kappa\text{B}$  (p65) (red) in the cytoplasmic vs. nuclear compartment in vimentin knockdown and its vector control cells. The nuclei (blue) were stained with DAPI. (C) Subcellular fractionation was carried out to separate cytoplasmic and nuclear fractions of vimentin knockdown and vector control clones. Western blot analysis shows the distribution of p65 in cytoplasmic and nuclear fractions. (D) Western blot analysis shows the protein levels of notch intracellular domain (NICD) in flag- $\Delta\text{Np63}\alpha$  and its vector control clones. (E) The confocal images (Bar: 20 $\mu\text{m}$ ) show the distribution of NF- $\kappa\text{B}$  (p65) (red) in the cytoplasmic vs. nuclear compartment in flag- $\Delta\text{Np63}\alpha$  and its vector control clones. The nuclei (blue) were stained with DAPI. (F) Subcellular fractionation was carried out to separate cytoplasmic and nuclear fractions of flag- $\Delta\text{Np63}\alpha$  and its vector control clones. Western blot analysis shows the distribution of p65 in cytoplasmic and nuclear fractions.  $\beta$ -actin was used as a loading control for

the whole cell lysates.  $\alpha$ -tubulin was used as a loading control for the cytoplasmic fraction while histone H3 protein was used as a loading control for the nuclear fraction. All the experiments were repeated independently in triplicates.

(TIF)

**S19 Fig. Graphs showing fold change in the protein level of NICD, nuclear NF- $\kappa$ B and transcript levels of their respective target genes.** (A) Fold-change in NICD protein level in vimentin knockdown clone is shown relative to that of its vector control clone. Also, fold-change in NICD protein level in flag- $\Delta$ Np63 $\alpha$  overexpressing clone is shown relative to that of its vector control clone. (B) Fold-change in NF- $\kappa$ B (p65) nuclear protein level in vimentin knockdown clone is shown relative to that of its vector control clone. Also, fold-change in NF- $\kappa$ B (p65) nuclear protein level in flag- $\Delta$ Np63 $\alpha$  overexpressing clone is shown relative to that of its vector control clone. Fold change for nuclear levels of NF- $\kappa$ B was calculated by normalizing to its respective histone H3 nuclear levels. (C) qRT-PCR analysis of Hes1 in vimentin knockdown clone is shown relative to that of its vector control clone. Also, qRT-PCR analysis of Hes1 in flag- $\Delta$ Np63 $\alpha$  overexpressing clone is shown relative to that of its vector control clone. (D) qRT-PCR analysis of  $\text{I}\kappa\text{B}\alpha$  in vimentin knockdown clone is shown relative to that of its vector control clone. Also, qRT-PCR analysis of  $\text{I}\kappa\text{B}\alpha$  in flag- $\Delta$ Np63 $\alpha$  overexpressing clone is shown relative to that of its vector control clone. Error bars denote  $\pm$  SEM from three independent experiments.

(TIF)

**S20 Fig. Immunohistochemistry analysis on human oral tumor tissues showed positive correlation between K5/K14 and vimentin expression.** (A) The upper panel show images (Bar: 200 $\mu$ m) of IHC staining for K1, K5, K14 and vimentin expression in cut margin tissues while lower panel show images (Bar: 200 $\mu$ m) of IHC staining for K1, K5, K14 and vimentin expression in tumor tissues. The negative control images represent tissue sections incubated with serum from non-immunized mice in place of primary antibodies. (B) Kaplan-Meier survival analysis (n = 91) of high vimentin-K5-K14-low K1 expression vs. the other combinations of vimentin-K5-K14-K1 expression.

(TIF)

**S1 Table. List of cell lines used in this study.** The table shows a list of cell lines along with their particulars.

(TIF)

**S2 Table. Antibodies used in this study.** The table shows a list of antibodies along with their particulars.

(TIF)

**S3 Table. Reagents used in this study.** The table shows a list of reagents along with their particulars.

(TIF)

**S4 Table. Primers used in this study.** The table shows a list of primer sequences used for RT-PCR and qRT-PCR analysis.

(TIF)

**S5 Table. Correlations of vimentin-K14 expression with clinicopathological parameters of the oral cancer patients (n = 100).**

(TIF)

**S6 Table. Correlations of high vimentin-K5-K14-low K1 expression with clinicopathological parameters of the oral cancer patients (n = 100).**

(TIF)

**Acknowledgments**

We thank Professor Robert Goldman (Feinberg School of Medicine, Northwestern University, USA) and Professor Thomas Magin (TRM & Biology II, University of Leipzig, Germany) for generously gifting the emerald vimentin pQCXIP and K5 pLNCX2 retroviral constructs respectively. We thank Dr. Daniela Elena Costea (Gade Laboratory for Pathology, Institute of Clinical Medicine, University of Bergen, Norway and Department of Pathology, Haukeland University Hospital, Bergen) for her generous gift of the DOK cell line. We thank following people from ACTREC, TMC, India for their kind help: Dr. Sorab Dalal for generously gifting the pTU6 PURO vector; Pratik Chaudhari, Indrajit Sahu and Harsh Dongre for their valuable experimental suggestions; Silvania Charles for performing western blotting during revision of the manuscript, Aarti Adate for formatting of the manuscript and Mrs. Pallavi Rane for her help with the statistical analysis of the data. We are also thankful to Mrs. Tejaswini Modak (Online trainer and instructor for English Writing Skills, Centre for e-learning and Training) for corrections of English spelling and grammar.

**Author Contributions****Conceptualization:** MV CD.**Data curation:** PG ZD.**Formal analysis:** CD SS PG SK.**Funding acquisition:** SS CD MV.**Investigation:** CD SS HA PG SM MN R. Thorat KP.**Methodology:** MV CD.**Project administration:** MV CD SS.**Resources:** CD SS HA R. Tiwari DC.**Supervision:** MV CD SS.**Validation:** CD ZD.**Visualization:** CD.**Writing – original draft:** CD MV.**Writing – review & editing:** CD MV ZD.**References**

1. Eriksson JE, Dechat T, Grin B, Helfand B, Mendez M, Pallari HM, et al. Introducing intermediate filaments: from discovery to disease. *The Journal of clinical investigation*. 2009; 119(7):1763–71. PubMed Central PMCID: PMC2701876. doi: [10.1172/JCI38339](https://doi.org/10.1172/JCI38339) PMID: [19587451](https://pubmed.ncbi.nlm.nih.gov/19587451/)
2. Franke WW, Grund C, Kuhn C, Jackson BW, Illmensee K. Formation of cytoskeletal elements during mouse embryogenesis. III. Primary mesenchymal cells and the first appearance of vimentin filaments. *Differentiation; research in biological diversity*. 1982; 23(1):43–59. PMID: [6759279](https://pubmed.ncbi.nlm.nih.gov/6759279/)
3. Tapscott SJ, Bennett GS, Toyama Y, Kleinbart F, Holtzer H. Intermediate filament proteins in the developing chick spinal cord. *Developmental biology*. 1981; 86(1):40–54. PMID: [7197239](https://pubmed.ncbi.nlm.nih.gov/7197239/)

4. Capetanaki Y, Smith S, Heath JP. Overexpression of the vimentin gene in transgenic mice inhibits normal lens cell differentiation. *The Journal of cell biology*. 1989; 109(4 Pt 1):1653–64. PubMed Central PMCID: PMC2115810.
5. Li B, Zheng YW, Sano Y, Taniguchi H. Evidence for mesenchymal-epithelial transition associated with mouse hepatic stem cell differentiation. *PLoS one*. 2011; 6(2):e17092. PubMed Central PMCID: PMC3037942. doi: [10.1371/journal.pone.0017092](https://doi.org/10.1371/journal.pone.0017092) PMID: [21347296](https://pubmed.ncbi.nlm.nih.gov/21347296/)
6. Lian N, Wang W, Li L, Elefteriou F, Yang X. Vimentin inhibits ATF4-mediated osteocalcin transcription and osteoblast differentiation. *The Journal of biological chemistry*. 2009; 284(44):30518–25. PubMed Central PMCID: PMC2781606. doi: [10.1074/jbc.M109.052373](https://doi.org/10.1074/jbc.M109.052373) PMID: [19726676](https://pubmed.ncbi.nlm.nih.gov/19726676/)
7. Sommers CL, Byers SW, Thompson EW, Torri JA, Gelmann EP. Differentiation state and invasiveness of human breast cancer cell lines. *Breast cancer research and treatment*. 1994; 31(2–3):325–35. PMID: [7881109](https://pubmed.ncbi.nlm.nih.gov/7881109/)
8. Kidd ME, Shumaker DK, Ridge KM. The role of vimentin intermediate filaments in the progression of lung cancer. *American journal of respiratory cell and molecular biology*. 2014; 50(1):1–6. PubMed Central PMCID: PMC3930939. doi: [10.1165/rcmb.2013-0314TR](https://doi.org/10.1165/rcmb.2013-0314TR) PMID: [23980547](https://pubmed.ncbi.nlm.nih.gov/23980547/)
9. Satelli A, Li S. Vimentin in cancer and its potential as a molecular target for cancer therapy. *Cellular and molecular life sciences: CMLS*. 2011; 68(18):3033–46. PubMed Central PMCID: PMC3162105. doi: [10.1007/s00018-011-0735-1](https://doi.org/10.1007/s00018-011-0735-1) PMID: [21637948](https://pubmed.ncbi.nlm.nih.gov/21637948/)
10. Sawant S, Vaidya M, Chaukar D, Alam H, Dmello C, Gangadaran P, et al. Clinical significance of aberrant vimentin expression in oral premalignant lesions and carcinomas. *Oral diseases*. 2014; 20(5):453–65. doi: [10.1111/odi.12151](https://doi.org/10.1111/odi.12151) PMID: [23865921](https://pubmed.ncbi.nlm.nih.gov/23865921/)
11. Liu LK, Jiang XY, Zhou XX, Wang DM, Song XL, Jiang HB. Upregulation of vimentin and aberrant expression of E-cadherin/beta-catenin complex in oral squamous cell carcinomas: correlation with the clinicopathological features and patient outcome. *Modern pathology: an official journal of the United States and Canadian Academy of Pathology, Inc*. 2010; 23(2):213–24.
12. Otsuki S, Inokuchi M, Enjoji M, Ishikawa T, Takagi Y, Kato K, et al. Vimentin expression is associated with decreased survival in gastric cancer. *Oncology reports*. 2011; 25(5):1235–42. doi: [10.3892/or.2011.1185](https://doi.org/10.3892/or.2011.1185) PMID: [21327330](https://pubmed.ncbi.nlm.nih.gov/21327330/)
13. Mendez MG, Kojima S, Goldman RD. Vimentin induces changes in cell shape, motility, and adhesion during the epithelial to mesenchymal transition. *FASEB journal: official publication of the Federation of American Societies for Experimental Biology*. 2010; 24(6):1838–51. PubMed Central PMCID: PMC2874471.
14. Moll R, Hage C, Thoenes W. Expression of intermediate filament proteins in fetal and adult human kidney: modulations of intermediate filament patterns during development and in damaged tissue. *Laboratory investigation; a journal of technical methods and pathology*. 1991; 65(1):74–86. PMID: [1712875](https://pubmed.ncbi.nlm.nih.gov/1712875/)
15. Boraas LC, Guidry JB, Pineda ET, Ahsan T. Cytoskeletal Expression and Remodeling in Pluripotent Stem Cells. *PLoS one*. 2016; 11(1):e0145084. doi: [10.1371/journal.pone.0145084](https://doi.org/10.1371/journal.pone.0145084) PMID: [26771179](https://pubmed.ncbi.nlm.nih.gov/26771179/)
16. Moll R, Divo M, Langbein L. The human keratins: biology and pathology. *Histochemistry and cell biology*. 2008; 129(6):705–33. PubMed Central PMCID: PMC2386534. doi: [10.1007/s00418-008-0435-6](https://doi.org/10.1007/s00418-008-0435-6) PMID: [18461349](https://pubmed.ncbi.nlm.nih.gov/18461349/)
17. Raul U, Sawant S, Dange P, Kalraiya R, Ingle A, Vaidya M. Implications of cytokeratin 8/18 filament formation in stratified epithelial cells: induction of transformed phenotype. *International journal of cancer Journal international du cancer*. 2004; 111(5):662–8. doi: [10.1002/ijc.20349](https://doi.org/10.1002/ijc.20349) PMID: [15252834](https://pubmed.ncbi.nlm.nih.gov/15252834/)
18. Alam H, Kundu ST, Dalal SN, Vaidya MM. Loss of keratins 8 and 18 leads to alterations in alpha6beta4-integrin-mediated signalling and decreased neoplastic progression in an oral-tumour-derived cell line. *Journal of cell science*. 2011; 124(Pt 12):2096–106.
19. Alam H, Sehgal L, Kundu ST, Dalal SN, Vaidya MM. Novel function of keratins 5 and 14 in proliferation and differentiation of stratified epithelial cells. *Molecular biology of the cell*. 2011; 22(21):4068–78. PubMed Central PMCID: PMC3204069. doi: [10.1091/mbc.E10-08-0703](https://doi.org/10.1091/mbc.E10-08-0703) PMID: [21900500](https://pubmed.ncbi.nlm.nih.gov/21900500/)
20. Workman P, Aboagye EO, Balkwill F, Balmain A, Bruder G, Chaplin DJ, et al. Guidelines for the welfare and use of animals in cancer research. *British journal of cancer*. 2010; 102(11):1555–77. PubMed Central PMCID: PMC2883160. doi: [10.1038/sj.bjc.6605642](https://doi.org/10.1038/sj.bjc.6605642) PMID: [20502460](https://pubmed.ncbi.nlm.nih.gov/20502460/)
21. Tataka RJ, Rajaram N, Damle RN, Balsara B, Bhisey AN, Gangal SG. Establishment and characterization of four new squamous cell carcinoma cell lines derived from oral tumors. *Journal of cancer research and clinical oncology*. 1990; 116(2):179–86. PMID: [1691185](https://pubmed.ncbi.nlm.nih.gov/1691185/)
22. Chang SE, Foster S, Betts D, Marnock WE. DOK, a cell line established from human dysplastic oral mucosa, shows a partially transformed non-malignant phenotype. *International journal of cancer Journal international du cancer*. 1992; 52(6):896–902. PMID: [1459732](https://pubmed.ncbi.nlm.nih.gov/1459732/)

23. Boukamp P, Petrussevska RT, Breitkreutz D, Hornung J, Markham A, Fusenig NE. Normal keratinization in a spontaneously immortalized aneuploid human keratinocyte cell line. *The Journal of cell biology*. 1988; 106(3):761–71. PubMed Central PMCID: PMC2115116. PMID: [2450098](#)
24. Giard DJ, Aaronson SA, Todaro GJ, Arnstein P, Kersey JH, Dosik H, et al. In vitro cultivation of human tumors: establishment of cell lines derived from a series of solid tumors. *Journal of the National Cancer Institute*. 1973; 51(5):1417–23. PMID: [4357758](#)
25. Dmello C, Sawant S, Alam H, Gangadaran P, Tiwari R, Dongre H, et al. Vimentin-mediated regulation of cell motility through modulation of beta4 integrin protein levels in oral tumor derived cells. *The international journal of biochemistry & cell biology*. 2015; 70:161–72.
26. Iyer SV, Dange PP, Alam H, Sawant SS, Ingle AD, Borges AM, et al. Understanding the role of keratins 8 and 18 in neoplastic potential of breast cancer derived cell lines. *PloS one*. 2013; 8(1):e53532. PubMed Central PMCID: PMC3546083. doi: [10.1371/journal.pone.0053532](#) PMID: [23341946](#)
27. Sniezek JC, Matheny KE, Westfall MD, Pietenpol JA. Dominant negative p63 isoform expression in head and neck squamous cell carcinoma. *The Laryngoscope*. 2004; 114(12):2063–72. doi: [10.1097/01.mlg.0000149437.35855.4b](#) PMID: [15564824](#)
28. Achtstaetter T, Hatzfeld M, Quinlan RA, Parmelee DC, Franke WW. Separation of cytokeratin polypeptides by gel electrophoretic and chromatographic techniques and their identification by immunoblotting. *Methods in enzymology*. 1986; 134:355–71. PMID: [2434826](#)
29. Jensen MM, Jorgensen JT, Binderup T, Kjaer A. Tumor volume in subcutaneous mouse xenografts measured by microCT is more accurate and reproducible than determined by 18F-FDG-microPET or external caliper. *BMC medical imaging*. 2008; 8:16. PubMed Central PMCID: PMC2575188. doi: [10.1186/1471-2342-8-16](#) PMID: [18925932](#)
30. Truong AB, Kretz M, Ridky TW, Kimmel R, Khavari PA. p63 regulates proliferation and differentiation of developmentally mature keratinocytes. *Genes & development*. 2006; 20(22):3185–97. PubMed Central PMCID: PMC1635152.
31. Watt FM. Involucrin and other markers of keratinocyte terminal differentiation. *The Journal of investigative dermatology*. 1983; 81(1 Suppl):100s–3s.
32. Wawersik M, Paladini RD, Noensie E, Coulombe PA. A proline residue in the alpha-helical rod domain of type I keratin 16 destabilizes keratin heterotetramers. *The Journal of biological chemistry*. 1997; 272(51):32557–65. PMID: [9405470](#)
33. Troy TC, Turksen K. In vitro characteristics of early epidermal progenitors isolated from keratin 14 (K14)-deficient mice: insights into the role of keratin 17 in mouse keratinocytes. *Journal of cellular physiology*. 1999; 180(3):409–21. doi: [10.1002/\(SICI\)1097-4652\(199909\)180:3<409::AID-JCP12>3.0.CO;2-V](#) PMID: [10430181](#)
34. Romano RA, Birkaya B, Sinha S. A functional enhancer of keratin14 is a direct transcriptional target of deltaNp63. *The Journal of investigative dermatology*. 2007; 127(5):1175–86. doi: [10.1038/sj.jid.5700652](#) PMID: [17159913](#)
35. Romano RA, Ortt K, Birkaya B, Smalley K, Sinha S. An active role of the DeltaN isoform of p63 in regulating basal keratin genes K5 and K14 and directing epidermal cell fate. *PloS one*. 2009; 4(5):e5623. PubMed Central PMCID: PMC2680039. doi: [10.1371/journal.pone.0005623](#) PMID: [19461998](#)
36. Restivo G, Nguyen BC, Dziunycz P, Ristorcelli E, Ryan RJ, Ozuysal OY, et al. IRF6 is a mediator of Notch pro-differentiation and tumour suppressive function in keratinocytes. *The EMBO journal*. 2011; 30(22):4571–85. PubMed Central PMCID: PMC3243593. doi: [10.1038/emboj.2011.325](#) PMID: [21909072](#)
37. Nguyen BC, Lefort K, Mandinova A, Antonini D, Devgan V, Della Gatta G, et al. Cross-regulation between Notch and p63 in keratinocyte commitment to differentiation. *Genes & development*. 2006; 20(8):1028–42. PubMed Central PMCID: PMC1472299.
38. Chiang CT, Chu WK, Chow SE, Chen JK. Overexpression of delta Np63 in a human nasopharyngeal carcinoma cell line downregulates CKIs and enhances cell proliferation. *Journal of cellular physiology*. 2009; 219(1):117–22. doi: [10.1002/jcp.21656](#) PMID: [19089994](#)
39. Lu H, Hesse M, Peters B, Magin TM. Type II keratins precede type I keratins during early embryonic development. *European journal of cell biology*. 2005; 84(8):709–18. doi: [10.1016/j.ejcb.2005.04.001](#) PMID: [16180309](#)
40. Dotto GP. Crosstalk of Notch with p53 and p63 in cancer growth control. *Nature reviews Cancer*. 2009; 9(8):587–95. doi: [10.1038/nrc2675](#) PMID: [19609265](#)
41. Blanpain C, Lowry WE, Pasolli HA, Fuchs E. Canonical notch signaling functions as a commitment switch in the epidermal lineage. *Genes & development*. 2006; 20(21):3022–35. PubMed Central PMCID: PMC1620020.

42. Watt FM, Estrach S, Ambler CA. Epidermal Notch signalling: differentiation, cancer and adhesion. *Current opinion in cell biology*. 2008; 20(2):171–9. PubMed Central PMCID: PMC2324124. doi: [10.1016/j.ceb.2008.01.010](https://doi.org/10.1016/j.ceb.2008.01.010) PMID: [18342499](https://pubmed.ncbi.nlm.nih.gov/18342499/)
43. Oeckinghaus A, Ghosh S. The NF-kappaB family of transcription factors and its regulation. *Cold Spring Harbor perspectives in biology*. 2009; 1(4):a000034. PubMed Central PMCID: PMC2773619. doi: [10.1101/cshperspect.a000034](https://doi.org/10.1101/cshperspect.a000034) PMID: [20066092](https://pubmed.ncbi.nlm.nih.gov/20066092/)
44. Hoffmann A, Natoli G, Ghosh G. Transcriptional regulation via the NF-kappaB signaling module. *Oncogene*. 2006; 25(51):6706–16. doi: [10.1038/sj.onc.1209933](https://doi.org/10.1038/sj.onc.1209933) PMID: [17072323](https://pubmed.ncbi.nlm.nih.gov/17072323/)
45. Hsu YC, Li L, Fuchs E. Emerging interactions between skin stem cells and their niches. *Nature medicine*. 2014; 20(8):847–56. PubMed Central PMCID: PMC4358898. doi: [10.1038/nm.3643](https://doi.org/10.1038/nm.3643) PMID: [25100530](https://pubmed.ncbi.nlm.nih.gov/25100530/)
46. Vaidya MM, Kanojia D. Keratins: markers of cell differentiation or regulators of cell differentiation? *Journal of biosciences*. 2007; 32(4):629–34. PMID: [17762135](https://pubmed.ncbi.nlm.nih.gov/17762135/)
47. Ding L, Paszkowski-Rogacz M, Nitzsche A, Slabicki MM, Heninger AK, de Vries I, et al. A genome-scale RNAi screen for Oct4 modulators defines a role of the Paf1 complex for embryonic stem cell identity. *Cell stem cell*. 2009; 4(5):403–15. doi: [10.1016/j.stem.2009.03.009](https://doi.org/10.1016/j.stem.2009.03.009) PMID: [19345177](https://pubmed.ncbi.nlm.nih.gov/19345177/)
48. Zeineddine D, Hammoud AA, Mortada M, Boeuf H. The Oct4 protein: more than a magic stemness marker. *American journal of stem cells*. 2014; 3(2):74–82. PubMed Central PMCID: PMC4163606. PMID: [25232507](https://pubmed.ncbi.nlm.nih.gov/25232507/)
49. Ma S, Rao L, Freedberg IM, Blumenberg M. Transcriptional control of K5, K6, K14, and K17 keratin genes by AP-1 and NF-kappaB family members. *Gene expression*. 1997; 6(6):361–70. PMID: [9495317](https://pubmed.ncbi.nlm.nih.gov/9495317/)
50. Yoh K, Prywes R. Pathway Regulation of p63, a Director of Epithelial Cell Fate. *Frontiers in endocrinology*. 2015; 6:51. PubMed Central PMCID: PMC4412127. doi: [10.3389/fendo.2015.00051](https://doi.org/10.3389/fendo.2015.00051) PMID: [25972840](https://pubmed.ncbi.nlm.nih.gov/25972840/)
51. Medawar A, Virolle T, Rostagno P, de la Forest-Divonne S, Gambaro K, Rouleau M, et al. DeltaNp63 is essential for epidermal commitment of embryonic stem cells. *PloS one*. 2008; 3(10):e3441. PubMed Central PMCID: PMC2562986. doi: [10.1371/journal.pone.0003441](https://doi.org/10.1371/journal.pone.0003441) PMID: [18927616](https://pubmed.ncbi.nlm.nih.gov/18927616/)
52. Su X, Chakravarti D, Flores ER. p63 steps into the limelight: crucial roles in the suppression of tumorigenesis and metastasis. *Nature reviews Cancer*. 2013; 13(2):136–43. PubMed Central PMCID: PMC4181578. doi: [10.1038/nrc3446](https://doi.org/10.1038/nrc3446) PMID: [23344544](https://pubmed.ncbi.nlm.nih.gov/23344544/)
53. Yao JY, Chen JK. Roles of p63 in epidermal development and tumorigenesis. *Biomedical journal*. 2012; 35(6):457–63. doi: [10.4103/2319-4170.104410](https://doi.org/10.4103/2319-4170.104410) PMID: [23442358](https://pubmed.ncbi.nlm.nih.gov/23442358/)
54. Zheng Y, Bie W, Yang R, Perekatt AO, Poole AJ, Tyner AL. Functions of p21 and p27 in the regenerating epithelial linings of the mouse small and large intestine. *Cancer biology & therapy*. 2008; 7(6):873–9. PubMed Central PMCID: PMC3005242.
55. Tetsu O, McCormick F. Proliferation of cancer cells despite CDK2 inhibition. *Cancer cell*. 2003; 3(3):233–45. PMID: [12676582](https://pubmed.ncbi.nlm.nih.gov/12676582/)
56. Lee KB, Ye S, Park MH, Park BH, Lee JS, Kim SM. p63-Mediated activation of the beta-catenin/c-Myc signaling pathway stimulates esophageal squamous carcinoma cell invasion and metastasis. *Cancer letters*. 2014; 353(1):124–32. doi: [10.1016/j.canlet.2014.07.016](https://doi.org/10.1016/j.canlet.2014.07.016) PMID: [25045846](https://pubmed.ncbi.nlm.nih.gov/25045846/)
57. Vuoriluoto K, Haugen H, Kiviluoto S, Mpindi JP, Nevo J, Gjerdrum C, et al. Vimentin regulates EMT induction by Slug and oncogenic H-Ras and migration by governing Axl expression in breast cancer. *Oncogene*. 2011; 30(12):1436–48 doi: [10.1038/onc.2010.509](https://doi.org/10.1038/onc.2010.509) PMID: [21057535](https://pubmed.ncbi.nlm.nih.gov/21057535/)
58. Flores ER. The roles of p63 in cancer. *Cell cycle*. 2007; 6(3):300–4. doi: [10.4161/cc.6.3.3793](https://doi.org/10.4161/cc.6.3.3793) PMID: [17264676](https://pubmed.ncbi.nlm.nih.gov/17264676/)
59. Mishra R, Palve V, Kannan S, Pawar S, Teni T. High expression of survivin and its splice variants survivin DeltaEx3 and survivin 2 B in oral cancers. *Oral surgery, oral medicine, oral pathology and oral radiology*. 2015; 120(4):497–507. doi: [10.1016/j.oooo.2015.06.027](https://doi.org/10.1016/j.oooo.2015.06.027) PMID: [26346910](https://pubmed.ncbi.nlm.nih.gov/26346910/)
60. Candi E, Amelio I, Agostini M, Melino G. MicroRNAs and p63 in epithelial stemness. *Cell death and differentiation*. 2015; 22(1):12–21. PubMed Central PMCID: PMC4262770. doi: [10.1038/cdd.2014.113](https://doi.org/10.1038/cdd.2014.113) PMID: [25168241](https://pubmed.ncbi.nlm.nih.gov/25168241/)
61. Manni I, Artuso S, Careccia S, Rizzo MG, Baserga R, Piaggio G, et al. The microRNA miR-92 increases proliferation of myeloid cells and by targeting p63 modulates the abundance of its isoforms. *FASEB journal: official publication of the Federation of American Societies for Experimental Biology*. 2009; 23(11):3957–66.
62. Thomas PA, Kirschmann DA, Cerhan JR, Folberg R, Seftor EA, Sellers TA, et al. Association between keratin and vimentin expression, malignant phenotype, and survival in postmenopausal breast cancer patients. *Clinical cancer research: an official journal of the American Association for Cancer Research*. 1999; 5(10):2698–703.